TECHNICAL REPORT STANDARD TITLE PAGE

1. Report No.	2. Government Accession No.	3. Recipient's Catalog No.

4. Title and Subtitle	5. Report Date
"Cumulative Damage of Asphalt Materials Under Repeated-Load Indirect Tension"	January 1975
	6. Performing Orgonization Code
7. Author(s)	8. Performing Orgonization Report No.
Calvin E. Cowher and Thomas W. Kennedy	Research Report 183-3
9. Performing Organization Name and Address	10. Work Unit No.
Center for Highway Research The University of Texas at Austin Austin, Texas 78712	11. Contract or Grant No. Research Study 3-9-72-183
	13. Type of Report and Period Covered Interim
12. Sponsoring Agency Name and Address	14. Sponsoring Agency Code
Texas Highway Department Planning & Research Division P. O. Box 5051 Austin, Texas 78763	

15. Supplementary Notes
Work done in cooperation with the Federal Highway Administration, Department of Transportation.
Research Study Title: "Tensile Characterization of Highway Pavement Materials"

16. Abstract

This report summarizes the results of an investigation of the applicability of Miner's Hypothesis to the fatigue data which were obtained using the dynamic indirect tensile test. Relationships between fatigue life and stress were established for simple-loading fatigue data from which Miner's Hypothesis could be verified for compound-loading fatigue life prediction. The hypothesis was evaluated experimentally by conducting compound-loading fatigue tests in which two stress levels were used. In addition, it was shown that it was possible to predict the permanent deformations which occur under two-level compound loading conditions from the simple summation of damage increments from simple-loading permanent deformation curves. Statistical estimates of the fatigue life of the asphalt mixtures investigated are presented for both the simple-loading and compound-loading test series.

17. Key Words	18. Distribution Statement
dynamic indirect tensile test, Miner's Hypothesis, simple-loading, compound-loading, sequence tests, asphalt concrete, fatigue, repeated-loading, fatigue life, blackbase	

19. Security Classif. (of this report)	20. Security Classif. (of this page)	21. No. of Pages	22. Price
Unclassified	Unclassified	242	

Form DOT F 1700.7 (8-69)

CUMULATIVE DAMAGE OF ASPHALT MATERIALS UNDER REPEATED-LOAD INDIRECT TENSION

by

Calvin E. Cowher
Thomas W. Kennedy

Research Report Number 183-3

Tensile Characterization of Highway Pavement Materials

Research Project 3-9-72-183

conducted for

Texas
State Department of Highways and Public Transportation

in cooperation with
U. S. Department of Transportation
Federal Highway Administration

by the

CENTER FOR HIGHWAY RESEARCH

THE UNIVERSITY OF TEXAS AT AUSTIN

January 1975

The contents of this report reflect the views of the authors, who are responsible for the facts and the accuracy of the data presented herein. The contents do not necessarily reflect the official views or policies of the Federal Highway Administration. This report does not constitute a standard, specification, or regulation.

PREFACE

This is the third in a series of reports dealing with the findings of a research project concerned with tensile and elastic characterization of highway pavement materials. This report summarizes the results of a study to determine the applicability of Miner's Hypothesis to the fatigue data which were acquired using the dynamic indirect tensile test.

This report would not have been possible without the assistance of many people. Special appreciation is due Messrs. James N. Anagnos, Pat S. Hardeman, Victor N. Toth, and Harold H. Dalrymple for their involvement with the testing program; to Messrs. Avery Smith, Gerald Peck, and James L. Brown of the State Department of Highways and Public Transportation, who provided technical liaison for the project; and to Adedare S. Adedimila, Byron W. Porter, and Michael W. Cooper, who at various times aided in the actual specimen testing. Thanks are due the Center for Highway Research staff who assisted in the preparation of this manuscript. The support of the Federal Highway Administration, Department of Transportation, is gratefully acknowledged.

Calvin E. Cowher
Thomas W. Kennedy

January 1975

LIST OF REPORTS

Report No. 183-1, "Tensile and Elastic Characteristics of Pavement Materials," by Bryant P. Marshall and Thomas W. Kennedy, summarizes the results of a study on the magnitude of the tensile and elastic properties of highway pavement materials and the variations associated with these properties which might be expected in an actual roadway.

Report No. 183-2, "Fatigue and Repeated-Load Elastic Characteristics of Inservice Asphalt-Treated Materials," by Domingo Navarro and Thomas W. Kennedy, summarizes the results of a study on the fatigue response of highway pavement materials and the variation in fatigue life that might be expected in an actual roadway.

Report No. 183-3, "Cumulative Damage of Asphalt Materials Under Repeated-Load Indirect Tension," by Calvin E. Cowher and Thomas W. Kennedy, summarizes the results of a study on the applicability of a linear damage rule, Miner's Hypothesis, to fatigue data obtained utilizing the dynamic indirect tensile test.

ABSTRACT

This report summarizes the results of an investigation of the applicability of Miner's Hypothesis to the fatigue data which were obtained using the dynamic indirect tensile test. Relationships between fatigue life and stress were established for simple-loading fatigue data from which Miner's Hypothesis could be verified for compound-loading fatigue life prediction. The hypothesis was evaluated experimentally by conducting compound-loading fatigue tests in which two stress levels were used. In addition, it was shown that it was possible to predict the permanent deformations which occur under two-level compound loading conditions from the simple summation of damage increments from simple-loading permanent deformation curves. Statistical estimates of the fatigue life of the asphalt mixtures investigated are presented for both the simple-loading and compound-loading test series.

KEY WORDS: dynamic indirect tensile test, Miner's Hypothesis, simple-loading, compound-loading, sequence tests, asphalt concrete, fatigue, repeated-loading, fatigue life, blackbase.

SUMMARY

This report summarizes the findings of a study conducted to evaluate the applicability of Miner's Hypothesis to fatigue data which were obtained using the dynamic indirect tensile test. Two asphaltic concrete mixtures were tested, differing only in the type of aggregate utilized. The two aggregate types employed were a crushed limestone and a smooth river gravel.

Relationships between fatigue life and stress were established for both mixtures in simple-loading and it was found that the best-fit curves for each data set were virtually coincident, indicating only a minor influence on fatigue life due to aggregate type. Compound-loading tests with two levels of stress were performed; the initial and final stress levels were varied from 16 psi to 40 psi in increments of 8 psi so that the fatigue life under compound-loading conditions could be measured experimentally.

A predicted fatigue life was calculated from simple-loading information using Miner's Hypothesis and was compared to the compound-loading fatigue life measured experimentally. The experimental cumulative cycles ratio was found to vary from 0.65 to 1.18 for the limestone test series and from 0.57 to 1.01 for the gravel test series. This variation in experimental cycles ratio was found to be well within the range of variation reported by other investigators for two-level sequence tests.

The time-deformation data which were recorded indicate that it is possible to predict permanent deformation under compound-loading conditions from simple-loading considerations. Further, it was found that a simple geometrical construction could be used to determine a service fatigue life different from fracture and that the cycles ratio at which this service life occurred was reproducible from specimen to specimen and from mixture to mixture for a narrow range of cycles ratios (75-85%).

IMPLEMENTATION STATEMENT

The results of this study are of a preliminary nature. It has been established that compound-loading fatigue life predictions using Miner's Hypothesis are subject to variation; however, the available data suggest that the hypothesis can be used as a predictor, considering the numerous factors which affect the fatigue life of an asphalt mixture. Additional study is needed using loading spectra, which are representative of down-the-road and across-the-road traffic patterns and which include measurements within the actual loading cycle, and incorporate a solution which accounts for the inelastic behavior of asphaltic materials.

TABLE OF CONTENTS

PREFACE iii

LIST OF REPORTS v

ABSTRACT vii

SUMMARY ix

IMPLEMENTATION STATEMENT xi

CHAPTER 1. INTRODUCTION 1

CHAPTER 2. CURRENT STATUS OF KNOWLEDGE

Compound Loading 5
Linear Summation of Cycles Ratio Hypothesis 5
Deacon's Investigation 8
McElvaney's Investigation 20
Summary of Current-Status of Knowledge 32
Deacon's Investigation 32
McElvaney's Investigation 34
General 34

CHAPTER 3. EXPERIMENTAL PROGRAM

Experimental Program 37
Materials 37
Testing Method 40
Experiment Design 42

CHAPTER 4. EXPERIMENTAL RESULTS

Simple-Loading Constant-Stress Amplitude Tests 47
Fatigue-Life Estimates 48
Probability Estimates of Fatigue Life 48
Time Deformation Characteristics 58
Compound-Loading Two-Level Sequence Tests 60
Fatigue-Life Estimates 63
Probability Estimates of Compound-Loading Fatigue Life . . . 70
Evaluation of Miner's Hypothesis 70
Time-Deformation Characteristics Under Compound-Loading . . . 76

Deformation Prediction 77
Failure 78

CHAPTER 5. CONCLUSIONS

Conclusions 81
Simple-Loading Constant Stress Amplitude Tests 81
Compound-Loading Two-Level Sequence Tests 81
General 82
Recommendations 82

REFERENCES 83

APPENDIX A. BATCHING AND MIXING, COMPACTION, AND CURING PROCEDURES FOR ASPHALT-TREATED MATERIALS 87

APPENDIX B. PHYSICAL INFORMATION FOR ALL SPECIMENS 91

APPENDIX C. SIMPLE-LOADING CONSTANT STRESS AMPLITUDE SPECIMEN DATA 99

APPENDIX D. COMPOUND-LOADING TWO-LEVEL SEQUENCE SPECIMEN DATA . . . 129

CHAPTER 1. INTRODUCTION

The term fatigue has been in common use among engineers for well over half a century. As defined in the ASTM Standards (Ref 1), fatigue is the process of progressive localized permanent structural change occurring in a material subjected to conditions which produce fluctuating stresses and strains at some point or points and which may culminate in cracks or complete fracture after sufficient repetitions of load. Materials subjected to such conditions generally behave quite differently from those under steady loads, failing at stresses substantially less than the ultimate strength and exhibiting significantly different stress-strain characteristics.

The intense interest that has developed during the past several years concerning accumulation of fatigue damage in engineering materials is the result of the following needs:

(1) predicting the life of an engineering material or structure under an arbitrary load history in a given environment,

(2) determining the quantitative amount and distribution of damage in the material or structure under the arbitrary loading spectrum, and

(3) determining the manner and rate of accumulation of damage.

Unanimity as to the modes of distress exhibited by pavement materials does not exist in the literature. Distress can be categorized into three major classes: (1) fracture, (2) distortion, and (3) disintegration (Refs 2 and 3). Distress can also be equated with the end result of an accumulated "damage" phenomenon. McCullough (Ref 2) describes three modes of distress, giving manifestations and mechanisms (Table 1). It should be noted that "mode" refers to a failure condition, "manifestation" is the first visual observation of the mode, and "mechanism" is a causative phenomenon that initiates the mode of failure. The use of stabilized subbases as part of pavement structures requires a rational understanding of the damage phenomena associated with the materials employed in such projects. Further, these damage phenomena must be explored on both a static and a dynamic level so that the simple and compound

TABLE 1. MODES, MANIFESTATIONS, AND MECHANISMS OF TYPES OF DISTRESS

Mode	Manifestation	Mechanism
Fracture	Cracking	Excessive loading Repeated loading (i.e., fatigue) Thermal changes Moisture changes Slippage (horizontal forces) Shrinkage
	Spalling	Excessive loading Repeated loading (i.e., fatigue) Thermal changes Moisture changes
Distortion	Permanent deformation	Excessive loading Time-dependent deformation (e.g., creep) Densification (i.e., compaction) Consolidation Swelling
	Faulting	Excessive loading Densification (i.e., compaction) Consolidation Swelling
Disintegration	Stripping	Adhesion (i.e., loss of bond) Chemical reactivity Abrasion by traffic
	Raveling and scaling	Adhesion (i.e., loss of bond) Chemical reactivity Abrasion by traffic Degradation of aggregate Durability of binder

After McCullough (Ref 2).

fatigue behavior of these materials can be incorporated into the pavement design process.

The general objectives of this study were:

(1) to verify the previous work of Moore and Kennedy (Ref 4) by acquiring simple-fatigue data to be used to predict the fatigue life of an asphaltic concrete;

(2) to define the nature of the relationship between applied tensile stress and the number of load applications to failure, or fatigue life, in simple and compound loading;

(3) to investigate the deformation characteristics of an asphaltic concrete mixture in simple and compound loading; and

(4) to assess the applicability of Miner's Hypothesis as a predictor of the fatigue life of asphaltic concrete for compound-loading situations.

Chapter 2 contains a summary of the information available on the compound loading of asphaltic mixtures, with particular emphasis given to the hypothesis proposed by Miner (Ref 5) for the fatigue of metals under compound loading and subsequently applied to pavement materials and design. A review of the compound-loading investigations of Deacon (Ref 6) and McElvaney (Ref 7) is also presented in Chapter 2. Chapter 3 describes the experimental program in terms of test equipment, procedures, and experiment design. The findings of this study are presented in Chapter 4, with emphasis placed on the compound-loading phase of the investigation. The conclusions are summarized in Chapter 5.

CHAPTER 2. CURRENT STATUS OF KNOWLEDGE

The simple-fatigue behavior of asphalt mixtures under controlled laboratory conditions has been extensively treated in the literature and has been shown to be a stochastic phenomenon (Refs 4, 6, 7, 8, 9, and 10). In contrast, apparently only two major laboratory investigations concerning the fatigue behavior of bituminous mixtures subjected to compound loading have been completed (Refs 6 and 7). This chapter summarizes the current status of knowledge as it relates to the compound loading of bituminous mixtures.

COMPOUND LOADING

Compound-loading techniques have been employed in the investigation of fatigue of metals for over 60 years (Ref 11); however, few attempts at applying compound-loading hypotheses to the fatigue phenomena exhibited by asphalt mixtures have been made and, thus, knowledge with respect to the compound loading of bituminous mixtures is limited.

Monismith et al (Ref 8) were the first to suggest that the linear summation of cycles ratio hypothesis normally referred to as Miner's Hypothesis in the literature might prove valid for asphaltic concrete. In 1965, Deacon (Ref 6) completed the first comprehensive investigation of asphaltic concrete which considered the effects of compound loading in some detail. The published results and subsequent articles by Deacon (Refs 9, 12, and 13) concluded that the simple linear summation of cycles ratio hypothesis was adequate for predicting fatigue life under compound-loading conditions. A second in-depth investigation was completed in 1972, by McElvaney (Ref 7), who used the technique, introducing probability concepts into the method. This section reviews the hypothesis as proposed by Miner (Ref 5) in 1945 and summarizes the work of Deacon and McElvaney.

Linear Summation of Cycles Ratio Hypothesis

The linear summation of cycles ratio hypothesis was first proposed by

Palmgren in 1924 (Ref 14); however, credit is usually given to Langer (Ref 15) or Miner (Ref 5).

The hypothesis as proposed by Miner was the result of fatigue investigations of metals. Specimen damage had been alluded to as early as 1933, by French (Ref 16), who established "probable damage lines" on the conventional stress versus fatigue life diagram. These probable damage lines defined regions of damage and no-damage for steel specimens. Kommers (Ref 17), in 1938, reported results for steel specimens, expressing the damage incurred under load applications of overstress different from the test stress level as a percentage of the change in the fatigue limit. Investigators during this period searched for a simple method for predicting the fatigue life of an engineering material under changing load and environmental conditions; i.e., under compound loading (Refs 18, 19, 20, 21, and 22).

Miner's damage hypothesis is based on the assumption that the phenomenon of damage under repeated loads was related to the net work absorbed by a given specimen at failure. The governing equations developed by Miner were as follows:

$$\frac{w_1}{W_f} = \frac{n_1}{N_f} \tag{1}$$

where

W_f = the work absorbed at failure,

w_1 = the work absorbed after n_1 cycles of a given stress amplitude,

N_f = the number of cycles to first observation of cracking at a given stress amplitude,

n_1 = the applied number of cycles of a given stress amplitude.

Then if w_2 is the work absorbed after n_2 applications of a given stress amplitude, and if

$$w_1 + w_2 + \ldots + w_k = W_f \tag{2}$$

it follows that

$$\frac{w_1}{W_f} + \frac{w_2}{W_f} + \ldots + \frac{w_k}{W_f} = 1 \tag{3}$$

Substituting Eq 1 into Eq 3 gives

$$\frac{n_1}{N_f^1} + \frac{n_2}{N_f^2} + \ldots + \frac{n_k}{N_f^k} = 1 \tag{4}$$

and Eq 4 can be shown to be

$$\sum_{i=1}^{5} \frac{n_i}{N_f^i} = 1 \tag{5}$$

where i represents a given stress amplitude and the summation is defined to be the cycles ratio R, which equals unity in Miner's derivation.

The following assumptions are necessary for the derivations of Eqs 1 through 5:

(1) Fatigue failure occurs when a material absorbs a given amount of work W_f.

(2) Work absorbed per cycle of a given stress amplitude is constant.

(3) All work absorbed is irreversible.

The relationship given in Eq 1, therefore, defines a degree of damage in the specimen where the damage varies linearly with the cycles ratio n_i/N_f^i which ranges from zero to unity. Expressing the damage D in equation form,

$$D = \sum_{i=1}^{k} \frac{n_i}{N_f^i} \tag{6}$$

where $0 < D \leq 1$.

It also is assumed that the damage process is free of the effects of stress interaction. The concept of stress interaction can be explained as follows. If a test specimen is subjected to a first level of stress amplitude σ_1 and incurs an amount of damage following n_1 applications of load condition σ_1 and is then tested to failure at a second stress amplitude σ_2, the rate at which damage accumulates under the second load condition may or may not be

a function of the initial stress amplitude σ_1. No stress interaction exists if the rate at which damage accumulates under the second stress level is function of only the damage that existed in the specimen when the second load condition was applied and is independent of the manner in which the degree of damage was incurred. Figure 1 illustrates this concept. For no stress interaction the damage functions at all stress levels are coincident; however, with a stress interaction the curves are displaced relative to one another. Kommers (Ref 19) using Miner's Hypothesis for metals found a stress interaction; however, Kommers defined failure as complete specimen fracture, introducing the possibility that the time required for crack propagation could introduce significant variability in test results since Miner's definition of failure was crack inception. The data published by Miner show no evidence of stress interaction occurring; however, only 22 specimens were included in the test program, with no duplicates.

Deacon's Investigation

The investigation reported by Deacon (Ref 6) in 1965 was the first major attempt to study the effects of compound loading on bituminous mixtures under controlled laboratory conditions.

A two-point, pneumatically driven loading apparatus developed by Deacon produced a constant bending moment in the center third of a rectangular asphalt beam specimen. The loading system was capable of applying a pre-programmed controlled-stress loading sequence at a frequency of up to two load pulses per second. Figure 2 is a schematic of the repeated flexure apparatus used in the investigation. Figure 3 shows the load-pulse used. In it the downstroke portion was used to produce a stress reversal without a corresponding strain reversal. Deacon acquired both simple and compound-loading fatigue data during the course of his investigation.

Dynamic deflection measurements were taken during the course of a specimen test using an LVDT and a strip chart recorder. A stiffness modulus was then calculated by the following relationship:

$$E = \frac{KP}{I\Delta} \tag{7}$$

where

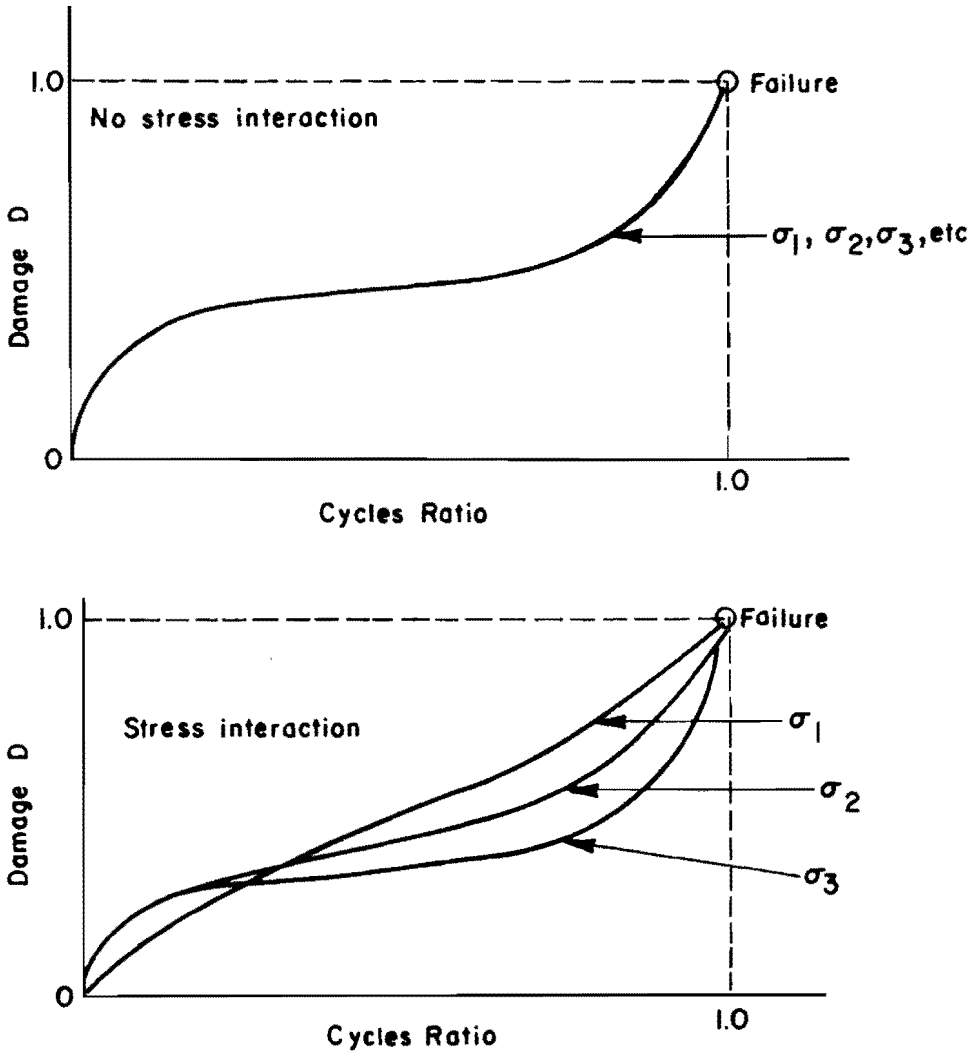

Fig 1. Damage-cycles ratio relationships.

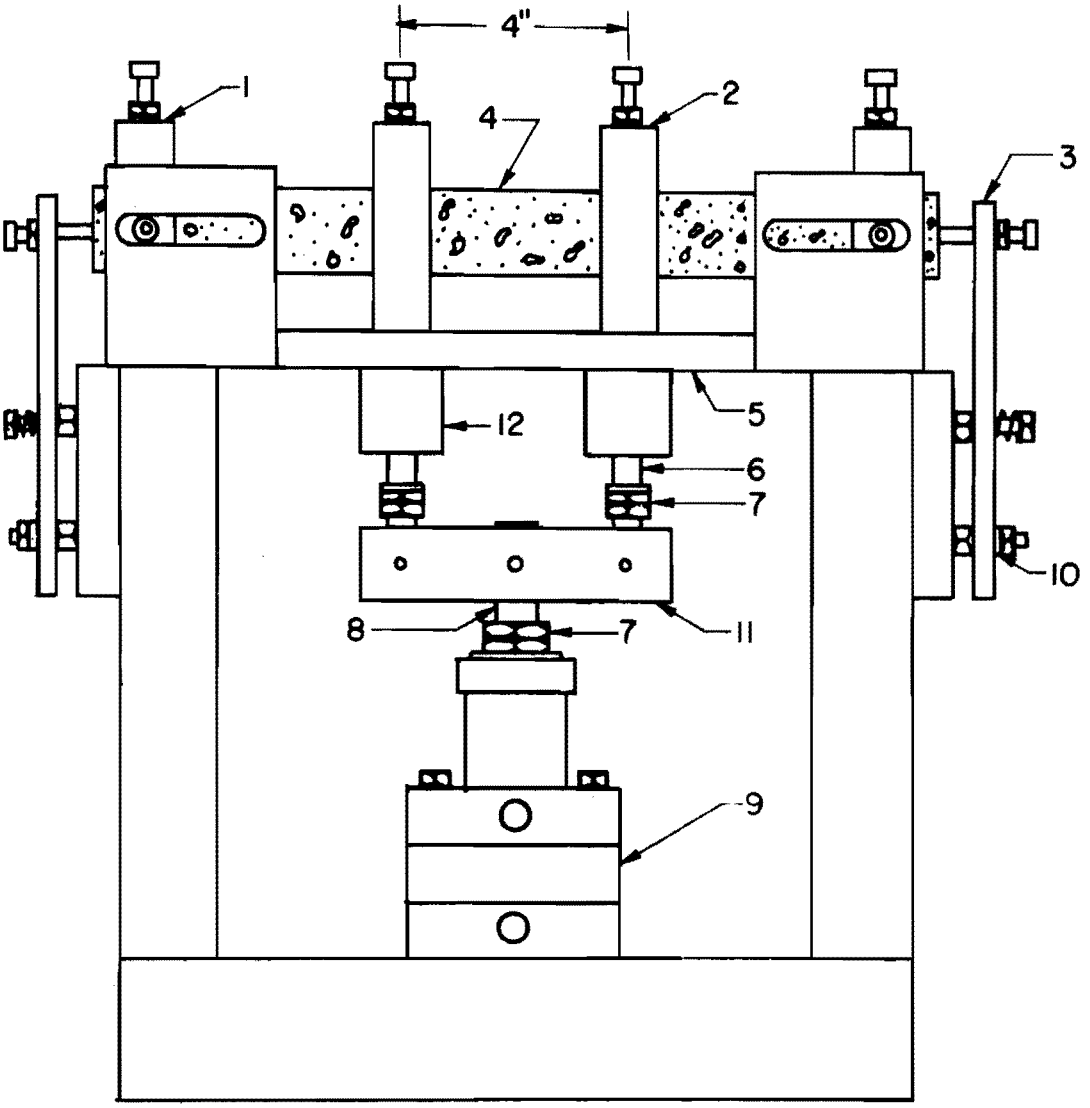

Key:

1. Reaction clamp
2. Load clamp
3. Restrainer
4. Specimen
5. Base plate
6. Loading rod
7. Stop nut
8. Piston rod
9. Double-acting, Bellofram cylinder
10. Rubber washer
11. Load bar
12. Thomson ball bushing

Fig 2. Repeated flexure apparatus (Ref 6).

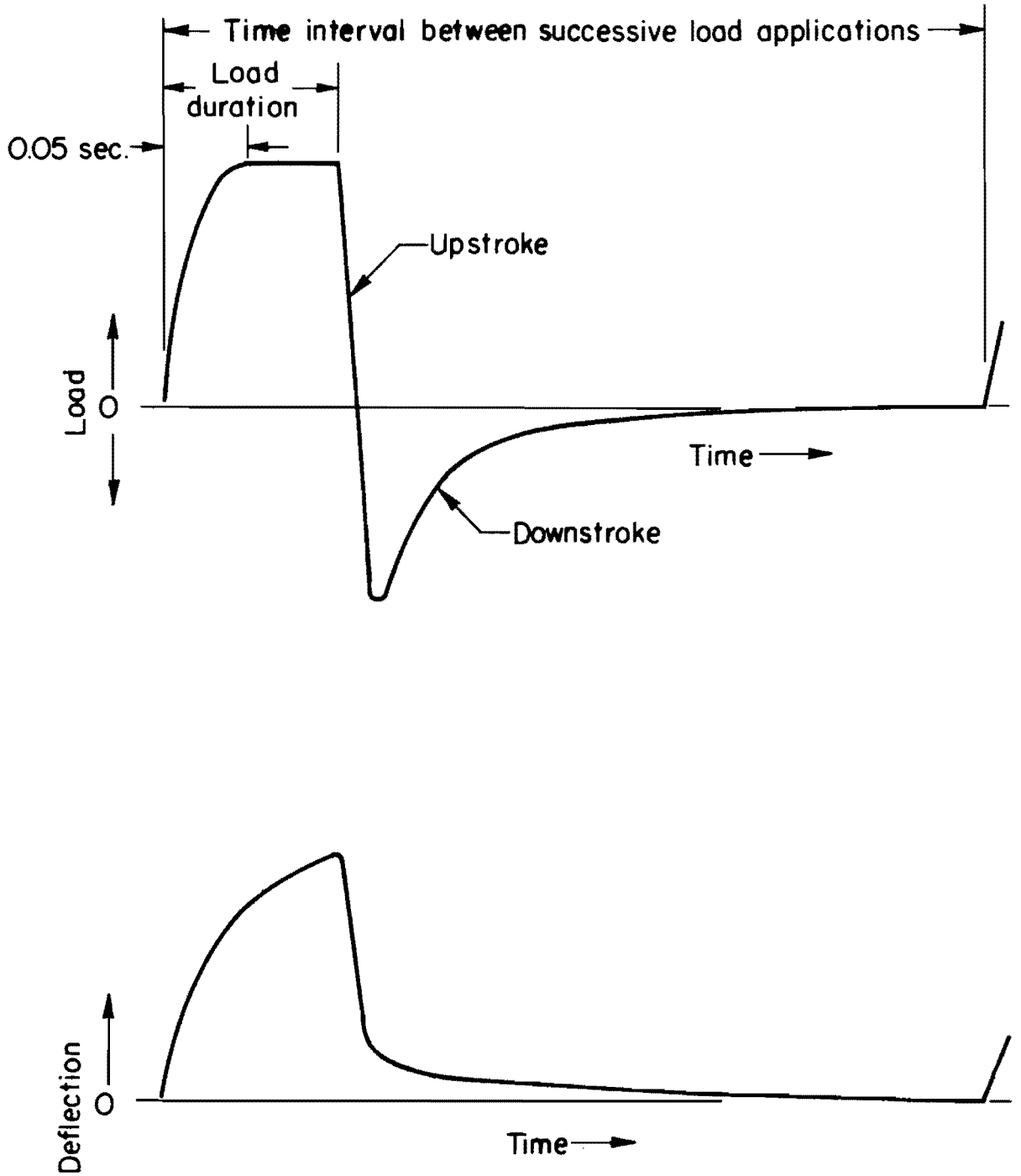

Fig 3. Load-pulse relationships (Ref 6).

E = deflection-based stiffness modulus,

K = constant dependent on specimen geometry,

P = total dynamic load applied upwards to the specimen,

I = moment of inertia of the beam cross section,

Δ = dynamic center deflection.

The calculated stiffness was found to decrease rapidly in the initial and final phases of the test, with a more gradual reduction in the intermediate phases of the test for all specimens observed (Fig 4). The magnitude of decrease at any given cycles ratio R was found to be a function of the stress level, the larger stress causing an increased reduction in stiffness.

In the study, 117 specimens were tested in simple loading and 133 specimens were subjected to compound-loading tests (Tables 2 and 3). All specimens were prepared from one mixture, the properties of which are summarized in Table 4. The asphalt and aggregate were mixed at 250°F by a mechanical mixer, cured 24 hours at 140°F, and then compacted at 250°F into 15-inch-long bars with rectangular cross sections, using a kneading compactor. Test specimens with final dimensions of 1.5" x 1.5" x 15.0" were cut from the compacted bars. The delay between compaction and testing was 1 to 4 weeks. The average void content for all specimens was 4.53 percent with an average specific gravity of 2.523, the latter having a standard deviation of 0.016.

The compound-loading tests performed were two-level, increasing and decreasing-sequence; two-level, repeated-block; three-level, repeated-block; and three-level, pseudo-random (Table 3). "Block" refers to a number of stress applications of a chosen stress "level," either high or low, depending on whether the stress sequence is "increasing" or "decreasing." Deacon performed all compound-loading tests at 75°F; however, the effect of temperature on an approximate dynamic modulus was evaluated for four specimens using resonant frequency techniques. The resulting data were analyzed using Miner's Hypothesis and variations of this hypothesis in an effort to choose the best predictive relationship for a mean compound-loading fracture life. Table 5 lists the predictive equations or techniques evaluated in Deacon's investigation. A comparison of compound-loading experimental results with the predicted results for the nine techniques is shown in Figs 5 and 6, constructed

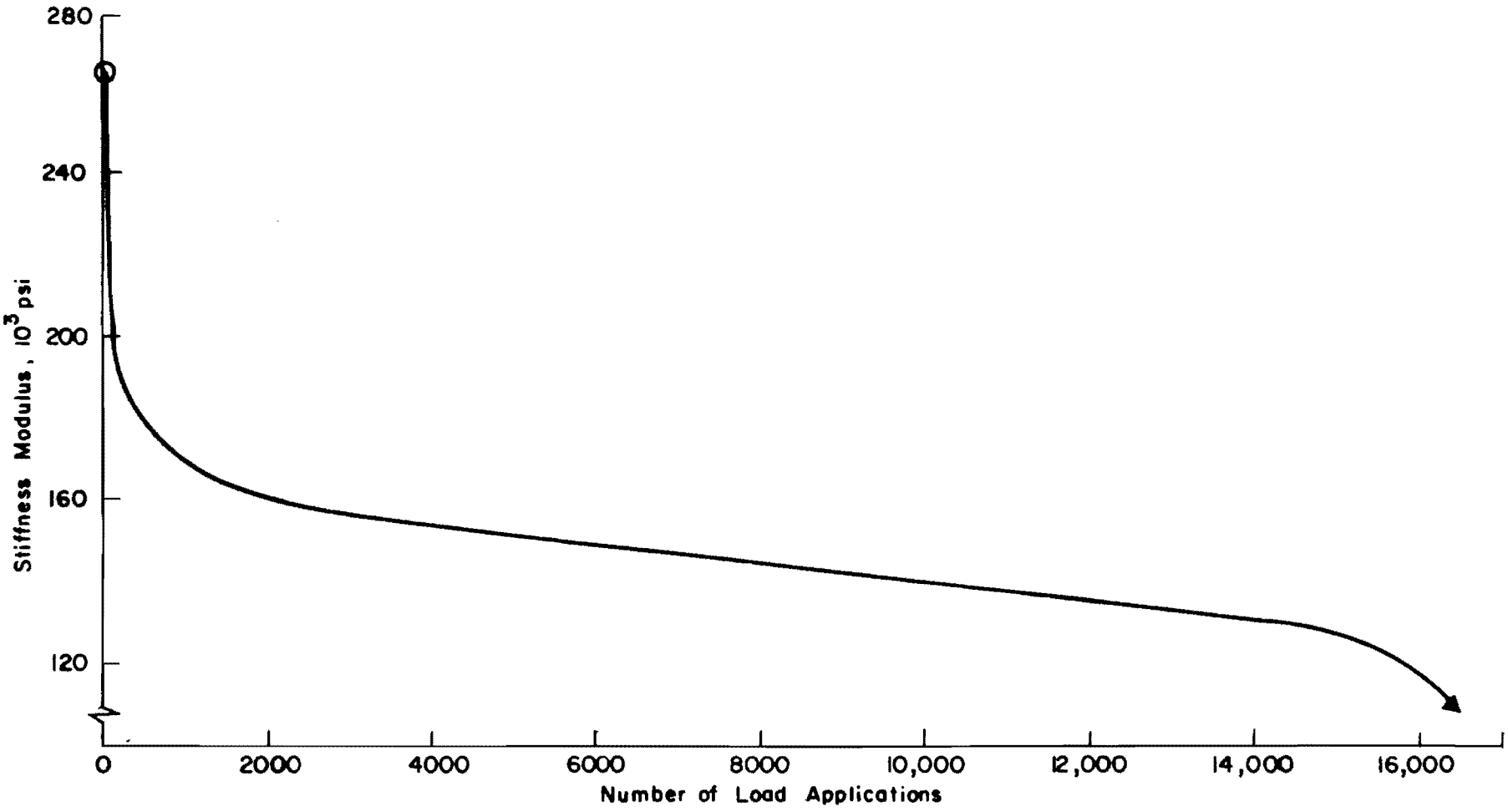

Fig 4. Dynamic deflection modulus - cycles ratio (Ref 6).

TABLE 2. NUMBER OF TEST SPECIMENS ASSIGNED TO SIMPLE-LOADING TEST SERIES

Test Series	No. of Specimens	Stress Levels, psi	Load Duration, sec	Rate of Loading, applic./min	Temperature, °F
A	58	78.5 to 507.2	0.1	100	75
B	3	90 to 125	0.1	100	75
	4	360 to 490	0.1	60 to 100	40
C	6	105	0.1	30 to 100	75
	24	400	0.1	30 to 100	40
D	12	88.5	0.1 to 0.18	100	75
E	10	93.5 to 128.5	0.1	100	75

After Deacon (Ref 6).

TABLE 3. NUMBER OF TEST SPECIMENS ASSIGNED TO COMPOUND-LOADING TEST SERIES

Test Series	Load History	Applied Percentage of Stress Level			No. of Specimens
		128.5 psi	113.5 psi	98.5 psi	
F	Two-level, increasing-sequence	Variable		Variable	24
	Two-level, decreasing-sequence	Variable		Variable	25
G	Two-level, repeated-block	5	95		4
		10	90		4
		25	75		4
		50	50		4
		5		95	4
		10		90	4
		25		75	4
		50		50	4
			5	95	4
			10	90	4
			25	75	4
			50	50	4
H	Three-level, repeated-block	10	30	60	6
		25	50	25	6
		60	30	10	6
I	Three-level, pseudo-random	10	30	60	6
		25	50	25	6
		60	30	10	6

After Deacon (Ref 6).

TABLE 4. LABORATORY TEST RESULTS

Asphalt Cement

Test	Test Result
Specific gravity	1.020
Penetration	
77°F, 100 g, 5 sec. (0.1 mm)	92
39.2°F, 200 g, 60 sec. (0.1 mm)	28
Penetration ratio	30.4
Flash point p.m.c.t. (°F)	465
Viscosity Saybolt Furol, 275°F (sec.)	164.5
Solubility in CCl_4 (%)	99.85
Softening point ring and ball (°F)	117

Aggregate Gradation*

Sieve Size	Percentage Passing	California Specifications
1/2-in.	100	100
3/8-in.	97.5	95-100
No. 4	74	65-85
No. 8	54	50-70
No. 16	40	
No. 30	29	28-40
No. 50	19.5	
No. 100	14.5	
No. 200	9	7-14

*aggregate continuous uniform gradation

After Deacon (Ref 6).

TABLE 5. SUMMARY OF COMPOUND-LOADING TECHNIQUES FOR PREDICTING MEAN FRACTURE LIFE

Technique No.	Type of Mean Predicted	Equation
1	Root-mean-square	$Y_1 = \left[1/\sum_i p_i/Z_1^i\right]^{\frac{1}{2}}$
2	Arithmetic mean	$Y_2 = \left[1/\sum_i p_i/(Z_2^i)^2\right]^{\frac{1}{2}}$
3	Arithmetic mean	$Y_2 = 1/\sum_i (p_i/Z_2^i)$
4	Arithmetic mean	$Y_2 = Z_2^k/\sum_i p_i (S^k/S^i)^b$
5	Arithmetic mean	$Y_2 = Z_2^1/\sum_i p_i (S^i/S^1)^r$
6	Arithmetic mean	$Y_2 = (Z_2^{max})^B/(Z_2^{min})^{B-1}$
7	Arithmetic mean	$Y_2 = Z_2^k\left[\prod_i (S^i/S^k)^{bp_i}\right]$
8	Geometric mean	$Y_3 = \text{antilog}\left[Z_3^k + \sum_i p_i \log (S^i/S^k)^{b'}\right]$
9	Harmonic mean	$Y_4 = \left[\sum_i p_i Z_4^i\right]^{-1}$

subscripts

1 = average squared fracture life

2 = average fracture life

3 = logarithm of fracture life

4 = reciprocal of fracture life

variables

Y = predicted means

Z = simple-loading mean

S = stress-level

p = applied percentage of a load condition or preset probabilities

b', B, r = constants (Ref 6)

superscripts

i = load-condition

k = load-condition which may or may not be the same as the i condition

b = slope of the log N_f-log S diagram in simple loading, where S indicates stress

After Deacon (Ref 6).

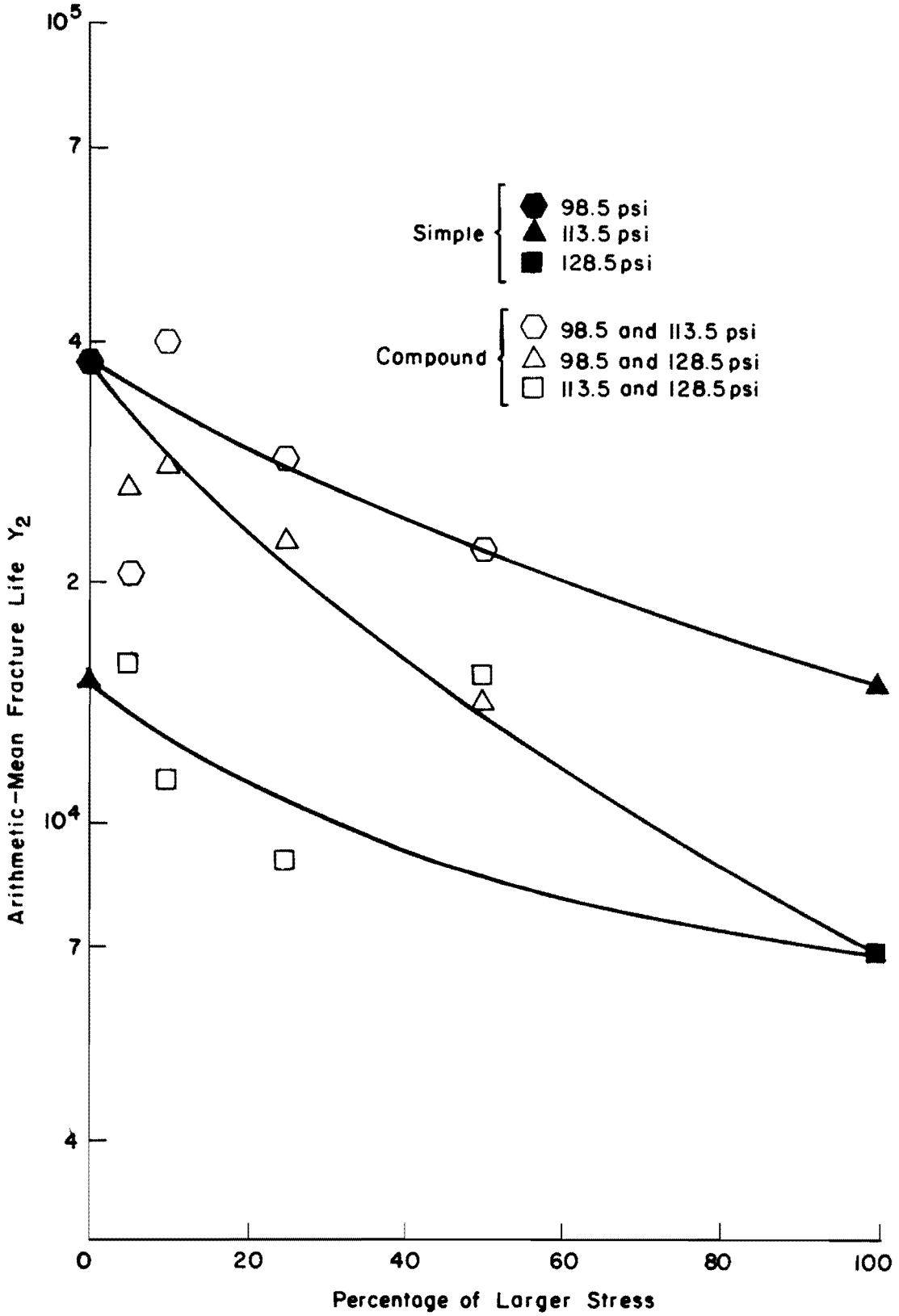

Fig 5. Experimental arithmetic-mean fracture lives Y_2: two-level, repeated-block loading (Ref 6).

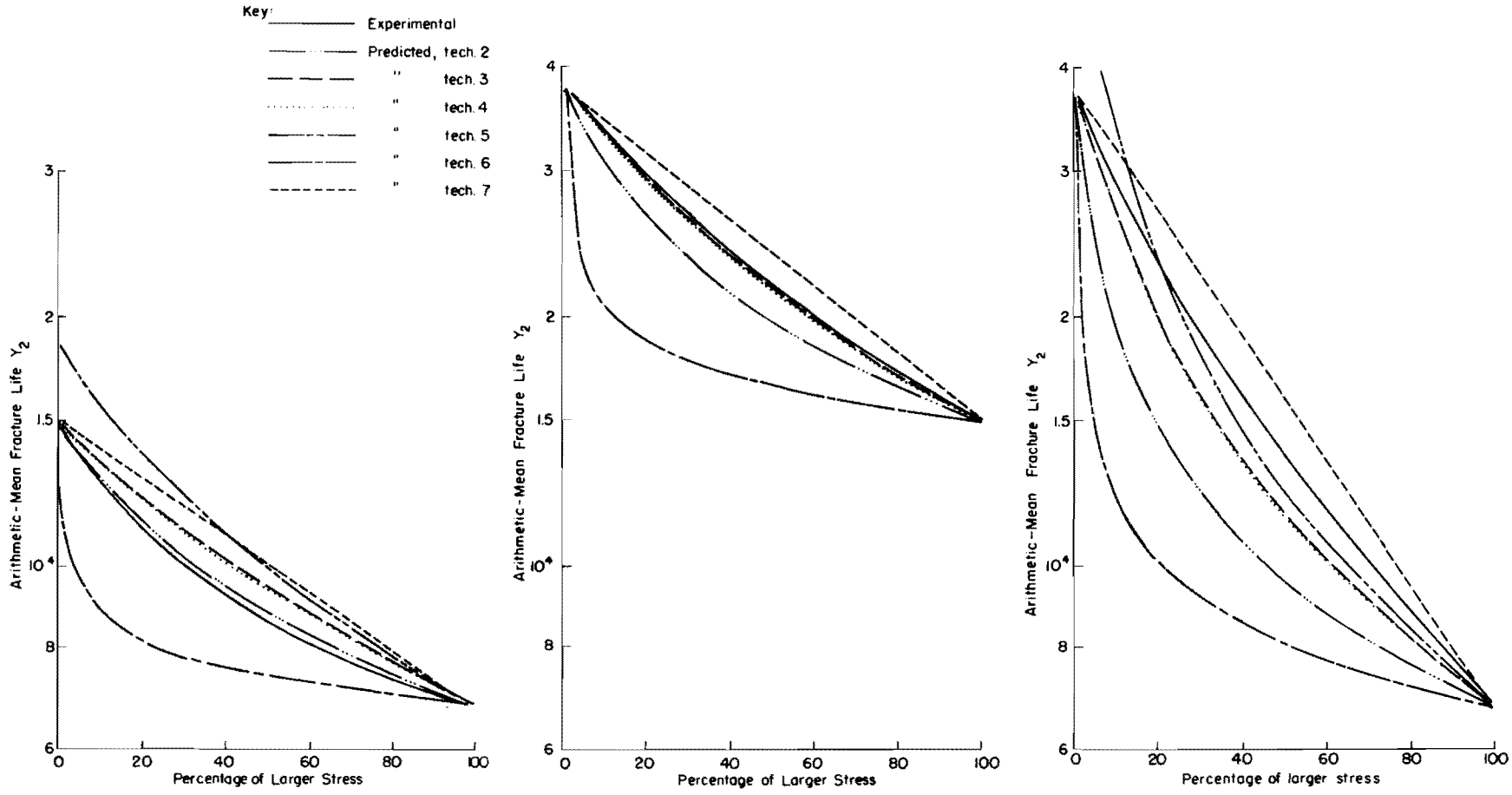

(a) 113.5 and 128.5 psi. (b) 98.5 and 113.5 psi. (c) 98.5 and 128.5 psi.

Fig 6. Experimental and predicted arithmetic-mean fracture lives Y_2: two-level, repeated-block loading (Ref 6).

from data in Tables 6 through 8. To choose the best predictive hypothesis Deacon calculated the deviation of the predicted mean fracture life from the measured mean fracture life for each technique (Table 5) and for each testing condition (Table 3), using the equation

$$\text{Deviation} = \frac{\text{Predicted Y - Measured Y}}{\text{Measured Y}} \tag{8}$$

The technique having the smallest average squared deviation was taken as the best technique. Table 9 gives the rank of predictive-accuracy based on all tests as determined by Eq 8. Deacon concluded that a modification of Miner's Hypothesis, technique 4, was superior in predictive accuracy.

Using two-level, increasing and decreasing-sequence tests, it was found that the order and magnitude of stress application were important (Figs 7 and 8). It was also found that the standard deviation of fracture life tends to increase as the stress level is decreased for simple-loading conditions.

McElvaney's Investigation

The most recent investigation concerning the compound-loading behavior of bituminous mixtures was completed by McElvaney in December of 1972 (Ref 7). The purpose of McElvaney's investigation was to study the fatigue response of laboratory prepared specimens of an asphalt basecourse mix to compound-loading and to determine the predictive accuracy of Miner's Hypothesis for a given set of conditions. McElvaney employed a technique developed by Wood (Ref 23) to evaluate Miner's Hypothesis which accounts for the probablistic nature of fatigue data.

Three types of constant-stress compound-loading tests were performed in addition to the simple-loading tests: (1) sequence tests, (2) repeated-block tests, and (3) temperature sequence tests at a constant stress level. The bituminous mixture investigated was a gap-graded, rolled asphalt base course. The mixture consisted of 60 percent coarse aggregate, 34 percent sand, and 6 percent (40-50 pen) bitumen.

The testing apparatus, schematically depicted in Fig 9, consisted of a rotating cantilevered beam. Temperature was maintained at the desired level during the test by a controlled-temperature water bath. Load was applied to the test specimen by a loading wire attached to the loading head. The specimen was rotated about a vertical axis at 1000 RPM under a constant-load perpen-

TABLE 6. COMPARISON OF MEAN FRACTURE LIVES - RANDOM VS REPEATED-BLOCK LOADING

Test[a]	Random		Repeated-Block	
	Mean Fracture Life	Mean Initial Stiffness Modulus, 1,000 psi	Mean Fracture Life	Mean Initial Stiffness Modulus, 1,000 psi
A	26,500	263	15,800	245
B	13,500	250	9,600	241
C	8,600	237	11,200	258

[a]Approximate applied percentages:
Test A: 10% of 128.5 psi, 30% of 113.5 psi, 60% of 98.5 psi;
Test B: 25% of 128.5 psi, 50% of 113.5 psi, 25% of 98.5 psi; and
Test C: 60% of 128.5 psi, 30% of 113.5 psi, 10% of 98.5 psi.

After Deacon (Ref 6).

TABLE 7. COMPARISON OF VARIABILITY OF FRACTURE LIFE - RANDOM VS REPEATED-BLOCK LOADING

Test[a]	Random		Repeated-Block	
	Std. Dev. of Fracture Life	Coeff. of Variation, %	Std. Dev. of Fracture Life	Coeff. of Variation, %
A	17,600	66	10,700	68
B	8,300	62	4.100	43
C	6,200	72	5,800	52

[a]Approximate applied percentages:
Test A: 10% of 128.5 psi, 30% of 113.5 psi, 60% of 98.5 psi;
Test B: 25% of 128.5 psi, 50% of 113.5 psi, 25% of 98.5 psi; and
Test C: 60% of 128.5 psi, 30% of 113.5 psi, 10% of 98.5 psi.

After Deacon (Ref 6).

TABLE 8. DATA FROM RANDOM TESTS

Fracture Life	Pre-Set Probability of Application, %			Actual Applied Percentage of Stress Level		
	128.5 psi	113.5 psi	98.5 psi	128.5 psi	113.5 psi	98.5 psi
51,592	10	30	60	10.0	30.1	59.9
45,449	10	30	60	10.4	29.6	60.0
16.491	10	30	60	10.1	29.6	60.3
22,200	10	30	60	10.3	28.8	60.9
14,432	10	30	60	—	—	—
9,074	10	30	60	—	—	—
27,348	25	50	25	24.1	51.6	24.3
12,313	25	50	25	24.8	50.9	24.3
17,658	25	50	25	24.5	49.4	26.1
3,684	25	50	25	24.3	52.6	23.0
7,937	25	50	25	25.2	51.2	23.6
11,897	25	50	25	24.2	49.4	26.4
20,829	60	30	10	60.2	29.6	10.2
3,032	60	30	10	59.6	31.3	9.1
6,700	60	30	10	60.5	29.9	9.6
7,423	60	30	10	60.2	29.8	10.0
6,139	60	30	10	59.5	30.6	9.9
7,691	60	30	10	60.5	30.1	9.4

After Deacon (Ref 6).

TABLE 9. PREDICTIVE-ACCURACY COMPARISON FOR MEAN FRACTURE LIFE, TWO-LEVEL TESTS

Rank	Technique	Average Squared Deviation, percent squared	Average Deviation, percent
1	4	780	0.9
2	3	831	1.6
3	7	916	13.1
4	9	947	16.0
5	2	962	-37.5
6	10	983	11.3
7	5	1083	13.1
8	8	1074	20.0
9	1	1259	-12.0
10	6	1646	-35.5

After Deacon (Ref 6).

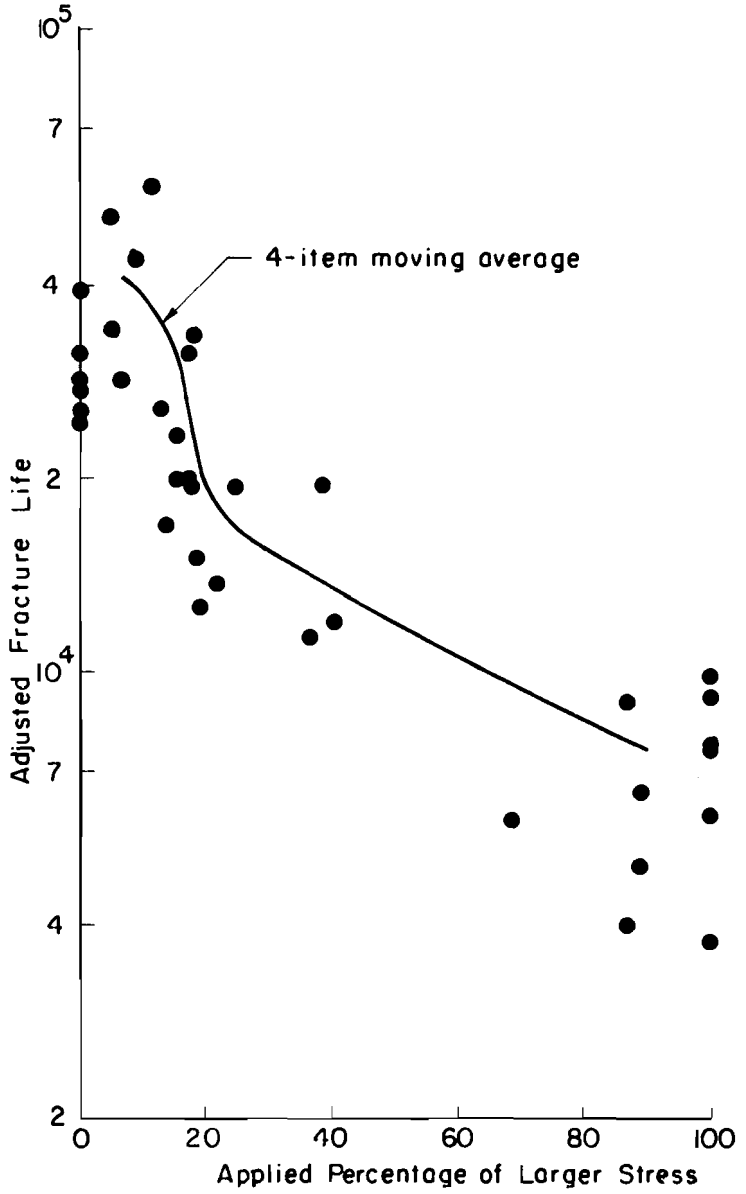

Fig 7. Two-level, decreasing-sequence tests, adjusted fracture lives (Ref 6).

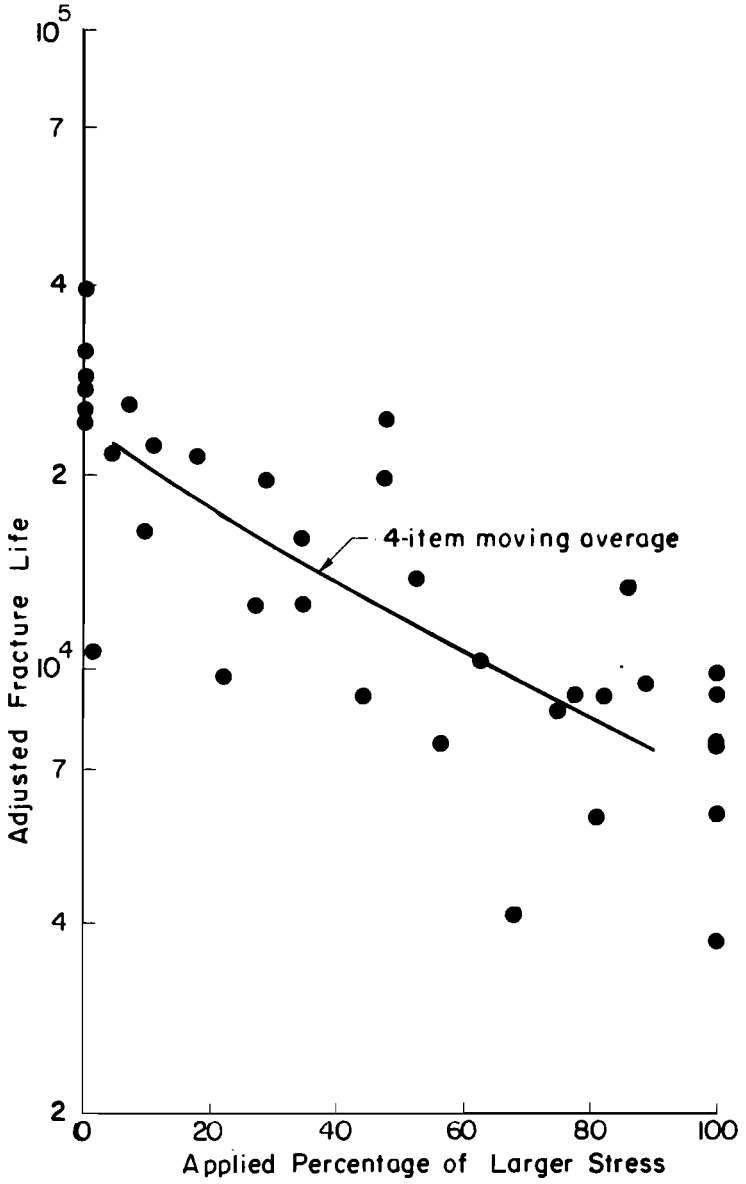

Fig 8. Two-level increasing-sequence tests, adjusted fracture lives (Ref 6).

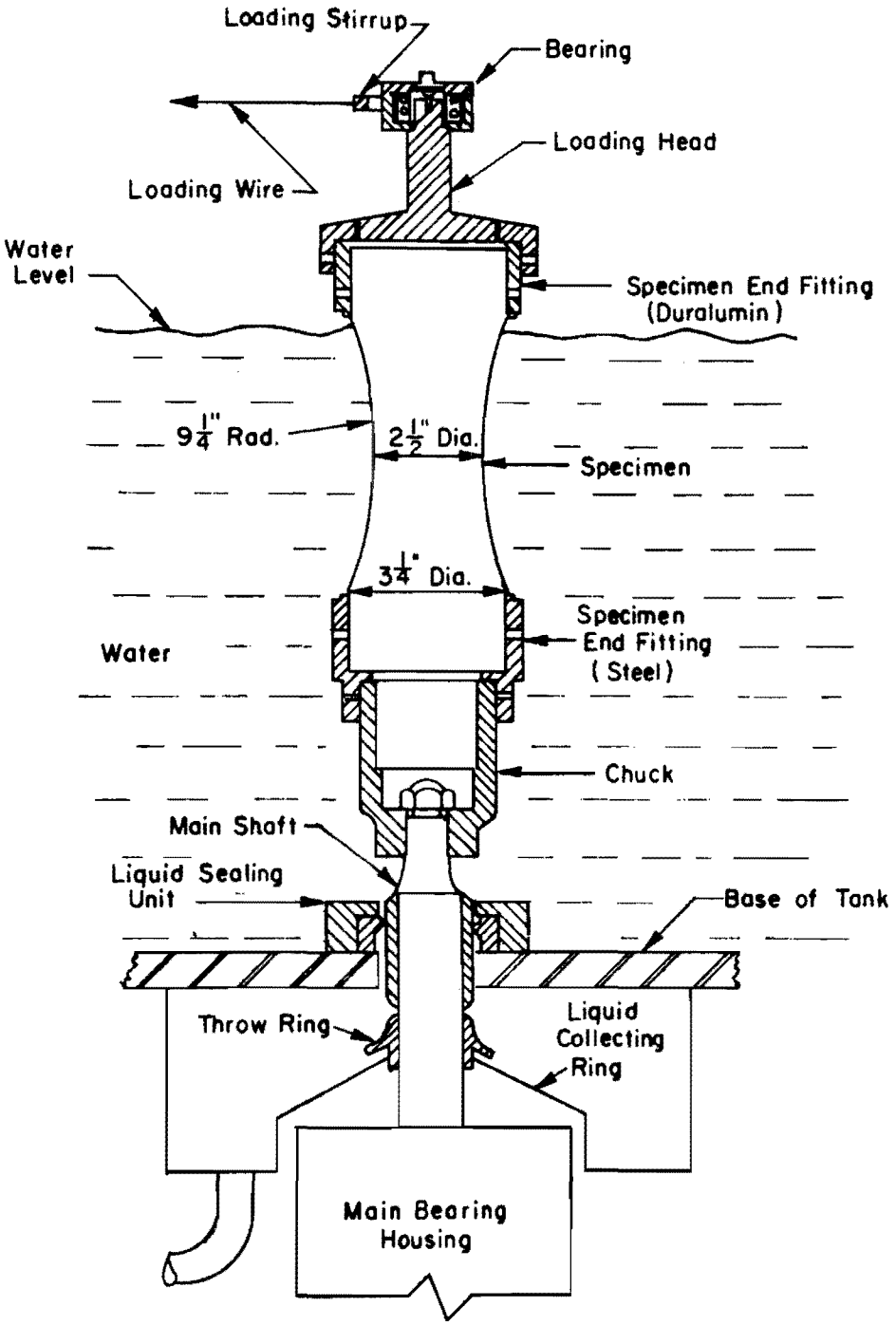

Fig 9. Detail of rotating cantilever specimen and loading system (Ref 7).

dicular to the axis of rotation, producing a maximum bending stress at the necked-down portion of the specimen.

McElvaney presented the results of his investigation in two ways: (1) the conventional stress versus fatigue life diagram (Fig 10), and (2) fatigue life versus probability of failure relationships assuming a log-normal distribution of fatigue life (Fig 11). A log-normal distribution of fatigue life was considered to be justified, based on experimental evidence reported by Pell and Taylor (Ref 24), the results of which show the validity of the log-normal distribution assumption in terms of a frequency histogram and a probability plot on normal probability paper (Fig 12). The knowledge of such a distribution allows the maximum amount of information to be extracted from a given set of fatigue data. The probability of failure, as used by McElvaney, was that proposed by Wiebull (Ref 25):

$$P(m) = \frac{m}{n+1} \tag{9}$$

where

m = the order number of fatigue life,
n = the number of observations,
P(m) = the probability of failure dependent on m and n.

The accuracy of a plot of $\log N_f$ versus the probability of failure $P(m)$ is entirely dependent on the number of observations. To obtain a linear relationship between fatigue life and the probability of failure, the reduced normal variates (the projection of the cumulative normal frequency curve on a linear axis) were used as recommended by Wiebull (Ref 25). The assumption of a log-normal distribution was tested using 24 specimens at a stress level of 140 pounds per square inch by establishing control curves at probabilities of failure of 15 and 85 percent (Fig 11). An additional feature of the $\log N_f$ vs $P(m)$ plots is that the slopes of the lines of best-fit give an indication of the scatter in the data, with a perfectly horizontal line indicating no scatter.

Table 10 contains data for the constant temperature two-level sequence tests. Columns 4, 5, and 6 represent the cumulative cycles ratio determined at prestress levels of 10, 30, and 50 percent (prestress level is the number

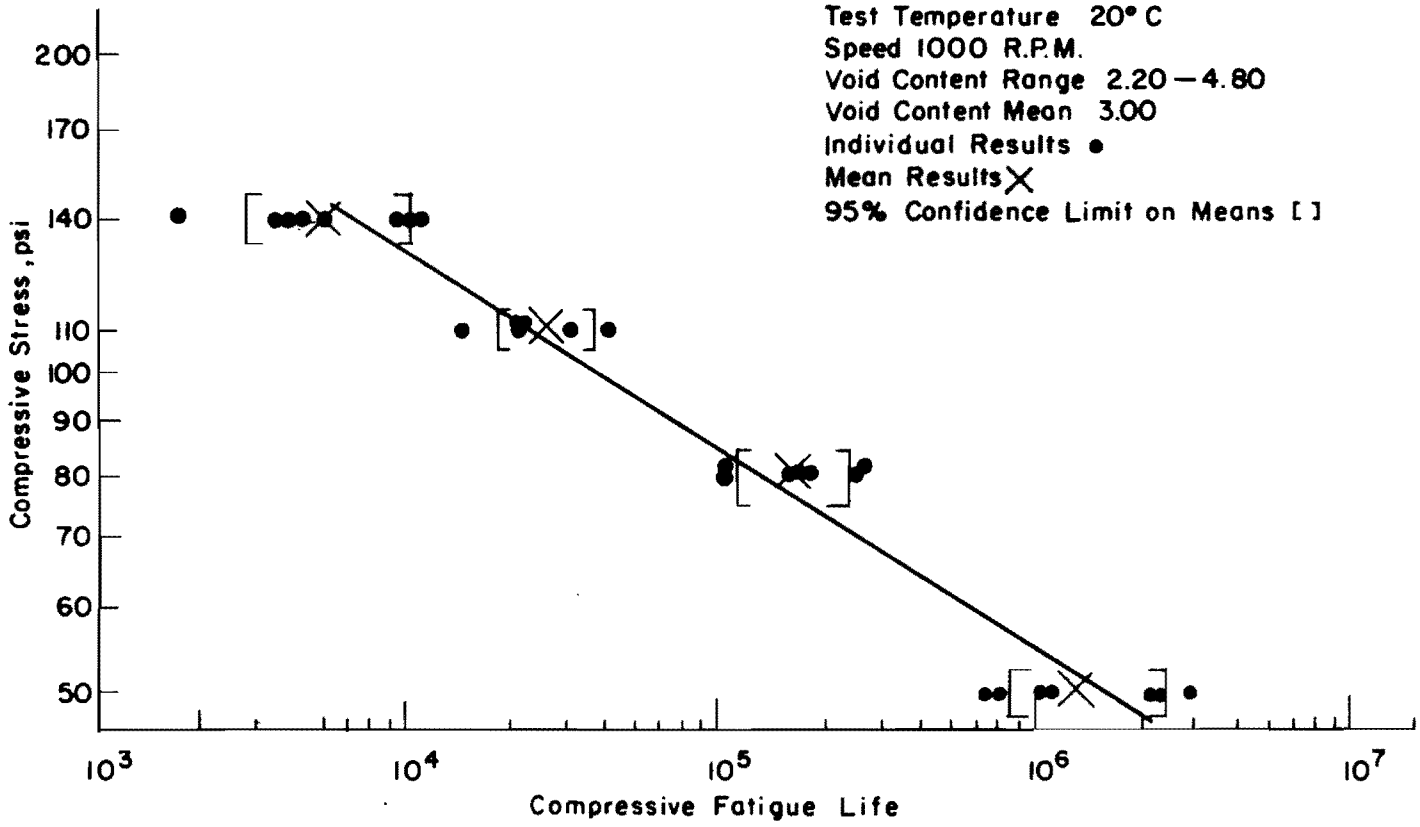

Fig 10. Compressive stress versus cycles to failure (Ref 7).

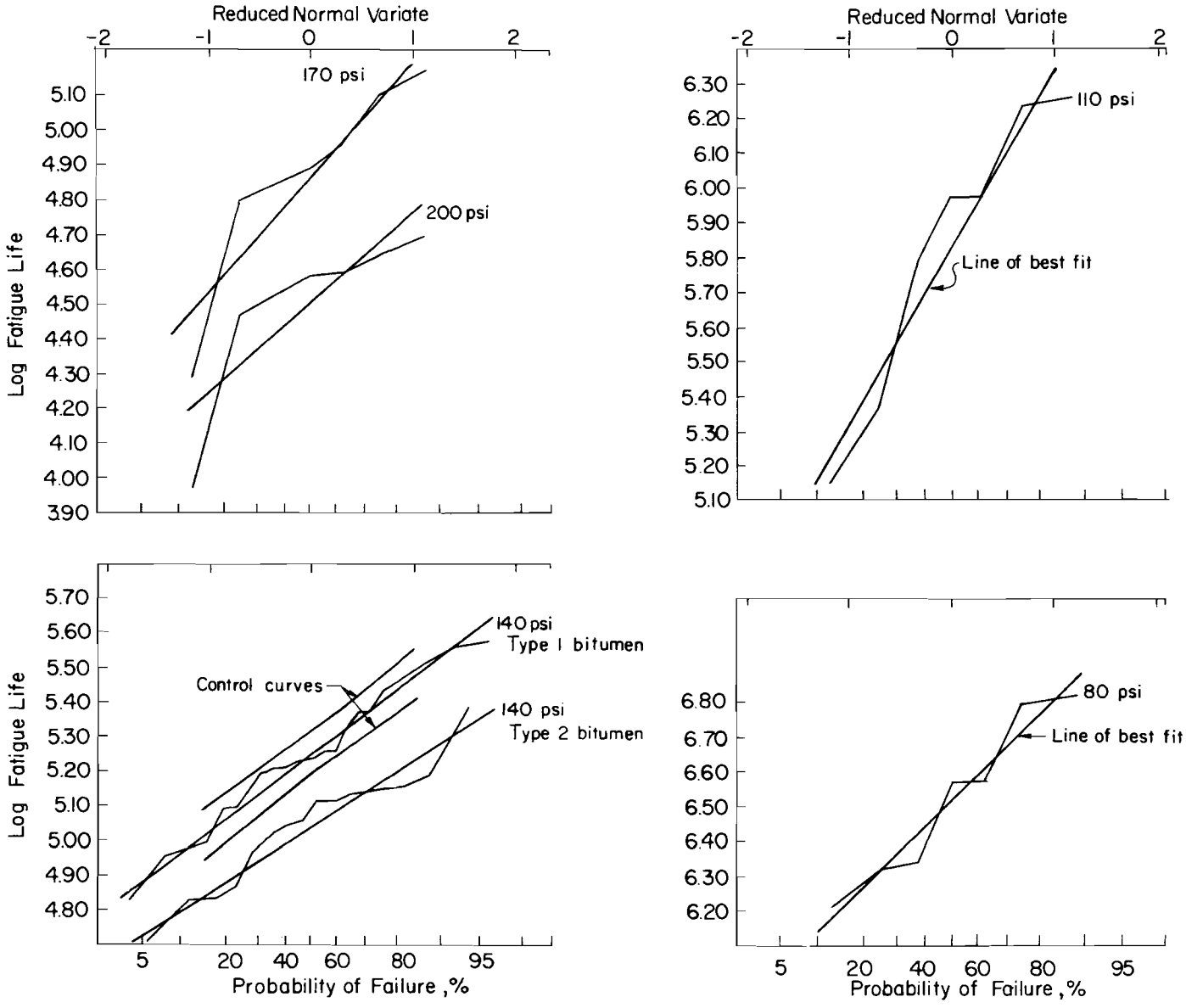

Fig 11. Probability of failure versus log service life: constant stress amplitude test data (Ref 7).

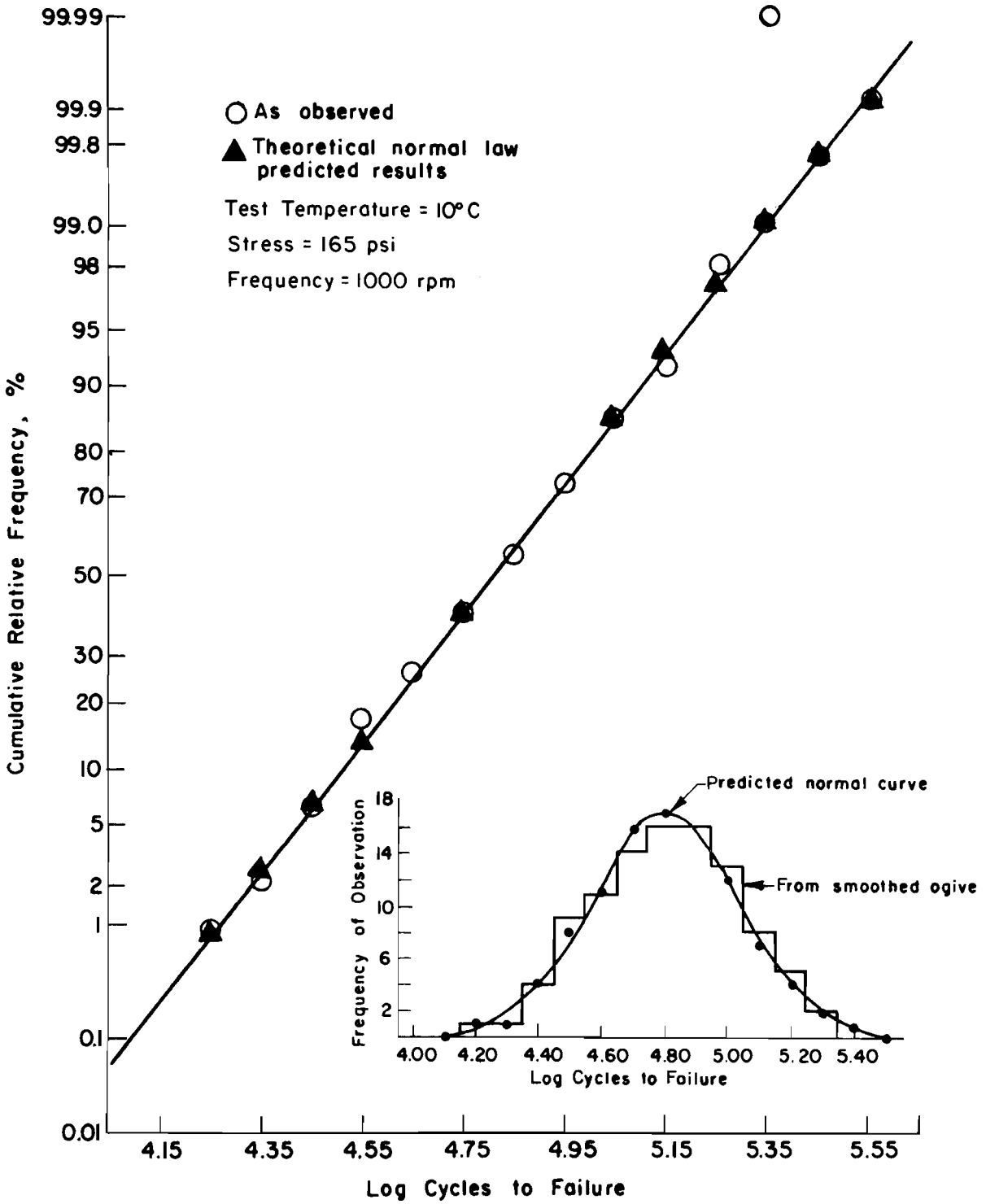

Fig 12. Normal probability plot of fatigue results with frequency histogram (Ref 24).

TABLE 10. TEST SERIES SEQUENCE FATIGUE RESULTS, TWO-LEVEL TESTS

Sequence Number	Prestress Value psi	Test Stress Value psi	$\Sigma(n/N)$ Prestress Level 10%	30%	50%
1(b)	200	140	—	0.99	1.04
2(f)	80	140	—	—	0.97
3(k)	170	140	1.21	0.64	1.07
4(n)	110	140	1.05	0.91	1.39
2(h)	80	200	—	—	1.23
4(p)	170	200	1.06	0.83	1.27
1(a)	200	170	1.07	0.79	1.20
2(g)	80	170	—	—	1.17
4(o)	140	170	0.78	0.55	1.15
1(c)	200	110	—	1.16	1.49
2(e)	80	110	1.46	1.28	2.00
3(l)	140	110	1.12	1.19	1.74
1(d)	200	80	—	1.63	1.60
3(m)	110	80	1.03	1.02	2.36

After McElvaney (Ref 7).

of cycles applied to a specimen at the first load condition). Each cycles ratio in the indicated prestress columns represents an average of seven specimens tested at the appropriate prestress level. The range in magnitude of the cumulative cycles ratio for the 30 percent prestress level was 0.55 to 1.63, which indicates the variability in predicted fracture life under compound loading using Miner's Hypothesis for two-level stress tests.

In an effort to determine the effects of stress history on fatigue life of the bituminous mixture the relationships (Fig 13) between fatigue life and test-stress level were established (test-stress level is the measured number of cycles to failure less the prestress level). The test-stress period N_t was shown to be the dominant influence for prestress levels of up to 50 percent for high levels of test stress, but low levels of test stress were noted to cause an increase in the cumulative cycles ratio.

SUMMARY OF CURRENT STATUS OF KNOWLEDGE

The compound-loading investigations of Deacon (Ref 6) and McElvaney (Ref 7) are valuable contributions to the increased understanding of the fatigue response of bituminous mixtures under controlled laboratory conditions. Deacon's intitial investigation yielded information concerning the fatigue behavior of bituminous mixtures for both simple and compound-loading. A major contribution by Deacon was his investigation of the various methods of predicting mean fatigue life. McElvaney considered the dispersion of fatigue life data in predicting compound-loading behavior utilizing Wood's method of probability (Ref 23). It is clear that the fatigue response of asphalt material is stochastic (Refs 4, 6 through 10, 12, 13, and 24 through 31). The major points of Deacon's and McElvaney's work are summarized in this section.

Deacon's Investigation

A linear relationship between the logarithm of the mean fatigue (fracture) life and the logarithm of stress (or strain) was found for specimens tested in the controlled-stress mode under simple-loading conditions. The standard deviation of fracture life was found to decrease as the stress level increased, with some evidence to suggest a linear relationship on a full logarithmic plot; however, the nature of the repetitive loading apparatus used in the testing program was admitted to have a profound influence on the observed fatigue behavior. Further, a larger load duration (of constant rate) was

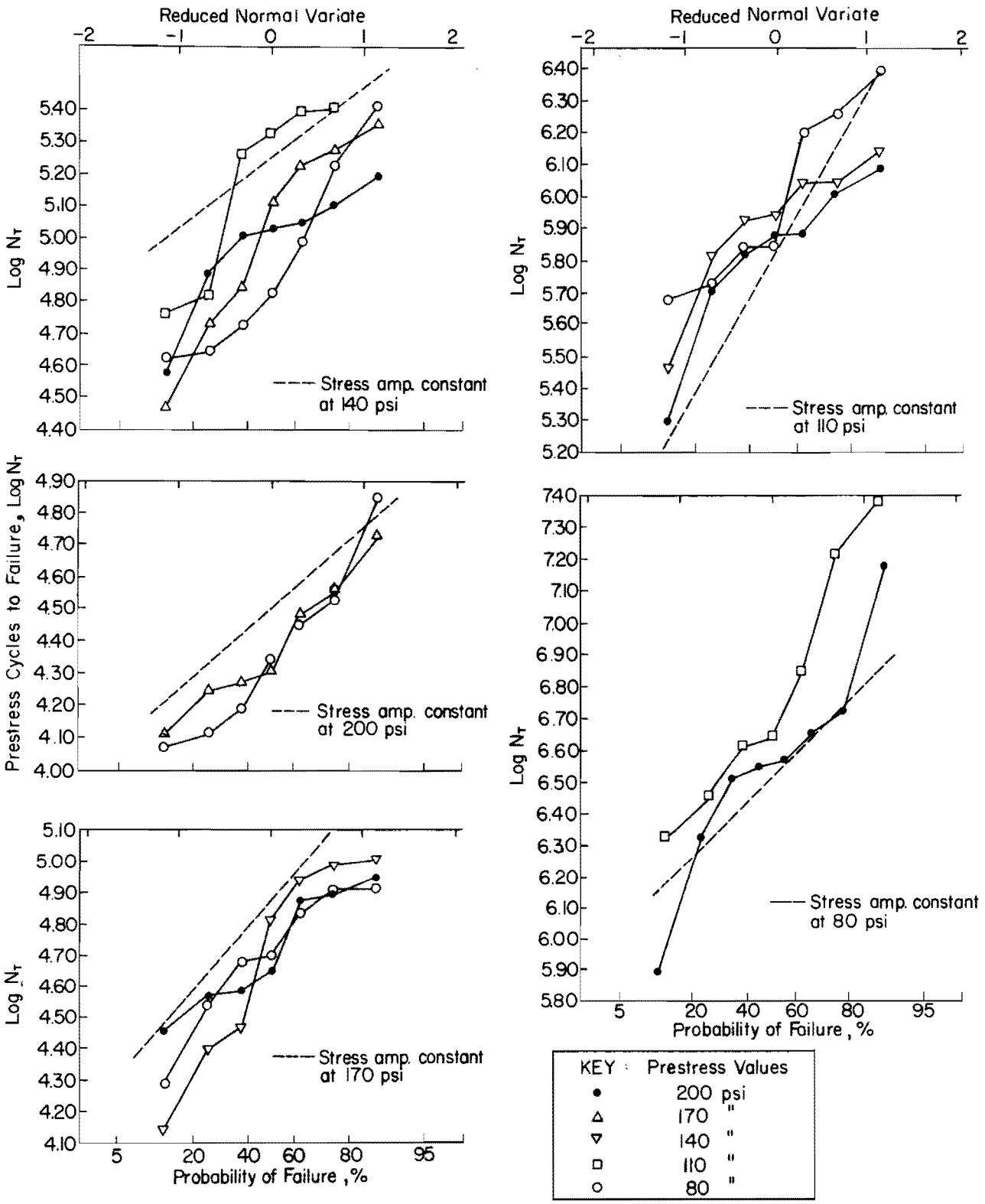

Fig 13. Probability of failure versus log test-stress level at 50 percent prestress level (Ref 7).

found to decrease the measured value of fracture life.

For two-level, decreasing-sequence tests, the mean fracture lives of specimens were greater than the corresponding tests of an increasing-sequence type for smaller applied percentages of the larger stress.

McElvaney's Investigation

McElvaney also found a linear relationship between the logarithm of applied stress and the logarithmic mean number of cycles to failure. Further, he found the fatigue life of a bituminous material was sensitive to temperature changes, an increase in temperature causing a decrease in fatigue life. He could not substantiate a linear relationship between the logarithm of the standard deviation of fatigue life and the logarithm of the applied stress level.

The influence of inherent material variability on the cumulative cycles ratio was found to be significant at all stress levels, particularly at low test-stress values. Finally, a linear damage rule such as Miner's Hypothesis was suggested as adequate for predicting fatigue life under compound-loading conditions.

General

The work of Deacon (Ref 6) and McElvaney (Ref 7) has provided considerable impetus for verifying damage rules, in particular, a linear damage hypothesis for bituminous materials. Deacon's conclusion with respect to testing apparatus introducing significant levels of variability into measured fatigue life values coupled with McElvaney's comment concerning the influence of inherent material variability on the cumulative cycles ratio has suggested the need for a method of testing bituminous materials which minimizes these factors. Such a testing method has been developed at the Center for Highway Research, The University of Texas at Austin. The method is the repeated-load indirect tensile test developed during the course of this investigation from a strong base provided by the previous work using static, or slowly applied, loads (Refs 4 and 32 through 35). The development of this test began in 1968, with the preliminary repeated-load investigation completed in 1971.

A natural step in the verification of the linear damage hypothesis is to include all major testing methods so as to determine the applicability of damage hypotheses to the different test methods. The three major testing methods for bituminous materials are

(1) the repeated-flexure test,

(2) the rotating cantilever test, and

(3) the repeated-load indirect tensile test,

which were developed at the University of California, Berkeley; the University of Nottingham, England; and The Center for Highway Research, The University of Texas at Austin, respectively. The repeated-flexure test and the rotating cantilever test have been verified for linear damage rules, such as Miner's Hypothesis. The purpose of this investigation was to provide such verification for the repeated-load indirect tensile test.

CHAPTER 3. EXPERIMENTAL PROGRAM

The principal objective of this investigation was to determine the applicability of Miner's Hypothesis (Ref 5) to the fatigue behavior of a bituminous mixture subjected to repeated tensile stresses using the repeated-load indirect tensile test. This chapter describes the procedures employed and the equipment utilized in the acquisition of simple and compound-loading data.

EXPERIMENTAL PROGRAM

There were essentially three distinct phases to the investigation of Miner's Hypothesis:

(1) the establishment of a reference logarithm stress versus logarithm fatigue life diagram, using simple-loading fatigue tests;

(2) the acquisition of compound-loading data, using fatigue tests in which the stress level was changed during the course of the test; and

(3) the analysis and evaluation of the resultant information.

This section will describe the materials investigated, the testing method, and the development of an experiment design.

Materials

Two different aggregate types were used, a crushed limestone and a smooth river gravel. Each aggregate was separated and recombined to produce the gradation curve shown in Fig 14. The aggregate-asphalt mixtures were prepared with an asphalt content of 7 percent by total weight of mixture using an AC-10 (88 pen) asphalt cement from the Cosden Refinery, Big Spring, Texas. Table 11 gives the pertinent physical information on this asphalt cement. The aggregates and the asphalt cement were combined by a mechanical mixer at a temperature of 300°F for three minutes (Appendix A). The mixture was then compacted, using the Texas Gyratory-Shear Compactor (Ref 36), into specimens nominally 2 inches in height and 4 inches in diameter. The specimens were

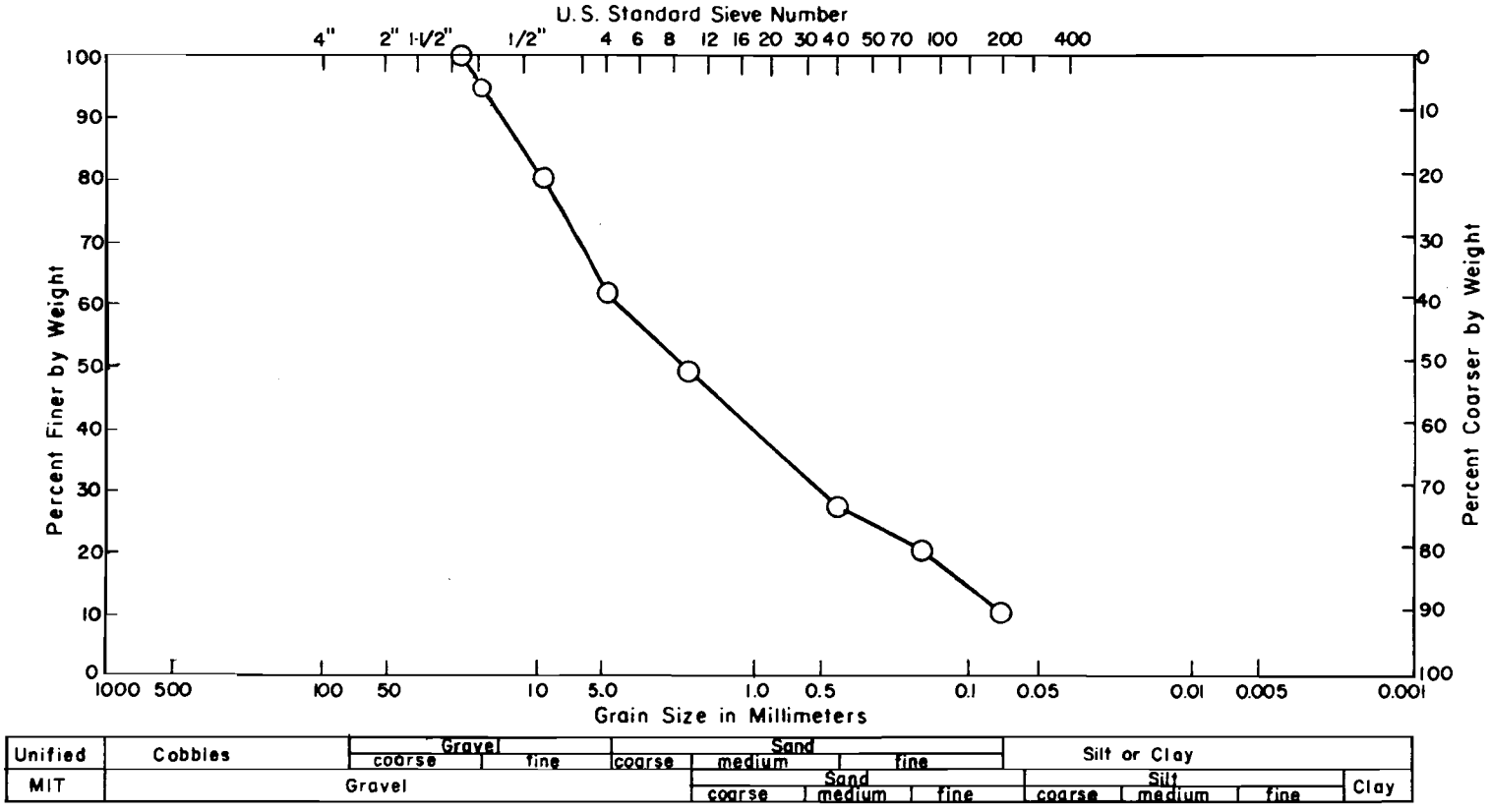

Fig 14. Gradation curve.

TABLE 11. PERTINENT PHYSICAL INFORMATION ON COSDEN ASPHALT CEMENT AC-10

Water, %	Nil
Viscosity at 275°F, stokes	2.45
Vixcosity at 140°F, stokes	940
Solubility in CCl_4, %	—
Flash point C.O.C., °F	585
Ductility, 77°F, 5 cm/min., cm	—
Pen at 77°F, 100 g, 5 sec.	88
Tests on residues from thin film oven test:	
Viscosity at 140°F, stokes	2052
Ductility at 77°F, 5 cm/min., cms.	141+
Res. pen 77°F	52
Original specific gravity 77°F	1.031

then cured for two days at room temperature, 75°F. The simple-fatigue response of a similar mixture was previously reported by Moore and Kennedy (Ref 4).

Testing Method

The dynamic indirect tensile test involves a right circular cylindrical specimen with repetitive compressive loads acting along two opposite generators (Fig 15). A rigid stainless steel loading strip which is curved at the interface with the specimen and has a 2-inch radius was employed to transmit the compressive load to the specimen in order to maintain a constant loading area. This loading configuration develops a relatively uniform tensile stress perpendicular to the directions of loading and along the vertical diametral plane through the center of the loading strips. Hondros (Ref 37) analyzed a circular specimen subjected to loading through a narrow strip, assuming that the body forces were negligible, and developed equations for the resulting stresses. Based on these equations, the tensile stress in the center of the specimen is given by

$$\sigma_t = \frac{2P}{\pi ah} (\text{SIN } 2\alpha - \frac{a}{2R}) \qquad (10)$$

where

σ_t = indirect tensile stress, in psi;
P = total vertical load applied to the specimen, in pounds;
a = width of the loading strip, in inches;
h = height of the specimen at the beginning of the test, in inches;
2α = angle at the center of the specimen subtended by the width of the loading strip, in radians;
R = the radius of the specimen, in inches.

The equations for stress, strain, modulus, and Poisson's ratio have been reported by Kennedy et al (Refs 4, 32, and 34).

The basic testing apparatus was a closed-loop electrohydraulically actuated loading system operating in the controlled-stress mode. The actual loading device was a commercially available die set, modified to accept the loading strips in the upper and lower platens (Fig 16). The data were recorded using

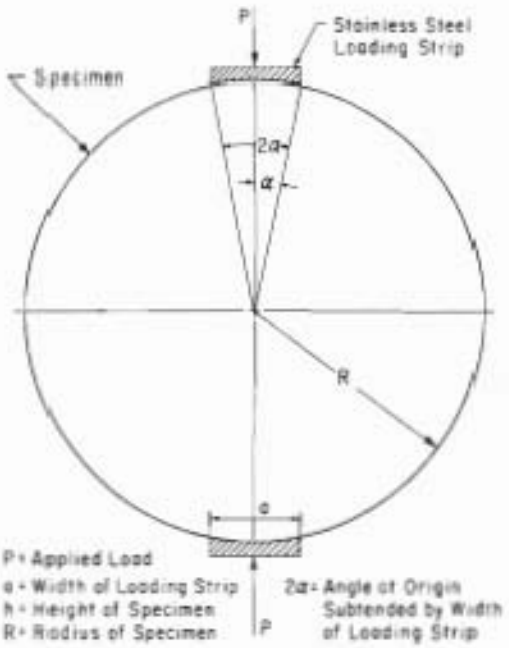

Fig 15. Schematic of the dynamic indirect tensile test.

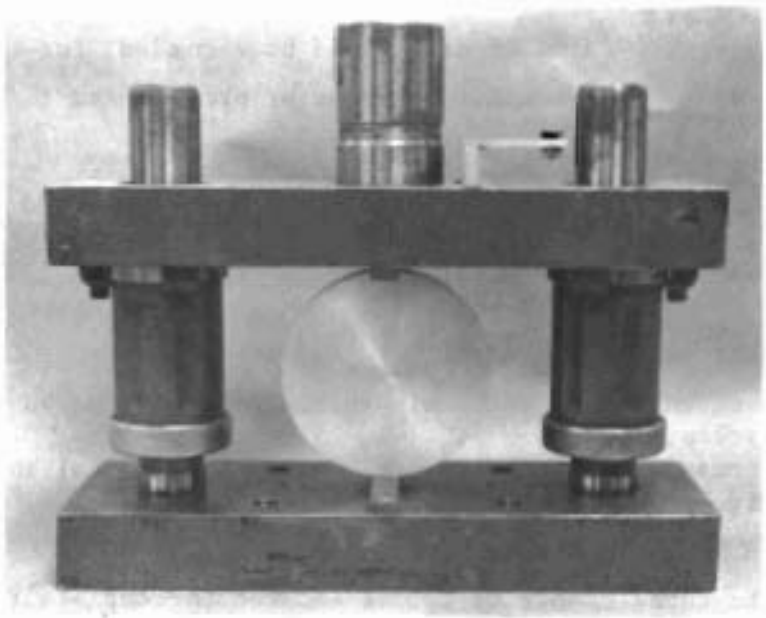

Fig 16. Loading device.

a two-channel strip chart recorder, an analog-digital recorder, and a digital voltmenter.

The load pulse was controlled with a strain-gage type load cell and was varied in magnitude pulsewise by combining the signals from two frequency generators. A frequency of 1 Hz was selected, with 0.4 second pulse time and 0.6 second rest time. Figure 17 shows a representative load pulse with the associated vertical and horizontal deformations. The data which were recorded with the analog-digital device can be reproduced graphically to give the plots shown in Fig 18 if the individual cyclic deformation is superimposed on the permanent deformation information. Although both individual cyclic information and total or permanent deformation data were recorded for all specimens tested, only the permanent deformation data were considered in this investigation.

Experiment Design

Insofar as possible the simple and compound-loading tests were scheduled at sufficient intervals of time to approximate a random experiment design. Failure was defined as the complete rupture of the specimen (Fig 18) in accordance with the convention used by others (Refs 4, 6 through 9, 24, and 26 through 31). It was decided that for a preliminary investigation such as this one all possible forms of data would be recorded; for each specimen the following records were made for purposes of present and future analysis:

(1) a specimen record sheet, including
    (a) aggregate and the gradation used,
    (b) weight measurements to determine the bulk specific gravity,
    (c) specimen dimensions, and
    (d) stress levels(s) and the sequence of application and duration;
(2) deformations, including
    (a) horizontal and vertical dynamic deformations on individual cycles, and
    (b) permanent deformation for both the horizontal and vertical directions; and
(3) fatigue life, including
    (a) the total number of cycles endured to complete fracture for both the simple and compound-loading specimens, and
    (b) the number of cycles of stress application at the two levels of stress chosen for the compound-loading tests.

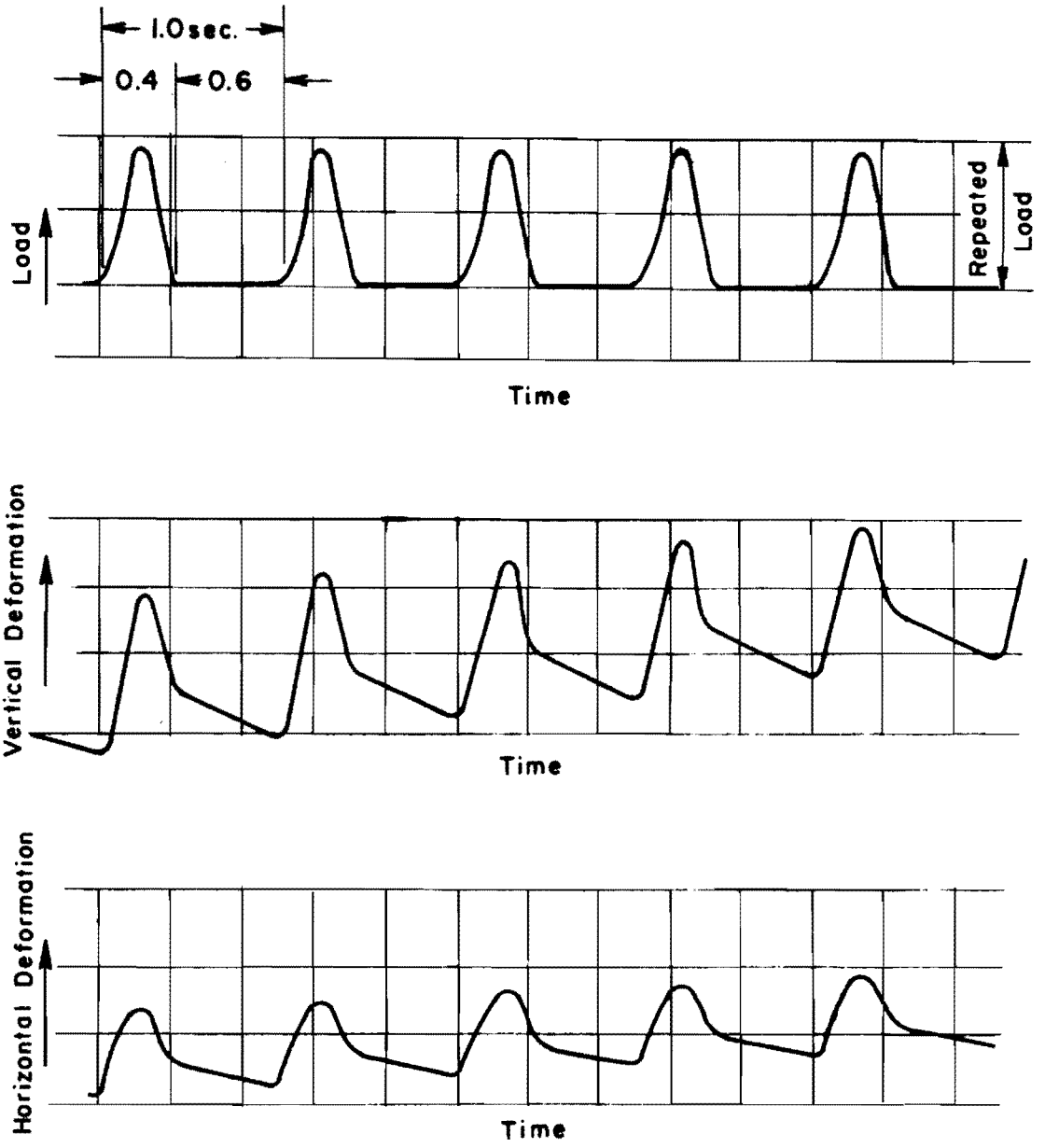

Fig 17. Load pulse and associated deformation data for the repeated-load indirect tensile test.

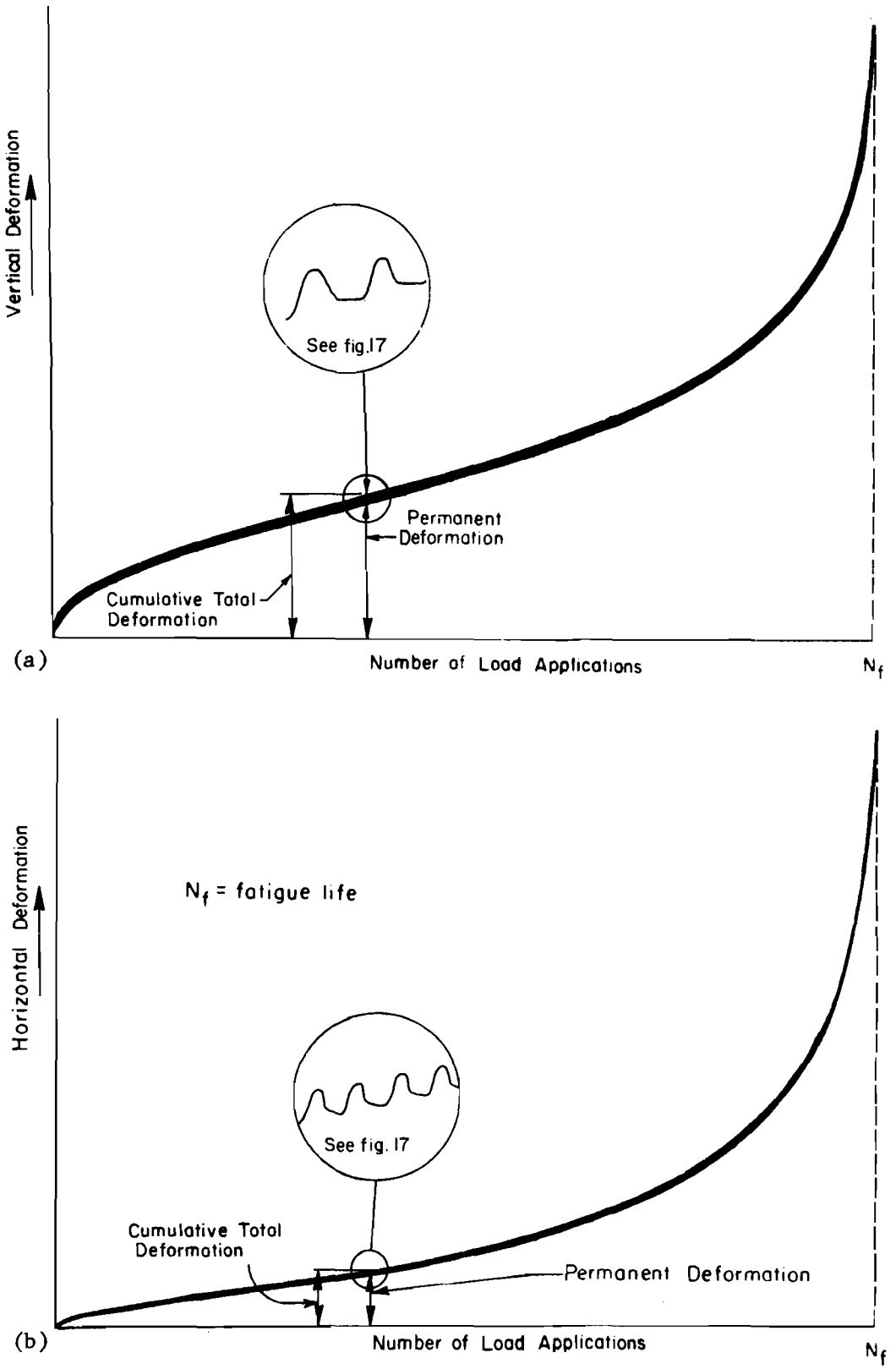

Fig 18. Relationships between number of load applications and vertical and horizontal deformation for the repeated-load indirect tensile test.

From this information it was possible to reconstruct the time-deformation history of each specimen and show the relationships for fatigue life prediction.

In view of the work reported by Deacon (Ref 6) and McElvaney (Ref 7), the investigation was limited to compound-loading tests involving only two stress levels. One series was performed for an increasing-stress sequence and one for a decreasing-stress sequence. A two-way block design was utilized, varying the first stress level (prestress level) from 16 psi to 40 psi. A total of 60 limestone and 60 gravel specimens were tested, with 5 specimens assigned to each stress sequence. The experiment design is schematically depicted in Fig 19.

As previously noted, a log-normal distribution of fatigue life at a given stress level was assumed, based on the evidence presented by Pell and Taylor (Ref 24) for the simple-loading fatigue data. Due to the small numbers of specimens tested in simple-loading at a given stress level and in compound-loading for a given stress sequence, only simple statistical estimates were feasible; however, the probabilistic techniques used by McElvaney were employed.

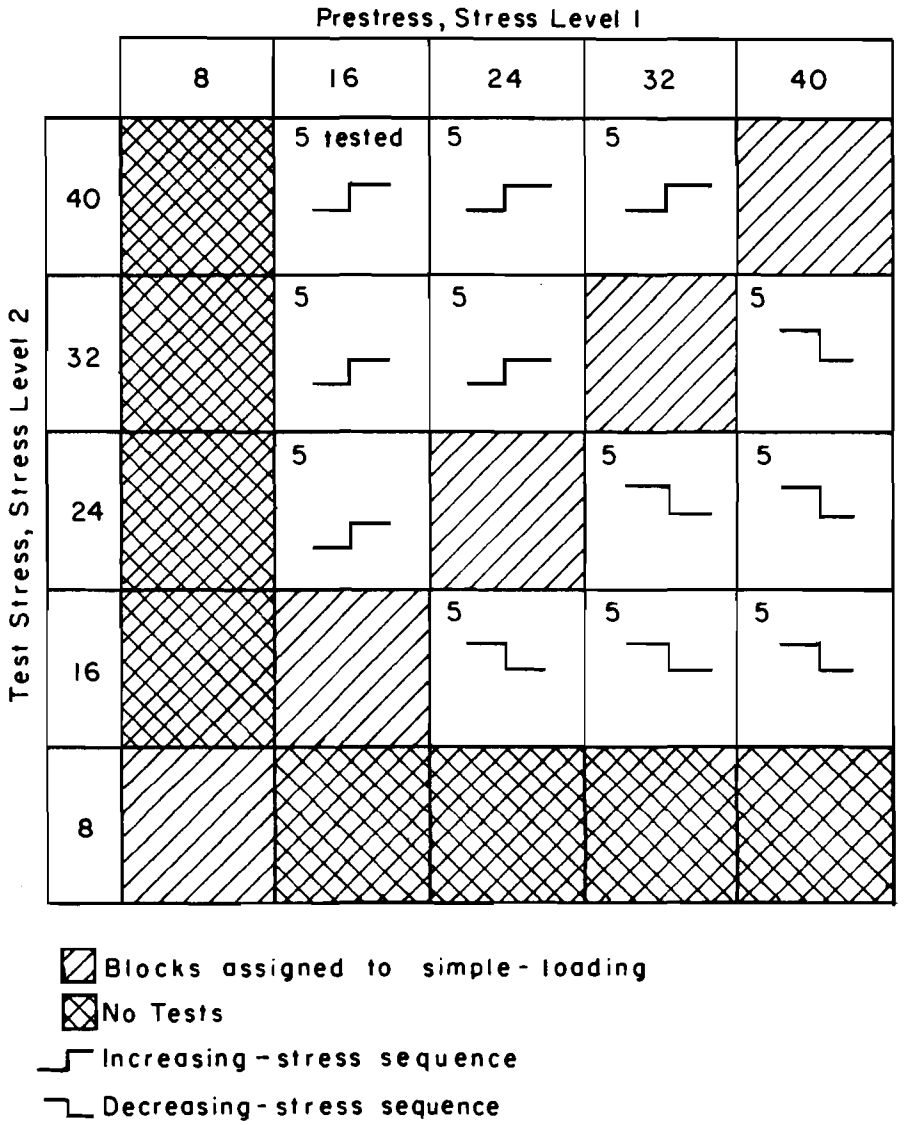

Fig 19. Experimental block design.

CHAPTER 4. EXPERIMENTAL RESULTS

The fatigue life of bituminous mixtures subjected to fatigue loading exhibits a significant amount of variation for a given load condition, and this variation is indicative of the statistical nature of fatigue behavior. For meaningful results to be derived from fatigue data the analytical techniques employed must give some measure of the distribution and dispersion of fatigue life for a set of environmental and load variables.

This chapter summarizes and discusses the results of the simple and compound-loading fatigue tests performed using the dynamic indirect tensile test. Data are presented for both fatigue life and time-deformation characteristics of the bituminous mixture investigated.

SIMPLE-LOADING CONSTANT-STRESS AMPLITUDE TESTS

The simple-loading phase of this investigation consisted of two test series which differed only in aggregate type. The mixtures consisted of either a rounded gravel or a crushed limestone and 7 percent asphalt (AC-10) and were selected from a factorial experiment designed to determine the fatigue characterisitcs of asphalt mixtures over a range of asphalt contents (Ref 38). Tables B-1 and B-2 (Appendix B) summarize the pertiment physical data for the 31 specimens of the limestone mixture and the 41 specimens of the gravel mixture, respectively. The simple-loading tests were performed in the controlled-stress mode over a stress range of 8 psi to 40 psi in increments of 8 psi.

To establish simple analytical techniques which can be applied to fatigue data, the form of the fatigue life distribution for a given load condition should be known; however, due to the limit on the number of specimens which could be tested at each stress level, the log-normal distribution was assumed for the analysis, on the basis of previously cited experimental evidence (Ref 24).

Fatigue-Life Estimates

The data for the limestone test series are presented in Table 12 and for the gravel test series in Table 13. The simple-fatigue life N_f is defined as the number of load cycles required to produce complete fracture of the specimen for a given stress level (Fig 18). The statistical parameters were calculated in accordance with procedures outlined in the ASTM STP 91-A (Ref 1) and are "point estimates" or single-valued parameters representing the fatigue life for a given stress level. From the mean and standard deviations, it is possible to calculate confidence intervals, which with a certain level of confidence contain the true mean of the population. The 95 percent confidence interval was calculated for each stress level and is contained in Tables C-1 through C-10 in Appendix C. These intervals will contain the true mean 95 times out of 100.

Figures 20 and 21 illustrate the log N_f versus log σ_t relationships for the limestone and gravel mixtures with the 95 percent confidence intervals superimposed on the diagram. Least-squares linear regression was performed on both test series with the resultant equations and simple-correlation coefficients indicated on the appropriate figure. The regression coefficients indicate only minor differences in slope and intercept values. In addition, Fig 22 indicates that aggregate type had a small effect on the fatigue life for this mixture gradation. The regression line is associated with different probability of failure estimates at each stress level, whereas the mean fatigue life value is associated with a probability of failure of 50 percent. The disadvantage in both techniques is the lack of information provided with regard to the dispersion of fatigue life at a given load condition. Figure 23 illustrates this point. It can be seen from the figure that the dispersion of fatigue life at particular stress levels is quite different for the limestone and gravel aggregate types. Thus a technique whereby the probability of failure can be related to the dispersion of fatigue life at a given stress level is necessary.

Probability Estimates of Fatigue Life

Due to the scatter in fatigue life at a given stress level, no unique relationship exists between applied stress and fatigue life. To adequately describe such a relationship requires consideration of the probability of

TABLE 12. LIMESTONE FAILURE CONDITION DATA FOR SIMPLE LOADING

7% AC-10
Medium Gradation
Sinusoidal Pulse (0.6 sec. rest), 1 Hz

Temperature 75°F
Preload 20 lb

Tensile Stress, psi	Spec. No.	Date of Test	Fatigue Life N_f	Arith. Mean	Log Mean N_f	Standard Deviation S	Variance S^2
	280	11-7-73	178200				
	282	11-9-73	190800				
8	285	11-14-73	200700	219720	214536	52351	2.74×10^9
	286	11-16-73	206700				
	288	11-21-73	322200				
	396	2-27-74	6041				
	395	2-27-74	6400				
	456	5-9-74	6800				
16	558	7-18-74	7172	8332	8117	2110	4.45×10^6
	557	7-18-74	8441				
	556	7-18-74	8909				
	457	5-9-74	11093				
	458	5-8-74	11801				
	453	5-8-74	1405				
	455	5-8-74	1412				
24	382	2-14-74	1645	1643	1629	241	5.81×10^4
	454	5-8-74	1812				
	381	2-14-74	1942				
	451	5-8-74	488				
	452	5-8-74	512				
32	391	2-21-74	569	575	571	82	6.72×10^3
	450	5-8-74	612				
	318	12-12-73	695				
	386	2-21-74	273				
	387	2-21-74	287				
	389	2-21-74	315				
40	388	2-21-74	333	360	353	78	6.08×10^3
	728	9-11-74	350				
	730	9-11-74	358				
	110	9-24-73	475				
	729	9-11-74	490				

TABLE 13. GRAVEL FAILURE CONDITION DATA FOR SIMPLE LOADING

7% AC-10 Temperature 75°F
Medium Gradation Preload 20 lb
Sinusoidal Pulse (0.6 sec. rest), 1 Hz

Tensile Stress, psi	Spec. No.	Date of Test	Fatigue Life N_f	Arith. Mean	Log Mean N_f	Standard Deviation S	Variance S^2
	115	9-26-73	199560				
	117	9-28-73	270780				
8	119	10-1-73	329100	350232	329003	145062	2.10×10^{10}
	129	10-12-73	378000				
	123	10-5-73	573720				
	465	5-15-74	3307				
	407	4-19-74	3648				
	466	5-15-74	5245				
	467	5-15-74	6137				
16	339	12-19-73	6293	6309	5955	2412	5.82×10^{8}
	561	7-18-74	6496				
	559	7-18-74	6987				
	560	7-18-74	7865				
	338	12-19-73	10807				
	462	5-8-74	784				
	463	5-8-74	784				
	464	5-8-74	850				
	521	7-18-74	1286				
24	519	7-18-74	1317	1532	1375	802	6.43×10^{5}
	566	7-24-74	1532				
	520	7-18-74	1719				
	102	9-21-73	2500				
	107	9-21-73	3012				
	461	5-8-74	258				
	459	5-8-74	273				
	460	5-8-74	296				
	524	7-18-74	536				
32	523	7-18-74	548	563	503	311	9.70×10^{4}
	522	7-18-74	586				
	565	7-24-74	609				
	380	12-21-73	866				
	103	9-21-73	1095				
	2011	5-1-74	163				
	564	7-24-74	266				
	563	7-24-74	292				
	562	7-24-74	313				
40	106	9-21-73	500	496	429	322	1.04×10^{5}
	101	9-21-73	525				
	105	9-21-73	650				
	104	9-21-73	690				
	130	10-12-73	1065				

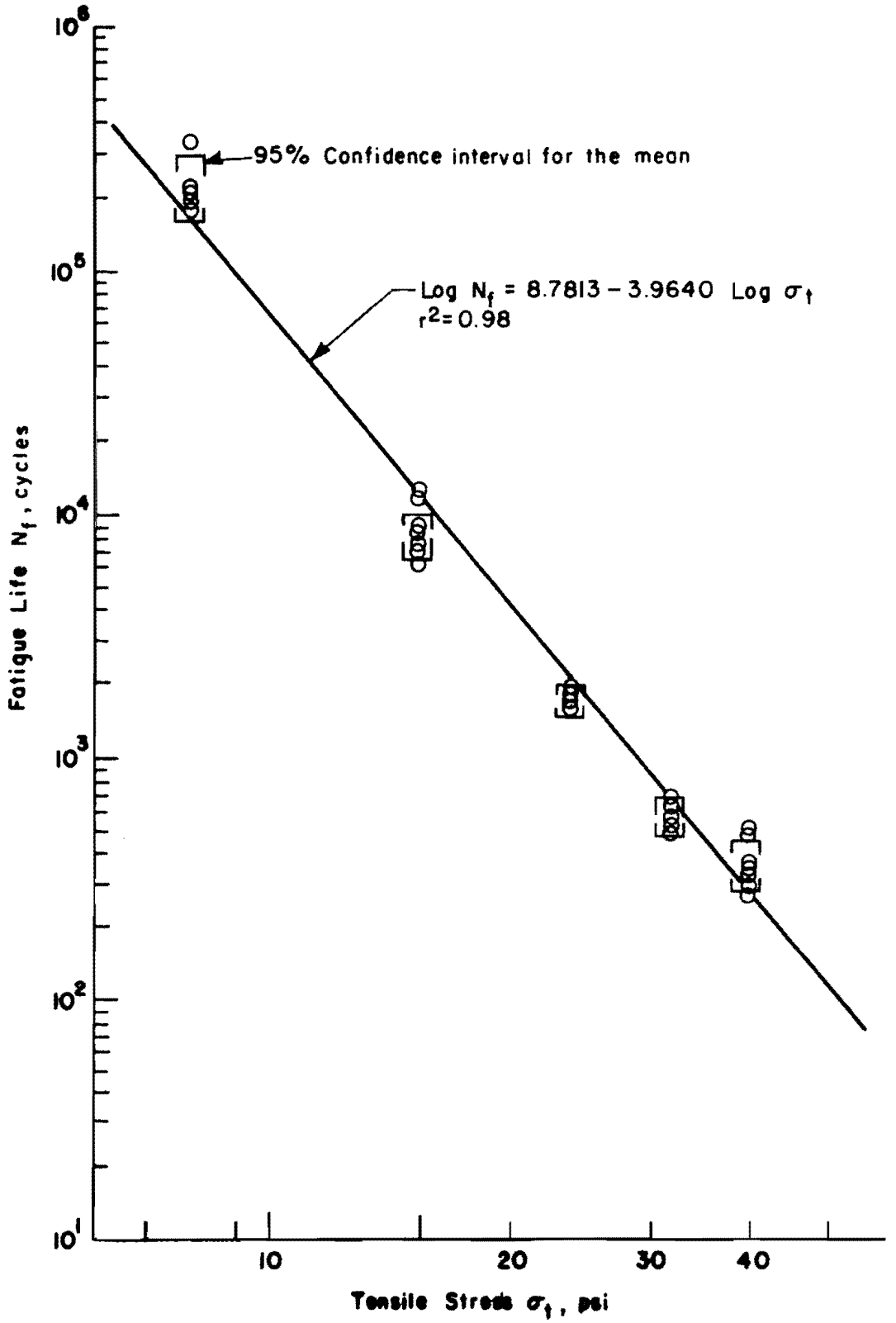

Fig 20. Fatigue life versus tensile stress: constant stress amplitude, limestone test series.

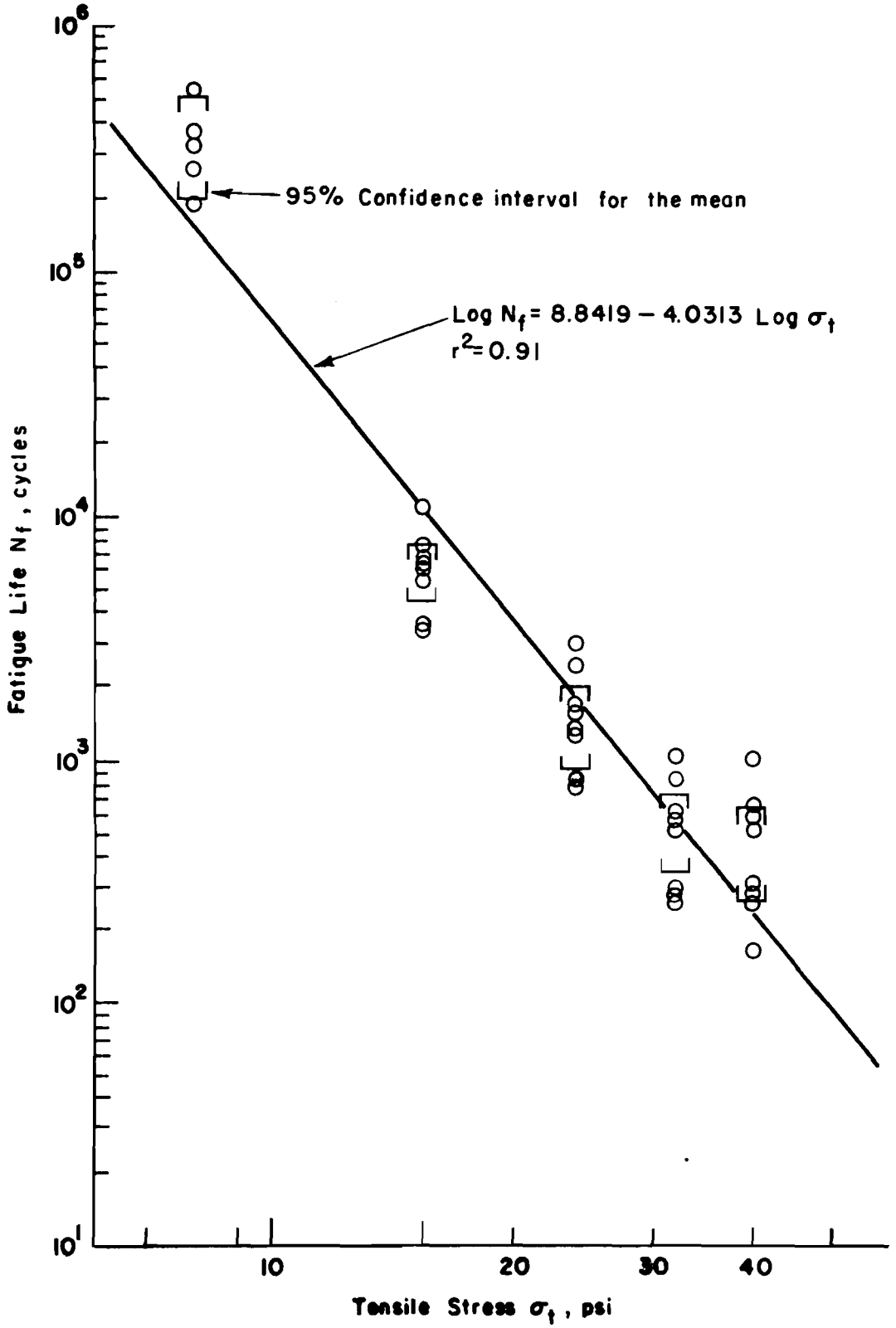

Fig 21. Fatigue life versus tensile stress: constant stress amplitude, gravel test series.

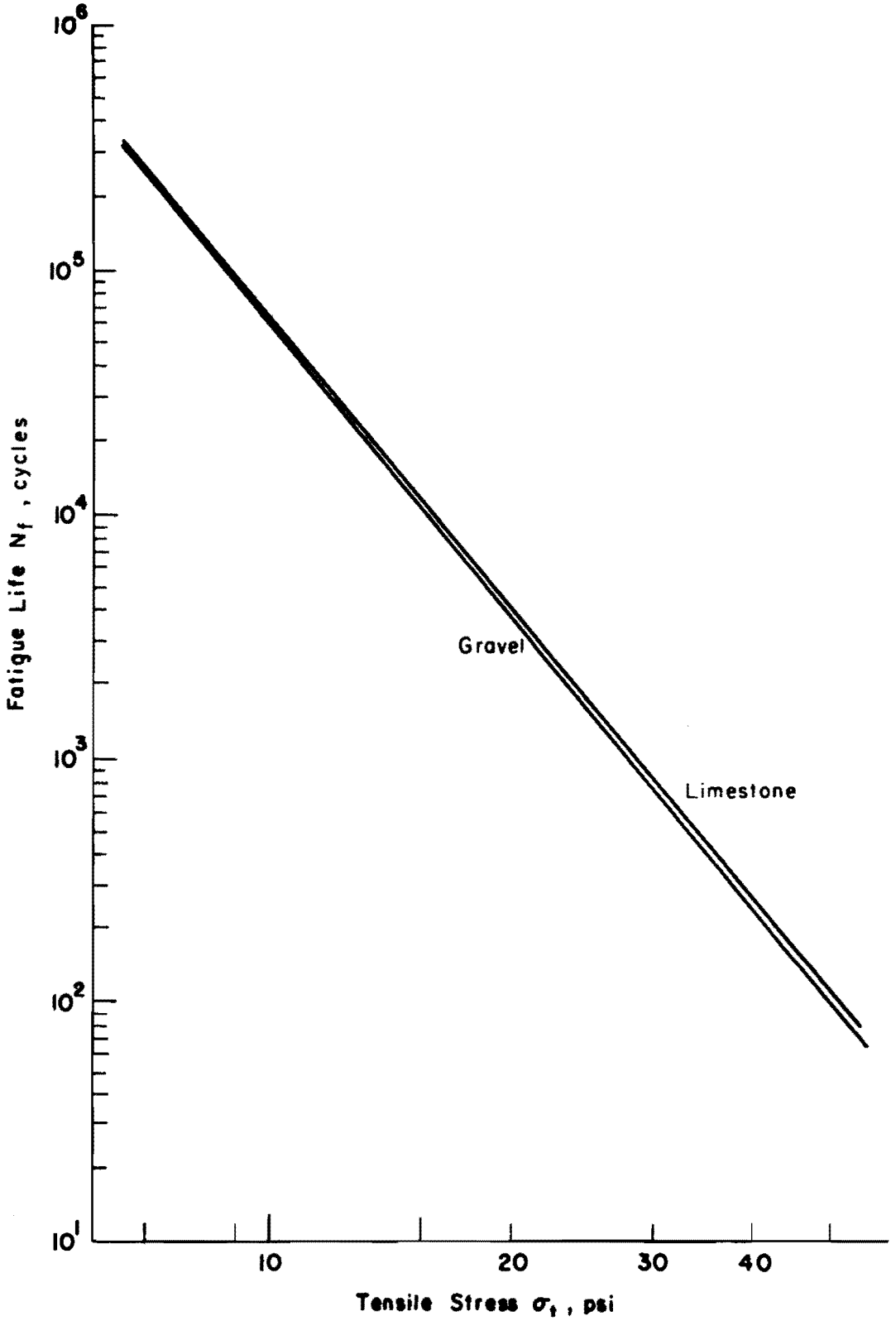

Fig 22. Comparison of regression lines for limestone and gravel test series.

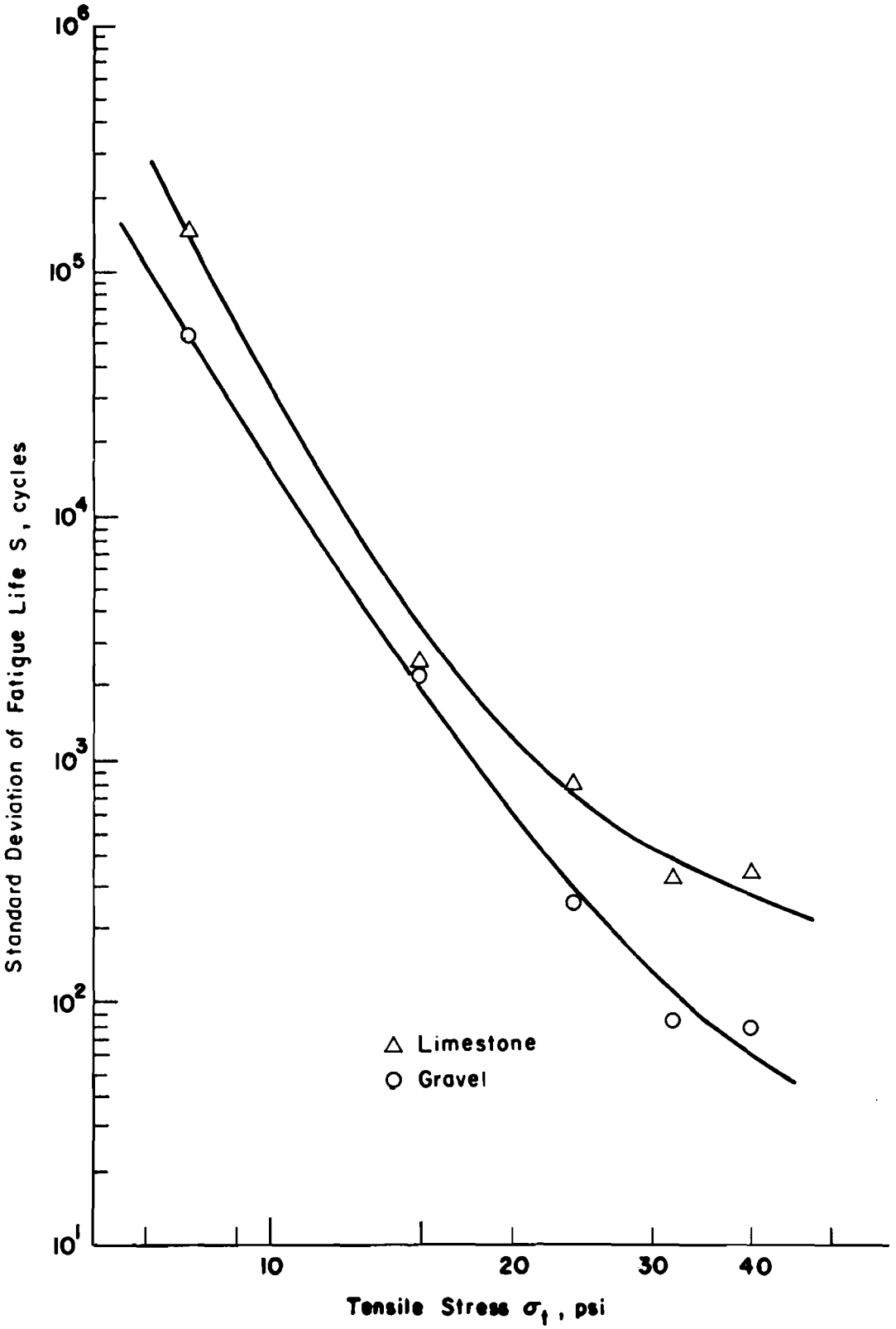

Fig 23. Standard deviation of fatigue life versus tensile stress.

failure P or survival. Using the three variables stress, fatigue life, and the probability of failure it is possible to construct curves of fatigue life versus stress for selected probability levels. The proper representation of the stress versus fatigue life relationship requires a knowledge of the variational characteristics and mean values of fatigue life at a given stress level. A curve fitted only to the mean or log-mean exhibits the same problems as the conventional regression line.

The construction of log N_f-P(m) functions at a given stress level was adopted for use in this investigation. In this investigation, techniques similar to those described by McElvaney (Ref 7) were adopted. The construction technique is as follows:

(1) Rank-order the sample values of fatigue life from least to greatest, assigning an order number m.

(2) Assign the appropriate probability of failure according to the equation

$$P(m) = \frac{m}{n+1} \tag{9}$$

(3) Determine the reduced normal variates X , i.e., the projection of the cumulative probability curve onto a linear axis corresponding to the appropriate level of probability (the reduced normal variates for the calculated probability levels are available in elementary statistical texts and mathematical handbooks).

(4) Plot the coordinate pairs (log N_f, X) on linear scales.

(5) Regress log N_f on X using the simple least-squares technique.

The simple-fatigue data have been reduced in this manner and are summarized in Appendix C. The log N_f-P(m) relationships are shown in Figs C-1 through C-10 (Appendix C). The regression equations for each stress level are given in Tables 14 and 15 for the limestone and gravel aggregate types, respectively. The median or 50 percent curve is defined immediately from the intercept value of these equations, and for an odd number of specimens the fitted median corresponds to the sample mean. An alternative and useful plot may be established by using these median values, which represent a probability of failure of 50 percent, to establish the conventional stress versus fatigue life diagram. Using the same probability of failure at each stress level it becomes obvious that the relationship is decidedly nonlinear (Fig 24), with this nonlinearity being masked by the sample scatter when the conventional regression line technique is used. Since the log N_f-X , or log N_f-P(m),

TABLE 14. REGRESSION COEFFICIENTS FOR CONSTANT STRESS, FAILURE CONDITION DATA FOR LIMESTONE

7% AC-10 — Temperature 75°F
Medium Gradation — Preload 20 lbs.
Sinusoidal Pulse (0.6 sec. rest time), 1 Hz

Tensile Stress, psi	Intercept A_0	Slope A_1	Predictor Equation* $\text{Log } N_f = A_0 + A_1 X$
8	5.3315	0.1176	$\text{Log } N_8 = 5.3315 + 0.1176X$
16	3.9086	0.1311	$\text{Log } N_{16} = 3.9086 + 0.1311X$
24	3.2120	0.0815	$\text{Log } N_{24} = 3.2120 + 0.0815X$
32	2.7563	0.0811	$\text{Log } N_{32} = 2.7563 + 0.0811X$
40	2.5475	0.1106	$\text{Log } N_{40} = 2.5475 + 0.1106X$

* X = reduced normal variate.

TABLE 15. REGRESSION COEFFICIENTS FOR CONSTANT STRESS, FAILURE CONDITION DATA FOR GRAVEL

7% AC-10 — Temperature 75°F
Medium Gradation — Preload 20 lbs.
Sinusoidal Pulse (0.6 sec. rest time), 1 Hz

Tensile Stress, psi	Intercept A_0	Slope A_1	Predictor Equation* $\text{Log } N_f = A_0 + A_1 X$
8	5.5172	0.2257	$\text{Log } N_8 = 5.5172 + 0.2257X$
16	3.7749	0.1880	$\text{Log } N_{16} = 3.7749 + 0.1880X$
24	3.1382	0.2515	$\text{Log } N_{24} = 3.1382 + 0.2515X$
32	2.7018	0.2604	$\text{Log } N_{32} = 2.7018 + 0.2604X$
40	2.6329	0.3034	$\text{Log } N_{40} = 2.6329 + 0.3034X$

* X = reduced normal variate.

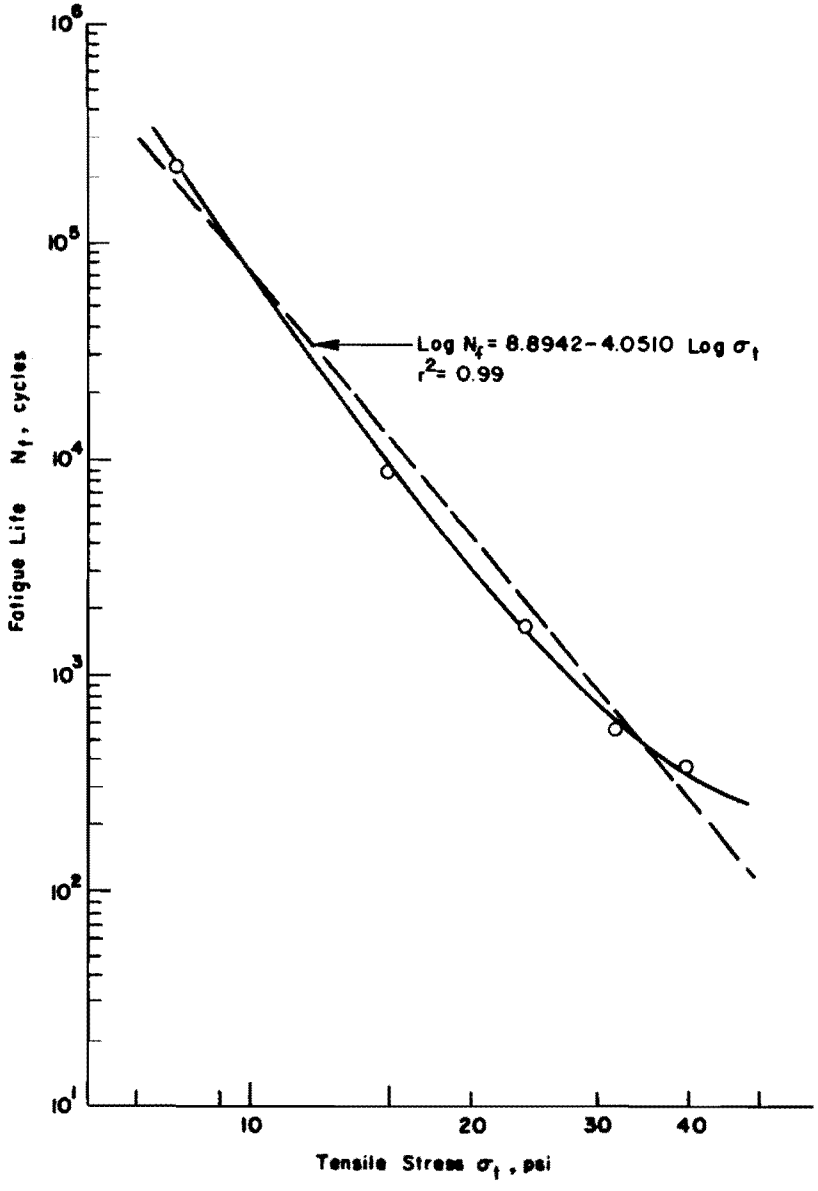

(a) Limestone.

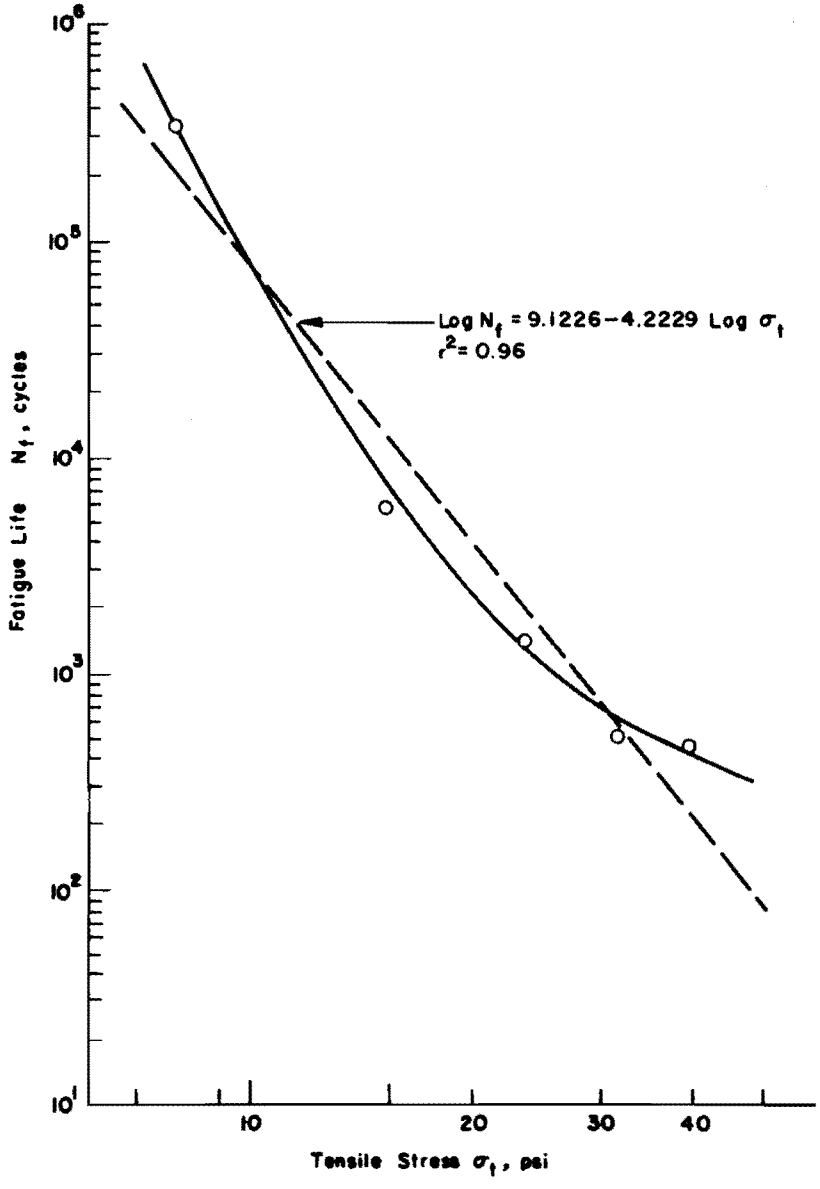

(b) Gravel.

Fig 24. Fatigue life versus tensile stress: probability of failure level at 50 percent.

relationship is dependent on the sample size, the assumption of linearity between the logarithm of stress and the logarithm of fatigue life may be untrue and such an assumption should be tested with significantly larger sample sizes. Further, the slopes of the log N_f-X diagrams represent scatter in the data and are highly sensitive to outlier data; however, in Tables 14 and 15 it cannot be verified from the simple slope values whether variability in test results decreases with an increase in stress level, as reported by McElvaney (Ref 7).

The log N_f-X functions can be used to construct stress versus fatigue life relationships for various probability levels of failure, which can then be used for design. An example of such a family of probability curves is shown in Fig 25, for probability of failure levels of 10, 50, and 90 percent, using the data from the constant-stress amplitude limestone test series.

Time Deformation Characteristics

The deformations of the specimens were monitored throughout a given test. Individual cyclic information was recorded at preselected intervals and the permanent deformation was taken at the corresponding cycles. For this investigation only the permanent deformation information was considered. Since the purpose of this investigation was to determine the applicability of Miner's Hypothesis to the fatigue life data measured in dynamic indirect tension, it was felt that the possibility existed that permanent deformation might also be predicted with such an hypothesis. Figures C-11 through C-20 (Appendix C) were constructed from the deformation data recorded in the horizontal direction on the limestone and gravel specimens. The deformation curves from a controlled-stress test are of interest since the general character of the curve is that of the familar creep curve, suggesting that perhaps the simple-fatigue characteristics of a bituminous material may be determined from creep tests of the material under investigation. This is the subject of a preliminary evaluation conducted as a part of this research project and reported by Porter and Kennedy (Ref 39).

The creep curve has been characterized by various investigators as consisting of three distinct zones of material response (Refs 28, 40, and 41):

(1) transient creep, characterized by an initial high rate of deformation which rapidly decreases to a constant value, also known as "primary creep;"

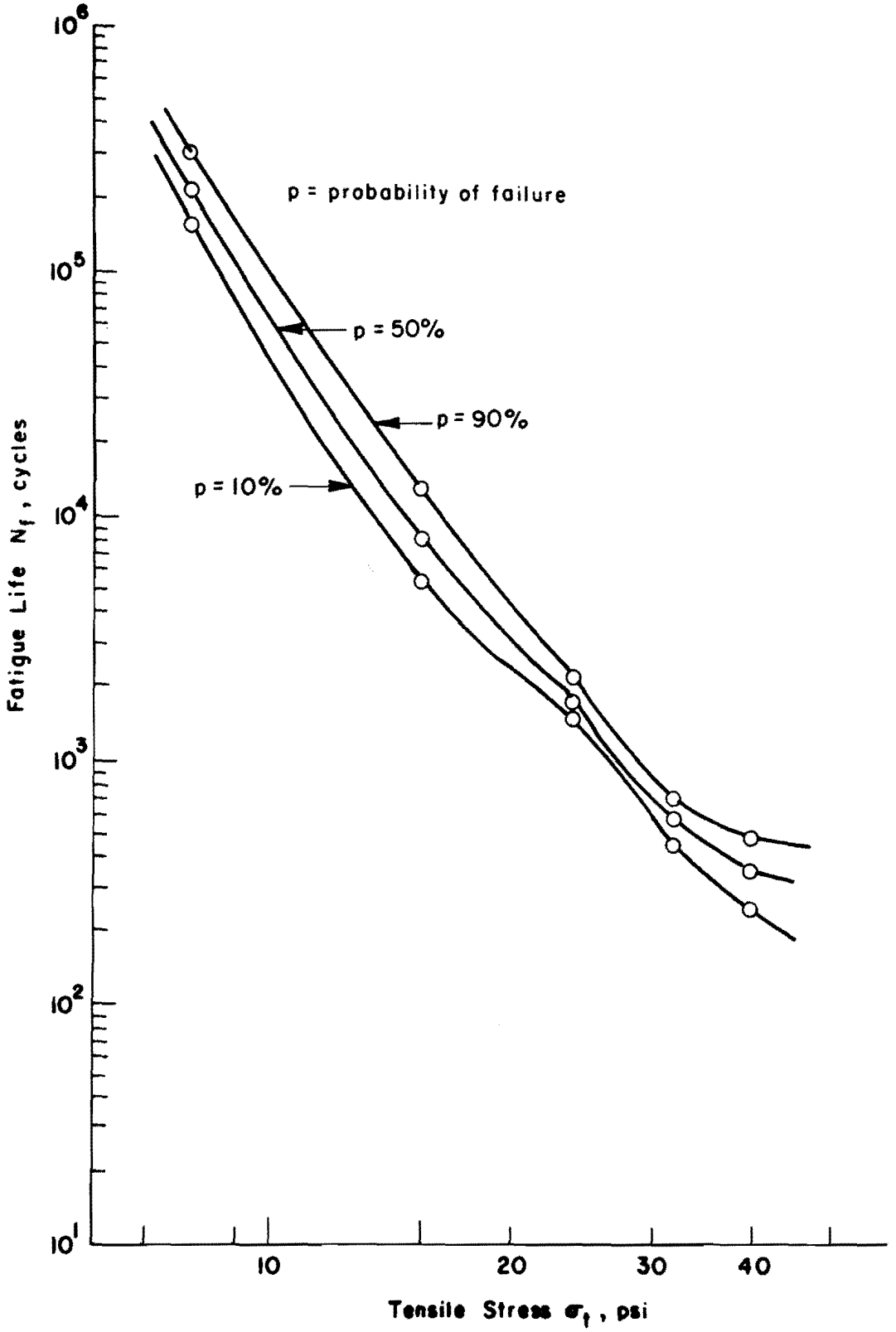

Fig 25. Fatigue life versus tensile stress: comparison of probability of failure levels 10, 50, and 90 percent for limestone test series.

(2) secondary creep, characterized by a constant rate of deformation; and

(3) tertiary creep, characterized by an increase in the rate of deformation and generally culminates in specimen fracture if allowed to continue with time.

These three stages of material behavior are analogous to the observed deformation characteristics of the asphalt mixtures under repeated loads. A typical relationship between horizontal deformation and cycles ratio of load is shown in Fig 26, reproduced here for convenience from Appendix C.

The curves for the horizontal deformations of both the limestone and the gravel test series were normalized by using Miner's cycles ratio n_i/N_f. Any difference in the rate of deformation with respect to the defined failure point is normalized, subject only to the limitations imposed by inherent material variability and the applied stress level. If the summation of "damage" increments by Miner's Hypothesis holds true and if the sample sizes tested in simple loading are representative of the sample population, then it should be possible to predict the deformation of samples subjected to compound-loading conditions from simple-loading deformation information. This suggested possibility is analyzed and discussed in the following section, which deals with the compound-loading phase of the investigation.

COMPOUND-LOADING TWO-LEVEL SEQUENCE TESTS

The specimens tested in compound-loading were prepared in the same manner as those in the simple-loading phase of this investigation. Two types of two-level sequence tests were performed, increasing and decreasing stress (Fig 27), for a range of stress levels in accordance with the previously defined experimental program (Fig 19). Each stress-sequence group was subjected to statistical analysis for point estimates of fatigue life and the probabilistic techniques previously described for simple-loading specimens so that an estimate of the dispersion of fatigue life for a given stress sequence could be obtained. Tables B-3 and B-4 (Appendix B) summarize the physical data for the 60 limestone specimens and the 60 gravel specimens, respectively. A log-normal distribution of compound-loading fatigue life was assumed, based on previous fatigue work using simple loading (Refs 6, 7, and 24).

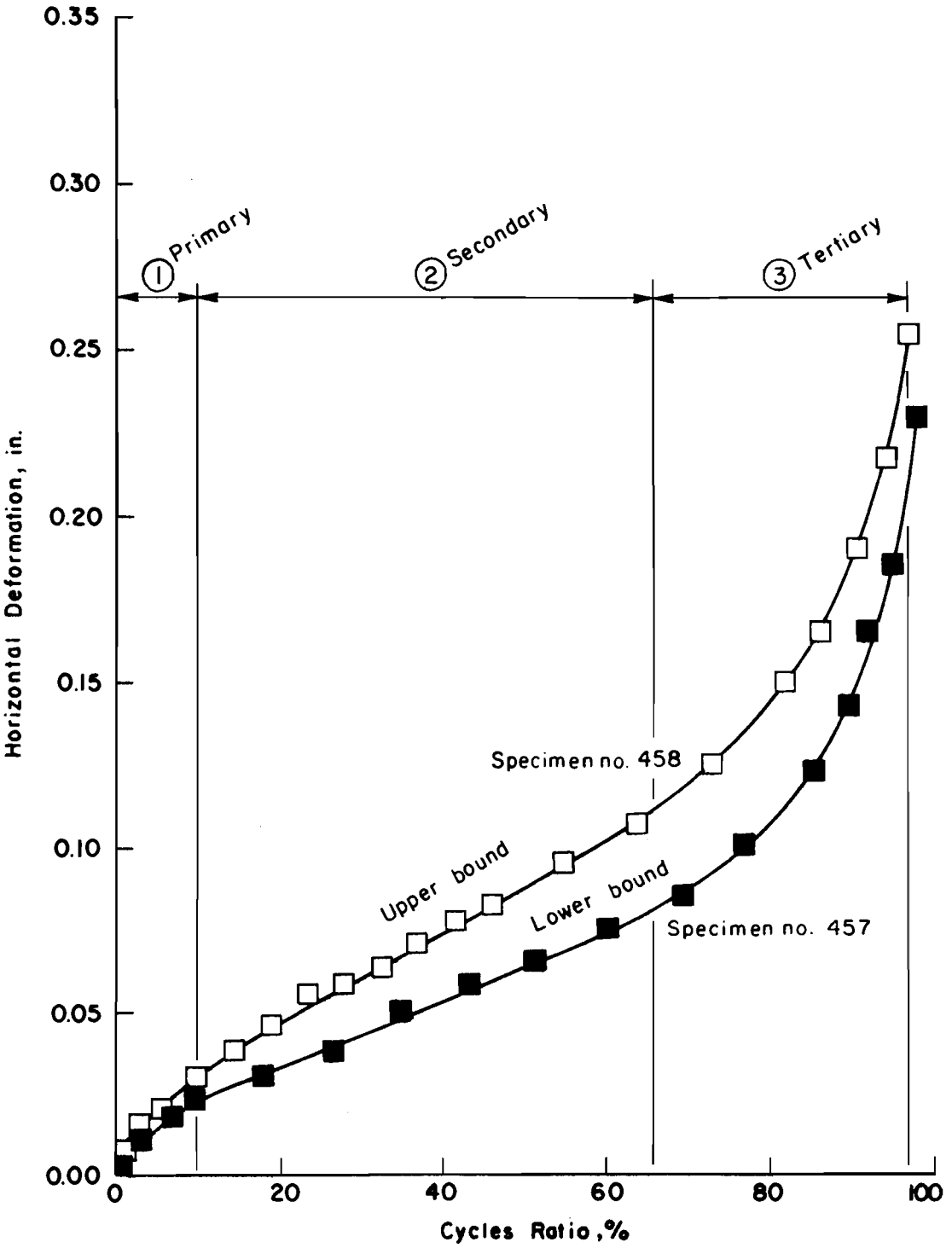

Fig 26. Limiting horizontal deformations in simple-loading: 16-psi limestone.

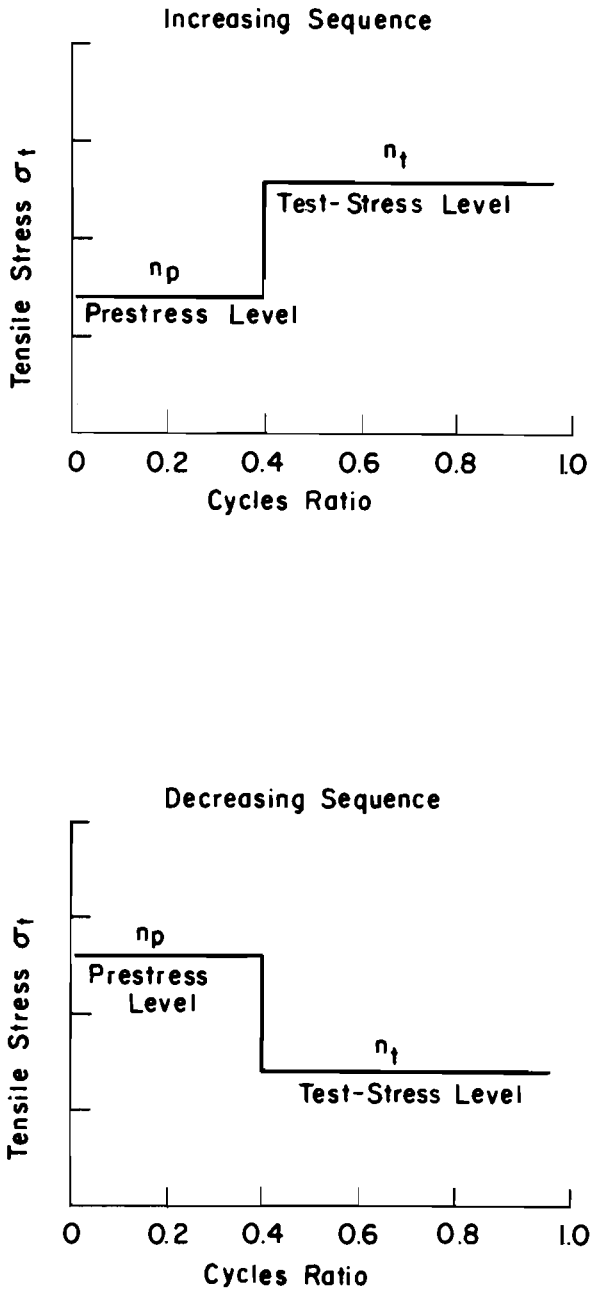

Fig 27. Schematic of two-level increasing and decreasing sequence tests.

Fatigue-Life Estimates

Point estimates of the compound-fatigue life data are presented in Tables 16 and 17 for the limestone and gravel mixtures, respectively. The compound fatigue life for two-level sequence tests consists of two parts: (1) an applied number of prestress cycles at the first stress level and (2) the number of cycles to failure or test stress cycles at the second stress level. The fatigue life under compound-loading can then be expressed as

$$N_p + N_t = N_e \tag{10}$$

where

N_p = a preselected number of cycles at the prestress level,

N_t = the measured number of cycles to failure at the test stress level,

N_e = the compound-loading fatigue life for two-level sequence tests (increasing or decreasing), measured experimentally.

The statistical estimates in Tables 16 and 17 are based on the measured values of N_e.

Since two stress levels are involved in each compound-loading test sequence the conventional stress versus fatigue life diagram cannot be constructed. Instead, it is possible to construct diagrams of fatigue life under compound loading versus a percentage of the fatigue life based on the number of cycles applied at the larger stress level. Figures 28 through 31 give such relationships for the limestone and gravel mixtures. These relationships represent the 25 percent prestress level and are a part of a family of experimental curves that could be constructed by varying the applied number of cycles of prestress. The actual percentage of prestress cycles for each point is shown. The slight variation is due to the insignificant changes in simple-loading mean values at each stress level as the simple-loading populations were increased in number during the testing program, while the compound-loading tests were being performed.

TABLE 16. STATISTICAL ESTIMATES OF COMPOUND-LOADING FATIGUE LIFE, LIMESTONE TEST SERIES

	Tensile Stress Sequence, psi	Arithmetic Average	Log Mean $\overline{N}_f$	Standard Deviation S	Variance S^2
Increasing Sequence	16-24	3567	3554	0.338×10^3	0.1142×10^6
	16-32	2568	2567	0.082×10^3	0.0072×10^6
	16-40	2112	2100	0.256×10^3	0.0723×10^6
	24-32	819	818	0.034×10^3	0.0012×10^6
	24-40	668	666	0.062×10^3	0.0038×10^6
	32-40	427	420	0.087×10^3	0.0076×10^6
Decreasing Sequence	24-16	4435	4360	0.916×10^3	0.8391×10^6
	32-16	4586	4453	1.360×10^3	1.8496×10^6
	32-24	1316	1312	0.115×10^3	0.0132×10^6
	40-16	3397	3328	0.767×10^3	0.5883×10^6
	40-24	1091	1086	0.112×10^3	0.0125×10^6
	40-32	606	600	0.092×10^3	0.0085×10^6

TABLE 17. STATISTICAL ESTIMATES OF COMPOUND-LOADING FATIGUE LIFE, GRAVEL TEST SERIES

	Tensile Stress Sequence, psi	Arithmetic Average	Log Mean $\overline{N}_f$	Standard Deviation S	Variance S^2
Increasing Sequence	16-24	2210	2197	0.264×10^3	0.0697×10^6
	16-32	1917	1916	0.071×10^3	0.0050×10^6
	16-40	1997	1992	0.156×10^3	0.0243×10^6
	24-32	758	755	0.065×10^3	0.0042×10^6
	24-40	554	554	0.028×10^3	0.0008×10^6
	32-40	324	324	0.016×10^3	0.0003×10^6
Decreasing Sequence	24-16	2866	2852	0.319×10^3	0.1018×10^6
	32-16	1361	1317	0.401×10^3	0.1608×10^6
	32-24	833	791	0.341×10^3	0.1163×10^6
	40-16	1838	1170	4.069×10^3	16.6557×10^6
	40-24	721	714	0.118×10^3	0.0139×10^6
	40-32	310	308	0.031×10^3	0.0010×10^6

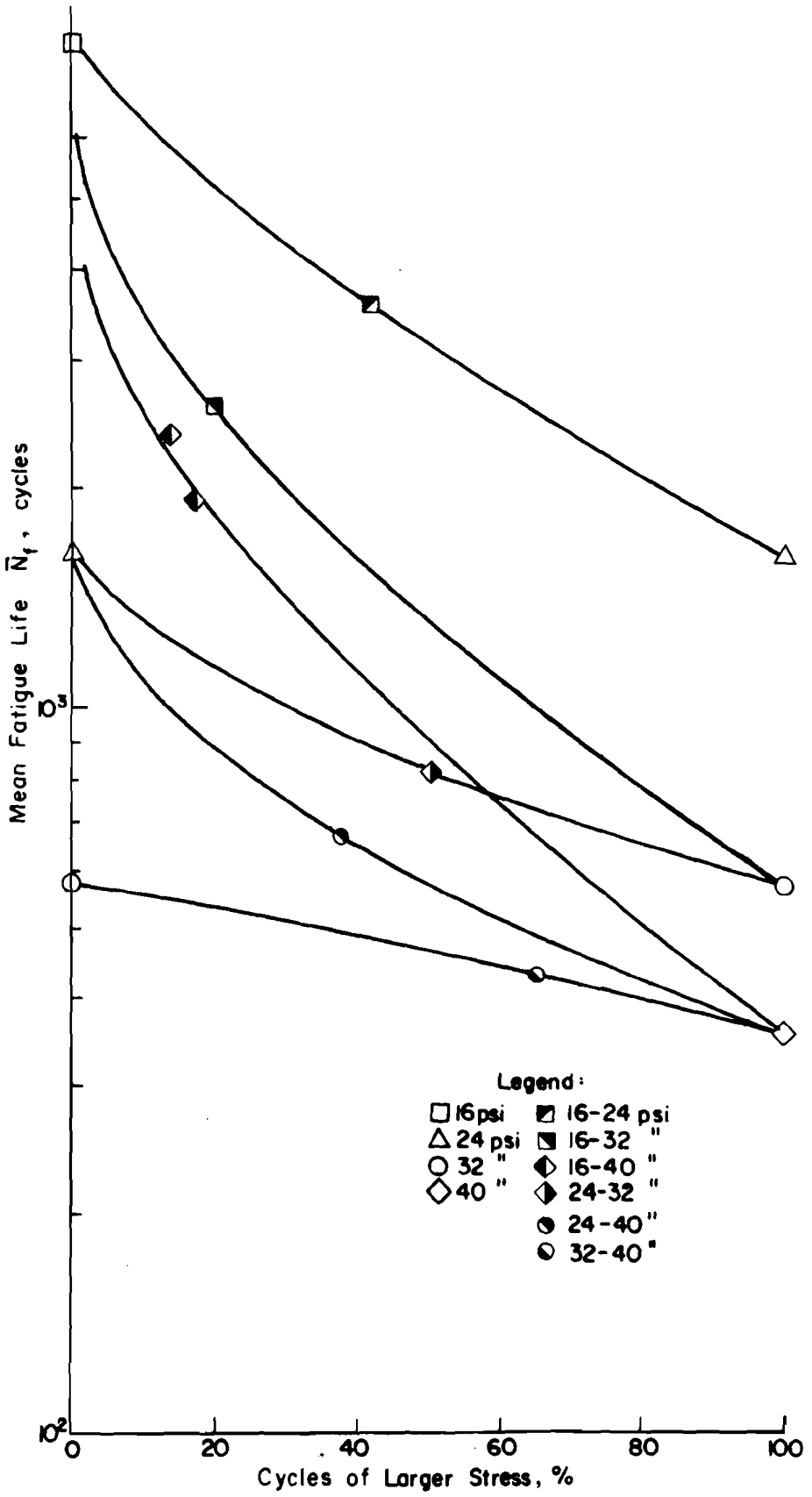

Fig 28. Mean fatigue life versus percent cycles at the larger stress, increasing-sequence limestone test series at the 25 percent prestress level.

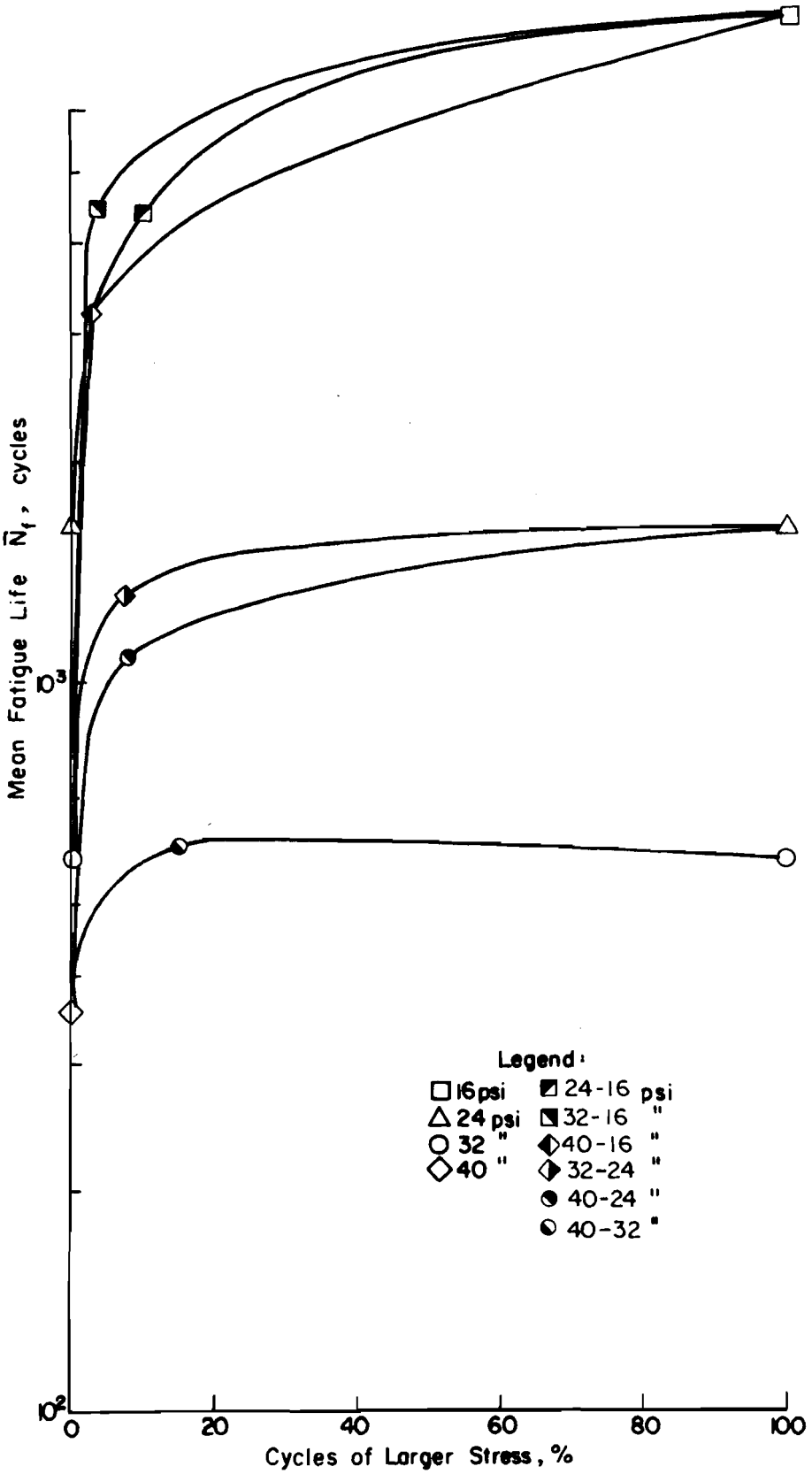

Fig 29. Mean fatigue life versus percent cycles at the larger stress, decreasing-sequence limestone test series at the 25 percent prestress level.

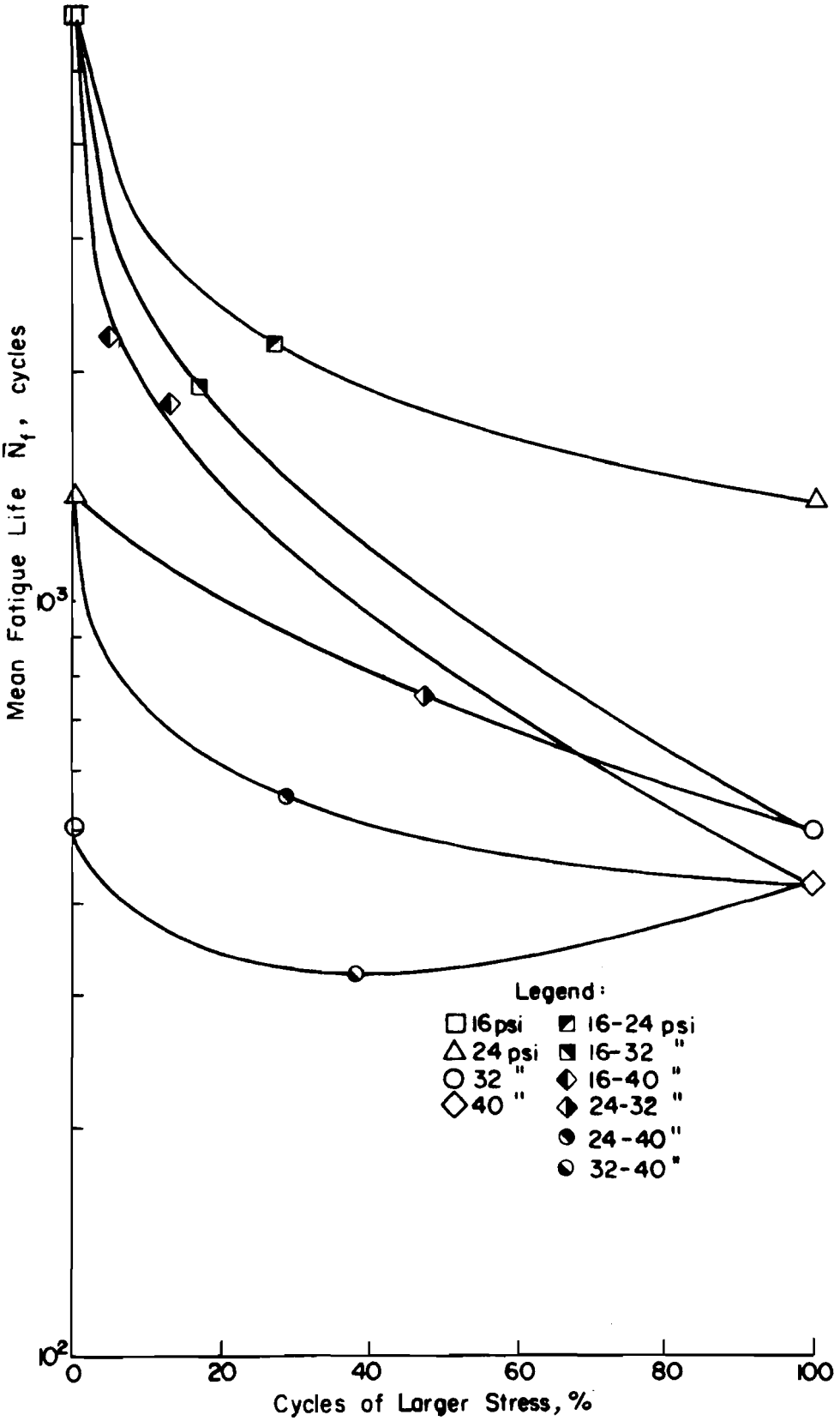

Fig 30. Mean fatigue life versus percent cycles of the larger stress, increasing-sequence gravel test series at the 25 percent prestress level.

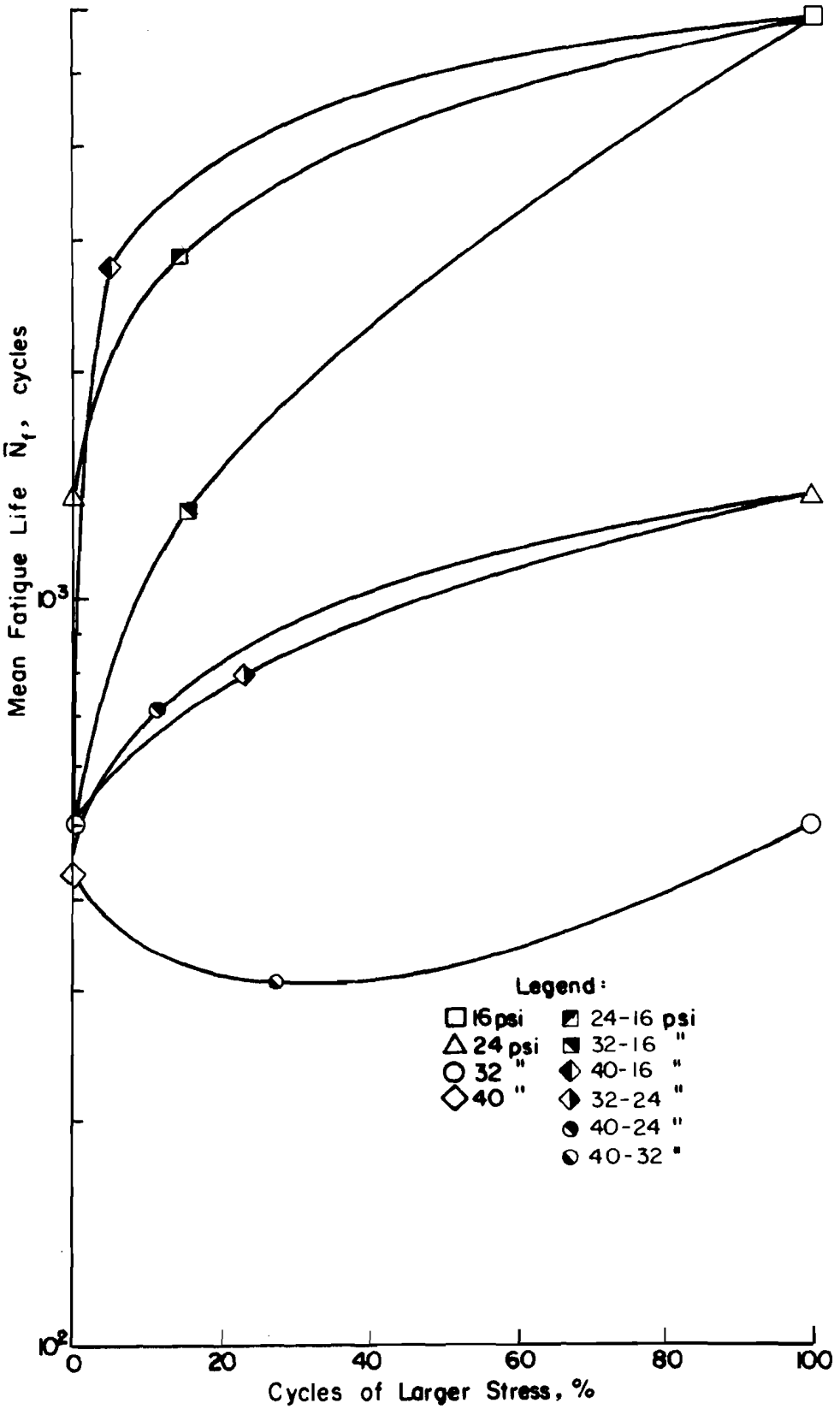

Fig 31. Mean fatigue life versus percent cycles of the larger stress, decreasing-sequence gravel test series at the 25 percent prestress level.

For the decreasing sequence tests (Figs 29 and 31) it can be seen that the prestress level had little influence on the fatigue life since approximately 80 percent of the fracture life was consumed at the lower stress level. For the increasing sequence tests (Figs 28 and 30) approximately 50 percent of the compound-loading fatigue life was consumed at the lower stress level. Generally, it can be said that the increasing sequence tests are more severe with respect to fatigue life, since for the decreasing sequence tests only 8 to 20 percent of the compound-loading fatigue life was consumed at the prestress level.

Probability Estimates of Compound-Loading Fatigue Life

As described in the section dealing with simple-loading fatigue life, it is possible to construct log N_f-X relationships at a given stress level. The compound-loading fatigue life data have been reduced in this manner and are given in Appendix D (Tables D-1 through D-48) with the corresponding log N_f-X relationships shown in Figs D-1 through D-24. The predictor equations from simple least-squares fit of the data for each stress sequence are given in Tables 18 and 19. As before, the method of data reduction gives the median or 50 percent probability curve directly from the equation intercept value, and for an odd number of specimens this corresponds to the sample mean.

Evaluation of Miner's Hypothesis

It is of interest to know whether or not compound-loading fatigue life can be predicted from the linear summation of cycles ratio as determined from simple loading fatigue data. This hypothesis, as proposed by Miner (Ref 5), is attractive due to the simplicity with which it can be applied. In a compound-loading test the fatigue life can be predicted from a knowledge of the simple-loading stress versus fatigue life relationship and the applied percentage of applications of a given stress level. The predictive ability of Miner's Hypothesis can then be checked by first measuring the experimental compound-loading fatigue life N_e from simple-loading considerations and comparing the calculated value with the experimental value. The form of Miner's Hypothesis for a two-level sequence test is given by

TABLE 18. REGRESSION COEFFICIENTS FOR SEQUENCE LEVEL, FAILURE CONDITION DATA FOR LIMESTONE

7% AC-10 — Temperature 75°F
Medium Gradation — Preload 20 lbs.
Sinusoidal Pulse (0.6 sec. rest time), 1 Hz

Tensile Stress Sequence	Intercept B_0	Slope B_1	Predictor Equation* Log $N_f = B_0 + B_1 X$
16-40	3.3222	0.0643	Log N_{16-40} = 3.3222 + 0.0643X
16-32	3.4095	0.0189	Log N_{16-32} = 3.4095 + 0.0189X
16-24	3.5507	0.0529	Log N_{16-24} = 3.5507 + 0.0529X
24-40	2.8233	0.0534	Log N_{24-40} = 2.8233 + 0.0534X
24-32	2.9128	0.0231	Log N_{24-32} = 2.9128 + 0.0231X
24-16	3.6395	0.1088	Log N_{24-16} = 3.6395 + 0.1088X
32-40	2.6231	0.1149	Log N_{32-40} = 2.6231 + 0.1149X
32-24	3.1179	0.0498	Log N_{32-24} = 3.1179 + 0.0498X
32-16	3.6487	0.1438	Log N_{32-16} = 3.6487 + 0.1438X
40-32	2.7783	0.0816	Log N_{40-32} = 2.7783 + 0.0816X
40-24	3.0358	0.0563	Log N_{40-24} = 3.0358 + 0.0563X
40-16	3.5222	0.1247	Log N_{40-16} = 3.5222 + 0.1247X

* X = reduced normal variate

TABLE 19. REGRESSION COEFFICIENTS FOR SEQUENCE LEVEL, FAILURE CONDITION DATA FOR GRAVEL

7% AC-10 Temperature 75°F
Medium Gradation Preload 20 lbs.
Sinusoidal Pulse (0.6 sec. rest time), 1 Hz

Tensile Stress Sequence	Intercept B_0	Slope B_1	Predictor Equation* $\text{Log } N_f = B_0 + B_1 X$
16-40	3.2993	0.0418	$\text{Log } N_{16-40} = 3.2993 + 0.0418X$
16-32	3.2825	0.0203	$\text{Log } N_{16-32} = 3.2825 + 0.0203X$
16-24	3.3418	0.0630	$\text{Log } N_{16-24} = 3.3418 + 0.0630X$
24-40	2.7434	0.0284	$\text{Log } N_{24-40} = 2.7434 + 0.0284X$
24-32	2.8783	0.0477	$\text{Log } N_{24-32} = 2.8783 + 0.0477X$
24-16	3.4551	0.0594	$\text{Log } N_{24-16} = 3.4551 + 0.0594X$
32-40	2.5101	0.0258	$\text{Log } N_{32-40} = 2.5101 + 0.0258X$
32-24	2.8980	0.2035	$\text{Log } N_{32-24} = 2.8980 + 0.2035X$
32-16	3.1196	0.1642	$\text{Log } N_{32-16} = 3.1196 + 0.1642X$
40-32	2.4890	0.0585	$\text{Log } N_{40-32} = 2.4890 + 0.0585X$
40-24	2.8535	0.0788	$\text{Log } N_{40-24} = 2.8535 + 0.0788X$
40-16	3.0682	0.6584	$\text{Log } N_{40-24} = 3.0682 + 0.6584X$

* X = reduced normal variate

$$\frac{n_p}{\bar{N}_p} + \frac{n_t}{\bar{N}_t} = R_e \tag{11}$$

where

n_p = the number of applied prestress cycles,

n_t = the number of cycles to failure at the test stress,

$\bar{N}_p$ = the simple-loading mean fatigue life at the prestress level,

$\bar{N}_t$ = the simple-loading mean fatigue life at the test-stress level, and

R_e = the experimentally determined cumulative cycle ratio.

If Miner's Hypothesis could predict the compound-loading fatigue life then the cumulative cycle ratio R_e would always be unity and the equation could be rewritten in the following form:

$$N_c = \frac{1}{\frac{f_p}{\bar{N}_p} + \frac{f_t}{\bar{N}_t}} \tag{12}$$

where

N_c = the predicted compound-loading fatigue life,

f_p and f_t are chosen percentages of the experimental compound fatigue life.

Since

$$f_p = \frac{n_p}{N_e} \tag{13}$$

and

$$f_t = \frac{n_t}{N_e} \tag{14}$$

it follows that

$$N_c = \frac{N_e}{R_e} \tag{15}$$

and after determining the values of R_e for a given stress sequence it is a simple matter to calculate the predicted value of compound-loading fatigue life N_c.

The experimental and calculated values of fatigue life under compound-loading are presented in Appendix D (Tables D-1 through D-48) and the appropriate values of N_c have been superimposed on Figs D-1 through D-24 to make simple comparisons of measured fatigue life values and predicted fatigue life values possible. The experimentally determined values of cumulative cycles ratios are also presented in these tables. Utilizing the technique suggested by Deacon (Ref 6), the values of N_e and N_c were compared by using the mean values associated with the particular stress sequence and calculating a percent difference by

$$\Delta = \frac{\overline{N}_c - \overline{N}_e}{\overline{N}_e} \quad (100) \tag{16}$$

Values are presented in Table 20 for both the gravel and limestone test series. The algebraic sign and magnitude of Δ are significant in that a negative value indicates that $N_c < N_e$ and a positive sign indicates the value of N_c exceeds the experimental value. The amount by which N_c underestimates or overestimates the experimental value depends on the stress sequence, the stress range, and the aggregate type. For the gravel mixtures, $\overline{N}_c$ always exceeded $\overline{N}_e$, with Δ ranging from 0.1 percent to 85.9 percent. For limestone the related relationship between $\overline{N}_c$ and $\overline{N}_e$ was not consistent, with Δ ranging from -14.2 percent to 54.9 percent. Observing the values of N_c superimposed on the log N_f-X relationships it is possible to conclude that for decreasing-sequence tests of both the limestone and gravel series the predicted values N_c were always greater than the measured values N_e and that the slopes of the log N_c-X lines were positive, indicating cumulative cycles ratios less than or near unity. For the increasing-

TABLE 20. COMPARISON OF EXPERIMENTAL AND PREDICTED FATIGUE LIFE

	Tensile Prestress σ_{tp}, psi	Tensile Test-Stress σ_{tt}, psi	Mean Fatigue Life $\bar{N}_e$, cycles	Mean Fatigue Life $\bar{N}_c$, cycles	Deviation Δ, %
Limestone	16	40	2100	1819	-13.38
		32	2567	2250	-12.35
		24	3554	3048	-14.24
	24	40	666	690	3.60
		32	181	848	3.67
		16	4360	5879	34.84
	32	40	420	407	- 3.09
		24	1312	1355	3.28
		16	4453	5646	26.79
	40	32	600	525	-12.50
		24	1086	1272	17.13
		16	3328	5154	54.87
Gravel	16	40	1992	2944	47.79
		32	1916	2102	9.71
		24	2197	3145	43.15
	24	40	554	846	52.71
		32	755	756	0.13
		16	2852	4048	41.94
	32	40	324	472	45.68
		24	791	986	24.65
		16	1317	2234	69.63
	40	32	308	481	56.17
		24	714	1095	53.36
		16	1170	2175	85.90

sequence tests for both aggregates there was no such consistent relationship between N_c and N_e ; however, the slopes of the log N_c-X relationships were always negative, indicating cumulative cycles ratios always greater than or near unity. This would seem to support the previous findings of this study which indicated increasing stress sequence to be more severe.

The choice of the two-level sequence test to verify the applicability of Miner's Hypothesis was good from the standpoint of required testing effort. The values of cumulative cycles ratio reported by McElvaney (Ref 7) ranged from 0.55 to 1.63 at the 30 percent prestress level. The data taken in this investigation at the 25 percent prestress level in terms of cumulative cycles ratio ranged from 0.65 to 1.18 for the limestone and from 0.57 to 1.01 for the gravel. Both Deacon (Ref 6) and McElvaney (Ref 7) found that as the block size (Fig 27) of load applications decreases the value of the cycles ratio approaches unity for repeated block tests. Thus, if repeated block tests had been performed in this investigation in all likelihood convergence to unity would have been observed. Based on the evidence attained in this investigation, it is concluded that Miner's Hypothesis can be used to estimate compound-loading fatigue life from simple-loading fatigue life information obtained using the dynamic indirect tensile test, subject to the variations shown.

Time-Deformation Characteristics Under Compound-Loading

The deformations of the compound-loading tests were measured in the same manner as the deformations under simple-loading conditions. The horizontal deformations are shown in Figs E-1 through E-24 in Appendix E. The previous statements concerning the more severe loading sequence are borne out by the deformation plots, which have been normalized using the cumulative cycles ratio. A significant portion of the total deformation occurred at the prestress level for increasing sequence tests. There are two items of interest concerning the compound-loading time-deformation curves: (1) the possibility is suggested that the deformations may be predicted from simple-loading considerations through the use of Miner's Hypothesis and (2) more information may be derived concerning the actual failure point of the material under investigation, i.e., the point where an irreversible amount of damage has occurred to the test specimens. Both topics are of considerable interest

and have been a subject of concern to engineers involved with flexible pavement design (Refs 2, 3, 6 through 10, 12, 13, 24, and 26 through 32).

Deformation Prediction. Since Miner's Hypothesis is based on a damage concept it is possible that using deformation as a damage function would allow compound-loading deformations to be predicted from simple-loading considerations by the summation of damage (deformation) increments. Assuming that for a given set of load conditions specimens tested in simple loading exhibit a distribution of deformation characteristics that can be bounded by the maximum and minimum deformations occurring under such conditions, it is of interest to verify whether or not the simple summation of maximum and minimum deformations from simple loading can be used to predict deformations under compound-loading conditions. Using the simple linear summation of cycles ratio concept, the following method was developed for summing deformation damage increments.

(1) Obtain the simple deformation characteristics of the asphalt mixture for the range of stress levels of interest (in this investigation five specimens were tested per stress level).

(2) Determine the specimens which exhibit the maximum and minimum deformation characteristics when normalized with respect to end point failure N_f (the normalization removes the rate effect due to fatigue life scatter.

(3) Establish a set of simple-loading, limiting deformation curves for the range of stress of interest.

(4) Sum the deformation damage increments according to the percentage of each stress level applied, and record the deformation value as "total deformation at damage level D" as X_p .

(5) Compare the predicted value of deformation X_p to the measured value of deformation under compound-loading conditions X_e , and determine whether the prediction includes the measured value X_e .

The deformation relationships in Appendix E represent the graphical depiction of the above procedure. It was found for two-level sequence tests that deformations could be predicted that included either the measured deformation X_e in the predicted range or exceeded the measured deformation under compound-loading by a slight amount so that a safe deformation estimate was possible. In only two cases did the measured deformations exceed the predicted deformations, the differences being minor and explained in terms of creep which

occurred under the preload condition prior to the start of the fatigue test, i.e., deformation information which was lost in the experimental testing. As a result, the limiting deformation curves were displaced relative to one another depending on the time that creep was occurring prior to testing in both the simple-loading and compound-loading test series. In general, the predicted deformations were greater than those measured experimentally for the increasing sequence tests and the measured deformations were within the predicted range for the decreasing-sequence tests.

Failure. Through the use of the more severe stress sequence (increasing) it appears to be possible to determine further information concerning the irreversibility of the damage process. Observing that the increasing-stress sequence is the more severe in terms of compound-fatigue life consumed at the prestress level and analyzing the deformation characteristics under this loading condition, it becomes obvious that a significant portion of the fatigue life is consumed at approximately 80 percent of the cycles ratio with respect to total deformation experienced by the specimens under test. This suggests that by applying different percentages of the prestress level it is possible to determine the point of irreversible cracking or damage that occurs to a specimen during the fatigue process. The deformation characteristic that would be obvious if the specimen had reached the point of irreversible damage would be that of tertiary creep, or a rapidly increasing rate of deformation with time. If the irreversible damage level had not been reached, then the specimen should exhibit primary, secondary, and tertiary creep characteristics at the second, or test-stress, level. The figures in Appendix E bear out this discussion.

Prior to the beginning of the compound-loading test series it was noticed that a simple geometric construction seemed to give a fatigue life (i.e., a service life) at a consistent level of 80 percent of the cumulative cycles ratio. This method is given as a technique for determining a fatigue service life which is predictable and is based on both simple and compound-loading information. The technique is illustrated in Fig 32 and is as follows.

(1) Establish a vertical line at the fracture fatigue life of a test specimen on the deformation plot.

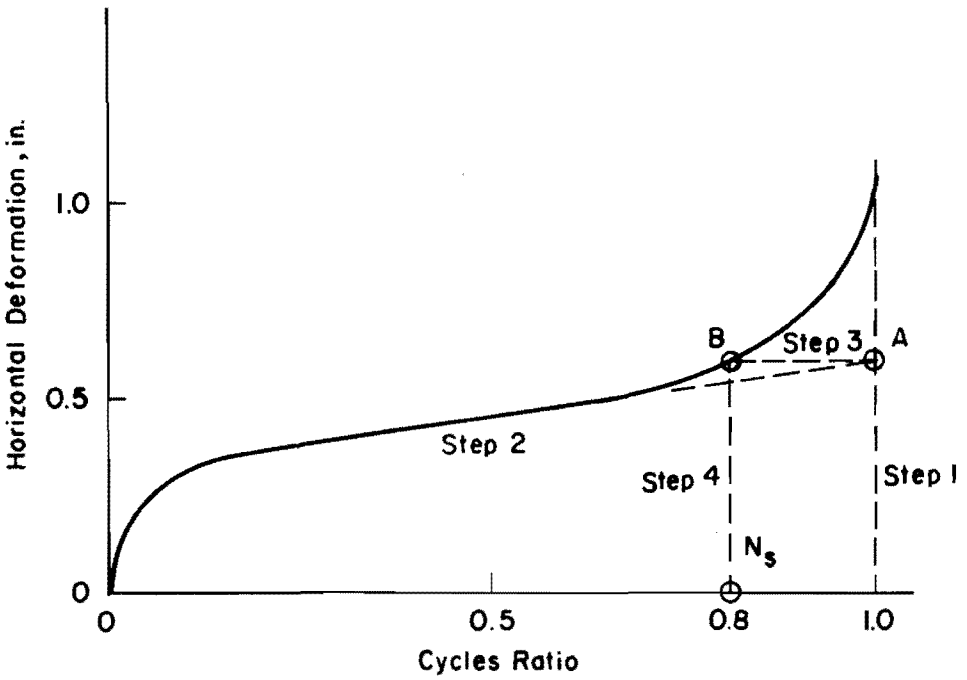

Fig 32. Graphical determination of a service fatigue life.

(2) Extend the secondary creep portion of the deformation plot until it intercepts the established vertical line at point A.

(3) Extend a horizontal line from the intercept point A until it touches the deformation plot at point B.

(4) Establish the fatigue service life N_s, i.e., the point at which irreversible damage occurred, with a vertical line extended from point B to the abcissa.

That the service life value occurs at approximately 80 percent of the measured fracture life of a given specimen is important, since in fact the construction may yield a range of values, depending entirely on the deformation characteristics of the mixture under investigation. The range has been found to be quite small (75 to 85 percent) and, if it is possible to predict a fatigue service life within 5 to 10 percent with repeatability, confidence can be developed with respect to handling fatigue information. Application of this method to the data presented by Deacon (Ref 6) and McElvaney (Ref 7) yields similar results, with values of 90 percent and 82 percent for the cumulative cycles ratios, respectively.

CHAPTER 5. CONCLUSIONS

The primary purpose of this study was to determine whether or not the dynamic indirect tension test simple-loading fatigue data could be used in conjunction with Miner's Hypothesis to predict the fatigue response of a bituminous mixture subjected to compound-loading conditions. This chapter summarizes the findings of the investigation.

CONCLUSIONS

Simple-Loading Constant Stress Amplitude Tests

(1) The logarithm of stress versus the logarithm of fatigue life for a given set of environmental conditions is essentially linear for the range of stresses investigated (8 psi to 40 psi); however, limited evidence suggests a nonlinear relationship if the same probability of failure is considered at each stress level.

(2) The standard deviation of fatigue life decreases with increasing stress level and is in agreement with previous findings.

(3) The probability of failure P(m) can be incorporated into the analysis of fatigue life data.

(4) The linear regression relationships formed by conventional least squares methods are nearly coincident for the gravel and limestone aggregates mixtures, indicating that aggregate type did not affect fatigue life for the entire range of stresses considered. This conclusion, however, does not account for the dispersion of fatigue life at a given stress level and the regression relationships may define different probability levels at the various stresses.

(5) Relationships between the logarithm of fatigue life and the probability of failure P(m) can be developed at each stress level by established techniques (Refs 7 and 23). The slopes of such functions give an indication of the scatter at the given stress level.

Compound-Loading Two-Level Sequence Tests

(1) The order and magnitude of the applied stresses have a significant effect on the fatigue life under compound-loading. For two-level tests with increasing stress approximately 80 percent of the measured fatigue life was consumed at the prestress level for the same preset prestress level. The two-level tests with decreasing stress exhibited only 8 to 20 percent of the measured fatigue life consumed at the prestress level.

(2) The number of test-stress cycles prior to fracture for a given stress sequence varied for duplicate specimens.

(3) Miner's Hypothesis is valid for the asphalt mixtures tested. The range in the value for the cumulative cycles ratio for all tests was from 0.65 to 1.18 for the limestone test series and from 0.57 to 1.01 for the gravel tests.

(4) Time-deformation under compound-loading conditions can be predicted from simple-loading considerations using a technique of linear summation of damage increments. This prediction is subject to a maximum and minimum deformation since inherent material variability and creep deformation under preload influence the results.

General

A technique to determine a fatigue service life, the number of load applications at which irreversible damage occurs, was developed. Based on the results of this study it was concluded that fatigue service life was equal to 75 to 85 percent of fatigue life.

RECOMMENDATIONS

(1) Future investigations into the nature of fatigue response of highway pavement materials should incorporate pseudo-random loading spectra which are more representative of actual field conditions, considering longitudinal and transverse distribution of traffic on the pavement. Such pseudo-random loading techniques have been used for several years by the automobile industry (Ref 42) and the test equipment and analytical techniques exist to perform such tests.

(2) Ideally any subsequent investigations should be coupled with field performance studies, incorporating the field conditions in the laboratory testing so that a direct comparison can be made between field and laboratory findings. This recommendation is made with the full knowledge that such an undertaking would be costly in terms of manpower and financial support.

REFERENCES

1. American Society for Testing and Materials, "A Guide for Fatigue Testing and the Statistical Analysis of Fatigue Data," Special Technical Publication 91-A, 2nd Ed., Philadelphia, 1963.

2. McCullough, B. F., "Distress Mechanisms - General," Special Report 126, Highway Research Board, 1970, pp 77-85.

3. Finn, F. N., "Observation of Distress in Full-Scale Pavements," Special Report 126, Highway Research Board, 1970, pp 86-90.

4. Moore, R. K., and Thomas W. Kennedy, "Tensile Behavior of Subbase Materials under Repetitive Loading," Research Report 98-12, Center for Highway Research, The University of Texas at Austin, October 1971.

5. Miner, M. A., "Cumulative Damage in Fatigue," Transactions, American Society of Mechanical Engineers, Vol. 66, 1945, pp A159-A164.

6. Deacon, J. A., "Fatigue of Asphalt Concrete," Doctor of Engineering Dissertation, Transportation Engineering Division, University of California, Berkeley, 1965.

7. McElvaney, J., "Fatigue of a Bituminous Mixture Under Compound-Loading," Doctor of Philosophy Thesis, University of Nottingham, England, 1972.

8. Monismith, C. L., K. E. Secor, and E. W. Blackmer, "Asphalt Behavior in Repeated Flexure," Proceedings, Association of Asphalt Paving Technologists, Vol. 31, 1962, pp 231-260.

9. Deacon, J. A., and C. L. Monismith, "Laboratory Flexural Fatigue Testing of Asphalt-Concrete with Emphasis on Compound-Loading Tests," Highway Research Record No. 158, 1967, pp 1-31.

10. Jiminez, R. A., "Fatigue Testing of Asphaltic Concrete Slabs," American Society for Testing and Materials, Special Technical Publication 508, 1971, pp 3-17.

11. Smith, J. H., "Some Experiments on Fatigue of Metals," Journal of the Iron and Steel Institute, Vol. LXXXII, Part II, 1910, pp 246-318.

12. Deacon, J. A., "Materials Characterization - Experimental Behavior," Special Report 126, Highway Research Board, 1971, pp 150-179.

13. Deacon, J. A., "Fatigue Life Prediction," Special Report 140, Highway Research Board, 1973, pp 78-92.

14. Palmgren, A., "Die Lebensdauer von Kuggellagern," Zeitschrift Verein Deutscher Ingenieure, Vol. 68, No. 14, 1924, pp 339-341. - as cited by Deacon (Ref 6).

15. Langer, B. F., "Fatigue Failure from Stress Cycles of Varying Amplitude," Transactions, American Society of Mechanical Engineers, Vol. 59, 1937, pp A160-A162.

16. French, H. J., "Fatigue and the Hardening of Steels," Transactions, American Society for Steel Testing, Vol XXI, No. 10, 1933, pp 889-946.

17. Kommers, J. B., "The Effect of Overstressing and Understressing in Fatigue," Proceedings, American Society for Testing Materials, Vol. 38, Part II, 1938, pp 249-268.

18. Lea, F. C., "The Effect of Repetition Stresses on Materials," Engineering, February 16, 1923, pp 217-219 and 252-254.

19. Kommers, J. B., "The Effect of Overstress in Fatigue on the Endurance Life of Steel," Proceedings, American Society for Testing Materials, Vol. 45, 1945, pp 532-543.

20. Bruggemann, W. C., M. Mayer, Jr., and W. H. Smith, "Axial Fatigue Tests at Two Stress Amplitudes of 0.032 Inch 245-T Sheet Specimens with a Circular Hole," NACA TN-983, 1945.

21. Kommers, J. B., "The Effect of Under-Stressing on Case Iron and Open Hearth Iron," Proceedings, American Society for Testing Materials Vol. 30, Part II, 1930, pp 368-383.

22. Kommers, J. B., "The Effect of Overstressing and Understressing in Fatigue," Proceedings, American Society for Testing Materials, Vol. 43, 1943, pp 749-764.

23. Wood, A. A., "The Fatigue Properties of Mild Steel Specimens Subject to Uniform and Random Variations of Repeated Load," Doctor of Philosophy Thesis, University of Sheffield, England, 1961. - as cited by McElvaney (Ref 7).

24. Pell, P. S., and I. F. Taylor, "Asphaltic Road Materials in Fatigue," Proceedings, Association of Asphalt Paving Technologists, Vol. 38, 1969, pp 371-422.

25. Wiebull, W., Fatigue Testing and Analysis of Results, Pergamon Press, Oxford, England, 1961.

26. Pell, P. S., "Fatigue Characteristics of Bitumen and Bituminous Mixes," Proceedings, International Conference on the Structural Design of Asphalt Pavement, Ann Arbor, Michigan, 1962, pp 310-323.

27. Pell, P. S., "Fatigue of Asphalt Pavement Mixes," Proceedings, Second International Conference on the Structural Design of Asphalt Pavements, Ann Arbor Michigan, 1967, pp 577-593.

28. Monismith, C. L., and K. E. Secor, "Thixotropic Characteristics of Asphalt Paving Mixtures with Reference to Behavior in Repeated Loading," Proceedings, Association of Asphalt Paving Technologists, Vol. 29, 1960, pp 114-140.

29. Monismith, C. L., Seed, H. B., Mitry, F. G., and C. K. Chan, "Prediction of Pavement Deflections from Laboratory Tests," Proceedings, Second International Conference on the Structural Design of Asphalt Pavement, Ann Arbor, Michigan, 1967, pp 109-140.

30. Epps, J. A., and C. L. Monismith, "Influence of Mixture Variables on Flexural Fatigue Properties of Asphalt Concrete," Proceedings, Association of Asphalt Paving Technologists, Vol. 38, 1969, pp 423-464.

31. Monismith, C. L., "Asphalt Mixture Behavior in Repeated Flexure," IER Report No. TE-65-9, University of California, November 1965.

32. Hadley, W. O., Hudson, W. R., and T. W. Kennedy, "A Method of Estimating Tensile Properties of Materials Tested in Indirect Tension," Research Report 98-7, Center for Highway Research, The University of Texas at Austin, July 1970.

33. Anagnos, J. N., Kennedy, T. W., and W. R. Hudson, "Evaluation and Prediction of the Tensile Properties of Cement-Treated Materials," Research Report 98-8, Center for Highway Research, The University of Texas at Austin, October 1970.

34. Hadley, W. O., Hudson, W. R., and T. W. Kennedy, "Evaluation and Prediction of the Tensile Properties of Asphalt-Treated Materials," Research Report 98-9, Center for Highway Research, The University of Texas at Austin, May 1971.

35. Hudson, W. R., and T. W. Kennedy, "An Indirect Tensile Test for Stabilized Materials," Research Report 98-1, Center for Highway Research, The University of Texas at Austin, January 1968.

36. Texas Highway Department, Construction Division, "Design of Laboratory Mixes, Selection of Optimum Asphalt Content," Bulletin C-14, September 1964, pp 10-12.

37. Hondros, G., "The Evaluation of Poisson's Ratio and the Modulus of Materials of a Low Tensile Resistance by the Brazilian (Indirect Tensile) Test with Particular Reference to Concrete," Australian Journal of Applied Science, Vol. 10, No. 3.

38. Adedimila, A. S., "Fatigue and Resilient Characteristics of Asphalt Mixtures by Repeated-Load Indirect Tensile Test," Research Report 183-5, Center for Highway Research, The University of Texas at Austin, in progress.

39. Porter, Byron W., and Thomas W. Kennedy, "Comparison of Fatigue Test Methods for Asphalt Materials," Research Report 183-4, Center for Highway Research, The University of Texas at Austin, April 1975.

40. Richards, C. W., Engineering Materials Science, Wadsworth Publishing Company, Inc., San Francisco, 1961.

41. Freeme, C. R., and C. P. Marais, "The Structural Behavior of Bituminous Surfacings in an Experimental Asphalt Pavement," Proceedings, 3rd International Conference on the Structural Design of Asphalt Pavements, Vol. I, London, England, pp 812-822.

42. Swanson, S. R., "Random Load Fatigue Testing: A State of the Art Survey," Materials Research and Standards, Vol. 8, No. 4, April, 1968, pp 10-44.

APPENDIX A

BATCHING AND MIXING, COMPACTION, AND CURING PROCEDURES FOR ASPHALT-TREATED MATERIALS

BATCHING AND MIXING, COMPACTION, AND CURING PROCEDURES FOR ASPHALT-TREATED MATERIALS

BATCHING AND MIXING PROCEDURES

(1) Batch material by dry weight in storage containers, mixing fines and coarse fractions.

(2) Heat aggregate and asphalt to the appropriate mixing temperature ($300^{\circ}F \pm 5^{\circ}F$).

(3) Mix aggregate and asphalt at the specified temperature ($300^{\circ}F \pm 5^{\circ}F$) for three minutes in an automatic mixer.

COMPACTION PROCEDURES

(1) Place the mixes in preheated ovens and bring to the required compaction temperature ($250^{\circ}F \pm 5^{\circ}F$).

(2) Compact the mixes at the specified temperature using the Texas gyratory-shear compactor as specified in test method TEX-206-F (Ref 36).

(3) Extrude the specimen and weigh and measure the height and diameter of the specimen.

CURING PROCEDURES

Cure the specimens for two days at room temperature ($75^{\circ}F \pm 2^{\circ}F$).

APPENDIX B

PHYSICAL INFORMATION FOR ALL SPECIMENS

TABLE B-1. PHYSICAL DATA FOR LIMESTONE SPECIMENS USED IN CONSTANT-STRESS AMPLITUDE TESTS: (SPECIMENS RANK-ORDERED ON N_f)

Tensile Stress, psi	Spec. No.	Height, in.	Diameter, in.	Volume, $in.^3$	Bulk Specific Gravity	Bulk Density, pcf
	282	1.906	4.010	24.071	--	--
	280	1.912	4.010	24.147	2.308	143.7
8	285	1.893	4.010	23.907	2.329	145.0
	288	1.882	4.010	23.768	2.338	145.6
	286	1.878	4.010	23.718	2.338	145.6
	396	1.877	4.017	23.788	2.343	145.9
	395	1.879	4.017	23.813	2.340	145.7
	456	1.891	4.010	23.882	2.328	144.9
16	558	1.888	4.010	23.884	2.336	145.4
	557	1.886	4.010	23.819	2.340	145.7
	556	1.877	4.010	23.705	2.335	145.4
	458	1.900	4.010	23.996	2.331	145.1
	457	1.891	4.010	23.882	2.334	145.3
	453	1.886	4.010	23.819	2.330	145.1
	455	1.894	4.010	23.920	2.329	145.0
24	382	1.887	4.010	23.831	2.330	145.1
	454	1.881	4.010	23.756	2.339	145.6
	381	1.889	4.010	23.857	2.340	145.7
	451	1.879	4.010	23.730	2.337	145.5
	452	1.889	4.010	23.857	2.331	145.1
32	391	1.871	4.010	23.629	2.339	145.6
	450	1.888	4.010	23.844	2.330	145.1
	318	1.892	4.010	23.895	2.344	145.9
	386	1.894	4.010	23.920	2.321	144.5
	387	1.875	4.010	23.680	2.339	145.6
	389	1.878	4.010	23.718	2.339	145.6
40	388	1.915	4.010	24.185	2.330	145.1
	728	1.887	4.010	23.831	2.336	145.4
	730	1.870	4.010	23.617	2.344	145.9
	110	1.891	4.010	23.882	--	--
	729	1.869	4.010	23.604	2.345	146.0

TABLE B-2. PHYSICAL DATA FOR GRAVEL SPECIMENS USED IN CONSTANT-STRESS AMPLITUDE TESTS: (SPECIMENS RANK-ORDERED ON N_f)

Tensile Stress, psi	Spec. No.	Height, in.	Diameter, in.	Volume, $in.^3$	Bulk Specific Gravity	Bulk Density, pcf
	115	1.898	4.010	23.970	--	--
	117	1.881	4.010	23.756	--	--
8	119	1.892	4.010	23.895	2.305	143.5
	129	1.902	4.010	24.021	2.300	143.2
	123	1.900	4.010	23.996	2.299	143.1
	465	1.907	4.010	24.084	2.292	142.7
	407	1.890	4.010	23.869	2.316	144.2
	466	1.902	4.010	24.021	2.303	143.4
	467	1.898	4.010	23.970	2.306	143.6
16	339	1.885	4.010	23.806	2.321	144.5
	561	1.884	4.010	23.794	2.309	143.8
	559	1.903	4.010	24.034	2.294	142.8
	560	1.892	4.010	23.895	2.304	143.4
	338	1.901	4.010	24.008	2.299	143.1
	462	1.894	4.010	23.920	2.305	143.5
	463	1.898	4.010	23.970	2.307	143.6
	464	1.896	4.010	23.945	2.310	143.8
	521	1.892	4.010	23.895	2.303	143.4
24	519	1.878	4.010	23.718	2.323	144.6
	566	1.893	4.010	23.907	2.308	143.7
	520	1.882	4.010	23.768	2.315	144.1
	102	1.903	4.010	24.034	--	--
	107	1.887	4.010	23.831	--	--
	461	1.901	4.010	24.008	2.299	143.1
	459	1.899	4.010	23.983	2.306	143.6
	460	1.893	4.010	23.907	2.305	143.5
	524	1.885	4.010	23.806	2.318	144.3
32	523	1.902	4.010	24.021	2.297	143.0
	522	1.889	4.010	23.857	2.311	143.9
	565	1.891	4.010	23.882	2.304	143.4
	380	1.900	4.010	23.996	2.304	143.4
	103	1.897	4.010	23.958	--	--
	2011	1.897	4.010	23.958	2.313	144.0
	564	1.889	4.010	23.857	2.304	143.4
	563	1.894	4.010	23.920	2.303	143.4
	562	1.889	4.010	23.857	2.310	143.8
40	106	1.893	4.010	23.907	--	--
	101	1.899	4.010	23.983	--	--
	105	1.887	4.010	23.831	--	--
	104	1.903	4.010	24.034	--	--
	130	1.884	4.010	23.794	2.314	144.1

TABLE B-3a. PHYSICAL DATA FOR LIMESTONE SPECIMENS USED IN COMPOUND-LOADING TESTS: INCREASING SEQUENCE (SPECIMENS RANK-ORDERED ON N_f)

Tensile Stress, psi	Spec. No.	Height, in.	Diameter, in.	Volume, $in.^3$	Bulk Specific Gravity	Bulk Density, pcf
	2020	1.889	4.010	23.857	2.337	145.5
	2023	1.892	4.010	23.895	2.334	145.3
16-24	2021	1.889	4.010	23.857	2.332	145.2
	2024	1.887	4.010	23.831	2.332	145.2
	2022	1.882	4.010	23.768	2.342	145.8
	2015	1.880	4.010	23.743	2.340	145.7
	2018	1.892	4.010	23.895	2.325	144.8
16-32	2016	1.896	4.010	23.945	2.324	144.7
	2017	1.897	4.010	23.958	2.324	144.7
	2019	1.893	4.010	23.907	2.331	145.1
	2002	1.888	4.010	23.844	2.329	145.0
	2001	1.883	4.010	23.781	2.334	145.3
16-40	2003	1.874	4.010	23.667	2.350	146.3
	2014	1.908	4.010	24.097	2.322	144.6
	2013	1.900	4.010	23.996	2.327	144.9
	2033	1.885	4.010	23.806	2.336	145.4
	2032	1.885	4.010	23.806	2.340	145.7
24-32	2030	1.878	4.010	23.718	2.342	145.8
	2031	1.878	4.010	23.718	2.342	145.8
	2034	1.891	4.010	23.882	2.330	145.1
	2027	1.892	4.010	23.895	2.332	145.2
	2025	1.898	4.010	23.970	2.329	145.0
24-40	2026	1.899	4.010	23.983	2.327	144.9
	2028	1.895	4.010	23.932	2.332	145.2
	2029	1.891	4.010	23.882	2.331	145.1
	2040	1.888	4.010	23.844	2.331	145.1
	2041	1.897	4.010	23.958	2.329	145.0
32-40	2042	1.890	4.010	23.869	2.333	145.3
	2043	1.886	4.010	23.819	2.335	145.4
	2044	1.890	4.010	23.869	2.329	145.0

TABLE B-3b. PHYSICAL DATA FOR LIMESTONE SPECIMENS USED IN COMPOUND-LOADING TESTS: DECREASING SEQUENCE (SPECIMENS RANK-ORDERED ON N_f)

Tensile Stress, psi	Spec. No.	Height, in.	Diameter, in.	Volume, $in.^3$	Bulk Specific Gravity	Bulk Density, pcf
	2037	1.893	4.010	23.907	2.335	145.4
	2035	1.877	4.010	23.705	2.342	145.8
24-16	2036	1.885	4.010	23.806	2.334	145.3
	2038	1.887	4.010	23.831	2.335	145.4
	2039	1.886	4.010	23.819	2.335	145.4
	2050	1.899	4.010	23.983	2.332	145.2
	2051	1.880	4.010	23.743	2.339	145.6
32-16	2054	1.885	4.010	23.806	2.337	145.5
	2052	1.881	4.010	23.756	2.339	145.6
	2053	1.882	4.010	23.768	2.341	145.8
	2045	1.886	4.010	23.819	2.336	145.4
	2046	1.890	4.010	23.869	2.328	144.9
32-24	2048	1.886	4.010	23.819	2.337	145.5
	2049	1.887	4.010	23.831	2.342	145.8
	2047	1.886	4.010	23.819	2.338	145.6
	2066	1.884	4.010	23.794	2.339	145.6
	2065	1.886	4.010	23.819	2.343	145.9
40-16	2004	1.887	4.010	23.831	2.345	146.0
	2006	1.887	4.010	23.831	2.339	145.6
	2005	1.882	4.010	23.768	2.340	145.7
	2063	1.886	4.010	23.819	2.338	145.6
	2064	1.898	4.010	23.970	2.327	144.9
40-24	2060	1.891	4.010	23.882	2.337	145.4
	2062	1.898	4.010	23.970	2.332	145.2
	2061	1.887	4.010	23.831	2.339	145.6
	2058	1.886	4.010	23.819	2.333	145.3
	2057	1.883	4.010	23.781	2.339	145.6
40-32	2055	1.886	4.010	23.819	2.334	145.3
	2059	1.885	4.010	23.806	2.336	145.4
	2056	1.878	4.010	23.718	2.346	146.1

TABLE B-4a. PHYSICAL DATA FOR GRAVEL SPECIMENS USED IN COMPOUND-LOADING TESTS: INCREASING SEQUENCE (SPECIMENS RANK-ORDERED ON N_f)

Tensile Stress, psi	Spec. No.	Height, in.	Diameter, in.	Volume, $in.^3$	Bulk Specific Gravity	Bulk Density, pcf
	2076	1.893	4.010	23.907	2.308	143.7
	2077	1.885	4.010	23.806	2.314	144.1
16-24	2080	1.902	4.010	24.021	2.299	143.1
	2079	1.895	4.010	23.932	2.304	143.4
	2078	1.894	4.010	23.920	2.298	143.1
	2075	1.902	4.010	24.021	2.304	143.4
	2074	1.885	4.010	23.806	2.318	144.3
16-32	2072	1.908	4.010	24.097	2.288	142.5
	2073	1.897	4.010	23.958	2.319	144.4
	2122	1.897	4.010	23.958	2.306	143.6
	2068	1.913	4.010	24.160	2.287	142.4
	2067	1.905	4.010	24.059	2.296	142.9
16-40	2010	1.889	4.010	23.857	2.310	143.8
	2008	1.886	4.010	23.819	2.318	144.3
	2007	1.880	4.010	23.743	2.324	144.7
	2088	1.886	4.010	23.819	2.322	144.6
	2086	1.878	4.010	23.718	2.320	144.4
24-32	2087	1.880	4.010	23.743	2.321	144.5
	2089	1.885	4.010	23.806	2.321	144.5
	2090	1.886	4.010	23.819	2.317	144.3
	2085	1.889	4.010	23.857	2.319	144.4
	2082	1.885	4.010	23.806	2.317	144.3
24-40	2084	1.890	4.010	23.869	2.317	.4413
	2083	1.876	4.010	23.693	2.326	144.8
	2081	1.905	4.010	24.059	2.301	143.3
	2099	1.900	4.010	23.996	2.306	143.6
	2100	1.891	4.010	23.882	2.310	143.8
32-40	2096	1.887	4.010	23.831	2.318	144.3
	2098	1.893	4.010	23.907	2.308	143.7
	2097	1.897	4.010	23.958	2.303	143.4

TABLE B-4b. PHYSICAL DATA FOR GRAVEL SPECIMENS USED IN COMPOUND-LOADING TESTS: DECREASING SEQUENCE (SPECIMENS RANK-ORDERED ON N_f)

Tensile Stress, psi	Spec. No.	Height, in.	Diameter, in.	Volume, $in.^3$	Bulk Specific Gravity	Bulk Density, pcf
	2092	1.886	4.010	23.819	2.316	144.2
	2094	1.896	4.010	23.945	2.308	143.7
24-16	2095	1.891	4.010	23.882	2.315	144.1
	2091	1.901	4.010	24.008	2.304	143.4
	2093	1.909	4.010	24.109	2.296	142.9
	2109	1.899	4.010	23.983	2.301	143.3
	2107	1.897	4.010	23.958	2.311	143.9
32-16	2110	1.895	4.010	23.932	2.309	143.8
	2106	1.881	4.010	23.756	2.322	144.6
	2108	1.898	4.010	23.970	2.309	143.8
	2102	1.897	4.010	23.958	2.310	143.8
	2104	1.884	4.010	23.794	2.320	144.4
32-24	2103	1.883	4.010	23.781	2.322	144.6
	2105	1.894	4.010	23.920	2.306	143.6
	2101	1.906	4.010	24.071	2.300	143.2
	2009	1.890	4.010	23.869	2.319	144.4
	2012	1.895	4.010	23.932	2.314	144.1
40-16	2069	1.907	4.010	24.084	2.294	142.8
	2116	1.889	4.010	23.857	2.320	144.4
	2070	1.878	4.010	23.718	2.324	144.7
	2121	1.885	4.010	23.806	2.316	144.2
	2119	1.885	4.010	23.806	2.318	144.3
40-24	2117	1.891	4.010	23.882	2.305	143.5
	2120	1.887	4.010	23.831	2.313	144.0
	2118	1.881	4.010	23.756	2.320	144.4
	2113	1.905	4.010	24.059	2.299	143.1
	2111	1.910	4.010	24.122	2.291	142.6
40-32	2115	1.891	4.010	23.882	2.310	143.8
	2114	1.892	4.010	23.895	2.312	143.9
	2112	1.898	4.010	23.970	2.304	143.4

APPENDIX C

SIMPLE-LOADING CONSTANT STRESS AMPLITUDE SPECIMEN DATA

TABLE C-1. LIMESTONE FAILURE CONDITION DATA FOR CONSTANT STRESS OF 8 PSI

7% AC-10
Medium Gradation
Sinusoidal Pulse (0.6 sec. rest time), 1 HZ

Temperature 75°F
Preload 20 lb

Spec. No.	Rank m	P(m), %	Reduced Normal Variate X	N_8	Log N_8	$\bar{N}_8$	S	CV, %
282	1	16.667	-0.967	178200	5.2509	5.3315 (214536)	0.1017 (52351)	24.40
280	2	33.333	-0.431	190800	5.2806			
285	3	50.000	0.000	200700	5.3025	Two-sided 95% conficence limits on N_8		
288	4	66.667	+0.431	206700	5.3153			
286	5	83.333	+0.967	322200	5.5081	5.2052 - 5.4578 (160398 - 286946)		

TABLE C-2. LIMESTONE FAILURE CONDITION DATA FOR CONSTANT STRESS OF 16 PSI

7% AC-10
Medium Gradation
Sinusoidal Pulse (0.6 sec. rest time), 1 HZ

Temperature 75°F
Preload 20 lb

Spec. No.	Rank m	P(m), %	Reduced Normal Variate X	$N_{1\varepsilon}$	Log $N_{1\varepsilon}$	$\overline{N}_{1\varepsilon}$	S	CV, %
396	1	11.111	-1.221	6041	3.7811	3.9094	0.1078	25.99
395	2	22.222	-0.765	6498	3.8062	(8117)	(2110)	
456	3	33.333	-0.431	6800	3.8325			
558	4	44.444	-0.140	7172	3.8556			
557	5	55.556	+0.140	8441	3.9264			
556	6	66.667	+0.431	8909	3.9498	Two-sided 95% confidence limits on $\overline{N}_{1\varepsilon}$		
458	7	77.778	+0.765	11093	4.0450			
457	8	88.889	+1.221	11801	4.0719	3.8177 - 3.9994 (6572 - 9986)		

TABLE C-3. LIMESTONE FAILURE CONDITION DATA FOR CONSTANT STRESS OF 24 PSI

7% AC-10
Medium Gradation
Sinusoidal Pulse (0.6 sec. rest time), 1 HZ

Temperature 75°F
Preload 20 lb

Spec. No.	Rank m	P(m), %	Reduced Normal Variate X	N_{24}	Log N_{24}	$\bar{N}_{24}$	S	CV, %
453	1	16.667	-0.967	1405	3.1477	3.2120 (1629)	0.0632 (241)	14.79
455	2	33.333	-0.431	1412	3.1498			
382	3	50.000	0.000	1645	3.2162	Two-sided 95% confidence limits on $\bar{N}_{24}$		
454	4	66.667	+0.431	1812	3.2582			
381	5	83.333	+0.967	1942	3.2882	3.1336 - 3.2905 (1360 - 1952)		

TABLE C-4. LIMESTONE FAILURE CONDITION DATA FOR CONSTANT STRESS OF 32 PSI

7% AC-10
Medium Gradation
Sinusoidal Pulse (0.6 sec. rest time), 1 HZ

Temperature 75°F
Preload 20 lb

Spec. No.	Rank m	P(m), %	Reduced Normal Variate X	N_{32}	Log N_{32}	$\bar{N}_{32}$	S	CV, %
451	1	16.667	-0.967	488	2.6884	2.7563 (571)	0.0614 (82)	14.36
452	2	33.333	-0.431	512	2.7043			
391	3	50.000	0.000	569	2.7551	Two-sided 95% confidence limits on $\bar{N}_{32}$		
450	4	66.667	+0.431	612	2.7868			
318	5	83.333	+0.967	695	2.8420	2.6800 - 2.8326 (479 - 680)		

TABLE C-5. LIMESTONE FAILURE CONDITION DATA FOR CONSTANT STRESS OF 40 PSI

7% AC-10
Medium Gradation
Sinusoidal Pulse (0.6 sec. rest time), 1 HZ

Temperature 75°F
Preload 20 lb

Spec. No.	Rank m	P(m), %	Reduced Normal Variate X	N_{40}	Log N_{40}	$\bar{N}_{40}$	S	CV, %
386	1	11.111	-1.221	273	2.4361	2.5475 (353)	0.0930 (78)	22.10
387	2	22.222	-0.765	287	2.4579			
389	3	33.333	-0.431	315	2.4983			
388	4	44.444	-0.140	333	2.5224			
728	5	55.556	+0.140	350	2.5441			
730	6	66.667	+0.431	358	2.5539	Two-sided 95% confidence limits on $\bar{N}_{40}$		
110	7	77.778	+0.765	475	2.6767			
729	8	88.889	+1.221	490	2.6902	2.4697 - 2.6252 (295 - 422)		

TABLE C-6. GRAVEL FAILURE CONDITION DATA FOR CONSTANT STRESS OF 8 PSI

7% AC-10
Medium Gradation
Sinusoidal Pulse (0.6 sec. rest time), 1 HZ

Temperature 75°F
Preload 20 lb

Spec. No.	Rank m	P(m), %	Reduced Normal Variate X	N_8	Log N_8	$\overline{N}_8$	S	CV, %
115	1	16.667	-0.967	199560	5.3001	5.5172 (329003)	0.1705 (145062)	44.09
117	2	33.333	-0.431	270780	5.4326			
119	3	50.000	0.000	329100	5.5173	Two-sided 95% confidence limits on $\overline{N}_8$		
129	4	66.667	+0.431	378000	5.5775			
123	5	83.333	+0.967	573720	5.7587	5.3056 - 5.7389 (202116 - 535673)		

TABLE C-7. GRAVEL FAILURE CONDITION DATA FOR CONSTANT STRESS OF 16 PSI

7% AC-10
Medium Gradation
Sinusoidal Pulse (0.6 sec. rest time), 1 HZ

Temperature 75°F
Preload 20 lb

Spec. No.	Rank m	P(m), %	Reduced Normal Variate X	N_{1e}	Log N_{1e}	$\bar{N}_{1e}$	S	CV, %
465	1	10.000	-1.282	3307	3.5194	3.7749 (5955)	0.1590 (2412)	40.50
407	2	20.000	-0.841	3648	3.5621			
466	3	30.000	-0.524	5245	3.7197			
467	4	40.000	-0.253	6137	3.7880			
339	5	50.000	0.000	6293	3.7989	Two-sided 95% confidence limits on $\bar{N}_{1e}$		
561	6	60.000	+0.253	6496	3.8126			
559	7	70.000	+0.524	6987	3.8443			
560	8	80.000	+0.841	7865	3.8957	3.6527 - 3.8971 (4495 - 7890)		
338	9	90.000	+1.282	10807	4.0337			

TABLE C-8. GRAVEL FAILURE CONDITION DATA FOR CONSTANT STRESS OF 24 PSI

7% AC-10
Medium Gradation
Sinusoidal Pulse (0.6 sec. rest time), 1 HZ

Temperature 75°F
Preload 20 lb

Spec. No.	Rank m	P(m), %	Reduced Normal Variate X	N_{24}	Log N_{24}	$\bar{N}_{24}$	S	CV, %
462	1	10.000	-1.282	784	2.8943	3.1382 (1375)	0.2118 (802)	58.33
463	2	20.000	-0.841	784	2.8943			
464	3	30.000	-0.524	850	2.9294			
521	4	40.000	-0.253	1286	3.1092			
519	5	50.000	0.000	1317	3.1196	Two-sided 95% confidence limits on $\bar{N}_{24}$		
566	6	60.000	+0.253	1532	3.1853			
520	7	70.000	+0.524	1719	3.2353			
102	8	80.000	+0.841	2500	3.3979	2.9754 - 3.3011 (945 - 2000)		
107	9	90.000	+1.282	3012	3.4789			

TABLE C-9. GRAVEL FAILURE CONDITION DATA FOR CONSTANT STRESS OF 32 PSI

7% AC-10
Medium Gradation
Sinusoidal Pulse (0.6 sec. rest time), 1 HZ

Temperature 75°F
Preload 20 lb

Spec. No.	Rank m	P(m), %	Reduced Normal Variate X	N_{32}	Log N_{32}	$\overline{N}_{32}$	S	CV, %
461	1	10.000	-1.282	258	2.4116	2.7018 (503)	0.2210 (311)	61.83
459	2	20.000	-0.841	273	2.4362			
460	3	30.000	-0.524	296	2.4713			
524	4	40.000	-0.253	536	2.7292			
523	5	50.000	0.000	548	2.7388	Two-sided 95% confidence limits on $\overline{N}_{32}$		
522	6	60.000	+0.253	586	2.7679			
565	7	70.000	+0.524	609	2.7846			
380	8	80.000	+0.841	866	2.9375	2.5320 - 2.8717 (340 - 744)		
103	9	90.000	+1.282	1095	3.0394			

TABLE C-10. GRAVEL FAILURE CONDITION DATA FOR CONSTANT STRESS OF 40 PSI

7% AC-10
Medium Gradation
Sinusoidal Pulse (0.6 sec. rest time), 1 HZ

Temperature 75°F
Preload 20 lb

Spec. No.	Rank m	P(m), %	Reduced Normal Variate X	N_{40}	Log N_{40}	$\bar{N}_{40}$	S	CV, %
2011	1	10.000	-1.282	163	2.2122	2.6329 (429)	0.2524 (322)	75.06
564	2	20.000	-0.841	266	2.4249			
563	3	30.000	-0.524	292	2.4654			
562	4	40.000	-0.253	313	2.4955			
106	5	50.000	0.000	500	2.6990	Two-sided 95% confidence limits on $\bar{N}_{40}$		
101	6	60.000	+0.253	525	2.7202			
105	7	70.000	+0.524	650	2.8129			
104	8	80.000	+0.841	690	2.8388	2.4389 - 2.8269 (275 - 671)		
130	9	90.000	+1.282	1065	3.0273			

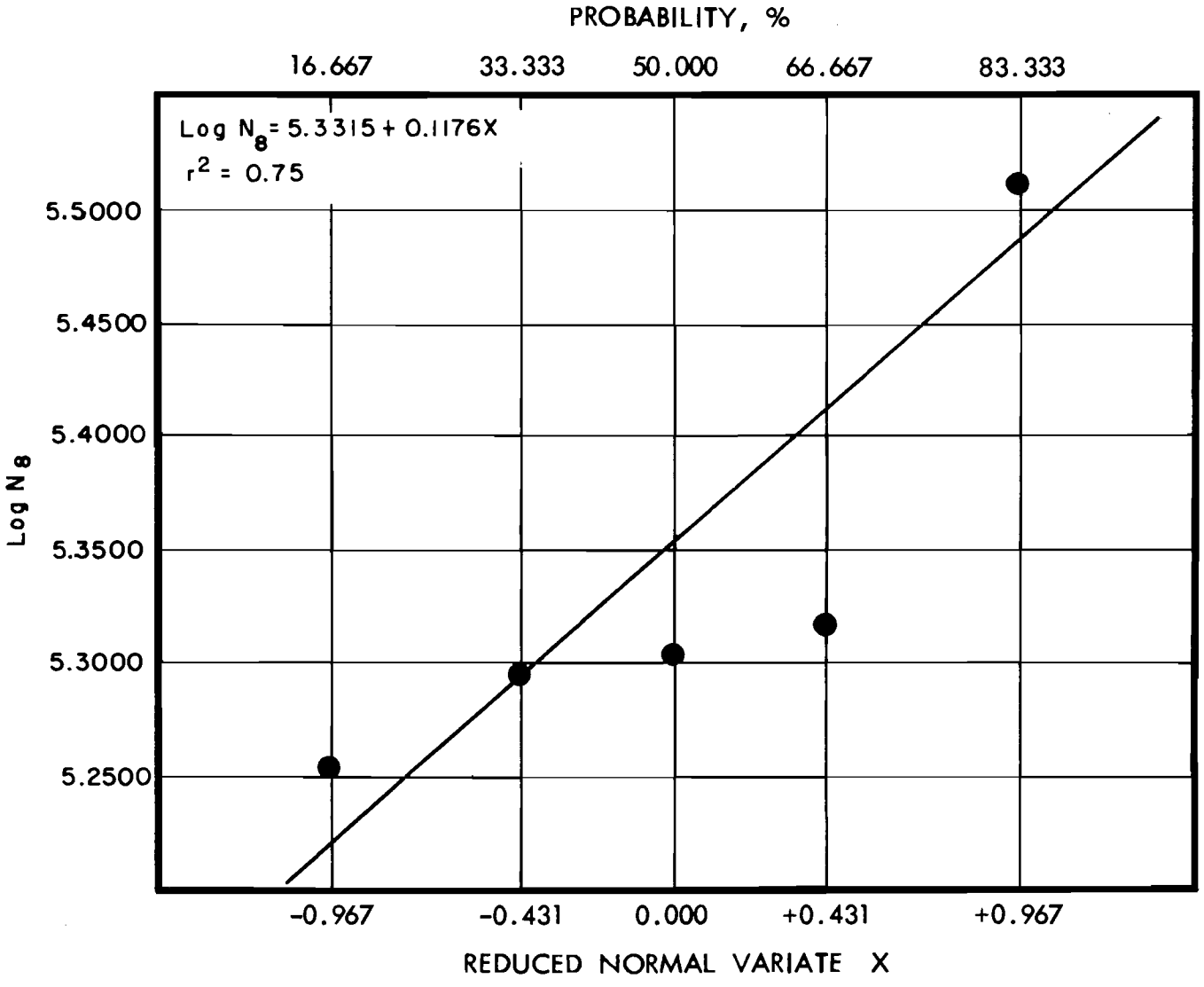

Fig C-1. Logarithm of fatigue life versus probability of failure: 8 psi, limestone.

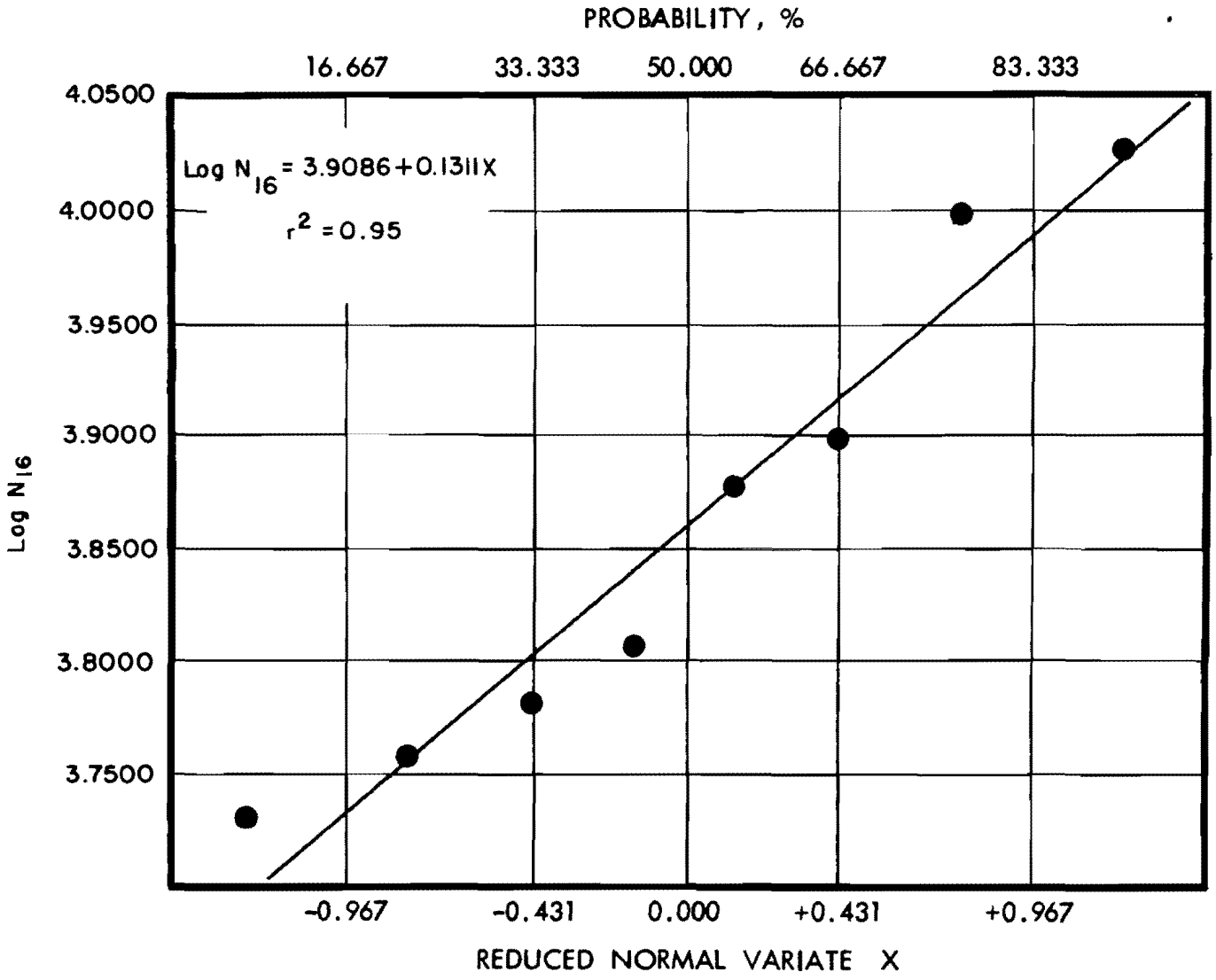

Fig C-2. Logarithm of fatigue life versus probability of failure: 16 psi, limestone.

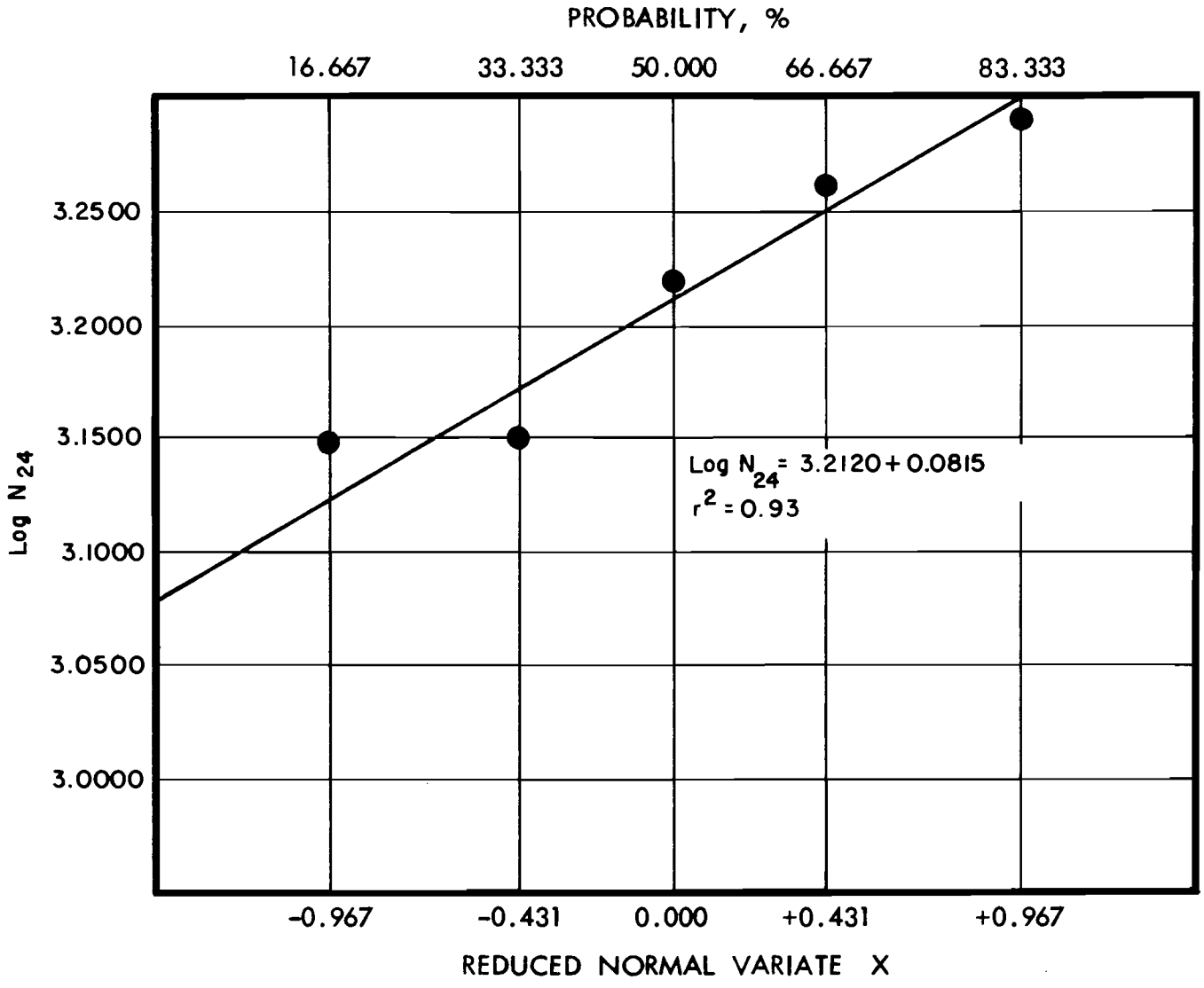

Fig C-3. Logarithm of fatigue life versus probability of failure: 24 psi, limestone.

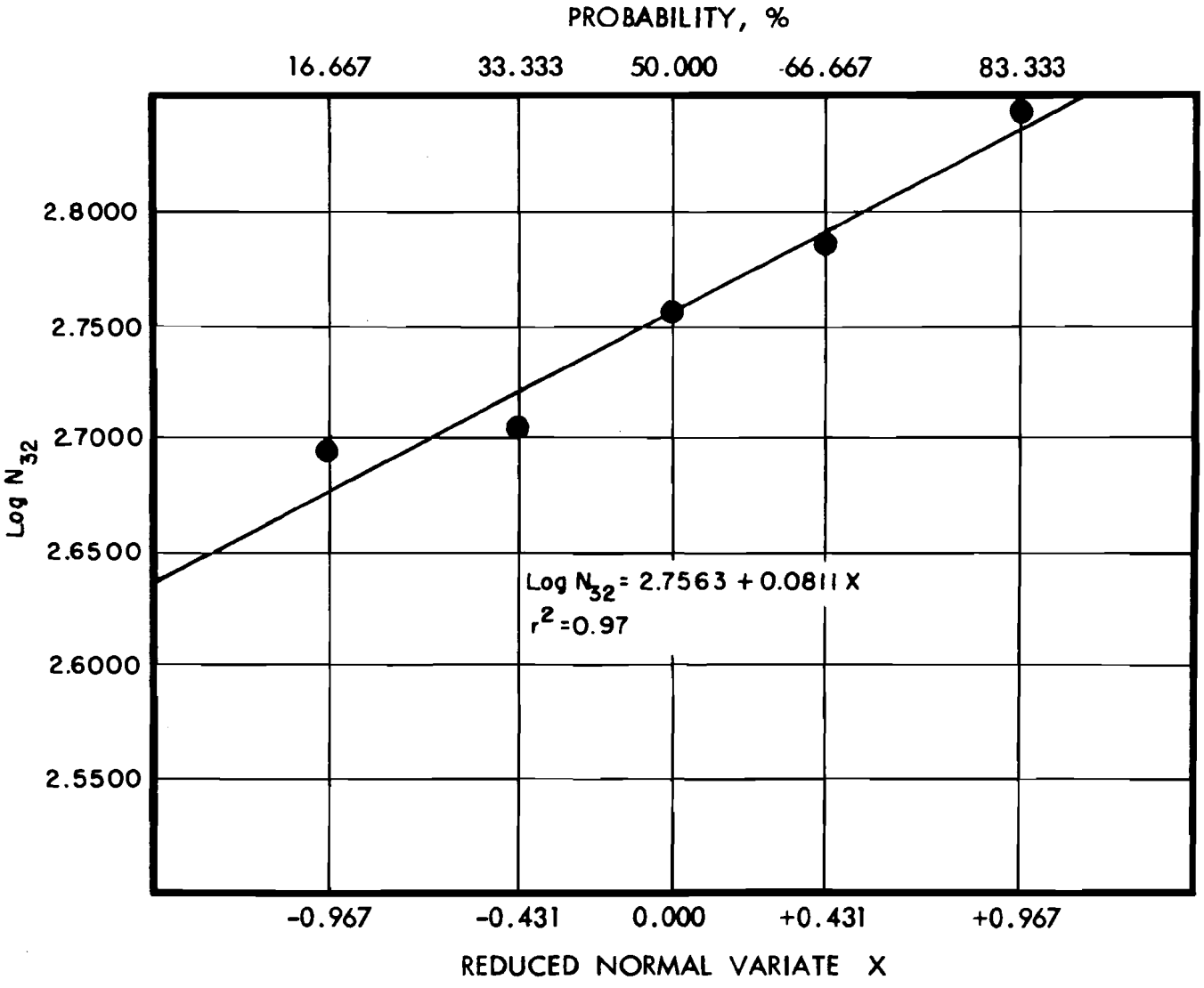

Fig C-4. Logarithm of fatigue life versus probability of failure: 32 psi, limestone.

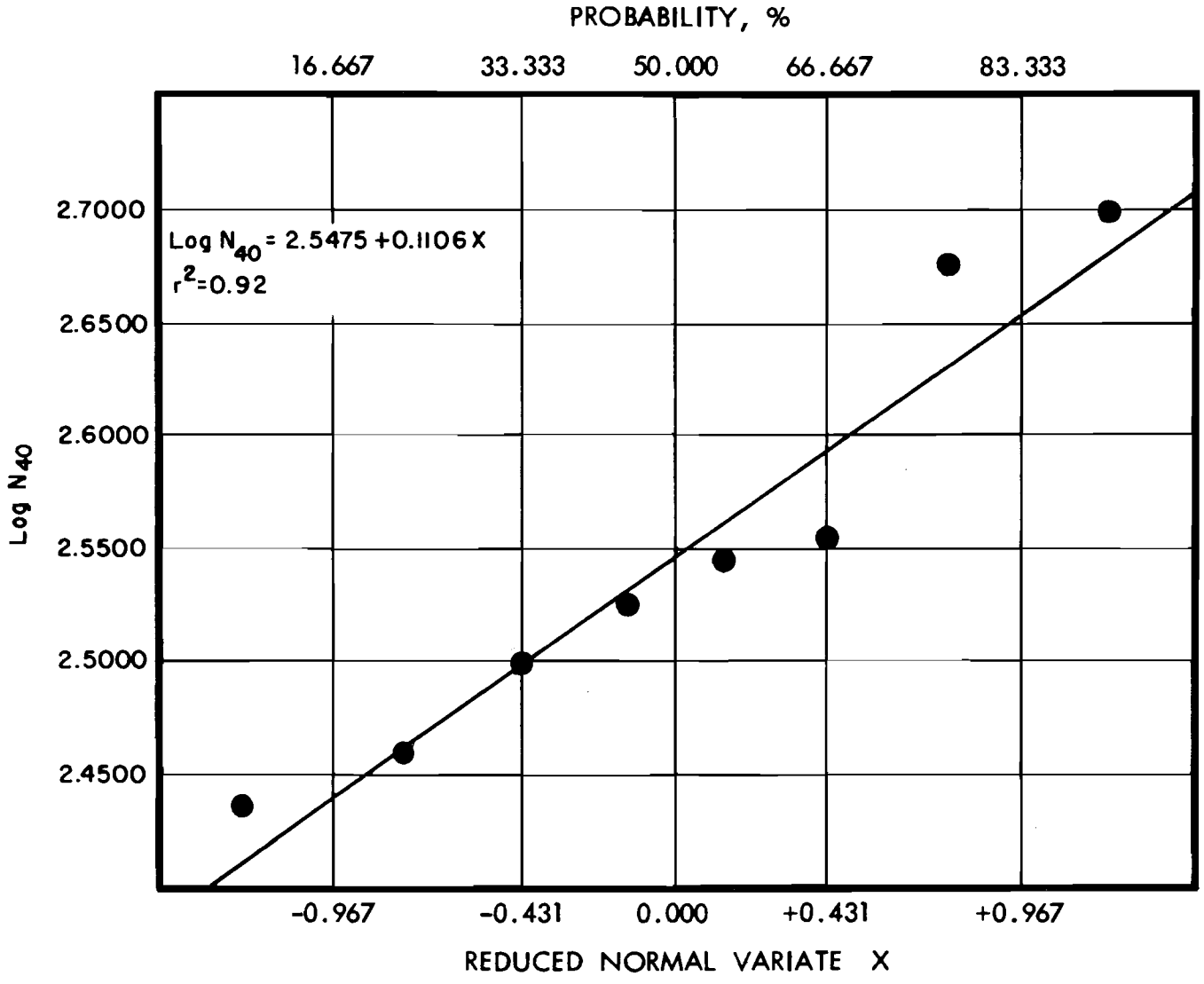

Fig C-5. Logarithm of fatigue life versus probability of failure: 40 psi, limestone.

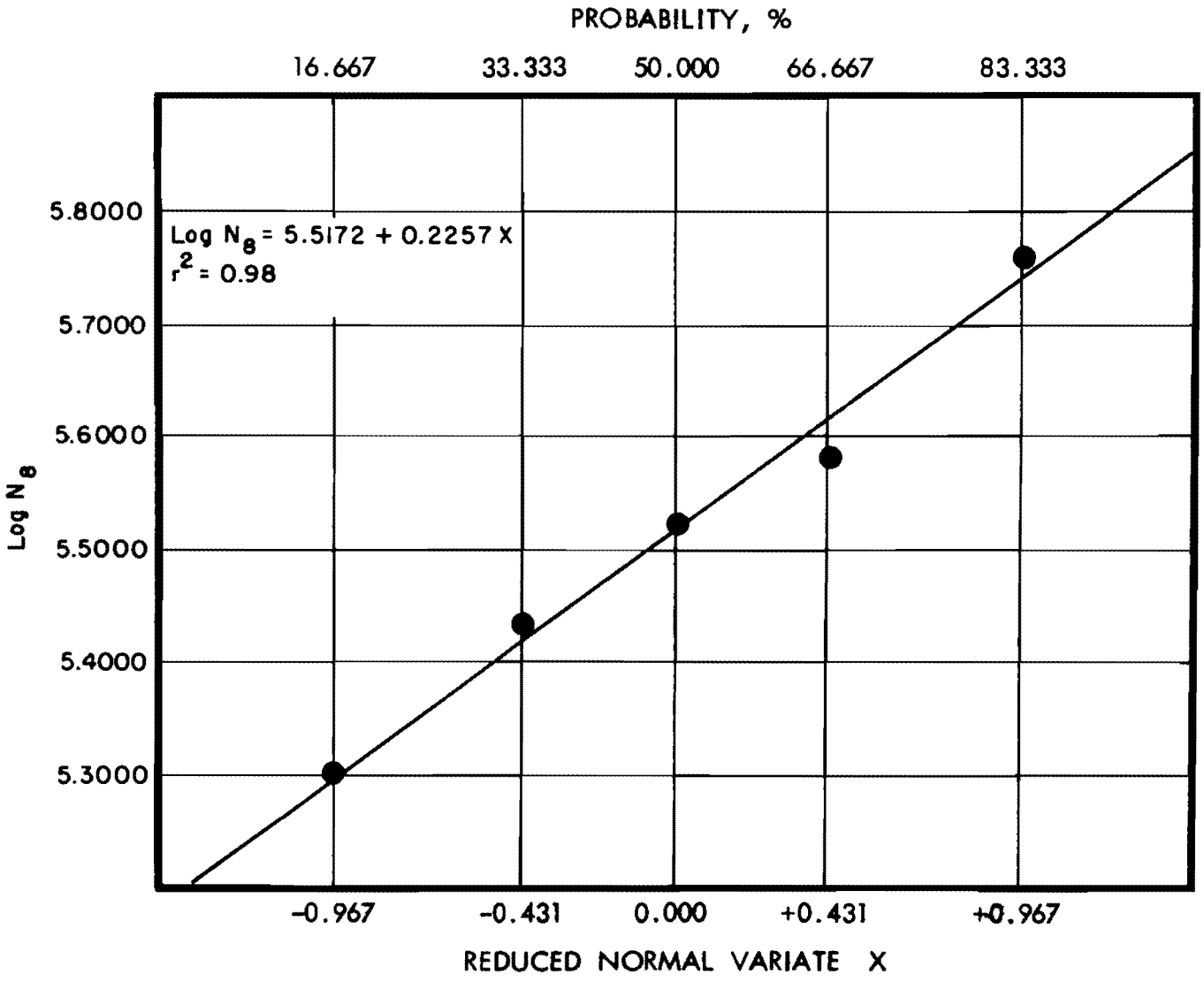

Fig C-6. Logarithm of fatigue life versus probability of failure: 8 psi, gravel.

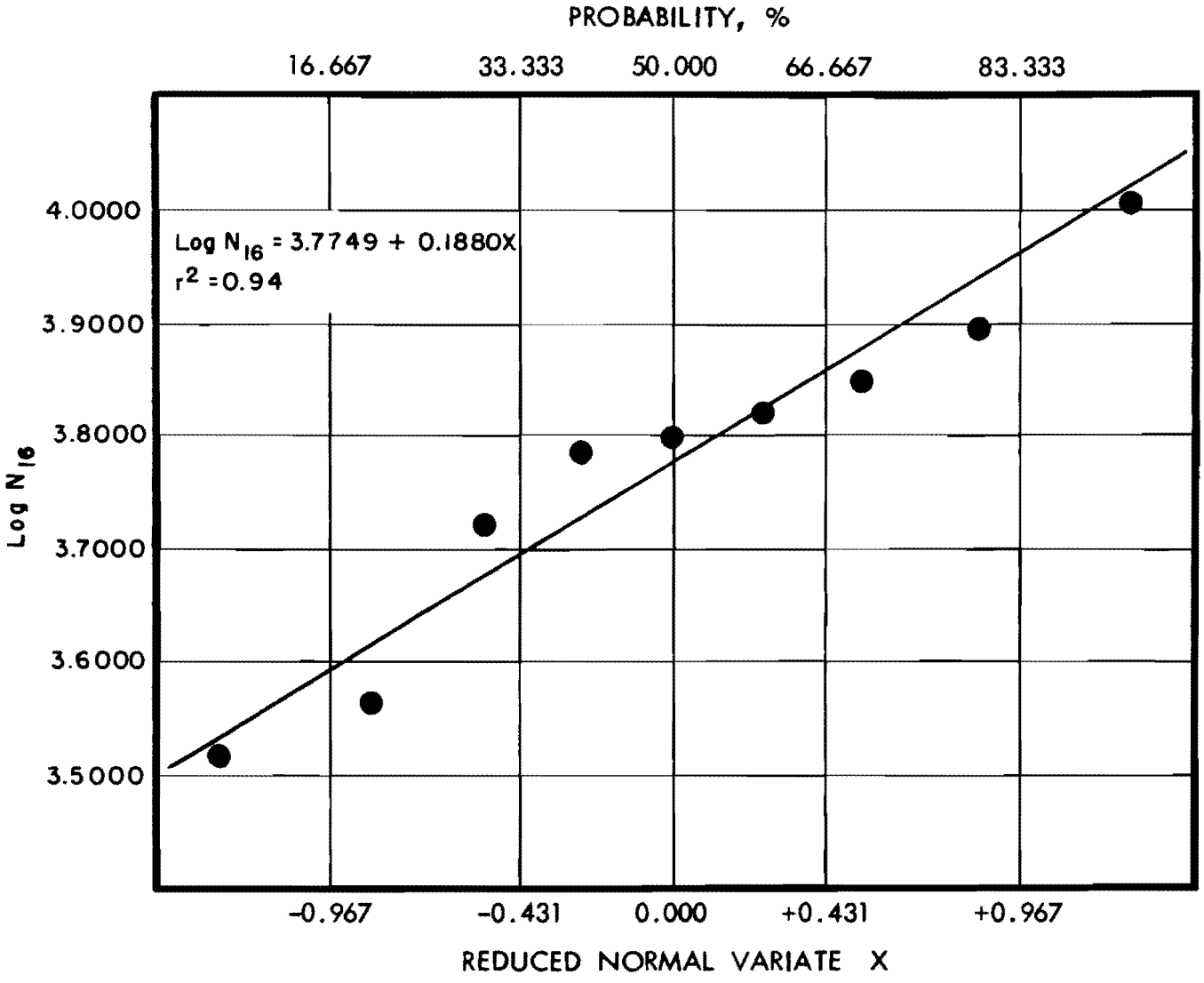

Fig C-7. Logarithm of fatigue life versus probability of failure: 16 psi, gravel.

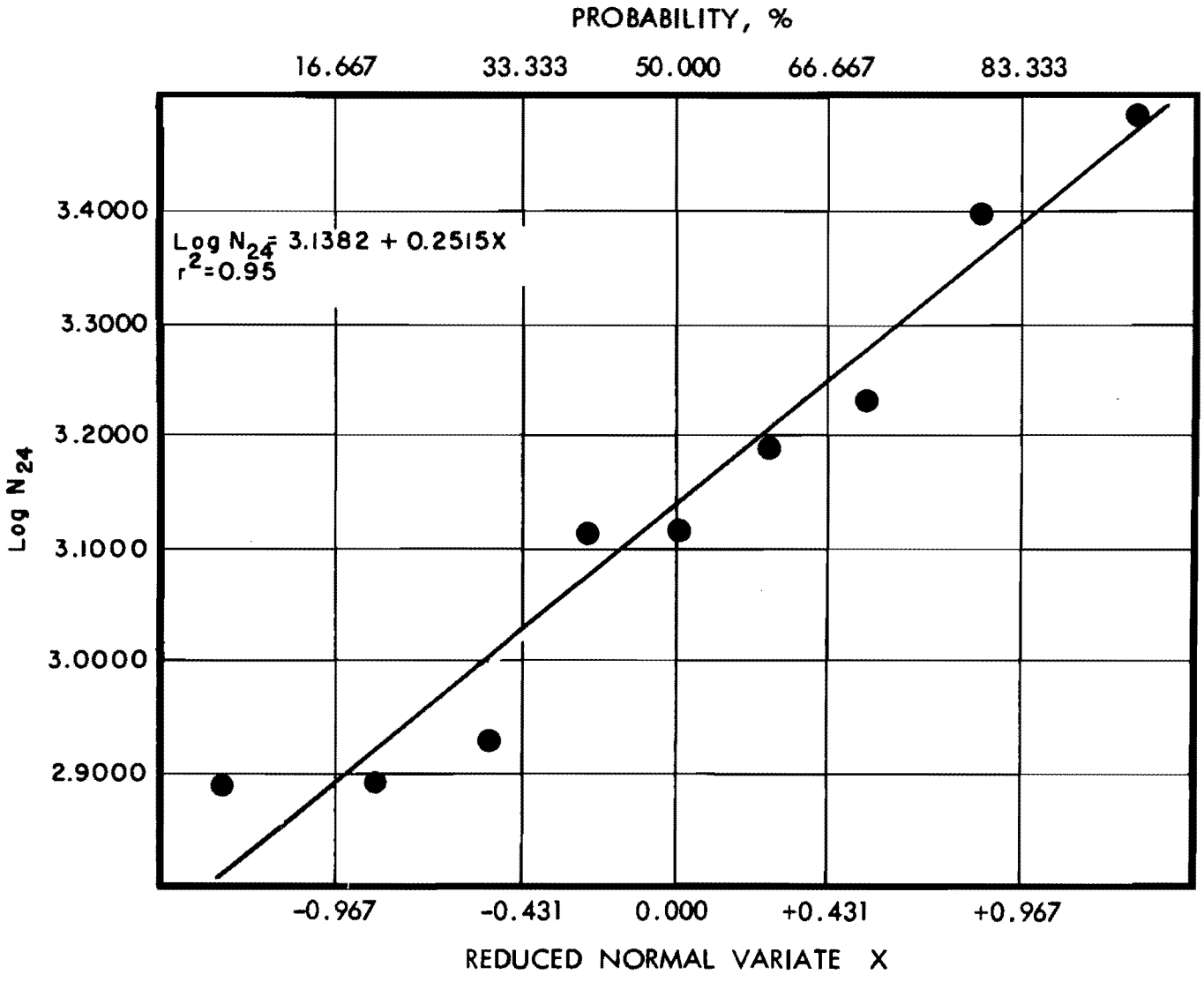

Fig C-8. Logarithm of fatigue life versus probability of failure: 24 psi, gravel.

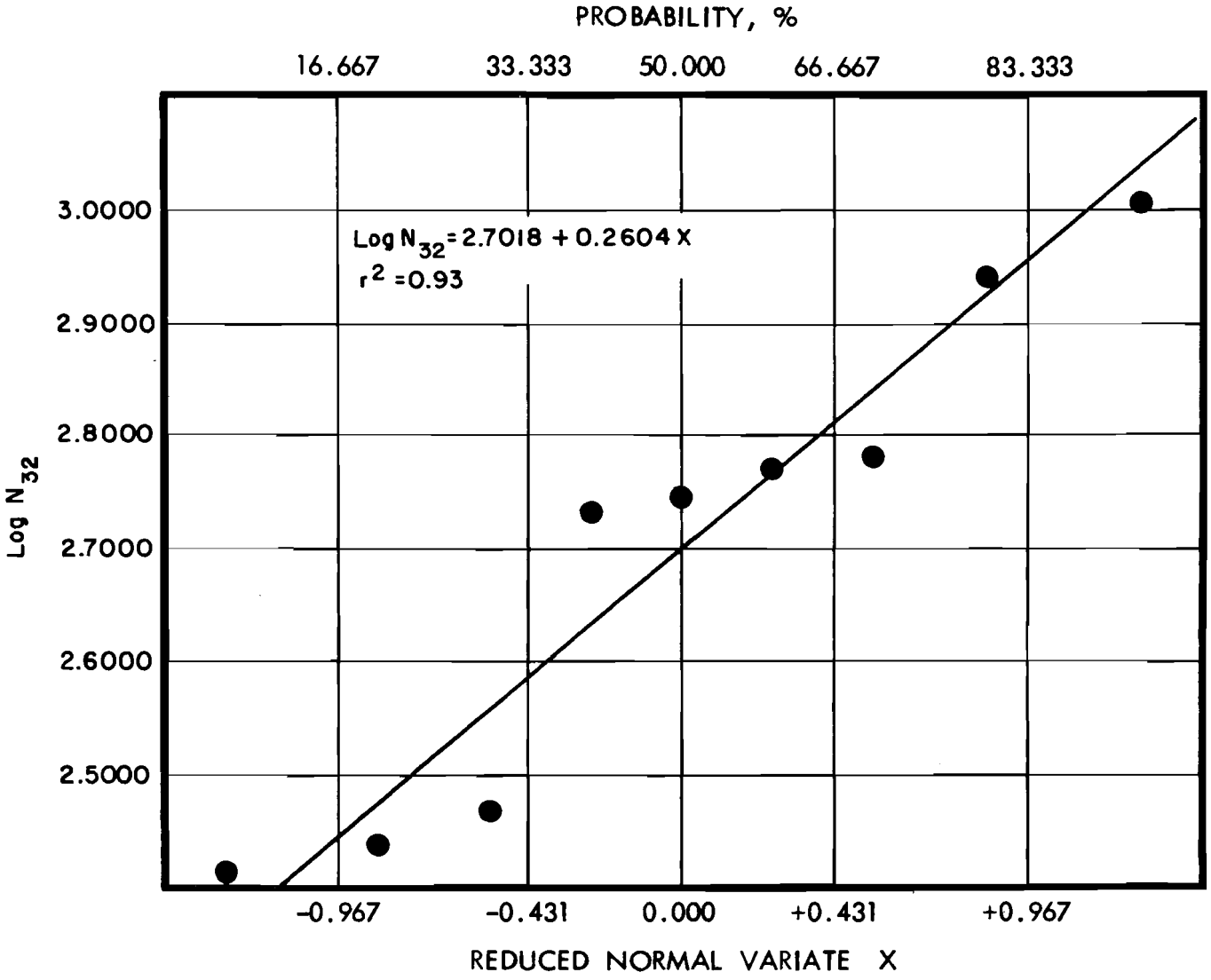

Fig C-9. Logarithm of fatigue life versus probability of failure: 32 psi, gravel.

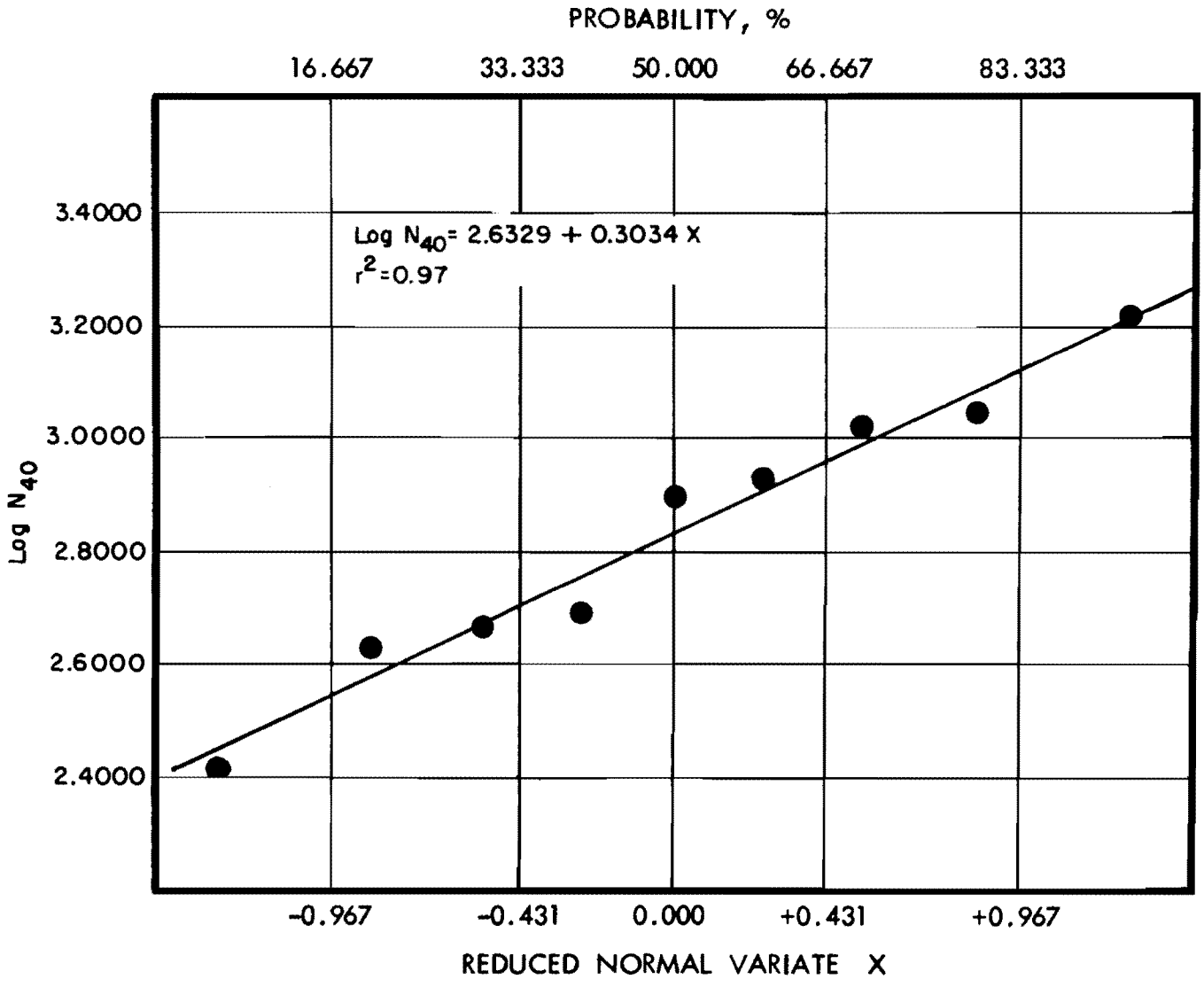

Fig C-10. Logarithm of fatigue life versus probability of failure: 40 psi, gravel.

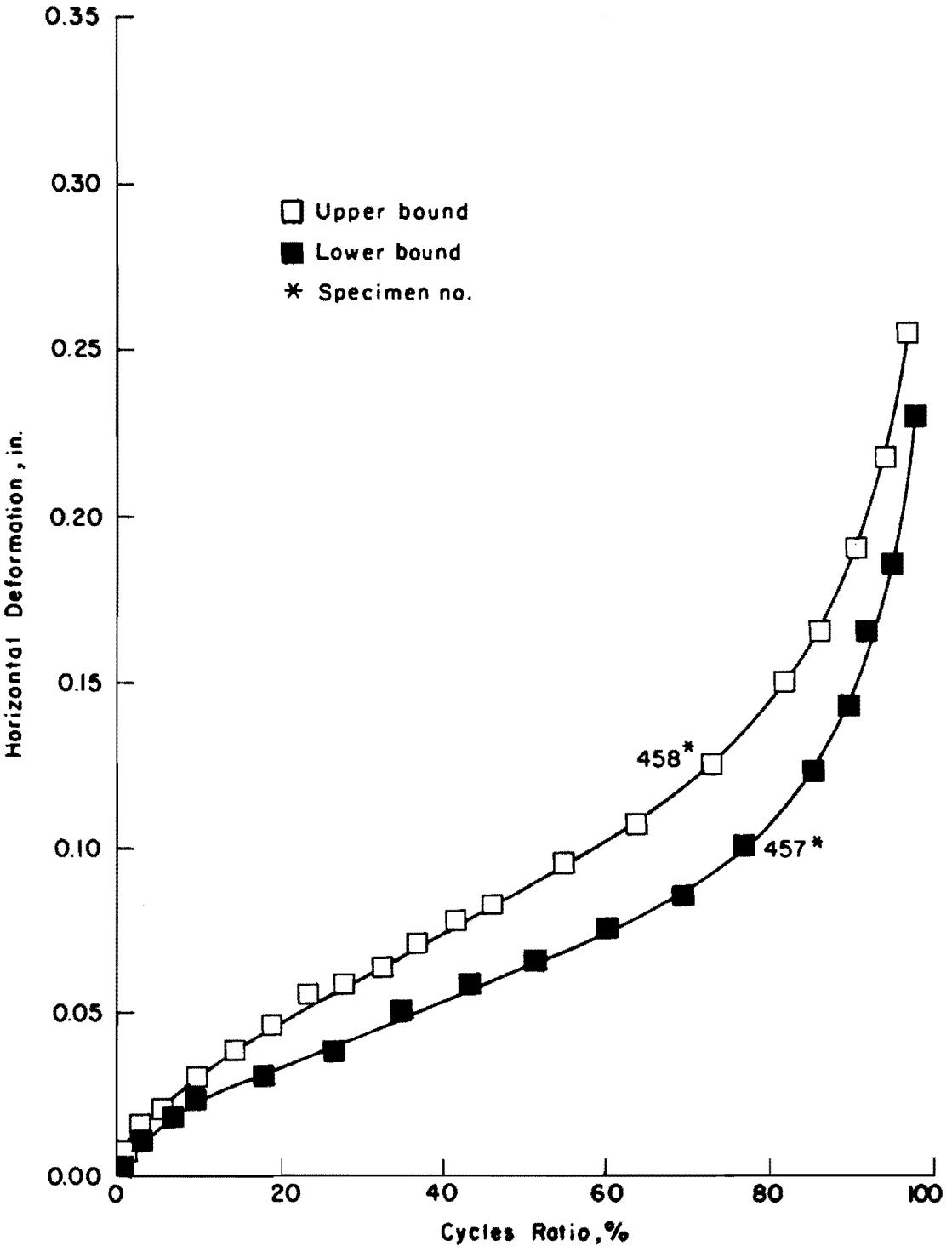

Fig C-11. Limiting horizontal deformations in simple-loading: 16 psi, limestone.

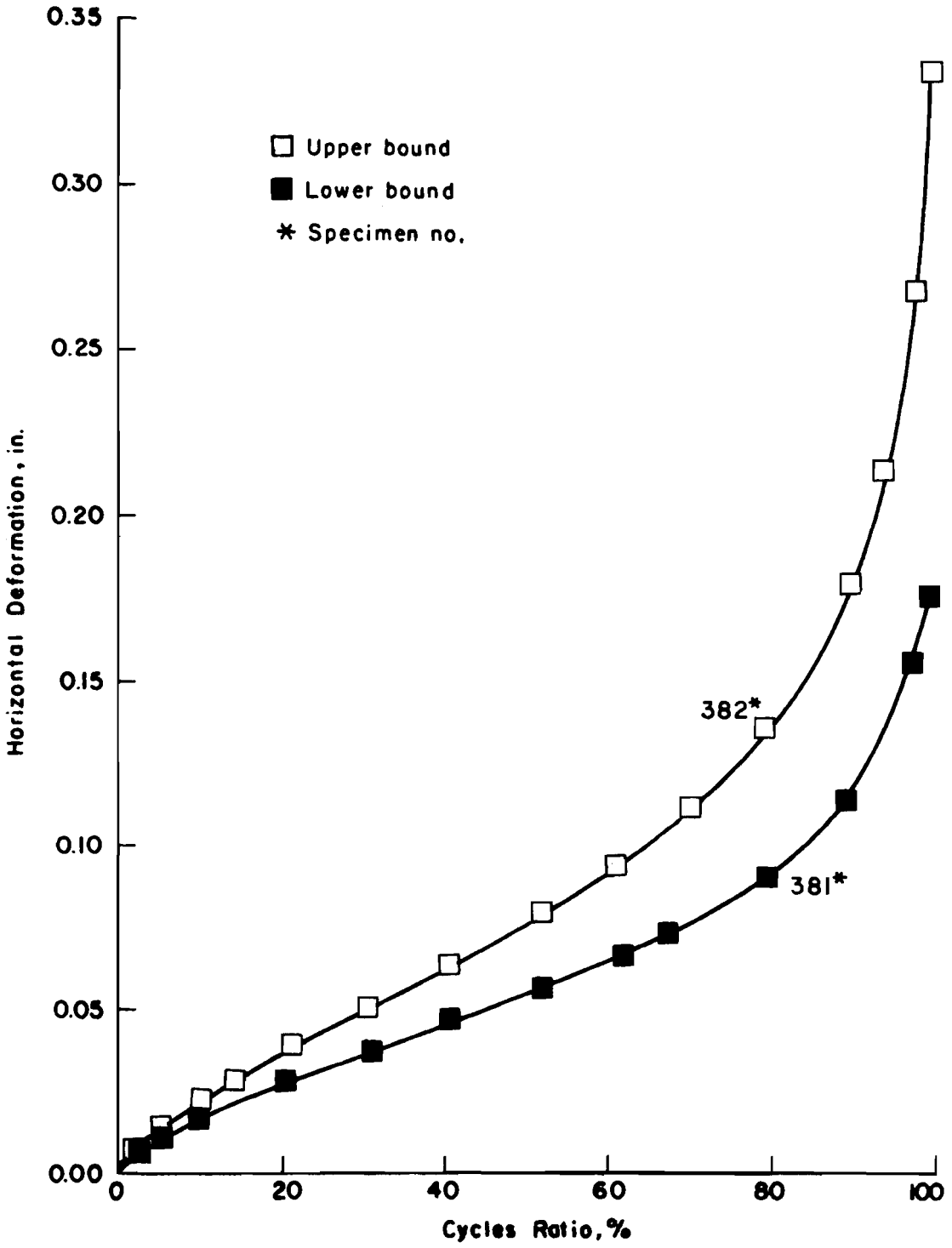

Fig C-12. Limiting horizontal deformations in simple-loading: 24 psi, limestone.

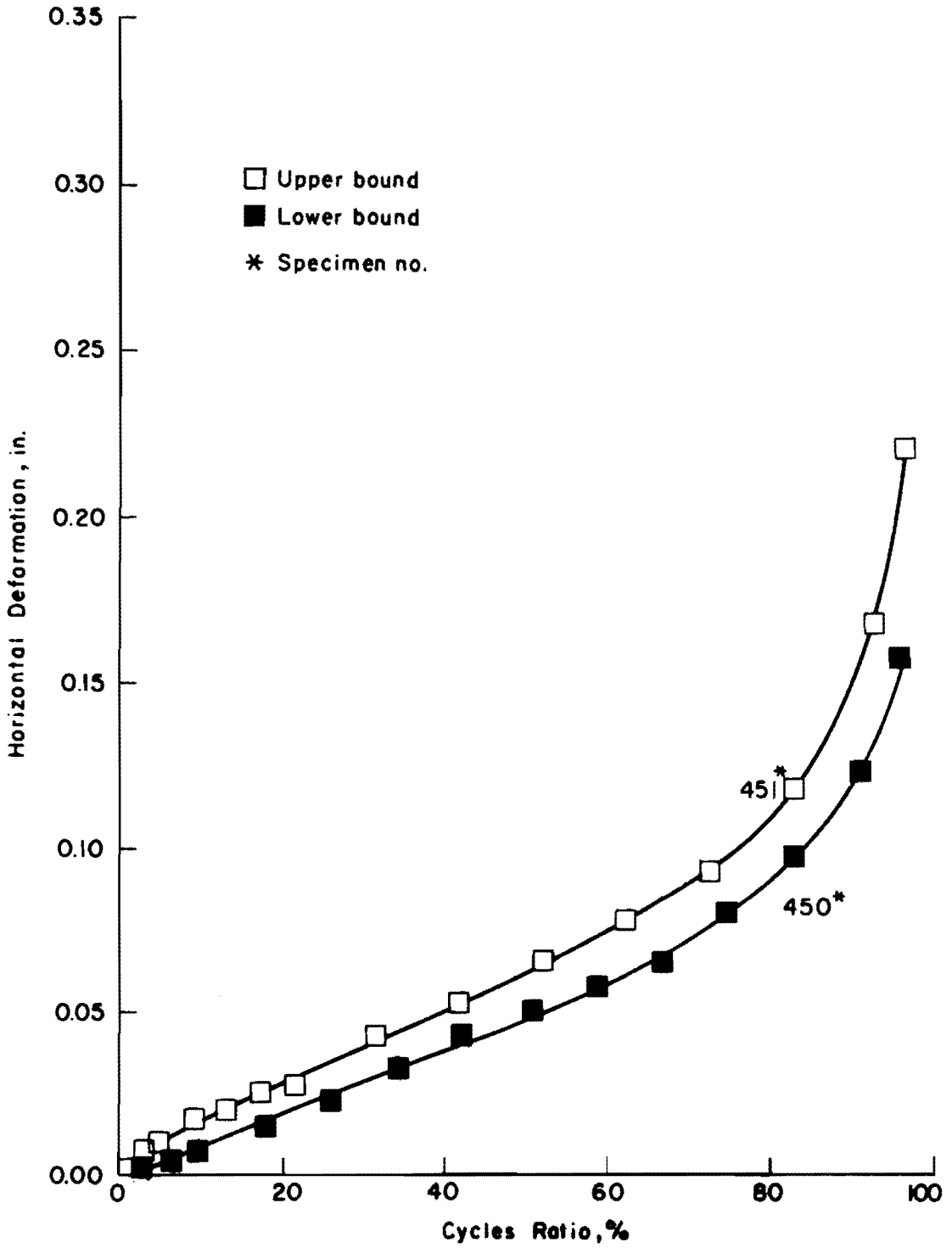

Fig C-13. Limiting horizontal deformations in simple-loading: 32 psi, limestone.

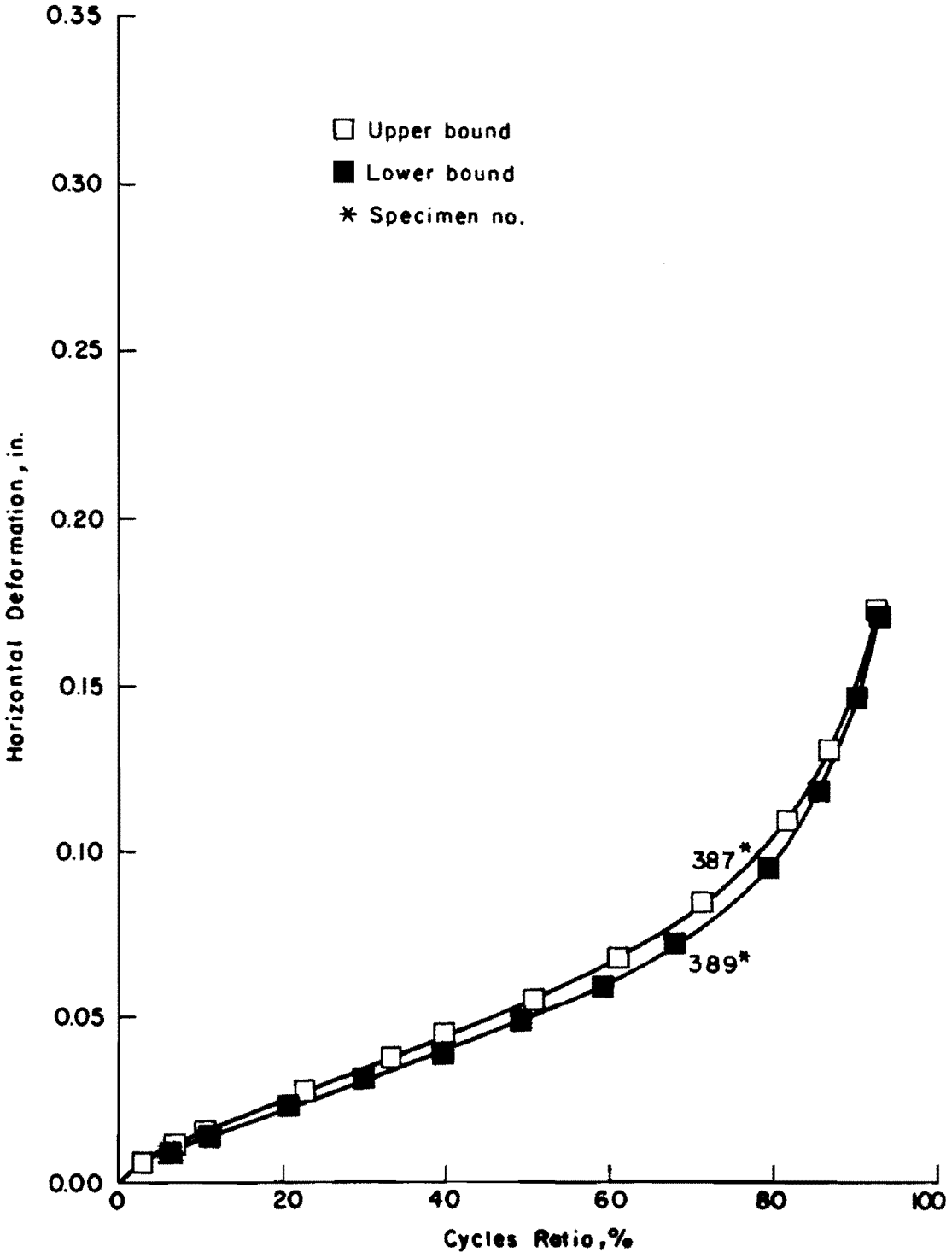

Fig C-14. Limiting horizontal deformations in simple-loading: 40 psi, limestone.

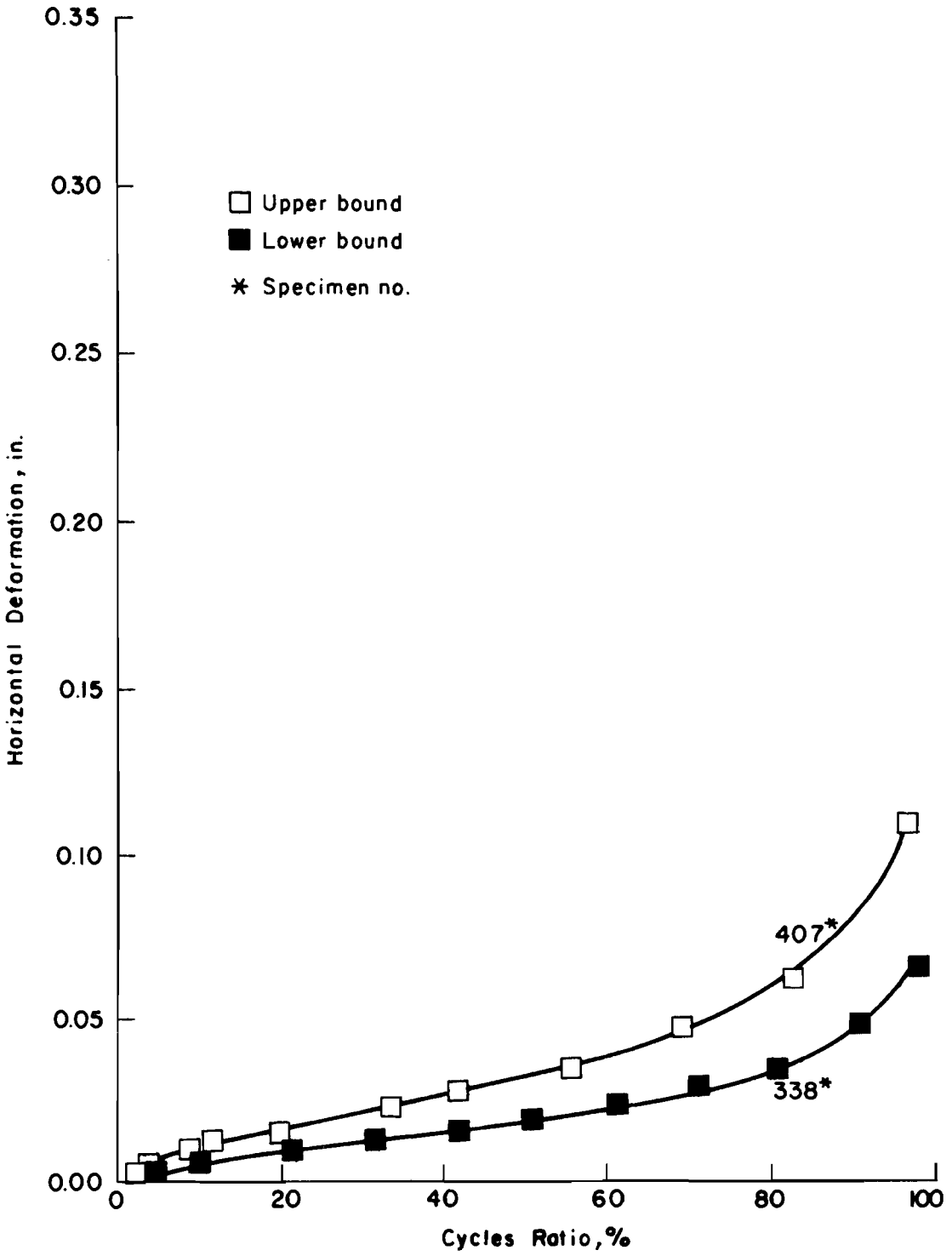

Fig C-15. Limiting horizontal deformations in simple-loading: 16 psi, gravel.

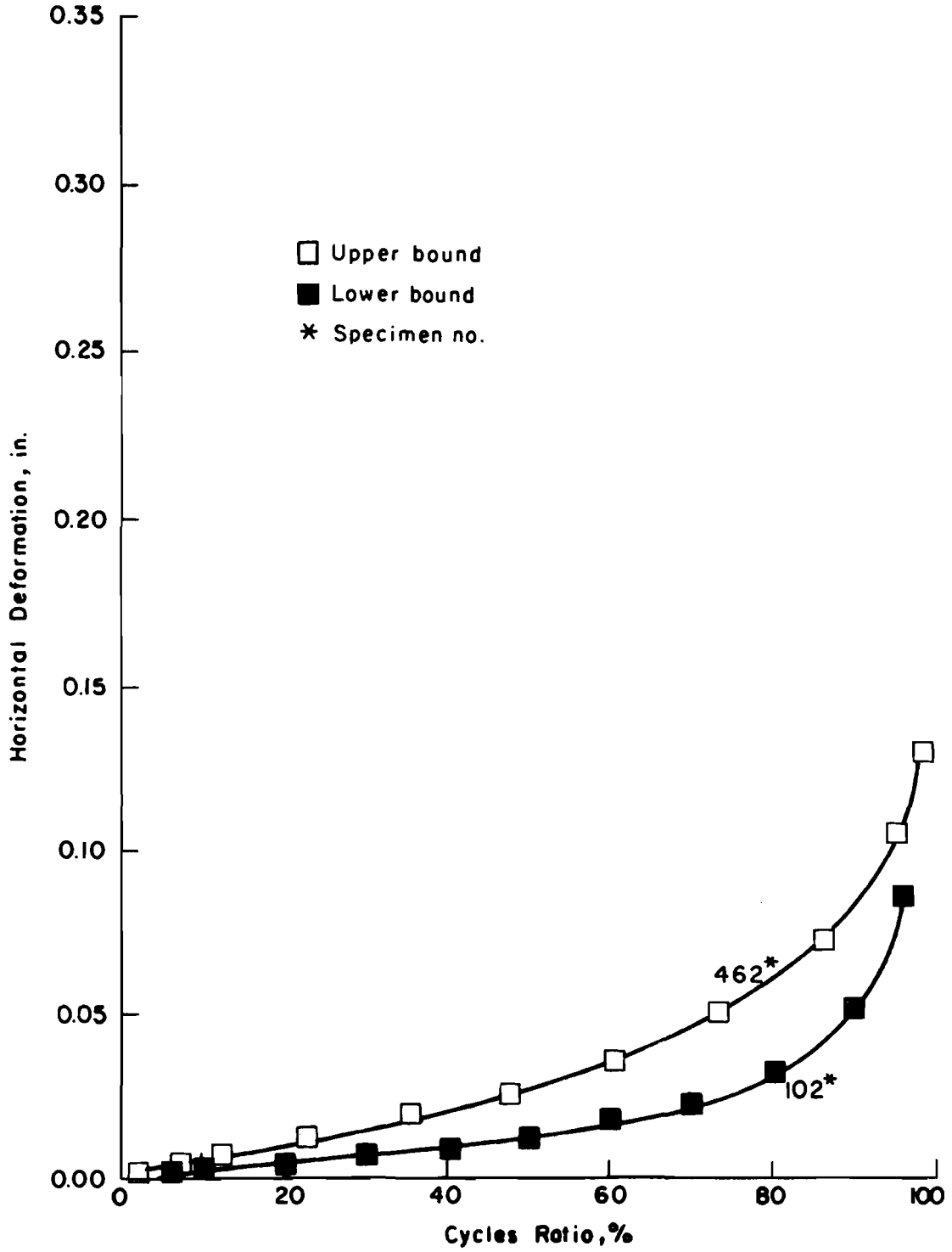

Fig C-16. Limiting horizontal deformations in simple-loading: 24 psi, gravel.

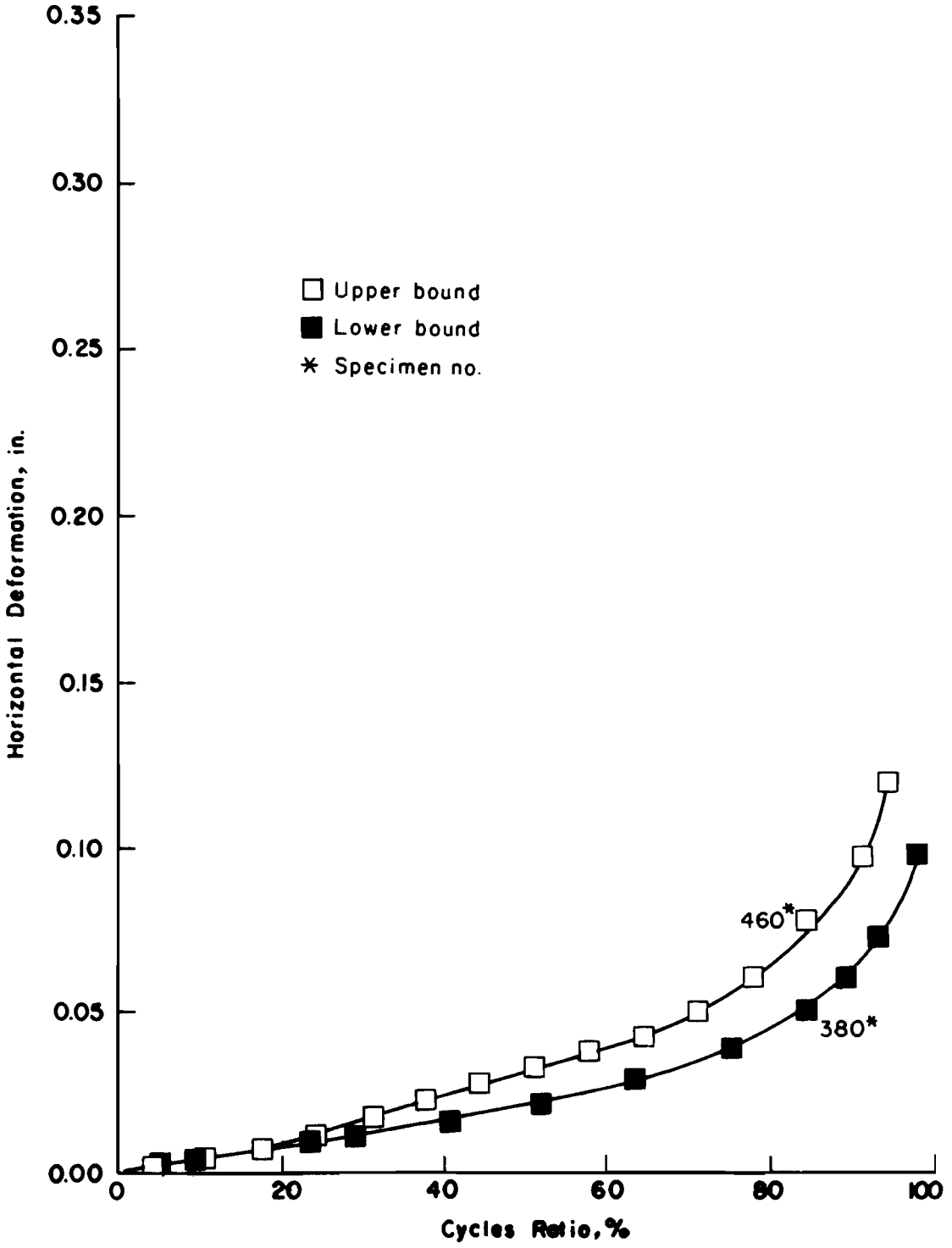

Fig C-17. Limiting horizontal deformations in simple-loading: 32 psi, gravel.

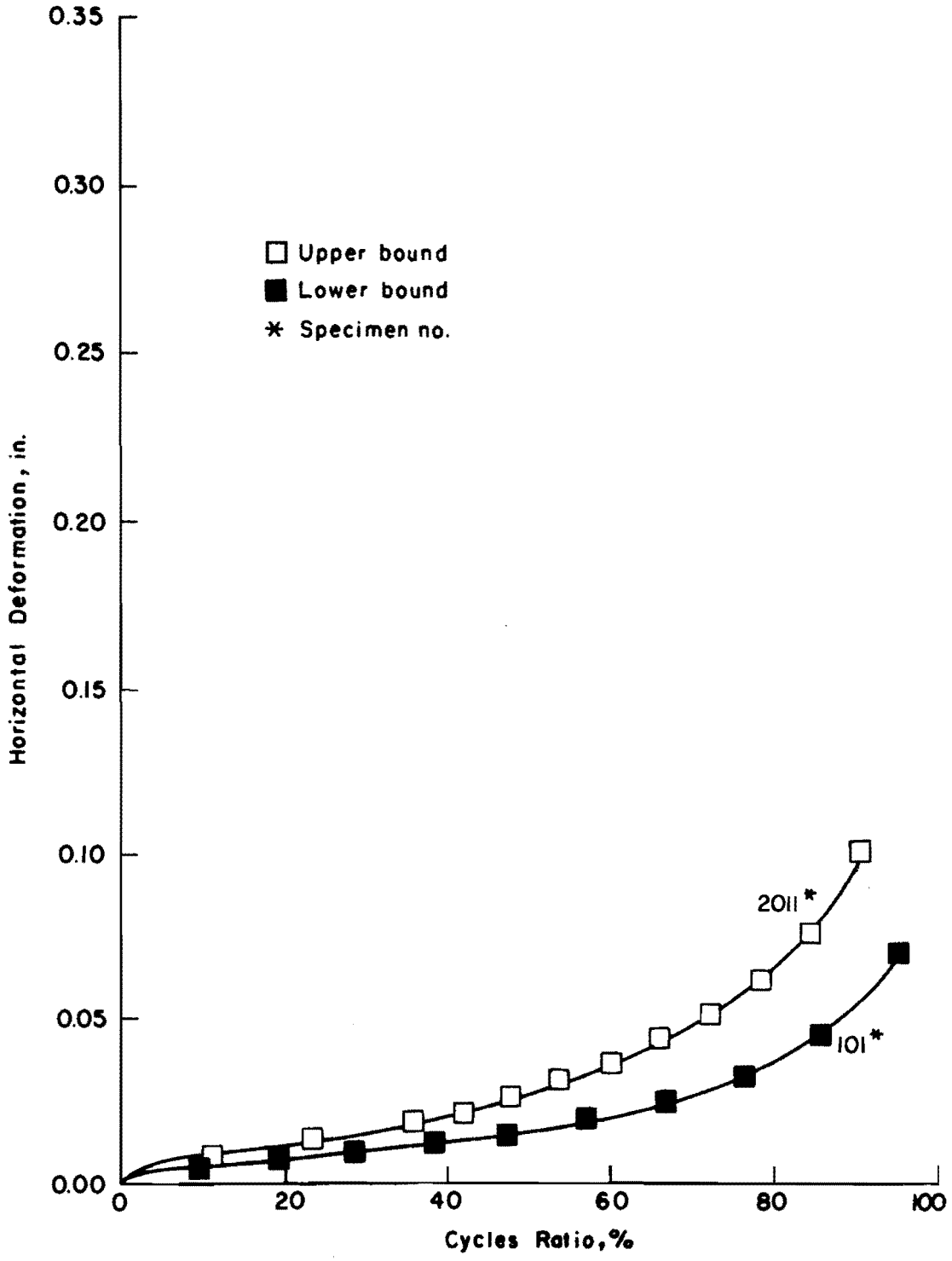

Fig C-18. Limiting horizontal deformations in simple-loading: 40 psi, gravel.

APPENDIX D

COMPOUND-LOADING TWO-LEVEL SEQUENCE SPECIMEN DATA

TABLE D-1. LIMESTONE FAILURE CONDITION DATA FOR INCREASING SEQUENCE LEVELS OF 16-24 PSI

7% AC-10
Medium Gradation
Sinusoidal Pulse (0.6 sec. rest time), 1 Hz

Temperature 75°F
Preload 20 lb

Spec. No.	Rank m	P(m), %	Reduced Normal Variate X	N_{16-24}	Log N_{16-24}	$\overline{N}_{16-24}$	S	CV, %
2020	1	16.667	-0.967	3236	3.5100	3.5507 (3554)	0.0410 (338)	9.51
2023	2	33.333	-0.431	3297	3.5181			
2021	3	50.000	0.000	3455	3.5384			
2024	4	66.667	+0.431	3834	3.5837			
2022	5	83.333	+0.967	4013	3.6035			

TABLE D-2. LIMESTONE FAILURE CONDITION DATA FOR INCREASING SEQUENCE LEVELS OF 16-32 PSI

7% AC-10
Medium Gradation
Sinusoidal Pulse (0.6 sec. rest time), 1 Hz

Temperature 75°F
Preload 20 lb

Spec. No.	Rank m	P(m), %	Reduced Normal Variate X	N_{16-32}	Log N_{16-32}	$\overline{N}_{16-32}$	S	CV, %
2015	1	16.667	-0.967	2470	3.3927	3.4095 (2567)	0.0144 (85)	3.31
2018	2	33.333	-0.431	2513	3.4002			
2016	3	50.000	0.000	2548	3.4062			
2017	4	66.667	+0.431	2638	3.4213			
2019	5	83.333	+0.967	2673	3.4270			

TABLE D-3. LIMESTONE FAILURE CONDITION DATA FOR INCREASING SEQUENCE LEVELS OF 16-40 PSI

7% AC-10
Medium Gradation
Sinusoidal Pulse (0.6 sec. rest time), 1 Hz

Temperature 75°F
Preload 20 lb

Spec. No.	Rank m	P(m), %	Reduced Normal Variate X	N_{16-40}	Log N_{16-40}	$\overline{N}_{16-40}$	S	CV, %
2002	1	16.667	-0.967	1884	3.2751	3.3222 (2100)	0.0523 (256)	12.17
2001	2	33.333	-0.431	1926	3.2847			
2003	3	50.000	0.000	1966	3.2936			
2014	4	66.667	+0.431	2358	3.3725			
2013	5	83.333	+0.967	2427	3.3851			

TABLE D-4. LIMESTONE FAILURE CONDITION DATA FOR INCREASING SEQUENCE LEVELS OF 24-32 PSI

7% AC-10
Medium Gradation
Sinusoidal Pulse (0.6 sec. rest time), 1 Hz

Temperature 75°F
Preload 20 lb

Spec. No.	Rank m	P(m), %	Reduced Normal Variate, X	N_{24-32}	Log N_{24-32}	$\overline{N}_{24-32}$	S	CV, %
2033	1	16.667	-0.967	771	2.8871	2.9128 (818)	0.0182 (34)	4.20
2032	2	33.333	-0.431	795	2.9004			
2030	3	50.000	0.000	835	2.9217			
2031	4	66.667	+0.431	842	2.9253			
2034	5	83.333	+0.967	850	2.9294			

TABLE D-5. LIMESTONE FAILURE CONDITION DATA FOR INCREASING SEQUENCE LEVELS OF 24-40 PSI

7% AC-10
Medium Gradation
Sinusoidal Pulse (0.6 sec. rest time), 1 Hz

Temperature 75°F
Preload 20 lb

Spec. No.	Rank m	P(m), %	Reduced Normal Variate X	N_{24-40}	Log N_{24-40}	$\overline{N}_{24-40}$	S	CV, %
2027	1	16.667	-0.967	591	2.7716	2.8233 (666)	0.0403 (62)	9.34
2025	2	33.333	-0.431	633	2.8014			
2026	3	50.000	0.000	657	2.8176			
2028	4	66.667	+0.431	714	2.8537			
2029	5	83.333	+0.967	745	2.8722			

TABLE D-6. LIMESTONE FAILURE CONDITION DATA FOR INCREASING SEQUENCE LEVELS OF 32-40 PSI

7% AC-10
Medium Gradation
Sinusoidal Pulse (0.6 sec. rest time), 1 Hz

Temperature 75°F
Preload 20 lb

Spec. No.	Rank m	P(m), %	Reduced Normal Variate X	N_{32-40}	Log N_{32-40}	$\overline{N}_{32-40}$	S	CV, %
2040	1	16.667	-0.967	334	2.5237	2.6231 (420)	0.0869 (87)	20.62
2041	2	33.333	-0.431	357	2.5527			
2042	3	50.000	0.000	424	2.6274			
2043	4	66.667	+0.431	475	2.6767			
2044	5	83.333	+0.967	543	2.7348			

TABLE D-7. LINEAR SUMMATION OF CYCLES RATIO FOR FAILURE CONDITION FOR INCREASING SEQUENCE OF 16-24 PSI, LIMESTONE

7% AC-10
Medium Gradation
Sinusoidal Pulse (0.6 sec. rest time), 1 Hz

Temperature 75°F
Preload 20 lb

Spec. No.	Rank m	P(m), %	Reduced Normal Variate X	N_{16-24}	n_{16}	n_{24}	$\bar{n}_{24}$	$\sum \frac{n}{N}$	N_c
2020	1	16.667	-0.967	3236	2057	1179	3.1703 (1480)	0.977	3312
2023	2	33.333	-0.431	3297	2057	1240		1.015	3249
2021	3	50.000	0.000	3455	2057	1398		1.112	3108
2024	4	66.667	+0.431	3834	2057	1777		1.344	2852
2022	5	83.333	+0.967	4013	2057	1956		1.454	2760

TABLE D-8. LINEAR SUMMATION OF CYCLES RATIO FOR FAILURE CONDITION FOR INCREASING SEQUENCE OF 16-32 PSI, LIMESTONE

7% AC-10
Medium Gradation
Sinusoidal Pulse (0.6 sec. rest time), 1 Hz

Temperature 75°F
Preload 20 lb

Spec. No.	Rank m	P(m), %	Reduced Normal Variate X	N_{16-32}	n_{16}	n_{32}	$\bar{n}_{32}$	$\sum \frac{n}{N}$	N_c
2015	1	16.667	-0.967	2470	2058	412	2.7038 (506)	0.975	2533
2018	2	33.333	-0.431	2513	2057	456		1.052	2389
2016	3	50.000	0.000	2548	2057	491		1.113	2289
2017	4	66.667	+0.431	2638	2057	581		1.271	2076
2019	5	83.333	+0.967	2673	2057	616		1.332	2006

TABLE D-9. LINEAR SUMMATION OF CYCLES RATIO FOR FAILURE CONDITION FOR INCREASING SEQUENCE OF 16-40 PSI, LIMESTONE

7% AC-10
Medium Gradation
Sinusoidal Pulse (0.6 sec. rest time), 1 Hz

Temperature 75°F
Preload 20 lb

Spec. No.	Rank m	P(m), %	Reduced Normal Variate X	N_{16-40}	n_{16}	n_{40}	$\bar{n}_{40}$	$\sum \frac{n}{N}$	N_c
2002	1	16.667	-0.967	1884	1596	288	2.5183 (330)	1.012	1861
2001	2	33.333	-0.431	1926	1597	329		1.129	1706
2003	3	50.000	0.000	1966	1596	370		1.245	1579
2014	4	66.667	+0.431	2358	2057	301		1.106	2132
2013	5	83.333	+0.967	2427	2057	370		1.302	1865

TABLE D-10. LINEAR SUMMATION OF CYCLES RATIO FOR FAILURE CONDITION FOR INCREASING SEQUENCE OF 24-32 PSI, LIMESTONE

7% AC-10
Medium Gradation
Sinusoidal Pulse (0.6 sec. rest time), 1 Hz

Temperature 75°F
Preload 20 lb

Spec. No.	Rank m	P(m), %	Reduced Normal Variate X	N_{24-32}	n_{24}	n_{32}	$\bar{n}_{32}$	$\sum \frac{n}{N}$	N_c
2033	1	16.667	-0.967	771	410	361	2.6092 (407)	0.884	872
2032	2	33.333	-0.431	795	411	384		0.925	860
2030	3	50.000	0.000	835	411	424		0.995	839
2031	4	66.667	+0.431	842	411	431		1.007	836
2034	5	83.333	+0.967	850	411	439		1.021	832

TABLE D-11. LINEAR SUMMATION OF CYCLES RATIO FOR FAILURE CONDITION FOR INCREASING SEQUENCE OF 24-40 PSI, LIMESTONE

7% AC-10
Medium Gradation
Sinusoidal Pulse (0.6 sec. rest time), 1 Hz

Temperature 75°F
Preload 20 lb

Spec. No.	Rank m	P(m), %	Reduced Normal Variate X	N_{24-40}	n_{24}	n_{40}	$\bar{n}_{40}$	$\sum \frac{n}{N}$	N_c
2027	1	16.667	-0.967	591	411	180	2.3966 (249)	0.762	775
2025	2	33.333	-0.431	633	412	221		0.879	720
2026	3	50.000	0.000	657	418	239		0.934	704
2028	4	66.667	+0.431	714	411	303		1.111	643
2029	5	83.333	+0.967	745	411	334		1.198	622

TABLE D-12. LINEAR SUMMATION OF CYCLES RATIO FOR FAILURE CONDITION FOR INCREASING SEQUENCE OF 32-40 PSI, LIMESTONE

7% AC-10
Medium Gradation
Sinusoidal Pulse (0.6 sec. rest time), 1 Hz

Temperature 75°F
Preload 20 lb

Spec. No.	Rank m	P(m), %	Reduced Normal Variate X	N_{32-40}	n_{32}	n_{40}	$\bar{n}_{40}$	$\sum \frac{n}{N}$	N_c
2040	1	16.667	-0.967	334	144	190	2.4350 (272)	0.790	423
2041	2	33.333	-0.431	357	144	213		0.856	417
2042	3	50.000	0.000	424	144	280		1.045	406
2043	4	66.667	+0.431	475	144	331		1.190	399
2044	5	83.333	+0.967	543	144	399		1.383	393

TABLE D-13. LIMESTONE FAILURE CONDITION DATA FOR DECREASING SEQUENCE LEVELS OF 24-16 PSI

7% AC-10
Medium Gradation
Sinusoidal Pulse (0.6 sec. rest time), 1 Hz

Temperature 75°F
Preload 20 lb

Spec. No.	Rank m	P(m), %	Reduced Normal Variate X	N_{24-16}	Log N_{24-16}	$\overline{N}_{24-16}$	S	CV, %
2037	1	16.667	-0.967	3705	3.5688	3.6395 (4360)	0.0884 (916)	21.01
2035	2	33.333	-0.431	3766	3.5759			
2036	3	50.000	0.000	3876	3.5884			
2038	4	66.667	+0.431	4986	3.6978			
2039	5	83.333	+0.967	5844	3.7667			

TABLE D-14. LIMESTONE FAILURE CONDITION DATA FOR DECREASING SEQUENCE LEVELS OF 32-16 PSI

7% AC-10
Medium Gradation
Sinusoidal Pulse (0.6 sec. rest time), 1 Hz

Temperature 75°F
Preload 20 lb

Spec. No.	Rank m	P(m), %	Reduced Normal Variate X	N_{32-16}	Log N_{32-16}	$\overline{N}_{32-16}$	S	CV, %
2050	1	16.667	-0.967	2704	3.4320	3.6487 (4453)	0.1247 (1360)	30.54
2051	2	33.333	-0.431	4615	3.6642			
2054	3	50.000	0.000	4852	3.6859			
2052	4	66.667	+0.431	5269	3.7217			
2053	5	83.333	+0.967	5492	3.7397			

TABLE D-15. LIMESTONE FAILURE CONDITION DATA FOR DECREASING SEQUENCE LEVELS OF 32-24 PSI

7% AC-10
Medium Gradation
Sinusoidal Pulse (0.6 sec. rest time), 1 Hz

Temperature 75°F
Preload 20 lb

Spec. No.	Rank m	P(m), %	Reduced Normal Variate X	N_{32-24}	Log N_{32-24}	$\overline{N}_{32-24}$	S	CV, %
2045	1	16.667	-0.967	1157	3.0633	3.1179 (1312)	0.0377 (115)	8.77
2046	2	33.333	-0.431	1261	3.1007			
2048	3	50.000	0.000	1324	3.1219			
2049	4	66.667	+0.431	1394	3.1443			
2047	5	83.333	+0.967	1443	3.1593			

TABLE D-16. LIMESTONE FAILURE CONDITION DATA FOR DECREASING SEQUENCE LEVELS OF 40-16 PSI

7% AC-10
Medium Gradation
Sinusoidal Pulse (0.6 sec. rest time), 1 Hz

Temperature 75°F
Preload 20 lb

Spec. No.	Rank m	P(m), %	Reduced Normal Variate X	N_{40-16}	Log N_{40-16}	$\bar{N}_{40-16}$	S	CV, %
2066	1	16.667	-0.967	2668	3.4262	3.5222 (3328)	0.0965 (767)	23.05
2065	2	33.333	-0.431	2883	3.4598			
2004	3	50.000	0.000	3095	3.4907			
2006	4	66.667	+0.431	3689	3.5669			
2005	5	83.333	+0.967	4652	3.6676			

TABLE D-17. LIMESTONE FAILURE CONDITION DATA FOR DECREASING SEQUENCE LEVELS OF 40-24 PSI

7% AC-10
Medium Gradation
Sinusoidal Pulse (0.6 sec. rest time), 1 Hz

Temperature 75°F
Preload 20 lb

Spec. No.	Rank m	P(m), %	Reduced Normal Variate X	N_{40-24}	Log N_{40-24}	$\overline{N}_{40-24}$	S	CV, %
2063	1	16.667	-0.967	988	2.9948	3.0358 (1086)	0.0445 (112)	10.31
2064	2	33.333	-0.431	1020	3.0086			
2060	3	50.000	0.000	1043	3.0183			
2062	4	66.667	+0.431	1125	3.0512			
2061	5	83.333	+0.967	1277	3.1062			

TABLE D-18. LIMESTONE FAILURE CONDITION DATA FOR DECREASING SEQUENCE LEVELS OF 40-32 PSI

7% AC-10
Medium Gradation
Sinusoidal Pulse (0.6 sec. rest time), 1 Hz

Temperature 75°F
Preload 20 lb

Spec. No.	Rank m	P(m), %	Reduced Normal Variate X	N_{40-32}	Log N_{40-32}	$\overline{N}_{40-32}$	S	CV, %
2058	1	16.667	-0.967	474	2.6758	2.7783 (600)	0.0656 (92)	15.33
2057	2	33.333	-0.431	599	2.7774			
2055	3	50.000	0.000	614	2.7882			
2059	4	66.667	+0.431	619	2.7917			
2056	5	83.333	+0.967	722	2.8585			

TABLE D-19. LINEAR SUMMATION OF CYCLES RATIO FOR FAILURE CONDITION FOR DECREASING SEQUENCE OF 24-16 PSI, LIMESTONE

7% AC-10
Medium Gradation
Sinusoidal Pulse (0.6 sec. rest time), 1 Hz

Temperature 75°F
Preload 20 lb

Spec. No.	Rank m	P(m), %	Reduced Normal Variate X	N_{24-16}	n_{24}	n_{16}	$\bar{n}_{16}$	$\sum \frac{n}{N}$	N_c
2037	1	16.667	-0.967	3705	411	3294	3.5956 (3941)	0.658	5630
2035	2	33.333	-0.431	3766	411	3355		0.666	5658
2036	3	50.000	0.000	3876	415	3461		0.681	5690
2038	4	66.667	+0.431	4986	411	4575		0.816	6111
2039	5	83.333	+0.967	5844	411	5433		0.922	6341

TABLE D-20. LINEAR SUMMATION OF CYCLES RATIO FOR FAILURE CONDITION FOR DECREASING SEQUENCE OF 32-16 PSI, LIMESTONE

7% AC-10
Medium Gradation
Sinusoidal Pulse (0.6 sec. rest time), 1 Hz

Temperature 75°F
Preload 20 lb

Spec. No.	Rank m	P(m), %	Reduced Normal Variate X	N_{32-16}	n_{32}	n_{16}	$\bar{n}_{16}$	$\sum \frac{n}{N}$	N_c
2050	1	16.667	-0.967	2704	144	2560	3.6339 (4304)	0.568	4764
2051	2	33.333	-0.431	4615	144	4471		0.803	5747
2054	3	50.000	0.000	4852	143	4709		0.831	5842
2052	4	66.667	+0.431	5269	145	5124		0.885	5952
2053	5	83.333	+0.967	5492	144	5348		0.911	6028

TABLE D-21. LINEAR SUMMATION OF CYCLES RATIO FOR FAILURE CONDITION FOR DECREASING SEQUENCE OF 32-24 PSI, LIMESTONE

7% AC-10
Medium Gradation
Sinusoidal Pulse (0.6 sec. rest time), 1 Hz

Temperature 75°F
Preload 20 lb

Spec. No.	Rank m	P(m), %	Reduced Normal Variate X	N_{32-24}	n_{32}	n_{24}	$\bar{n}_{24}$	$\sum \frac{n}{N}$	N_c
2045	1	16.667	-0.967	1157	144	1013	3.0676 (1168)	0.874	1324
2046	2	33.333	-0.431	1261	141	1120		0.934	1349
2048	3	50.000	0.000	1324	144	1180		0.977	1356
2049	4	66.667	+0.431	1394	144	1250		1.020	1367
2047	5	83.333	+0.967	1443	141	1302		1.046	1379

TABLE D-22. LINEAR SUMMATION OF CYCLES RATIO FOR FAILURE CONDITION FOR DECREASING SEQUENCE OF 40-16 PSI, LIMESTONE

7% AC-10
Medium Gradation
Sinusoidal Pulse (0.6 sec. rest time), 1 Hz

Temperature 75°F
Preload 20 lb

Spec. No.	Rank m	P(m), %	Reduced Normal Variate X	N_{40-16}	n_{40}	n_{16}	$\bar{n}_{16}$	$\sum \frac{n}{N}$	N_c
2066	1	16.667	-0.967	2668	86	2584	3.5109 (3243)	0.556	4796
2065	2	33.333	-0.431	2883	84	2799		0.583	4747
2004	3	50.000	0.000	3095	82	3013		0.609	5083
2006	4	66.667	+0.431	3689	90	3599		0.682	5408
2005	5	83.333	+0.967	4652	84	4568		0.801	5810

TABLE D-23. LINEAR SUMMATION OF CYCLES RATIO FOR FAILURE CONDITION FOR DECREASING SEQUENCE OF 40-24 PSI, LIMESTONE

7% AC-10
Medium Gradation
Sinusoidal Pulse (0.6 sec. rest time), 1 Hz

Temperature 75°F
Preload 20 lb

Spec. No.	Rank m	P(m), %	Reduced Normal Variate X	N_{40-24}	n_{40}	n_{24}	$\bar{n}_{24}$	$\sum \frac{n}{N}$	N_c
2063	1	16.667	-0.967	988	84	904	3.0007 (1002)	0.793	1246
2064	2	33.333	-0.431	1020	84	936		0.813	1255
2060	3	50.000	0.000	1043	84	959		0.827	1262
2062	4	66.667	+0.431	1125	84	1041		0.877	1283
2061	5	83.333	+0.967	1277	84	1193		0.970	1316

TABLE D-24. LINEAR SUMMATION OF CYCLES RATIO FOR FAILURE CONDITION FOR DECREASING SEQUENCE OF 40-32 PSI, LIMESTONE

7% AC-10
Medium Gradation
Sinusoidal Pulse (0.6 sec. rest time), 1 Hz

Temperature 75°F
Preload 20 lb

Spec. No.	Rank m	P(m), %	Reduced Normal Variate X	N_{40-32}	n_{40}	n_{32}	$\bar{n}_{32}$	$\sum \frac{n}{N}$	N_c
2058	1	16.667	-0.967	474	84	390	2.7106 (514)	0.921	515
2057	2	33.333	-0.431	599	84	515		1.140	525
2055	3	50.000	0.000	614	84	534		1.166	527
2059	4	66.667	+0.431	619	93	526		1.185	523
2056	5	83.333	+0.967	722	84	638		1.355	533

TABLE D-25. GRAVEL FAILURE CONDITION DATA FOR INCREASING SEQUENCE LEVELS OF 16-24 PSI

7% AC-10
Medium Gradation
Sinusoidal Pulse (0.6 sec. rest time), 1 Hz

Temperature 75°F
Preload 20 lb

Spec. No.	Rank m	P(m), %	Reduced Normal Variate X	N_{16-24}	Log N_{16-24}	$\overline{N}_{16-24}$	S	CV, %
2076	1	16.667	-0.967	1949	3.2898	3.3418 (2197)	0.0517 (264)	12.02
2077	2	33.333	-0.431	2094	3.3210			
2080	3	50.000	0.000	2145	3.3314			
2079	4	66.667	+0.431	2182	3.3389			
2078	5	83.333	+0.967	2679	3.4280			

TABLE D-26. GRAVEL FAILURE CONDITION DATA FOR INCREASING SEQUENCE LEVELS OF 16-32 PSI

7% AC-10
Medium Gradation
Sinusoidal Pulse (0.6 sec. rest time), 1 Hz

Temperature 75°F
Preload 20 lb

Spec. No.	Rank m	P(m), %	Reduced Normal Variate X	N_{16-32}	Log N_{16-32}	$\overline{N}_{16-32}$	S	CV, %
2075	1	16.667	-0.967	1850	3.2671	3.2825 (1916)	0.0160 (71)	3.71
2074	2	33.333	-0.431	1874	3.2728			
2072	3	50.000	0.000	1897	3.2781			
2073	4	66.667	+0.431	1932	3.2860			
2122	5	83.333	+0.967	2034	3.3084			

TABLE D-27. GRAVEL FAILURE CONDITION DATA FOR INCREASING SEQUENCE LEVELS OF 16-40 PSI

7% AC-10
Medium Gradation
Sinusoidal Pulse (0.6 sec. rest time), 1 Hz

Temperature 75°F
Preload 20 lb

Spec. No.	Rank m	P(m), %	Reduced Normal Variate X	N_{16-40}	Log N_{16-40}	$\overline{N}_{16-40}$	S	CV, %
2068	1	16.667	-0.967	1795	3.2541	3.2993 (1992)	0.0339 (156)	7.83
2067	2	33.333	-0.431	1870	3.2718			
2010	3	50.000	0.000	2088	3.3197			
2008	4	66.667	+0.431	2103	3.3228			
2007	5	83.333	+0.967	2129	3.3282			

TABLE D-28. GRAVEL FAILURE CONDITION DATA FOR INCREASING SEQUENCE LEVELS OF 24-32 PSI

7% AC-10
Medium Gradation
Sinusoidal Pulse (0.6 sec. rest time), 1 Hz

Temperature 75°F
Preload 20 lb

Spec. No.	Rank m	P(m), %	Reduced Normal Variate X	N_{24-32}	Log N_{24-32}	$\bar{N}_{24-32}$	S	CV, %
2088	1	16.667	-0.967	692	2.8401	2.8782 (755)	0.0369 (65)	8.61
2086	2	33.333	-0.431	720	2.8573			
2087	3	50.000	0.000	731	2.8639			
2089	4	66.667	+0.431	789	2.8971			
2090	5	83.333	+0.967	857	2.9330			

TABLE D-29. GRAVEL FAILURE CONDITION DATA FOR INCREASING SEQUENCE LEVELS OF 24-40 PSI

7% AC-10
Medium Gradation
Sinusoidal Pulse (0.6 sec. rest time), 1 Hz

Temperature 75°F
Preload 20 lb

Spec. No.	Rank m	P(m), %	Reduced Normal Variate X	N_{24-40}	Log N_{24-40}	$\overline{N}_{24-40}$	S	CV, %
2085	1	16.667	-0.967	522	2.7177	2.7434 (554)	0.0221 (28)	5.05
2082	2	33.333	-0.431	538	2.7308			
2084	3	50.000	0.000	544	2.7356			
2083	4	66.667	+0.431	581	2.7642			
2081	5	83.333	+0.967	587	2.7686			

TABLE D-30. GRAVEL FAILURE CONDITION DATA FOR INCREASING SEQUENCE LEVELS OF 32-40 PSI

7% AC-10
Medium Gradation
Sinusoidal Pulse (0.6 sec. rest time), 1 Hz

Temperature 75°F
Preload 20 lb

Spec. No.	Rank m	P(m), %	Reduced Normal Variate X	N_{32-40}	Log N_{32-40}	$\overline{N}_{32-40}$	S	CV, %
2099	1	16.667	-0.967	308	2.4886	2.5101 (324)	0.0212 (16)	4.94
2100	2	33.333	-0.431	317	2.5011			
2096	3	50.000	0.000	322	2.5079			
2098	4	66.667	+0.431	322	2.5079			
2097	5	83.333	+0.967	351	2.5453			

TABLE D-31. LINEAR SUMMATION OF CYCLES RATIO FOR FAILURE CONDITION FOR INCREASING SEQUENCE OF 16-24 PSI, GRAVEL

7% AC-10
Medium Gradation
Sinusoidal Pulse (0.6 sec. rest time), 1 Hz

Temperature 75°F
Preload 20 lb

Spec. No.	Rank m	P(m), %	Reduced Normal Variate X	N_{16-24}	n_{16}	n_{24}	$\bar{n}_{24}$	$\sum \frac{n}{N}$	N_c
2076	1	16.667	-0.967	1949	1589	360	2.7630 (579)	0.529	3687
2077	2	33.333	-0.431	2094	1589	505		0.634	3302
2080	3	50.000	0.000	2145	1589	556		0.671	3196
2079	4	66.667	+0.431	2182	1589	593		0.698	3126
2078	5	83.333	+0.967	2679	1590	1090		1.059	2530

TABLE D-32. LINEAR SUMMATION OF CYCLES RATIO FOR FAILURE CONDITION FOR INCREASING SEQUENCE OF 16-32 PSI, GRAVEL

7% AC-10
Medium Gradation
Sinusoidal Pulse (0.6 sec. rest time), 1 Hz

Temperature 75°F
Preload 20 lb

Spec. No.	Rank m	P(m), %	Reduced Normal Variate X	N_{16-32}	n_{16}	n_{32}	$\bar{n}_{32}$	$\sum \frac{n}{N}$	N_c
2075	1	16.667	-0.967	1850	1589	261	2.5091 (323)	0.786	2355
2074	2	33.333	-0.431	1874	1588	286		0.835	2244
2072	3	50.000	0.000	1897	1589	308		0.879	2158
2073	4	66.667	+0.431	1932	1589	343		0.949	2036
2122	5	83.333	+0.967	2034	1589	445		1.152	1766

TABLE D-33. LINEAR SUMMATION OF CYCLES RATIO FOR FAILURE CONDITION FOR INCREASING SEQUENCE OF 16-40 PSI, GRAVEL

7% AC-10
Medium Gradation
Sinusoidal Pulse (0.6 sec. rest time), 1 Hz

Temperature 75°F
Preload 20 lb

Spec. No.	Rank m	P(m), %	Reduced Normal Variate X	N_{16-40}	n_{16}	n_{40}	$\bar{n}_{40}$	$\sum \frac{n}{N}$	N_c
2068	1	16.667	-0.967	1795	1591	204	2.1751 (150)	0.743	2417
2067	2	33.333	-0.431	1870	1589	281		0.922	2029
2010	3	50.000	0.000	2088	1996	92		0.550	3799
2008	4	66.667	+0.431	2103	1996	107		0.585	3597
2007	5	83.333	+0.967	2129	1996	133		0.645	3300

TABLE D-34. LINEAR SUMMATION OF CYCLES RATIO FOR FAILURE CONDITION FOR INCREASING SEQUENCE OF 24-32 PSI, GRAVEL

7% AC-10
Medium Gradation
Sinusoidal Pulse (0.6 sec. rest time), 1 Hz

Temperature 75°F
Preload 20 lb

Spec. No.	Rank m	P(m), %	Reduced Normal Variate X	N_{24-32}	n_{24}	n_{32}	$\bar{n}_{32}$	$\sum \frac{n}{N}$	N_c
2088	1	16.667	-0.967	692	397	295	2.5518 (356)	0.875	791
2086	2	33.333	-0.431	720	397	323		0.931	773
2087	3	50.000	0.000	731	397	334		0.953	767
2089	4	66.667	+0.431	789	397	392		1.068	739
2090	5	83.333	+0.967	857	397	460		1.203	712

TABLE D-35. LINEAR SUMMATION OF CYCLES RATIO FOR FAILURE CONDITION FOR INCREASING SEQUENCE OF 24-40 PSI, GRAVEL

7% AC-10
Medium Gradation
Sinusoidal Pulse (0.6 sec. rest time), 1 Hz

Temperature 75°F
Preload 20 lb

Spec. No.	Rank m	P(m), %	Reduced Normal Variate X	N_{24-40}	n_{24}	n_{40}	$\bar{n}_{40}$	$\sum \frac{n}{N}$	N_c
2085	1	16.667	-0.967	522	397	125	2.1936 (156)	0.580	900
2082	2	33.333	-0.431	538	397	141		0.617	871
2084	3	50.000	0.000	544	397	147		0.631	862
2083	4	66.667	+0.431	581	397	184		0.718	810
2081	5	83.333	+0.967	587	392	195		0.740	794

TABLE D-36. LINEAR SUMMATION OF CYCLES RATIO FOR FAILURE CONDITION FOR INCREASING SEQUENCE OF 32-40 PSI, GRAVEL

7% AC-10
Medium Gradation
Sinusoidal Pulse (0.6 sec. rest time), 1 Hz

Temperature 75°F
Preload 20 lb

Spec. No.	Rank m	P(m), %	Reduced Normal Variate X	N_{32-40}	n_{32}	n_{40}	$\bar{n}_{40}$	$\sum \frac{n}{N}$	N_c
2099	1	16.667	-0.967	308	200	108	2.0892 (123)	0.649	474
2100	2	33.333	-0.431	317	201	116		0.670	473
2096	3	50.000	0.000	322	200	122		0.682	472
2098	4	66.667	+0.431	322	201	121		0.682	472
2097	5	83.333	+0.967	351	200	151		0.750	468

TABLE D-37. GRAVEL FAILURE CONDITION DATA FOR DECREASING SEQUENCE LEVELS OF 24-16 PSI

7% AC-10
Medium Gradation
Sinusoidal Pulse (0.6 sec. rest time), 1 Hz

Temperature 75°F
Preload 20 lb

Spec. No.	Rank m	P(m), %	Reduced Normal Variate X	N_{24-16}	Log N_{24-16}	$\overline{N}_{24-16}$	S	CV, %
2092	1	16.667	-0.967	2592	3.4136	3.4551 (2852)	0.0482 (319)	11.19
2094	2	33.333	-0.431	2643	3.4221			
2095	3	50.000	0.000	2667	3.4260			
2091	4	66.667	+0.431	3126	3.4950			
2093	5	83.333	+0.967	3302	3.5188			

TABLE D-38. GRAVEL FAILURE CONDITION DATA FOR DECREASING SEQUENCE LEVELS OF 32-16 PSI

7% AC-10
Medium Gradation
Sinusoidal Pulse (0.6 sec. rest time), 1 Hz

Temperature 75°F
Preload 20 lb

Spec. No.	Rank m	P(m), %	Reduced Normal Variate X	N_{32-16}	Log N_{32-16}	$\overline{N}_{32-16}$	S	CV, %
2109	1	16.667	-0.967	941	2.9736	3.1196 (1317)	0.1243 (401)	30.45
2107	2	33.333	-0.431	1045	3.0191			
2110	3	50.000	0.000	1360	3.1335			
2106	4	66.667	+0.431	1572	3.1965			
2108	5	83.333	+0.967	1885	3.2753			

TABLE D-39. GRAVEL FAILURE CONDITION DATA FOR DECREASING SEQUENCE LEVELS OF 32-24 PSI

7% AC-10
Medium Gradation
Sinusoidal Pulse (0.6 sec. rest time), 1 Hz

Temperature 75°F
Preload 20 lb

Spec. No.	Rank m	P(m), %	Reduced Normal Variate X	N_{32-24}	Log N_{32-24}	$\overline{N}_{32-24}$	S	CV, %
2102	1	16.667	-0.967	416	2.6191	2.8980 (791)	0.1673 (341)	43.11
2104	2	33.333	-0.431	801	2.9036			
2103	3	50.000	0.000	878	2.9435			
2105	4	66.667	+0.431	904	2.9562			
2101	5	83.333	+0.967	1168	3.0674			

TABLE D-40. GRAVEL FAILURE CONDITION DATA FOR DECREASING SEQUENCE LEVELS OF 40-16 PSI

7% AC-10
Medium Gradation
Sinusoidal Pulse (0.6 sec. rest time), 1 Hz

Temperature 75°F
Preload 20 lb

Spec. No.	Rank m	P(m), %	Reduced Normal Variate X	N_{40-16}	Log N_{40-16}	$\bar{N}_{40-16}$	S	CV, %
2009	1	16.667	-0.967	217	2.3365	3.0682 (1170)	0.5120 (4069)	346.34
2012	2	33.333	-0.431	753	2.8768			
2069	3	50.000	0.000	1042	3.0179			
2116	4	66.667	+0.431	3504	3.5446			
2070	5	83.333	+0.967	3674	3.5651			

TABLE D-41. GRAVEL FAILURE CONDITION DATA FOR DECREASING SEQUENCE LEVELS OF 40-24 PSI

7% AC-10
Medium Gradation
Sinusoidal Pulse (0.6 sec. rest time), 1 Hz

Temperature 75°F
Preload 20 lb

Spec. No.	Rank m	P(m), %	Reduced Normal Variate X	N_{40-24}	Log N_{40-24}	$\bar{N}_{40-24}$	S	CV, %
2121	1	16.667	-0.967	538	2.7308	2.8535 (714)	0.0703 (118)	16.53
2119	2	33.333	-0.431	745	2.8722			
2117	3	50.000	0.000	751	2.8756			
2120	4	66.667	+0.431	756	2.8785			
2118	5	83.333	+0.967	814	2.9106			

TABLE D-42. GRAVEL FAILURE CONDITION DATA FOR DECREASING SEQUENCE LEVELS OF 40-32 PSI

7% AC-10
Medium Gradation
Sinusoidal Pulse (0.6 sec. rest time), 1 Hz

Temperature 75°F
Preload 20 lb

Spec. No.	Rank m	P(m), %	Reduced Normal Variate X	N_{40-32}	Log N_{40-32}	$\overline{N}_{40-32}$	S	CV, %
2113	1	16.667	-0.967	271	2.4330	2.4890 (308)	0.0440 (31)	10.06
2111	2	33.333	-0.431	288	2.4594			
2115	3	50.000	0.000	310	2.4914			
2114	4	66.667	+0.431	331	2.5198			
2112	5	83.333	+0.967	348	2.5416			

TABLE D-43. LINEAR SUMMATION OF CYCLES RATIO FOR FAILURE CONDITION FOR DECREASING SEQUENCE OF 24-16 PSI, GRAVEL

7% AC-10
Medium Gradation
Sinusoidal Pulse (0.6 sec. rest time), 1 Hz

Temperature 75°F
Preload 20 lb

Spec. No.	Rank m	P(m), %	Reduced Normal Variate X	N_{24-16}	n_{24}	n_{16}	$\bar{n}_{16}$	$\sum \frac{n}{N}$	N_c
2092	1	16.667	-0.967	2592	400	2192	3.3887 (2447)	0.659	3933
2094	2	33.333	-0.431	2643	396	2247		0.665	3972
2095	3	50.000	0.000	2667	417	2250		0.681	3915
2091	4	66.667	+0.431	3126	397	2729		0.747	4185
2093	5	83.333	+0.967	3302	398	2904		0.777	4249

TABLE D-44. LINEAR SUMMATION OF CYCLES RATIO FOR FAILURE CONDITION FOR DECREASING SEQUENCE OF 32-16 PSI, GRAVEL

7% AC-10
Medium Gradation
Sinusoidal Pulse (0.6 sec. rest time), 1 Hz

Temperature 75°F
Preload 20 lb

Spec. No.	Rank m	P(m), %	Reduced Normal Variate X	N_{32-16}	n_{32}	n_{16}	$\bar{n}_{16}$	$\sum \frac{n}{N}$	N_c
2109	1	16.667	-0.967	941	200	741	3.0450 (1109)	0.522	1803
2107	2	33.333	-0.431	1045	200	845		0.540	1937
2110	3	50.000	0.000	1360	200	1160		0.592	2296
2106	4	66.667	+0.431	1572	200	1372		0.628	2503
2108	5	83.333	+0.967	1885	200	1685		0.681	2770

TABLE D-45. LINEAR SUMMATION OF CYCLES RATIO FOR FAILURE CONDITION FOR DECREASING SEQUENCE OF 32-24 PSI, GRAVEL

7% AC-10
Medium Gradation
Sinusoidal Pulse (0.6 sec. rest time), 1 Hz

Temperature 75°F
Preload 20 lb

Spec. No.	Rank m	P(m), %	Reduced Normal Variate X	N_{32-24}	n_{32}	n_{24}	$\bar{n}_{24}$	$\sum \frac{n}{N}$	N_c
2102	1	16.667	-0.967	416	140	276	2.7823 (606)	0.479	868
2104	2	33.333	-0.431	801	200	601		0.835	960
2103	3	50.000	0.000	878	199	679		0.889	987
2105	4	66.667	+0.431	904	200	701		0.910	994
2101	5	83.333	+0.967	1168	139	1029		1.025	1140

TABLE D-46. LINEAR SUMMATION OF CYCLES RATIO FOR FAILURE CONDITION FOR DECREASING SEQUENCE OF 40-16 PSI, GRAVEL

7% AC-10
Medium Gradation
Sinusoidal Pulse (0.6 sec. rest time), 1 Hz

Temperature 75°F
Preload 20 lb

Spec. No.	Rank m	P(m), %	Reduced Normal Variate X	N_{40-16}	n_{40}	n_{16}	$\bar{n}_{16}$	$\sum \frac{n}{N}$	N_c
2009	1	16.667	-0.967	217	175	42	2.8917 (779)	0.415	523
2012	2	33.333	-0.431	753	172	581		0.498	1511
2069	3	50.000	0.000	1042	84	958		0.357	2921
2116	4	66.667	+0.431	3504	83	3421		0.768	4563
2070	5	83.333	+0.967	3674	82	3592		0.794	4625

TABLE D-47. LINEAR SUMMATION OF CYCLES RATIO FOR FAILURE CONDITION FOR DECREASING SEQUENCE OF 40-24 PSI, GRAVEL

7% AC-10
Medium Gradation
Sinusoidal Pulse (0.6 sec. rest time), 1 Hz

Temperature 75°F
Preload 20 lb

Spec. No.	Rank m	P(m), %	Reduced Normal Variate X	N_{40-24}	n_{40}	n_{24}	$\bar{n}_{24}$	$\sum \frac{n}{N}$	N_c
2121	1	16.667	-0.967	538	83	455	2.7998 (631)	0.524	1026
2119	2	33.333	-0.431	745	82	663		0.673	1106
2117	3	50.000	0.000	751	81	670		0.676	1111
2120	4	66.667	+0.431	756	82	674		0.681	1110
2118	5	83.333	+0.967	814	82	732		0.724	1125

TABLE D-48. LINEAR SUMMATION OF CYCLES RATIO FOR FAILURE CONDITION FOR DECREASING SEQUENCE OF 40-32 PSI, GRAVEL

7% AC-10
Medium Gradation
Sinusoidal Pulse (0.6 sec. rest time), 1 Hz

Temperature 75°F
Preload 20 lb

Spec. No.	Rank m	P(m), %	Reduced Normal Variate X	N_{40-32}	n_{40}	n_{32}	$\bar{n}_{32}$	$\sum \frac{n}{N}$	N_c
2113	1	16.667	-0.967	271	82	189	2.3531 (225)	0.567	478
2111	2	33.333	-0.431	288	83	205		0.601	479
2115	3	50.000	0.000	310	83	227		0.645	481
2114	4	66.667	+0.431	331	82	249		0.686	482
2112	5	83.333	+0.967	348	82	266		0.720	483

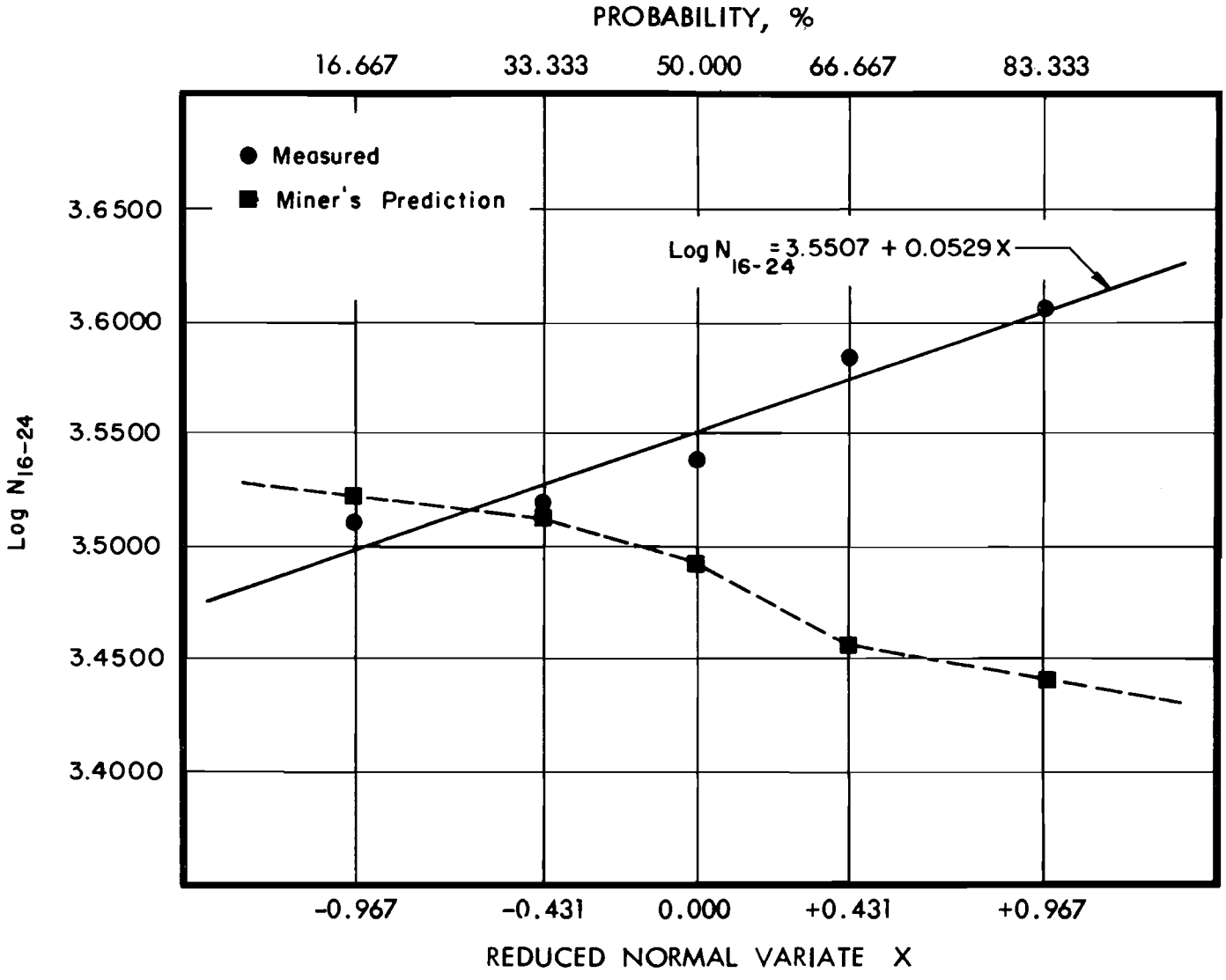

Fig D-1. Logarithm of compound fatigue life versus probability of failure: 16-24 psi, limestone.

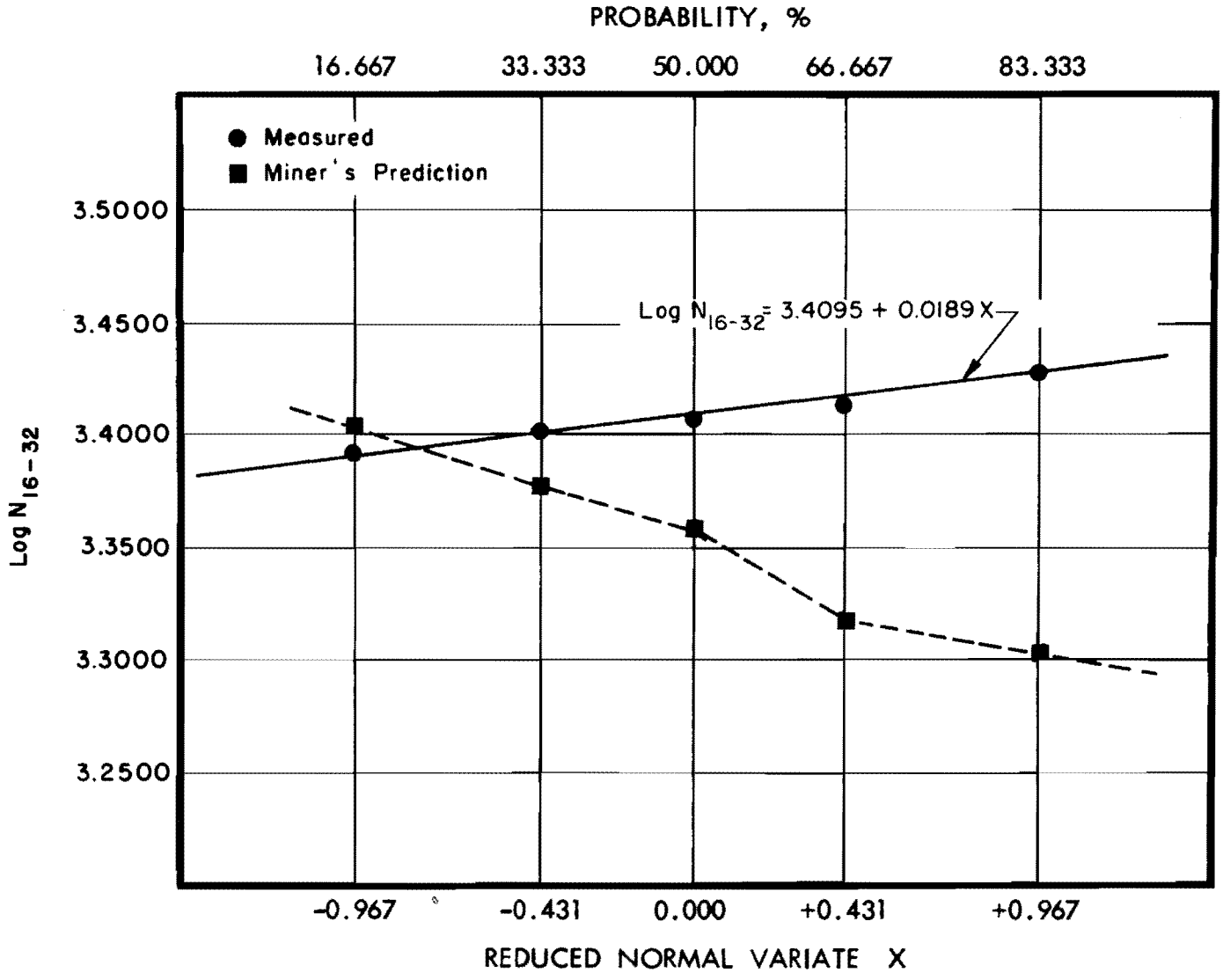

Fig D-2. Logarithm of compound fatigue life versus probability of failure: 16-32 psi, limestone.

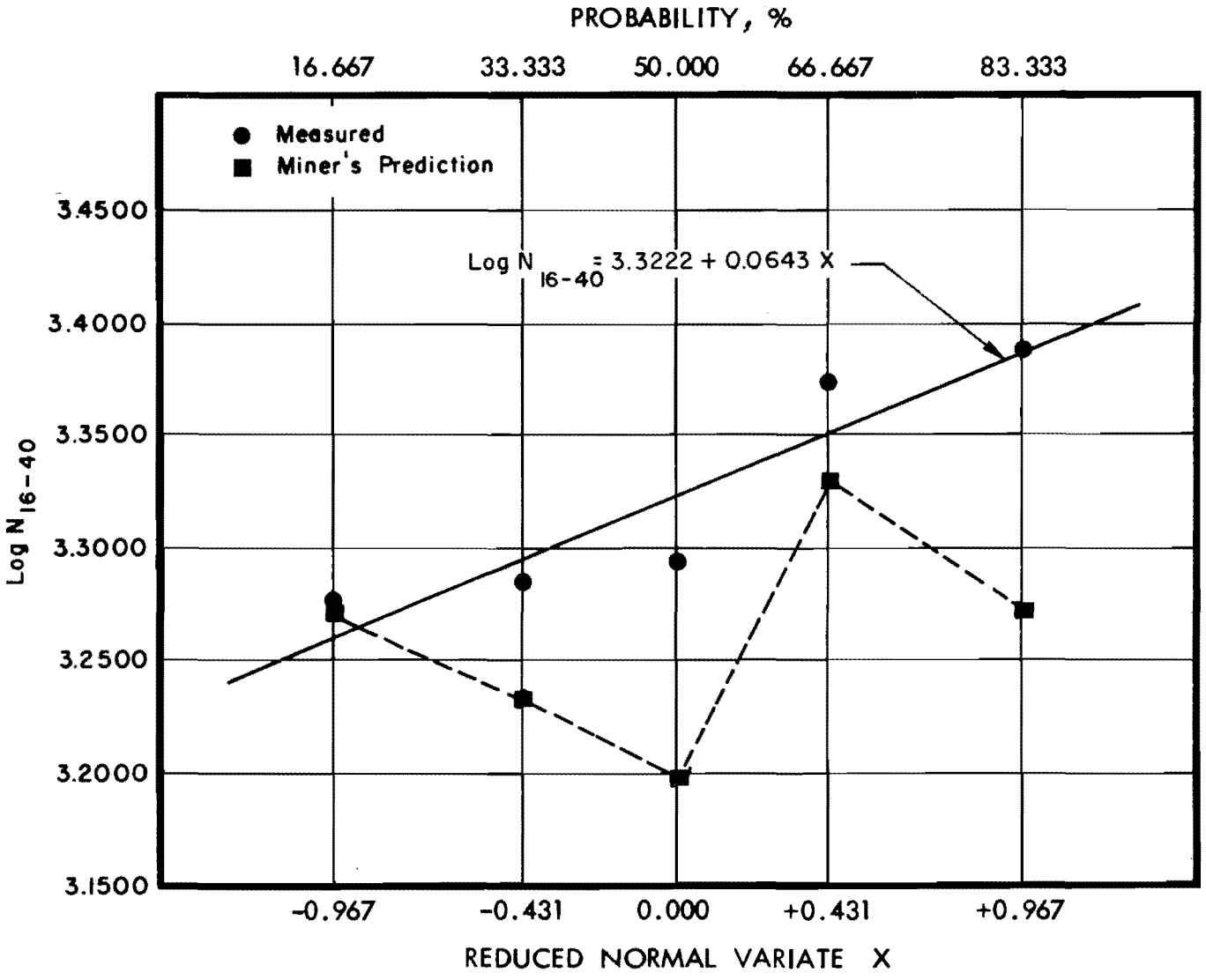

Fig D-3. Logarithm of compound fatigue life versus probability of failure: 16-40 psi, limestone.

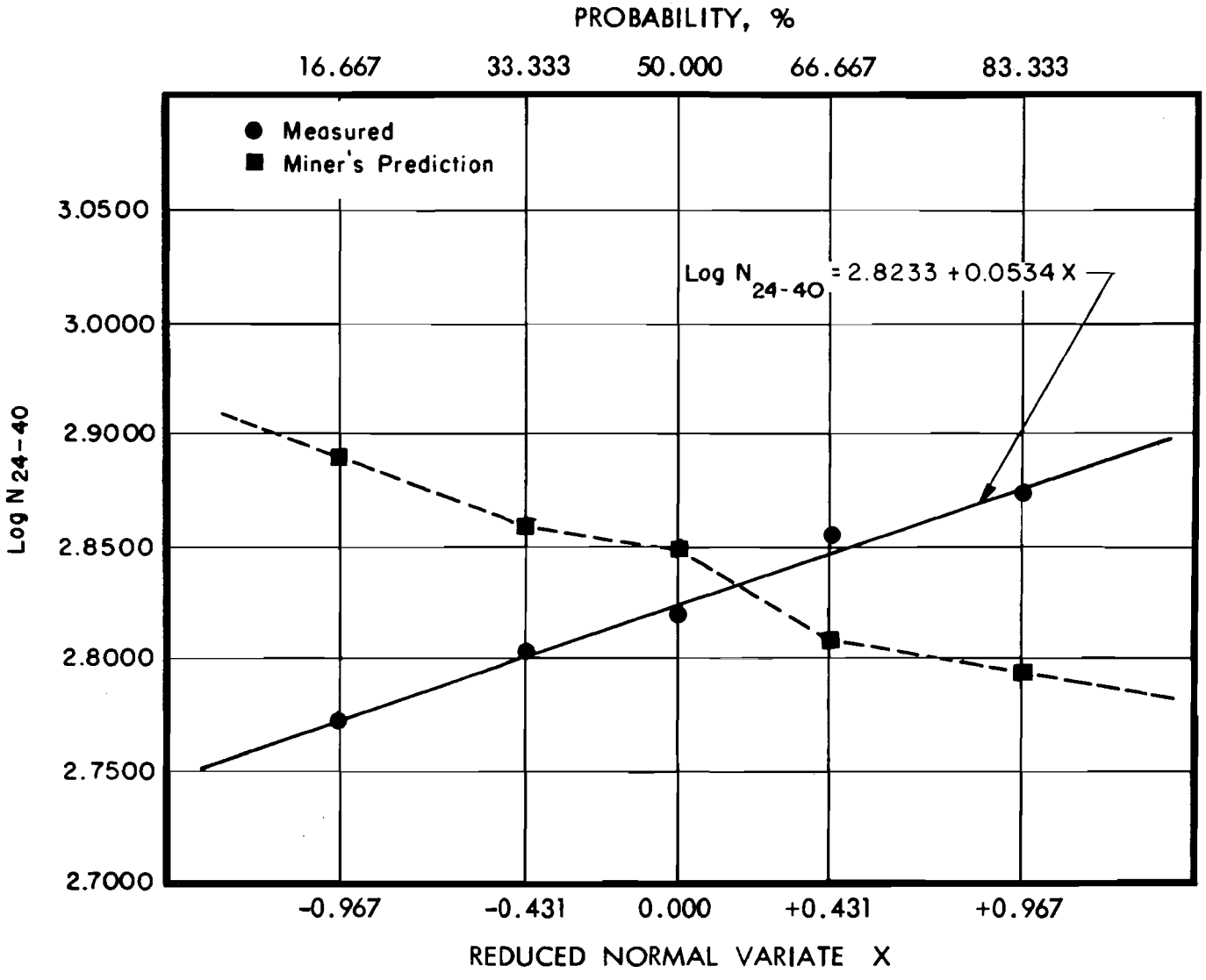

Fig D-4. Logarithm of compound fatigue life versus probability of failure: 24-40 psi, limestone.

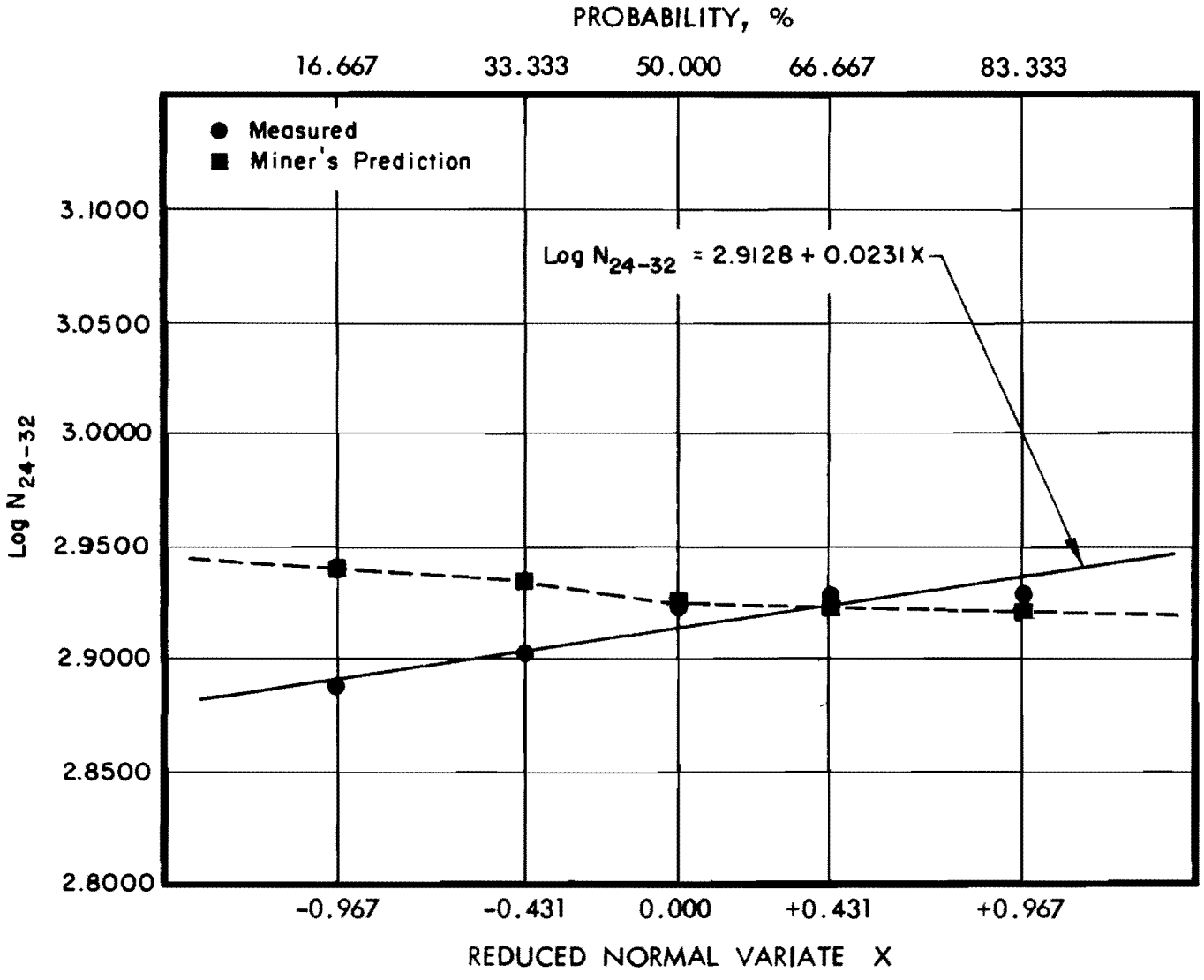

Fig D-5. Logarithm of compound fatigue life versus probability of failure: 24-32 psi, limestone.

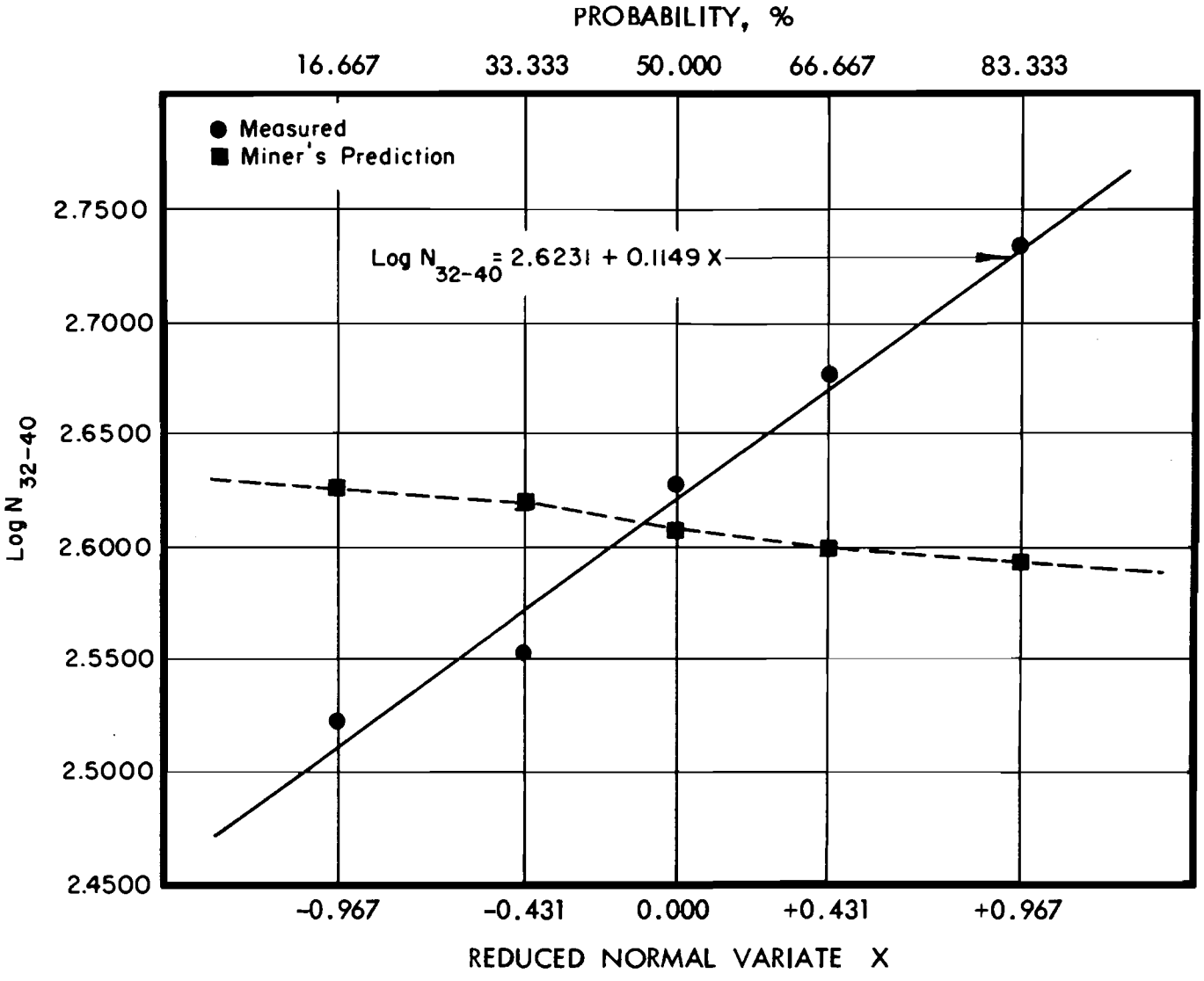

Fig D-6. Logarithm of compound fatigue life versus probability of failure: 32-40 psi, limestone.

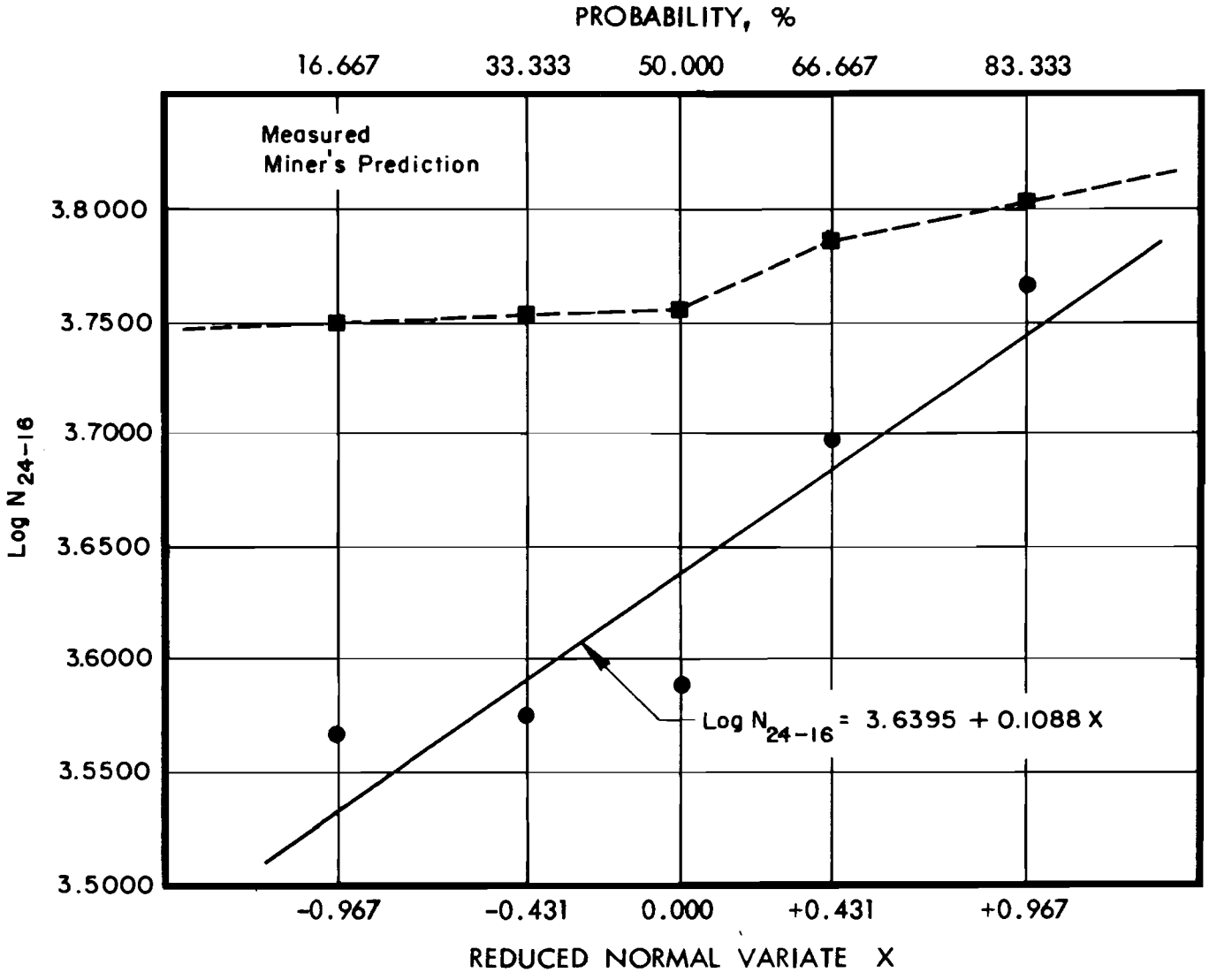

Fig D-7. Logarithm of compound fatigue life versus probability of failure: 24-16 psi, limestone.

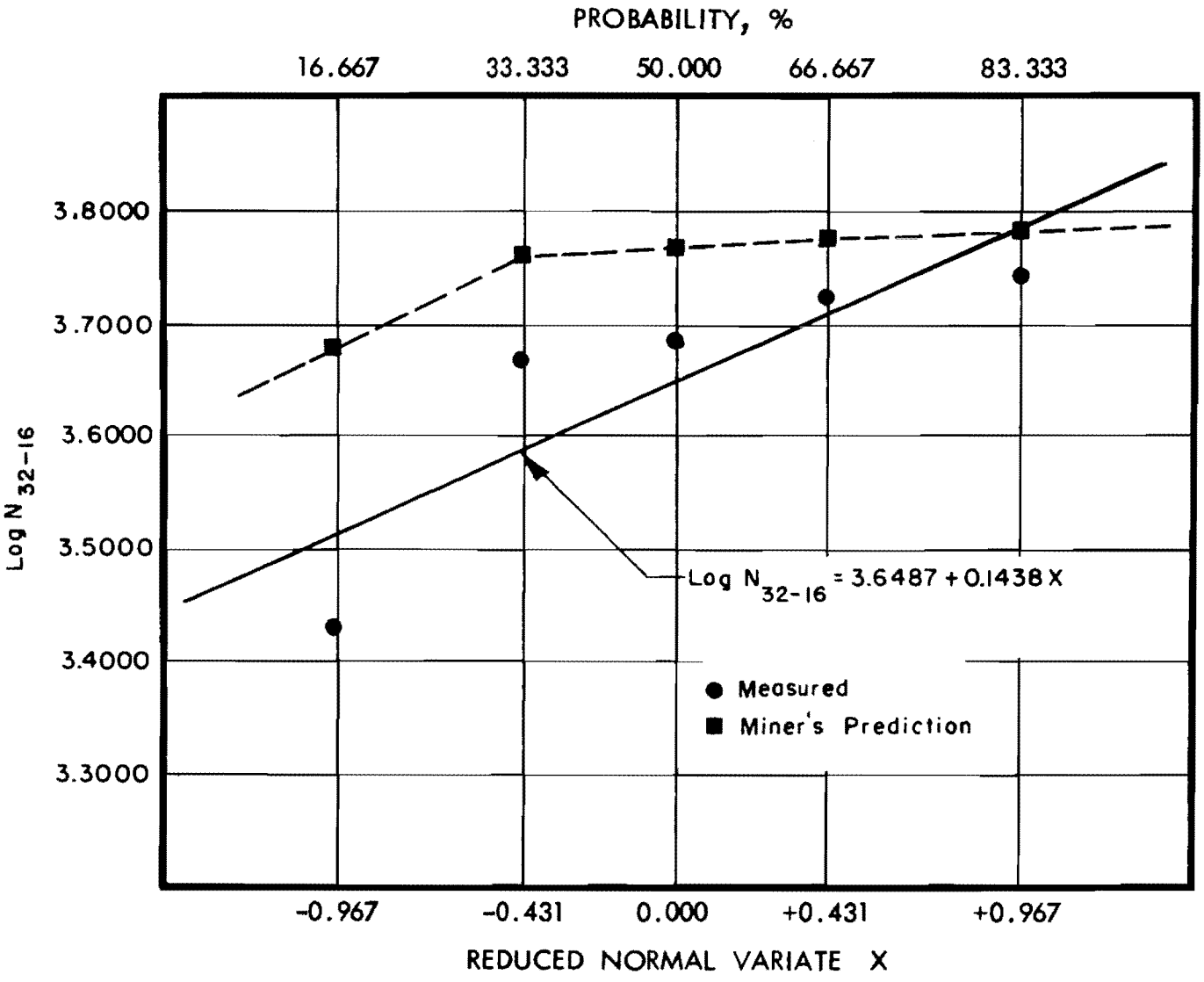

Fig D-8. Logarithm of compound fatigue life versus probability of failure: 32-16 psi, limestone.

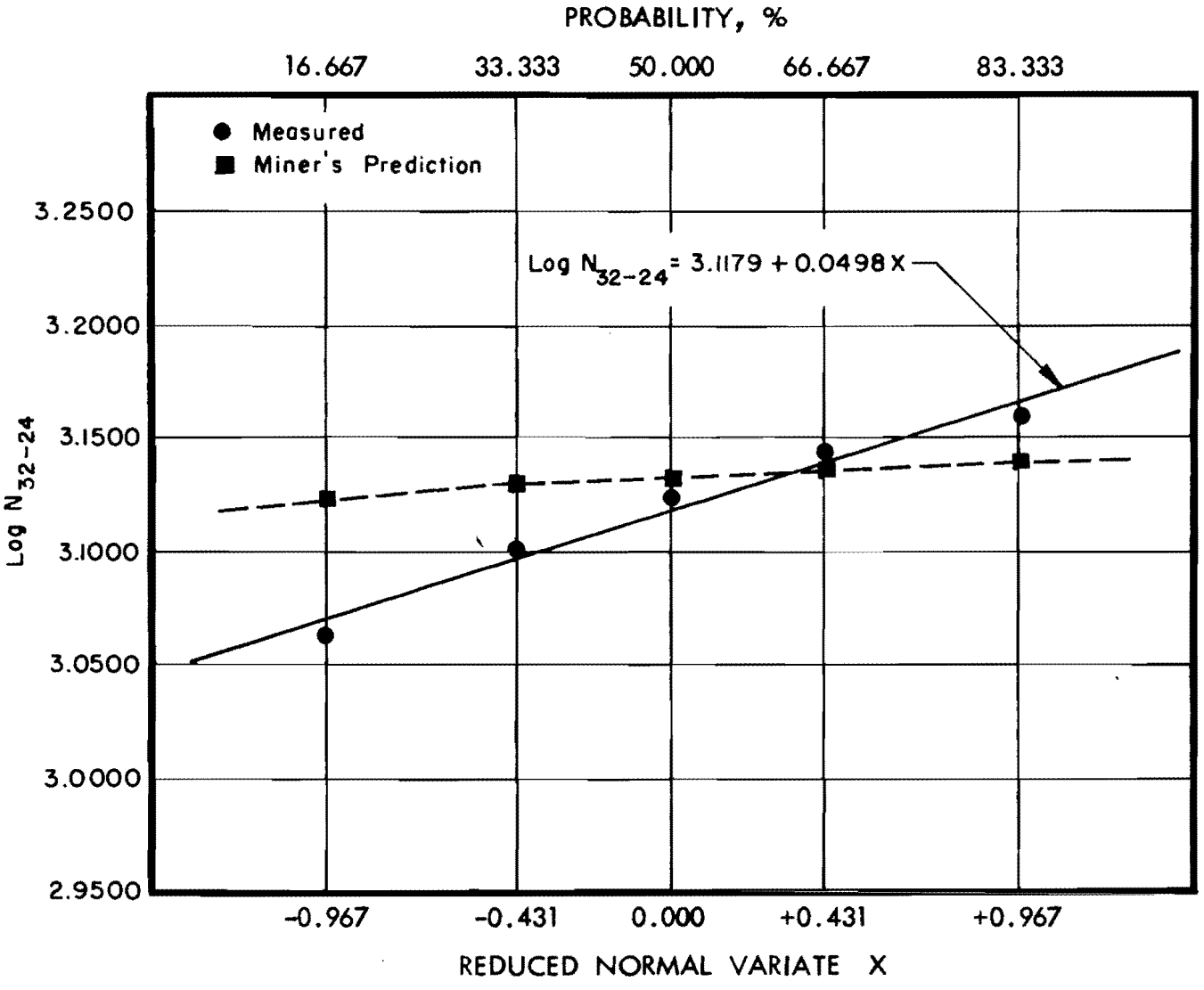

Fig D-9. Logarithm of compound fatigue life versus probability of failure: 32-24 psi, limestone.

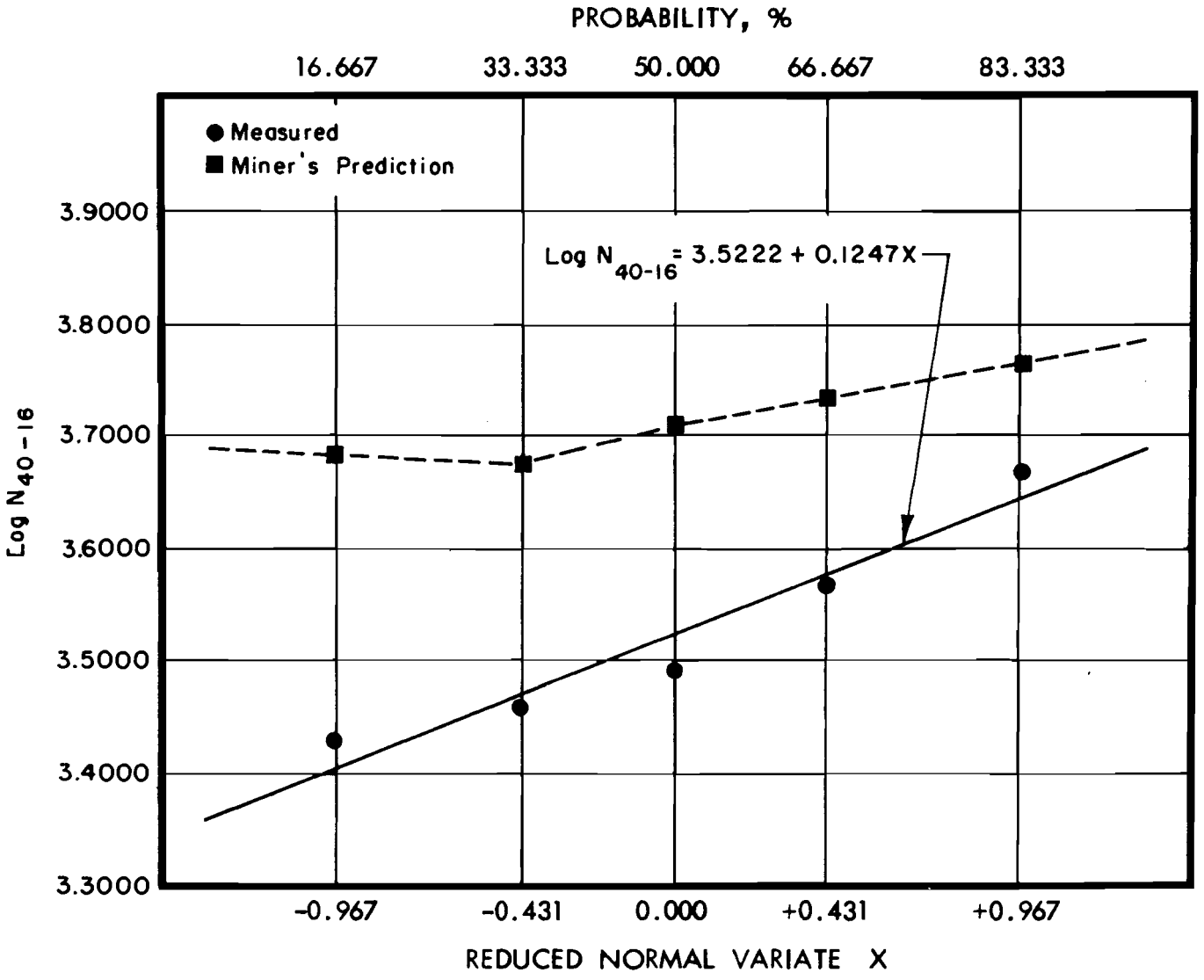

Fig D-10. Logarithm of compound fatigue life versus probability of failure: 40-16 psi, limestone.

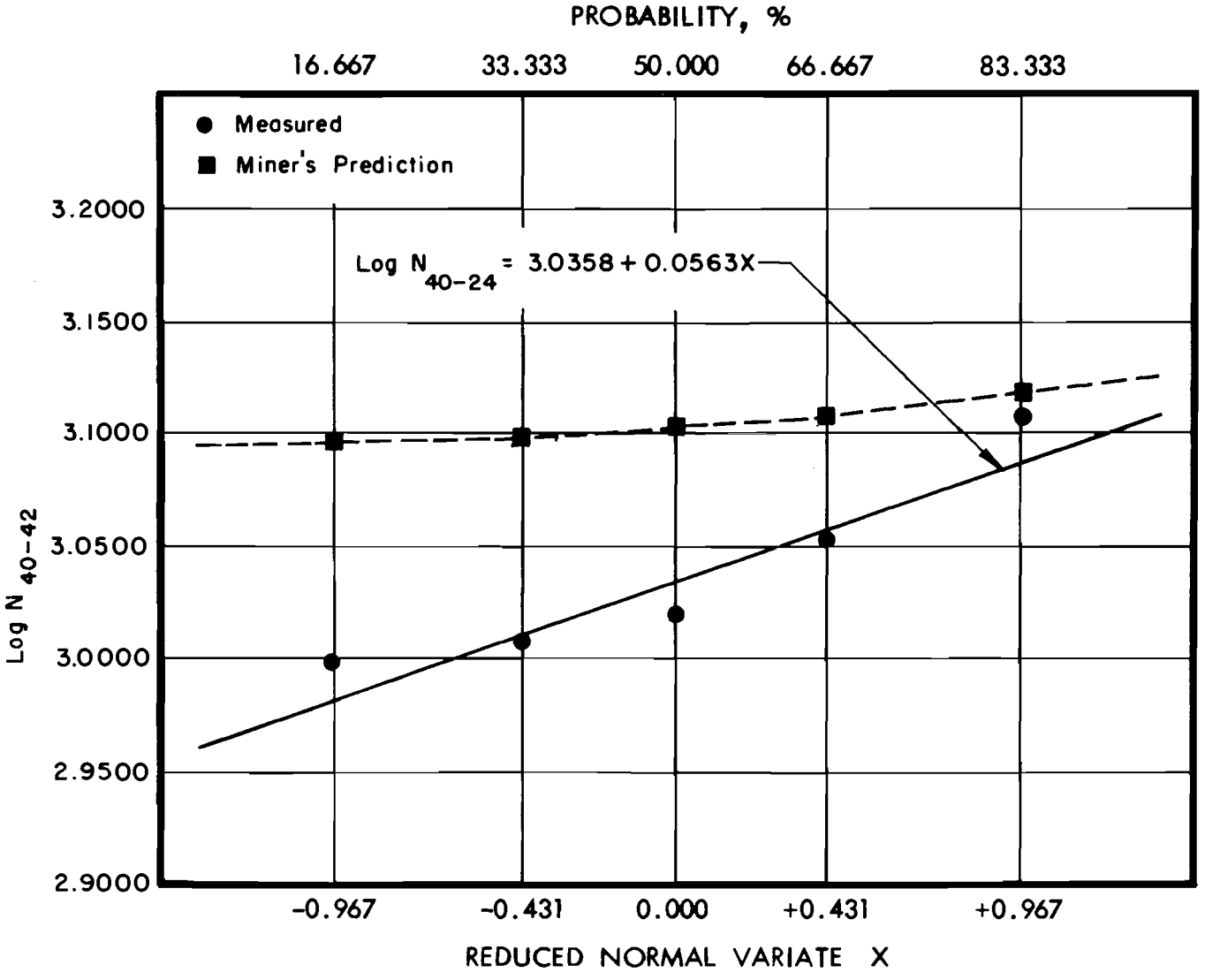

Fig D-11. Logarithm of compound fatigue life versus probability of failure: 40-24 psi, limestone.

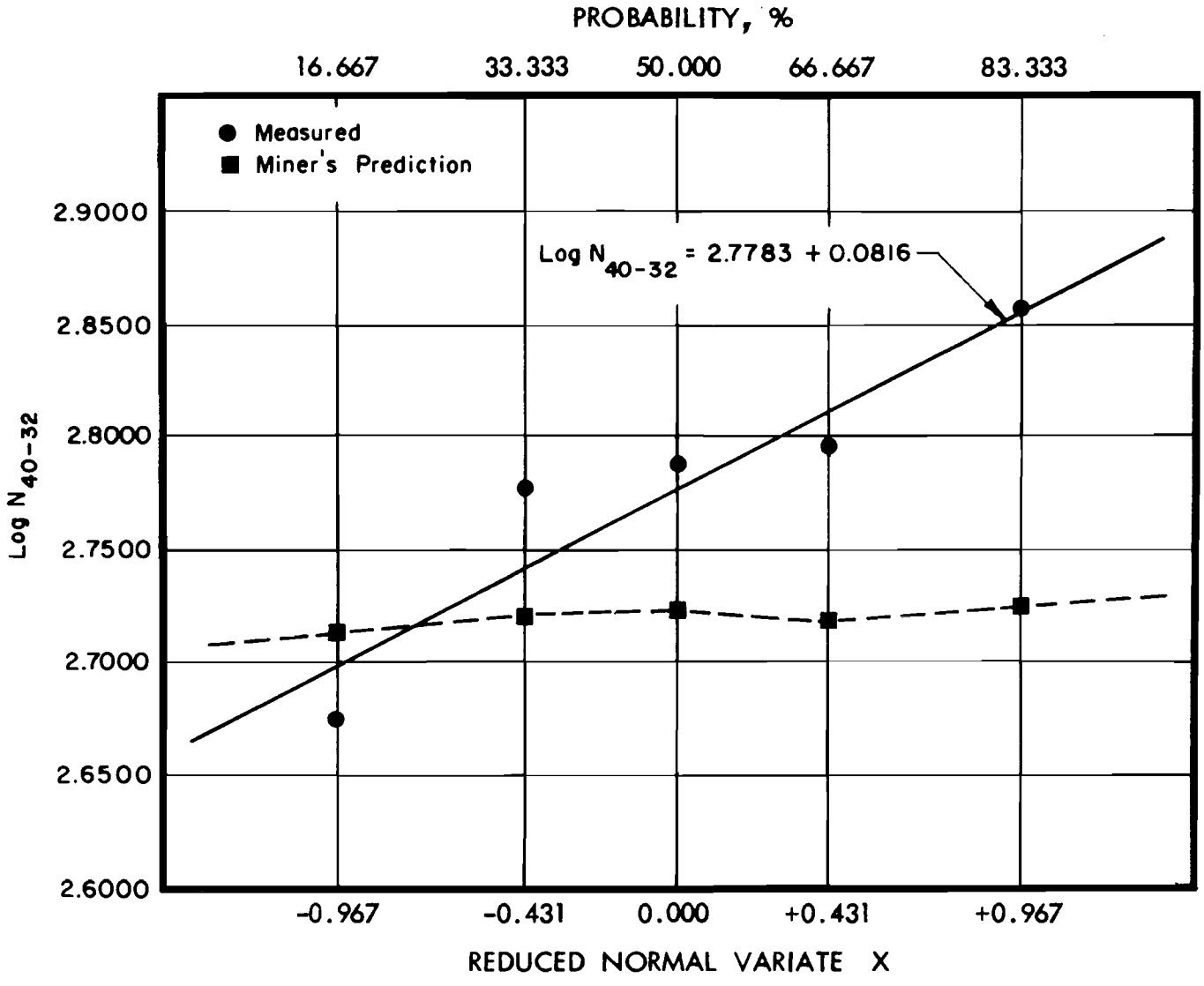

Fig D-12. Logarithm of compound fatigue life versus probability of failure: 40-32 psi, limestone.

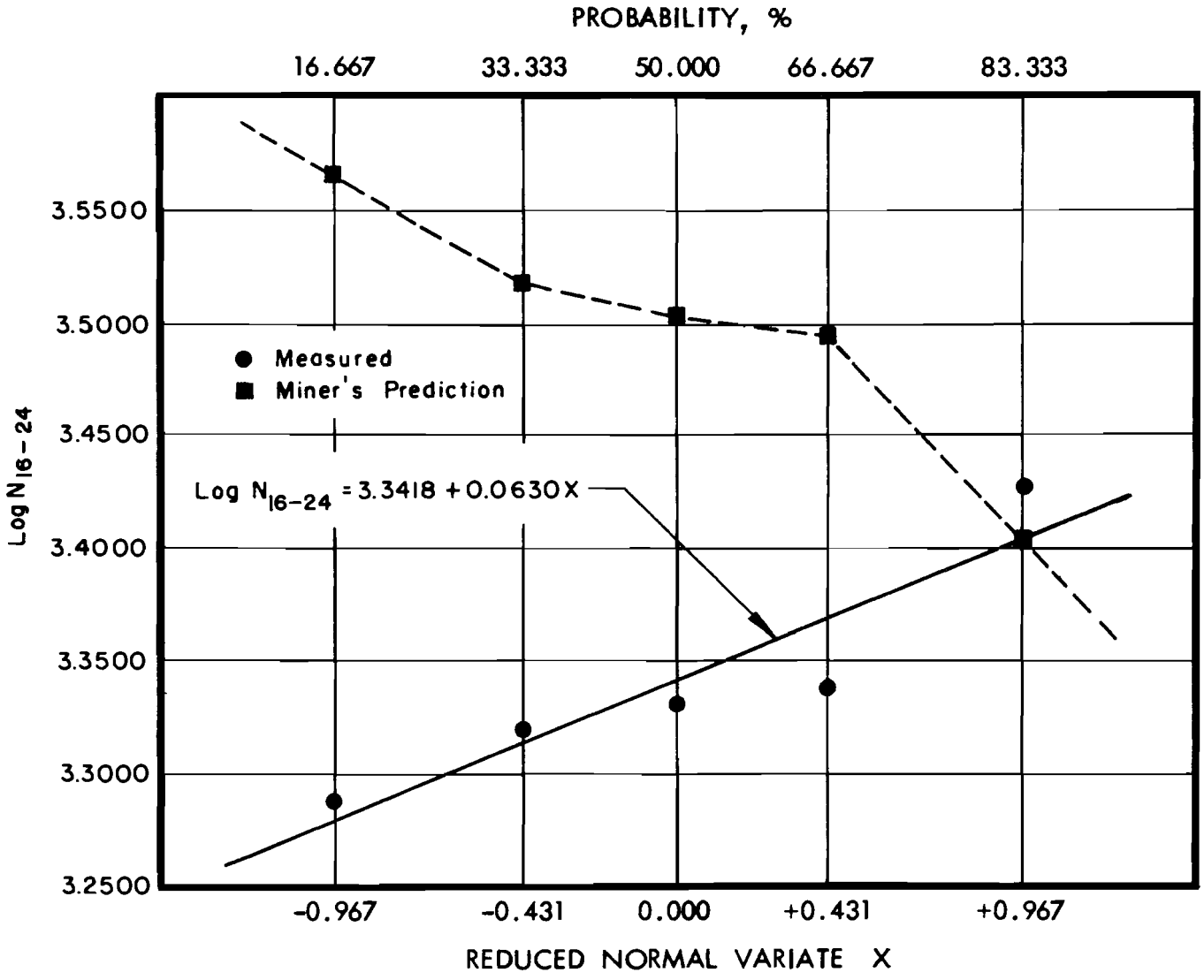

Fig D-13. Logarithm of compound fatigue life versus probability of failure: 16-24 psi, gravel.

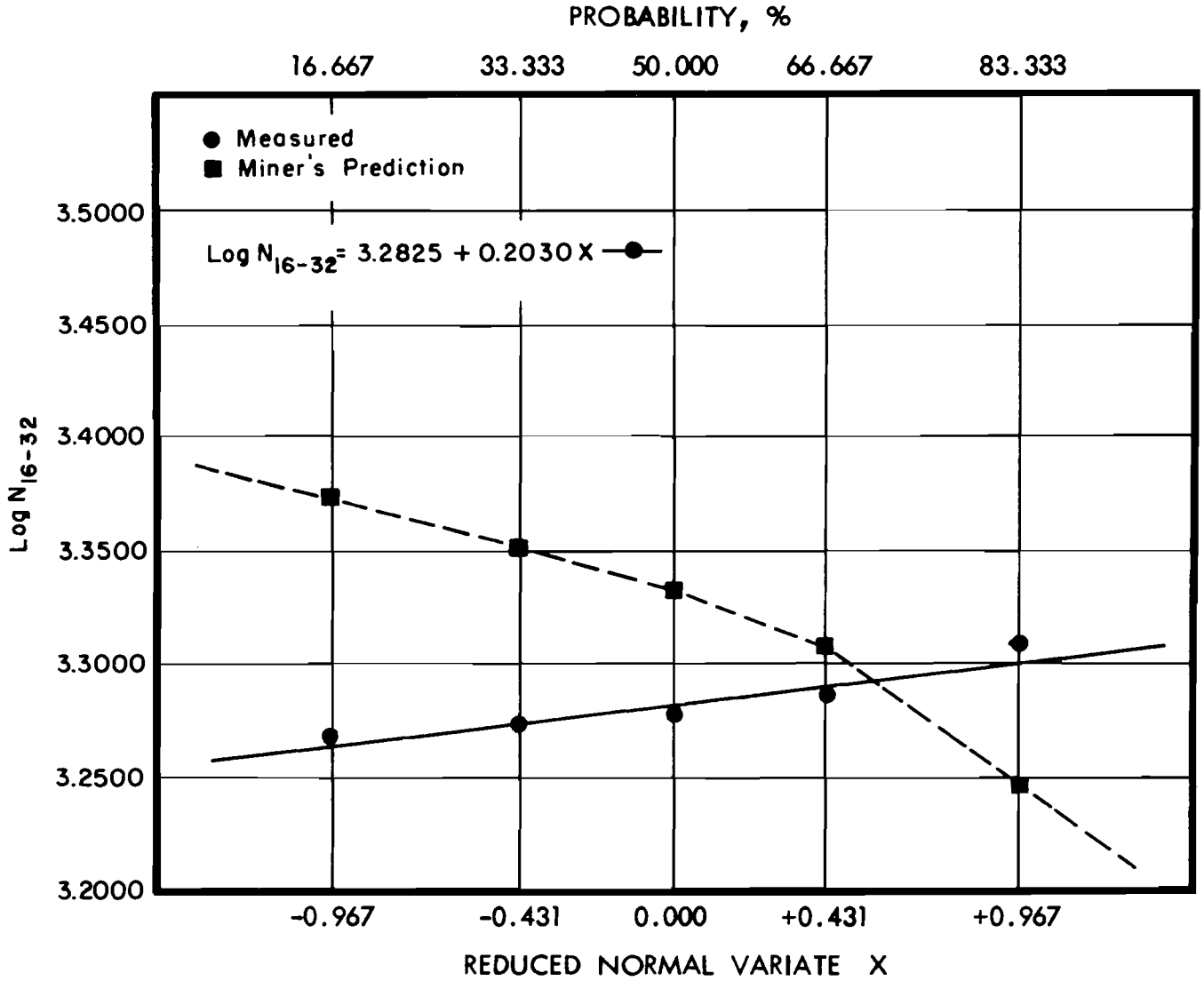

Fig D-14. Logarithm of compound fatigue life versus probability of failure: 16-32 psi, gravel.

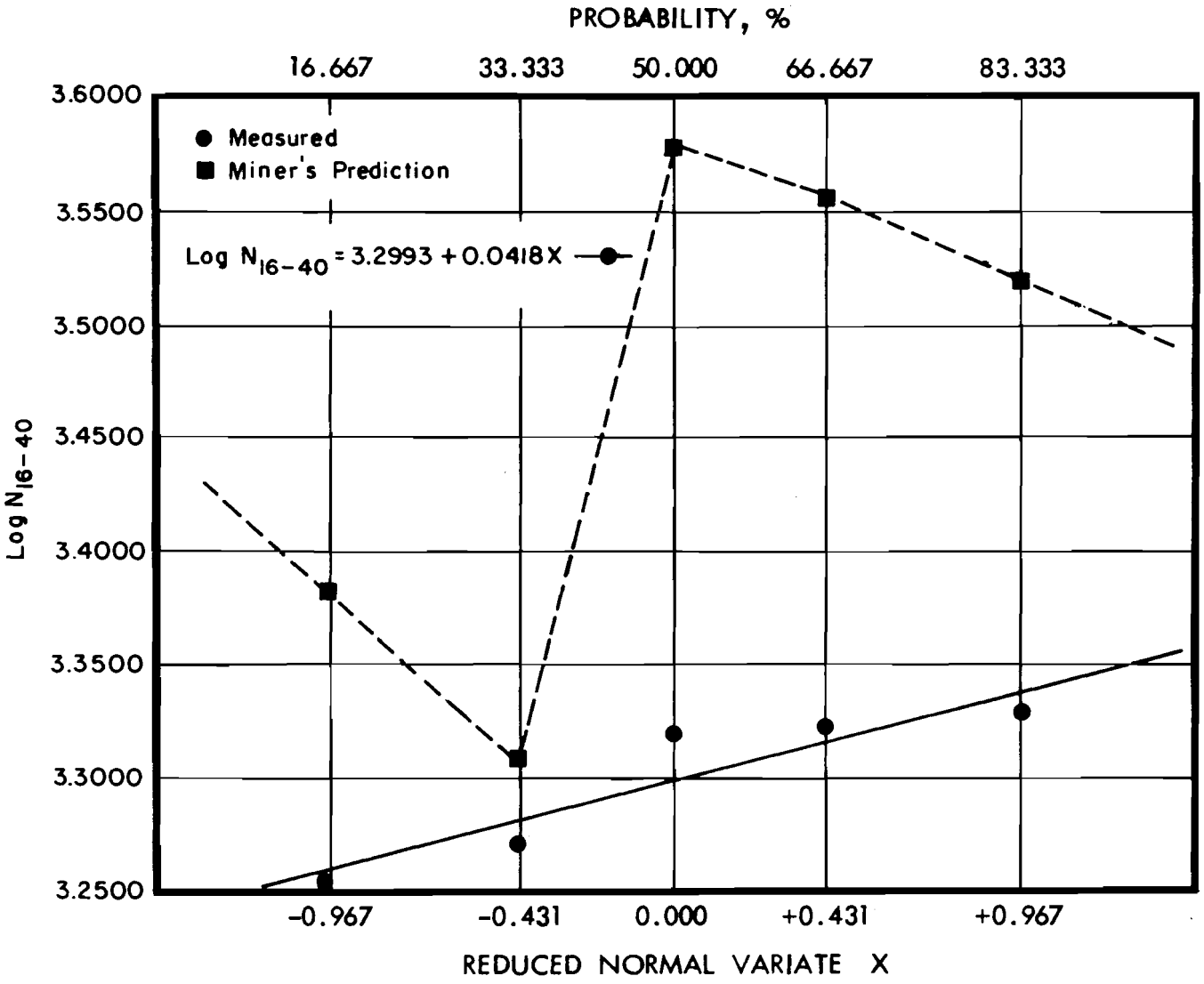

Fig D-15. Logarithm of compound fatigue life versus probability of failure: 16-40 psi, gravel.

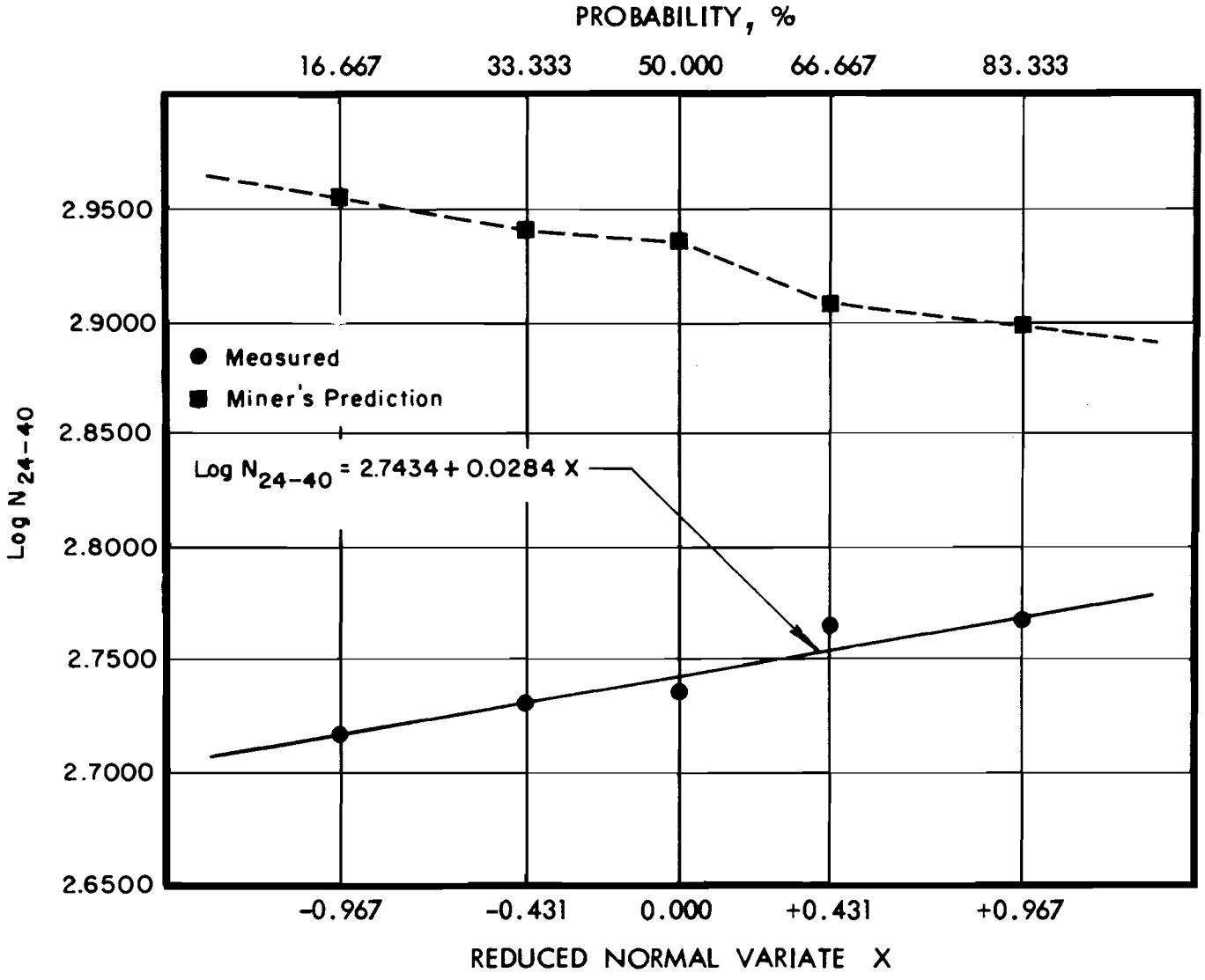

Fig D-16. Logarithm of compound fatigue life versus probability of failure: 24-40 psi, gravel.

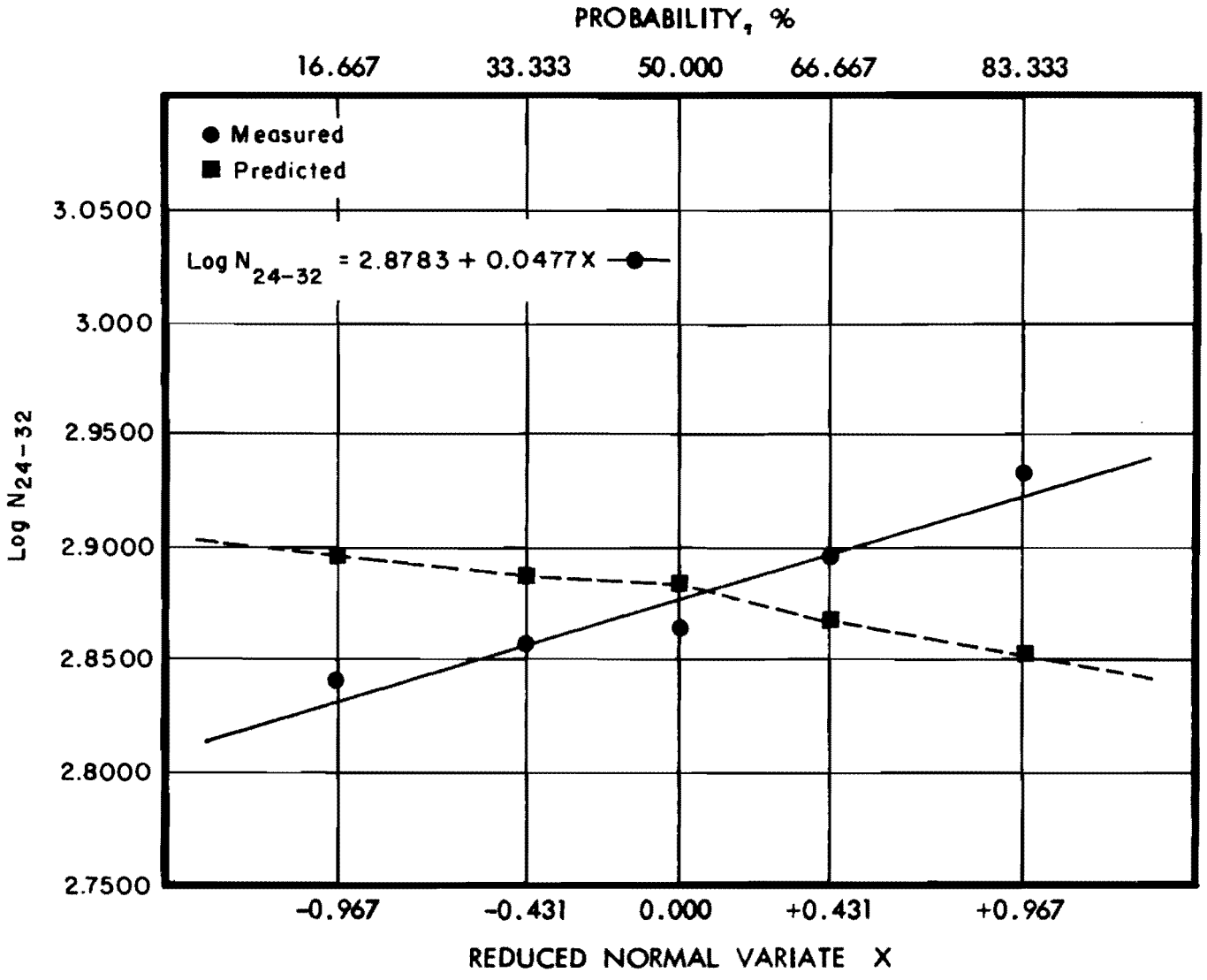

Fig D-17. Logarithm of compound fatigue life versus probability of failure: 24-32 psi, gravel.

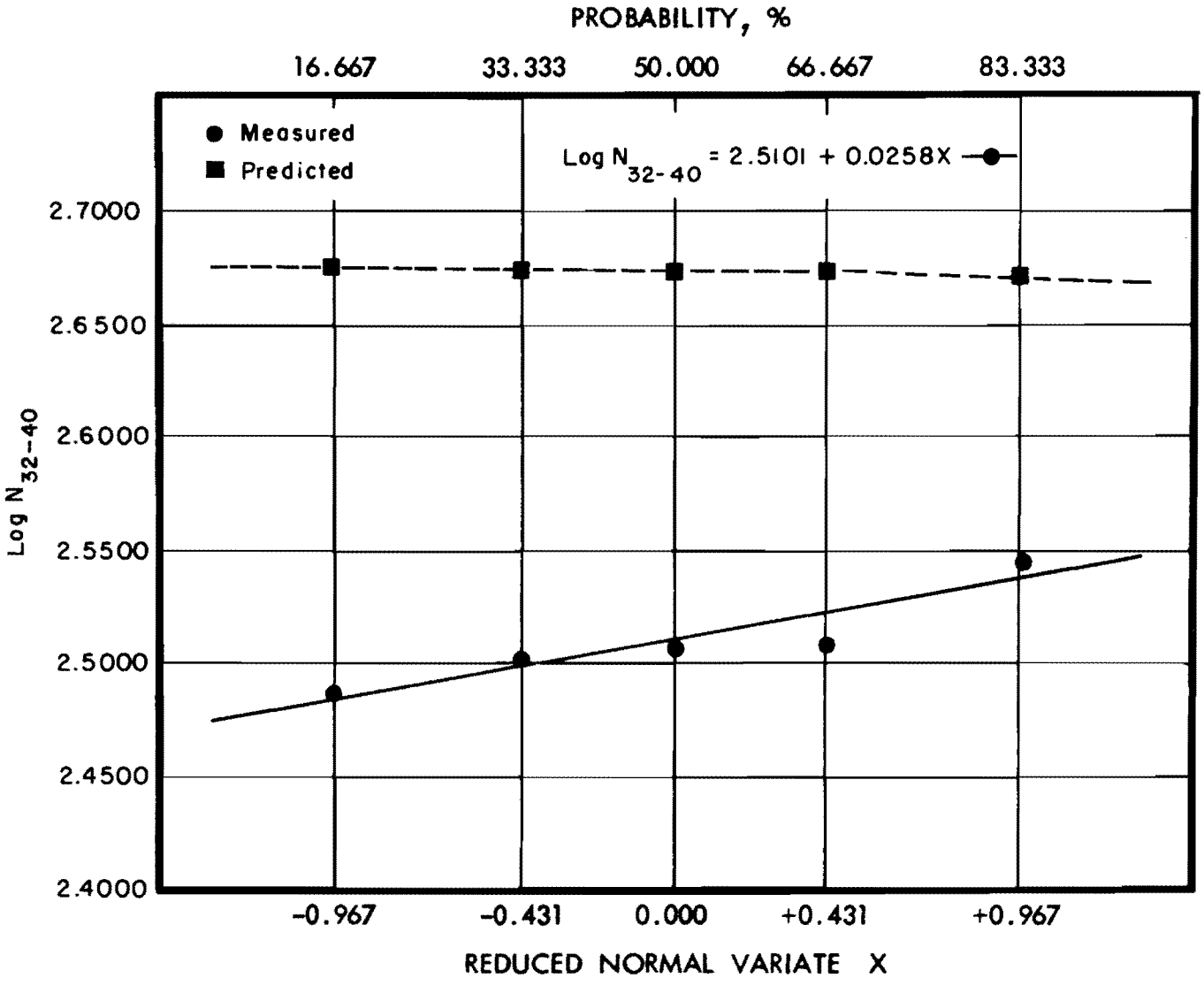

Fig D-18. Logarithm of compound fatigue life versus probability of failure: 32-40 psi, gravel.

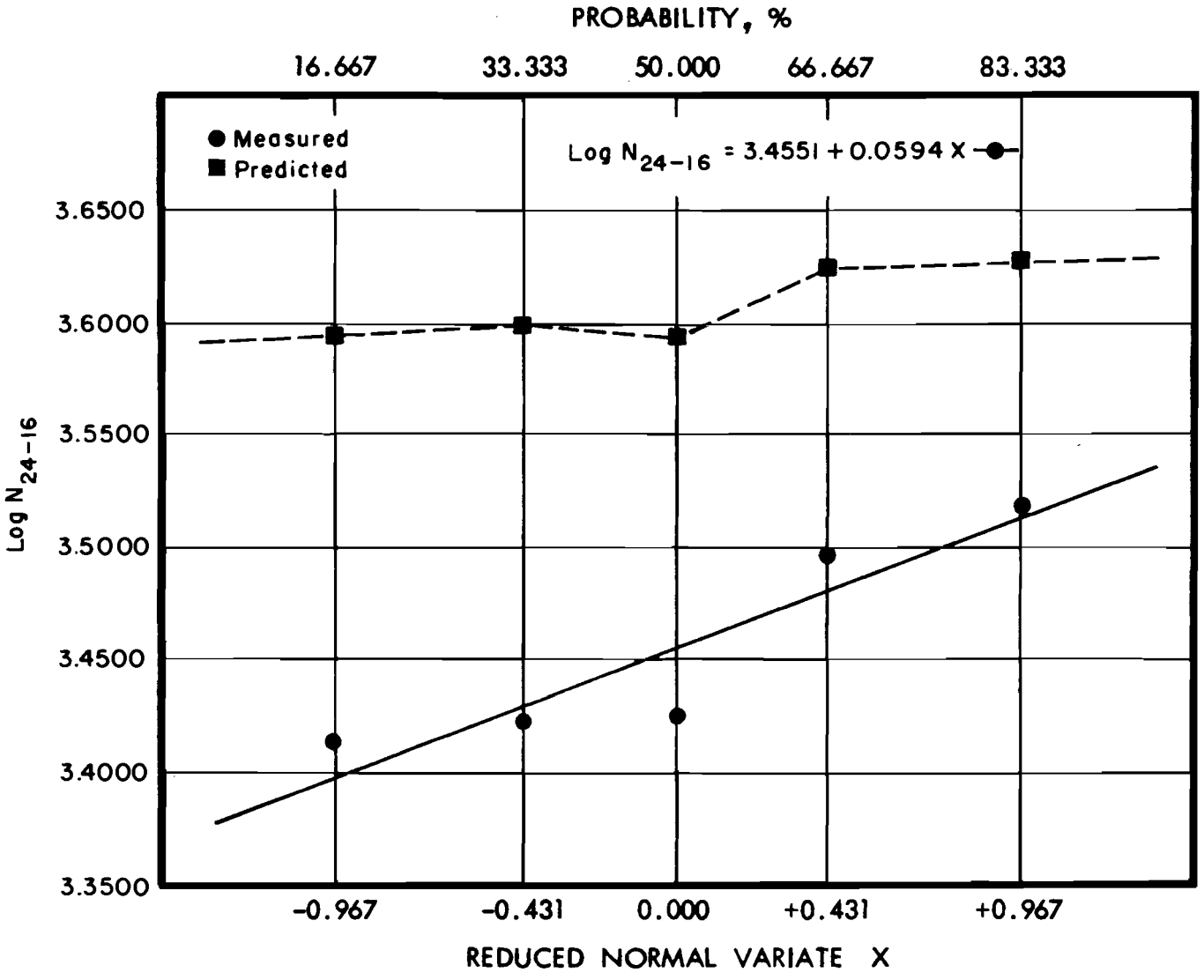

Fig D-19. Logarithm of compound fatigue life versus probability of failure: 24-16 psi, gravel.

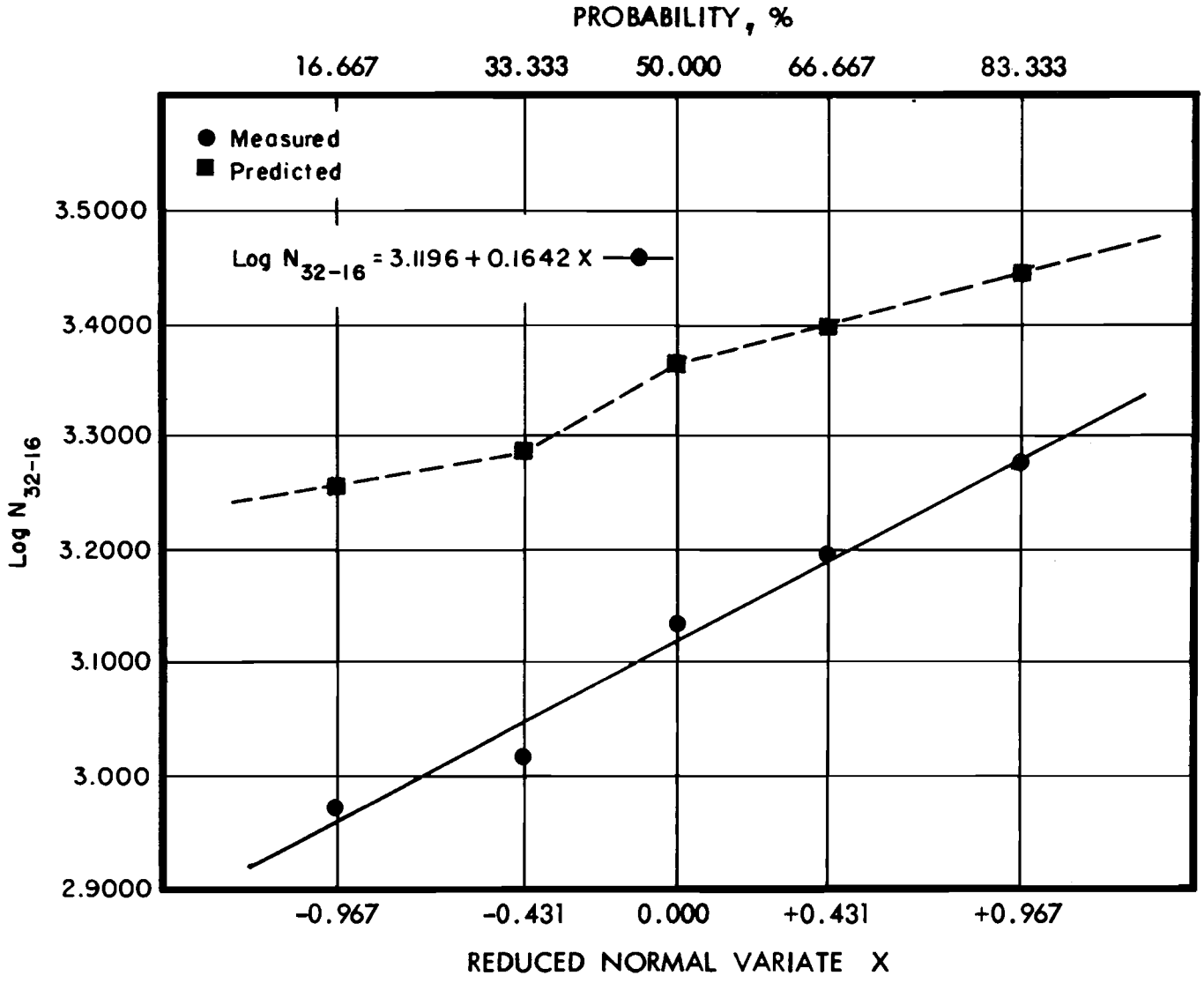

Fig D-20. Logarithm of compound fatigue life versus probability of failure: 32-16 psi, gravel.

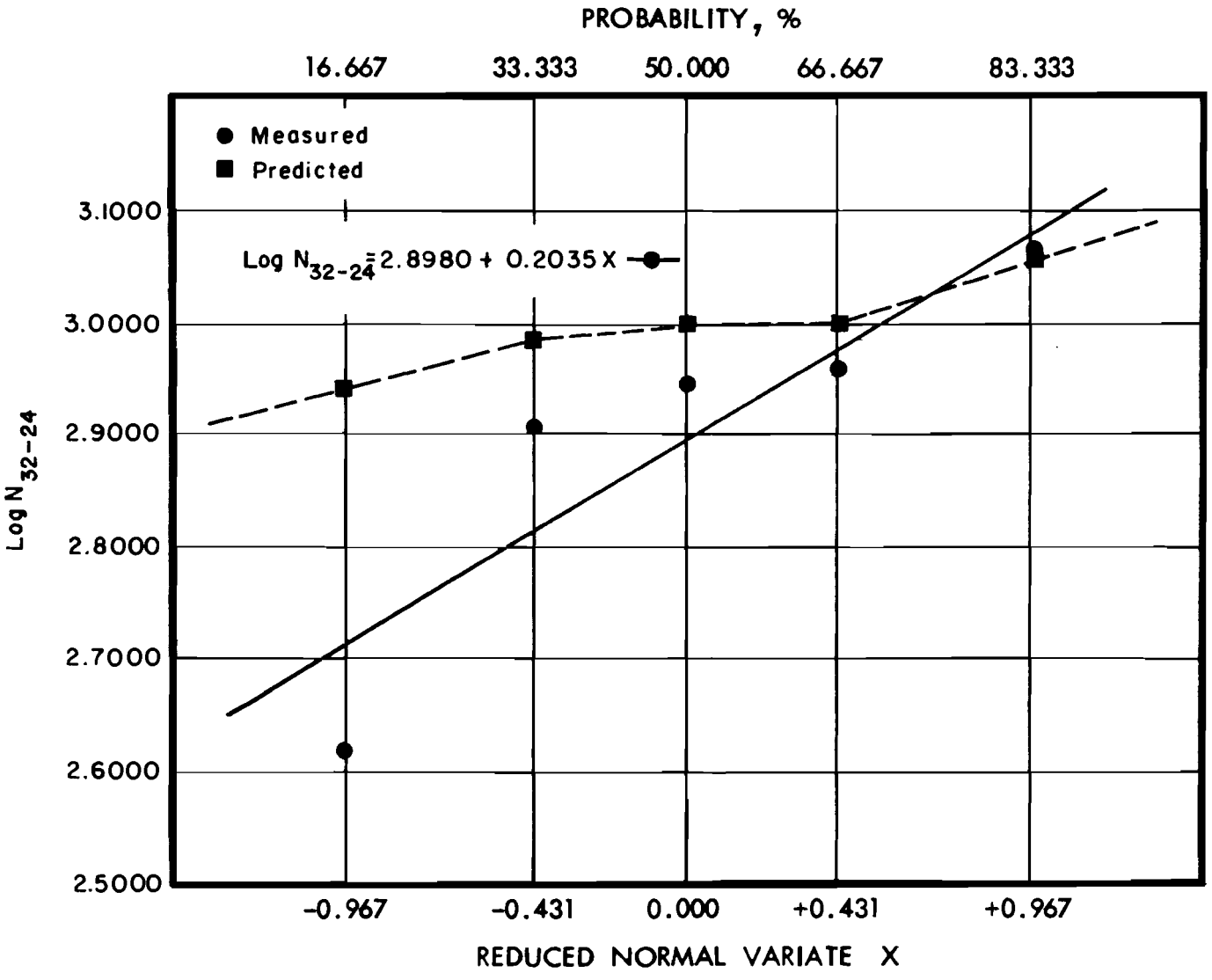

Fig D-21. Logarithm of compound fatigue life versus probability of failure: 32-24 psi, gravel.

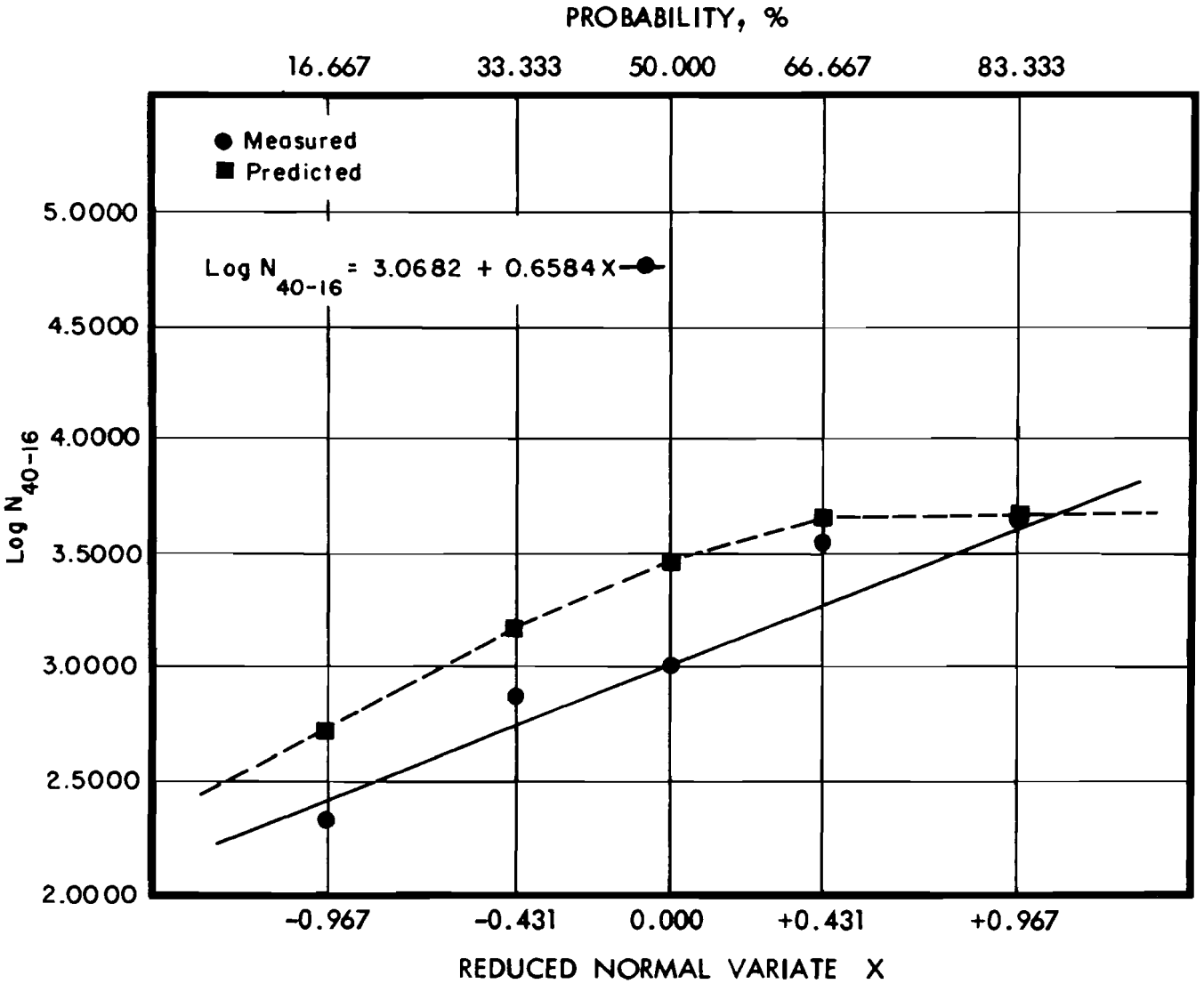

Fig D-22. Logarithm of compound fatigue life versus probability of failure: 40-16 psi, gravel.

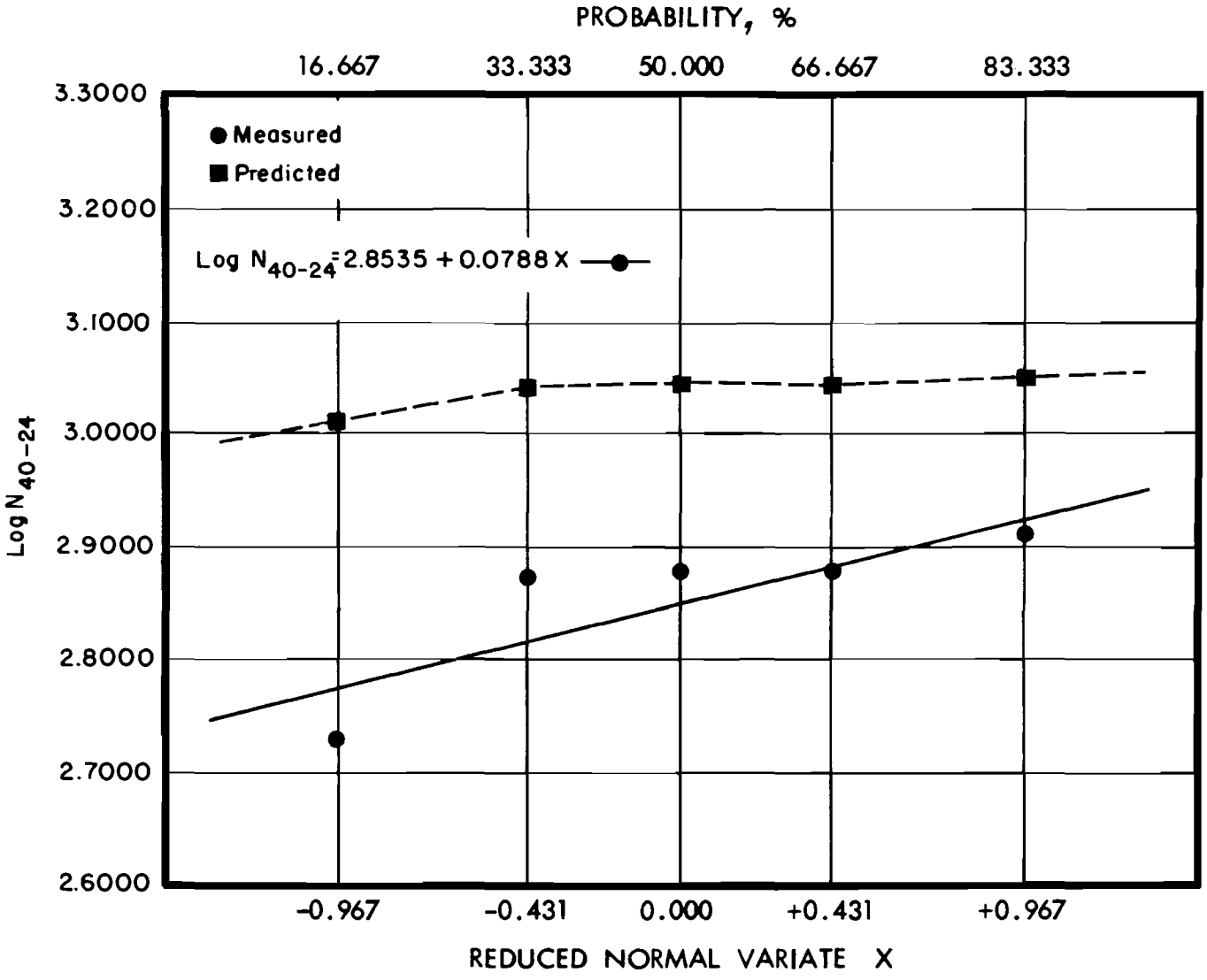

Fig D-23. Logarithm of compound fatigue life versus probability of failure: 40-24 psi, gravel.

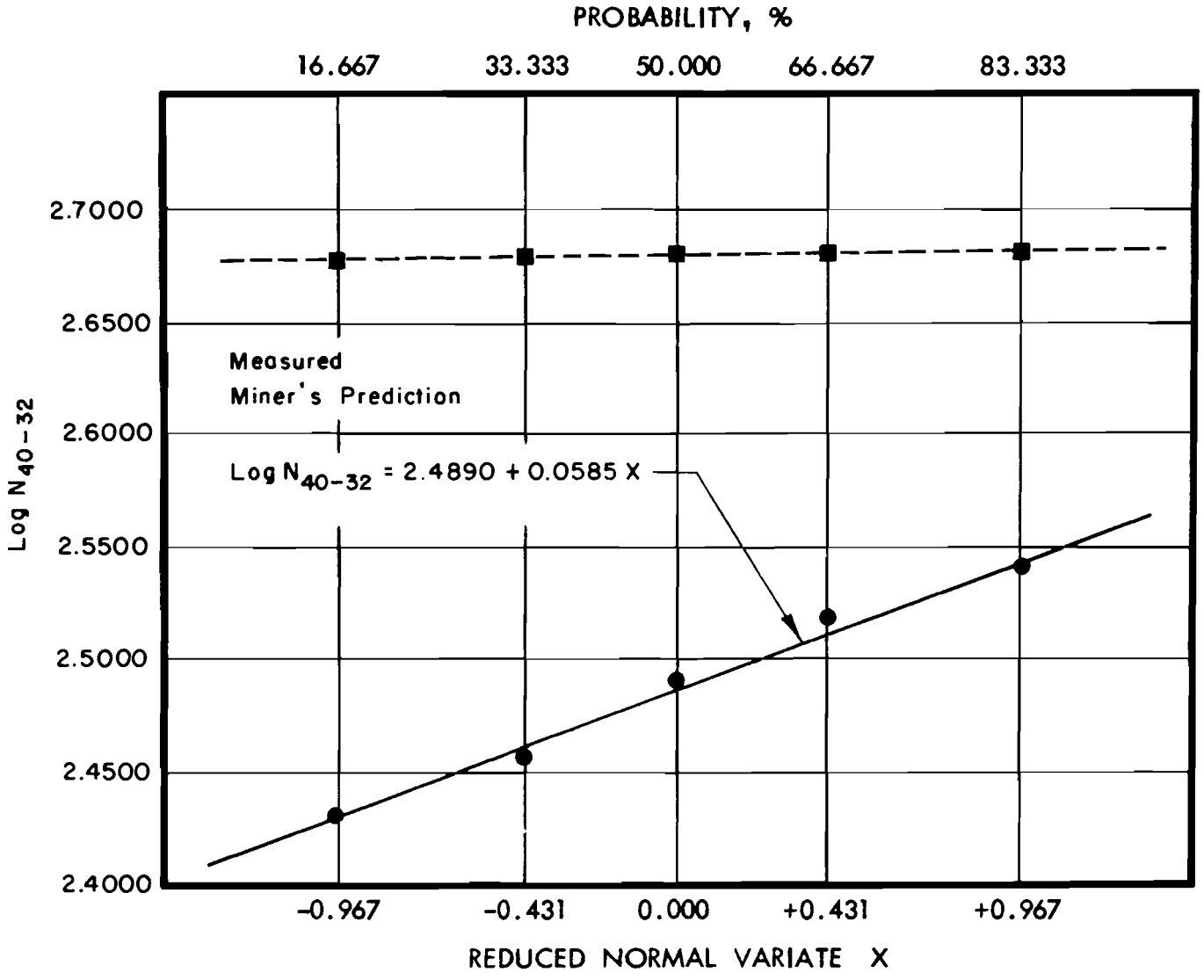

Fig D-24. Logarithm of compound fatigue life versus probability of failure: 40-32 psi, gravel.

APPENDIX E

TIME-DEFORMATION DAMAGE RELATIONSHIPS

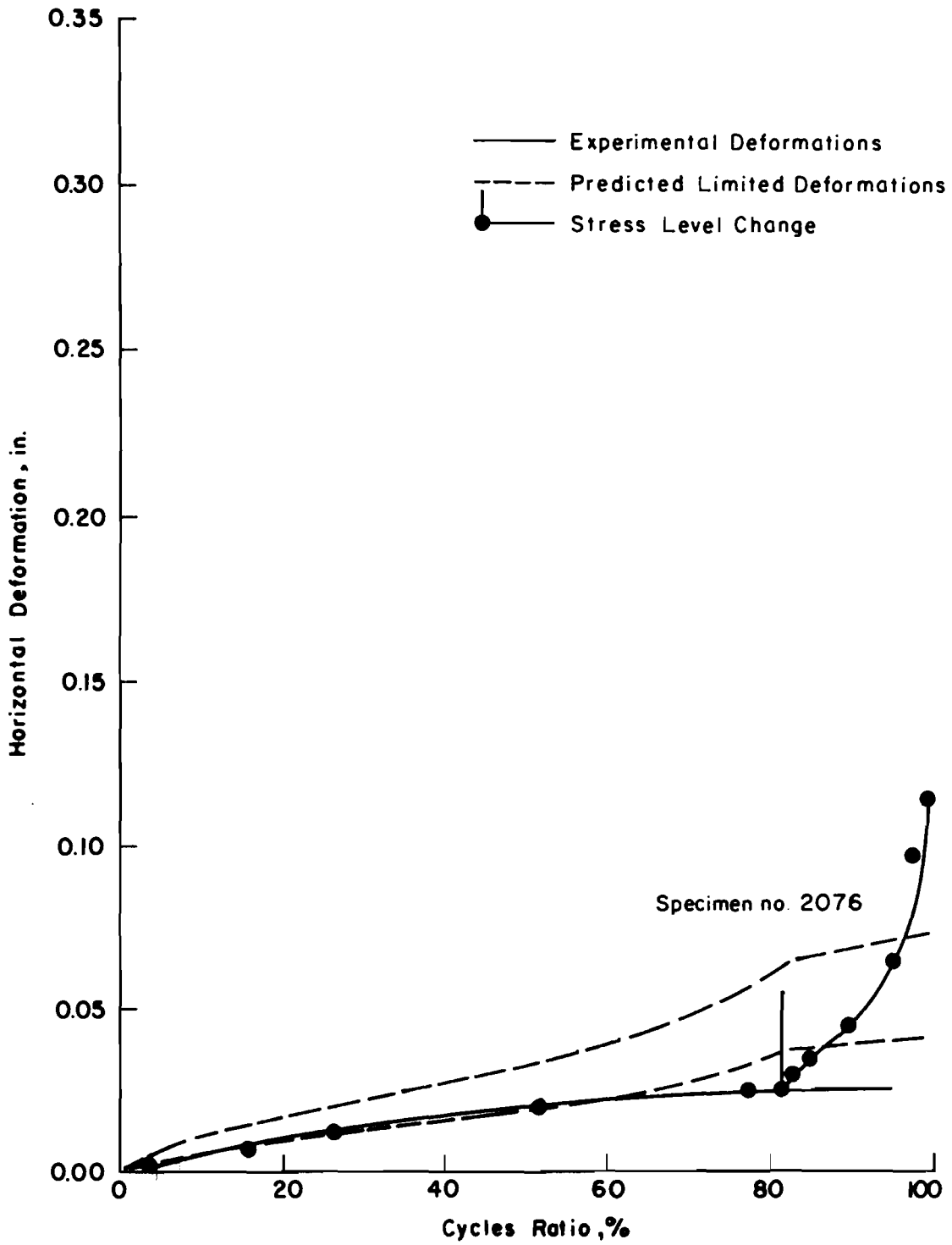

Fig E-1. Comparison of actual and predicted horizontal deformation: 16-24 psi, gravel.

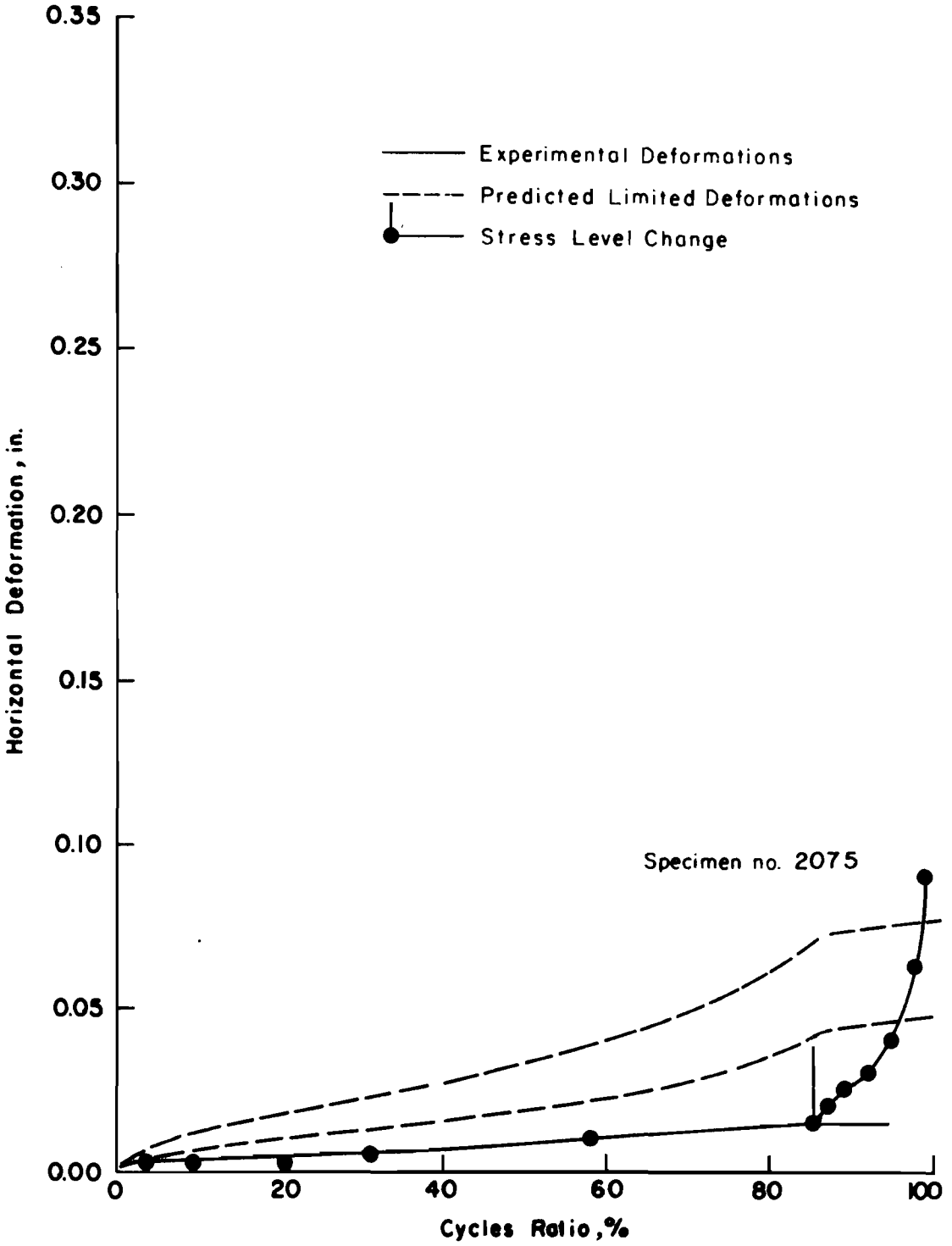

Fig E-2. Comparison of actual and predicted horizontal deformation: 16-32 psi, gravel.

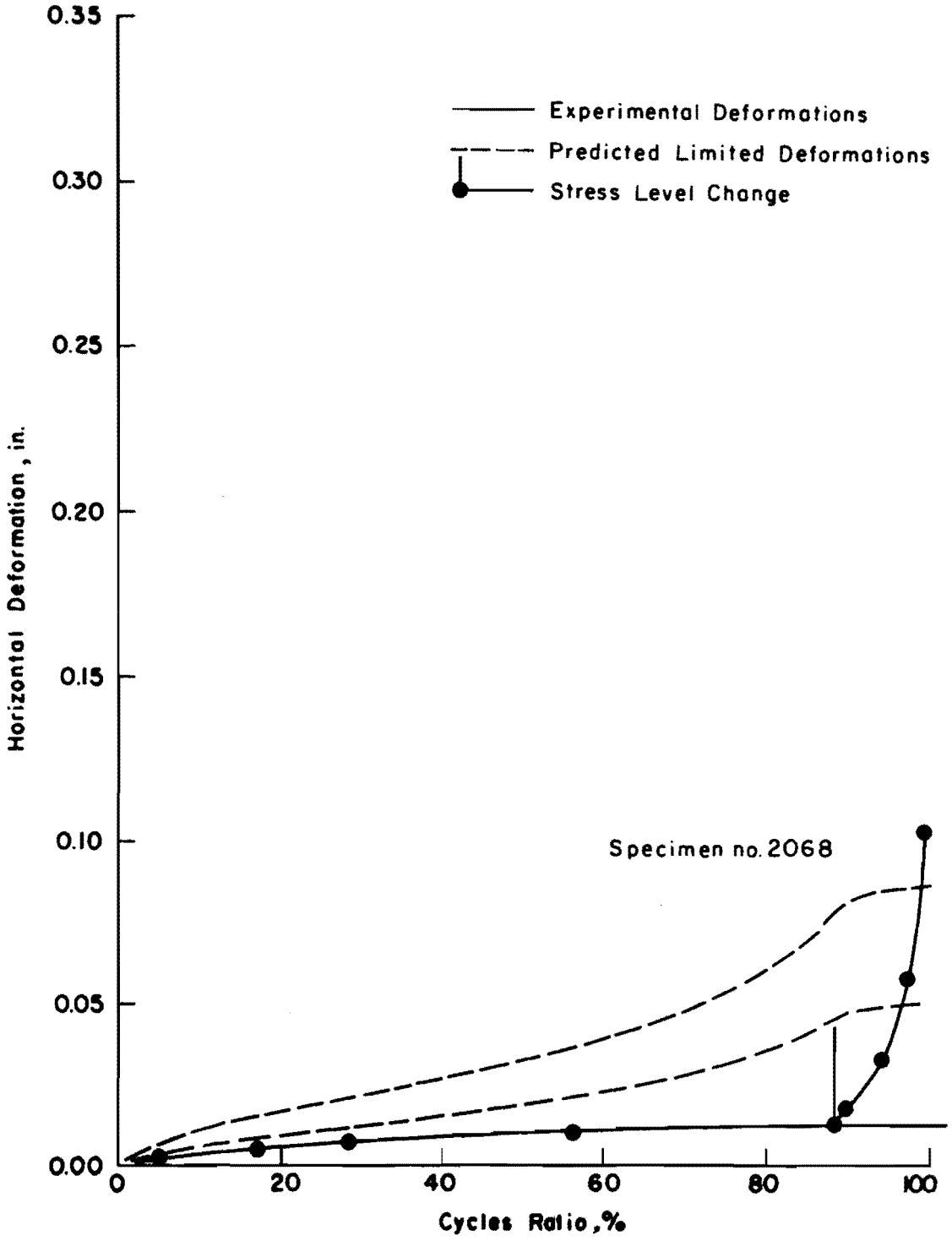

Fig E-3. Comparison of actual and predicted horizontal deformation: 16-40 psi, gravel.

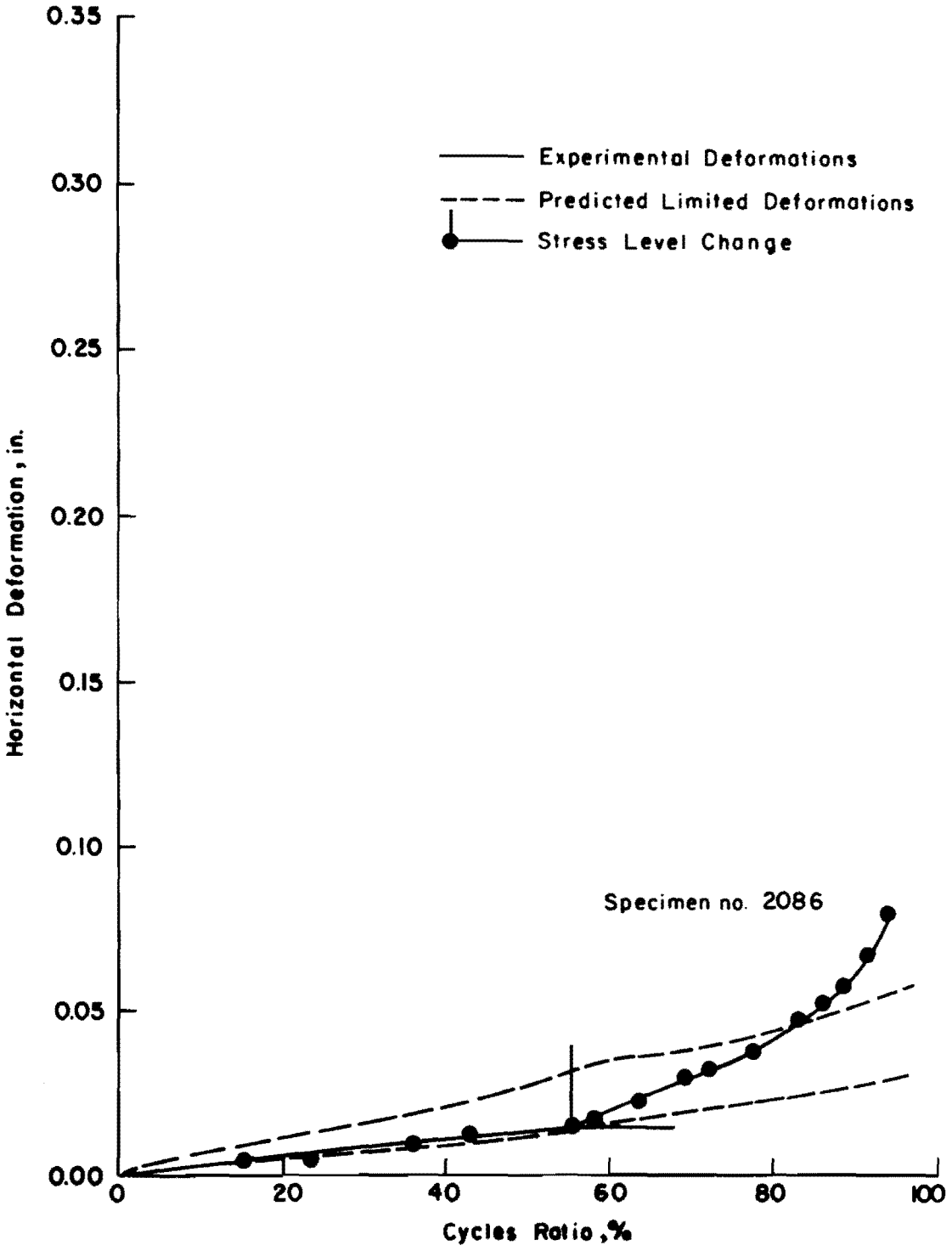

Fig E-4. Comparison of actual and predicted horizontal deformation: 24-32 psi, gravel.

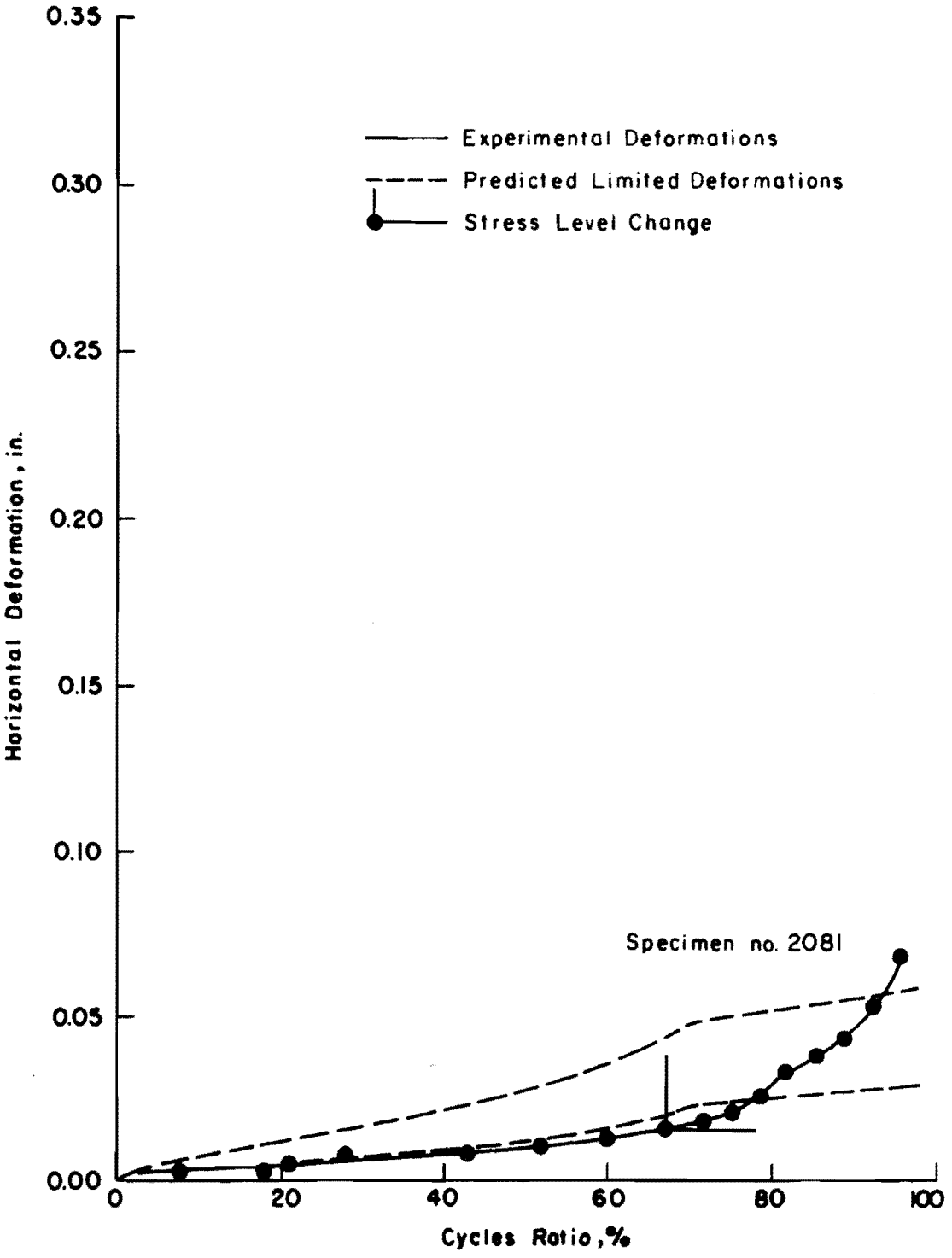

Fig E-5. Comparison of actual and predicted horizontal deformation: 24-40 psi, gravel.

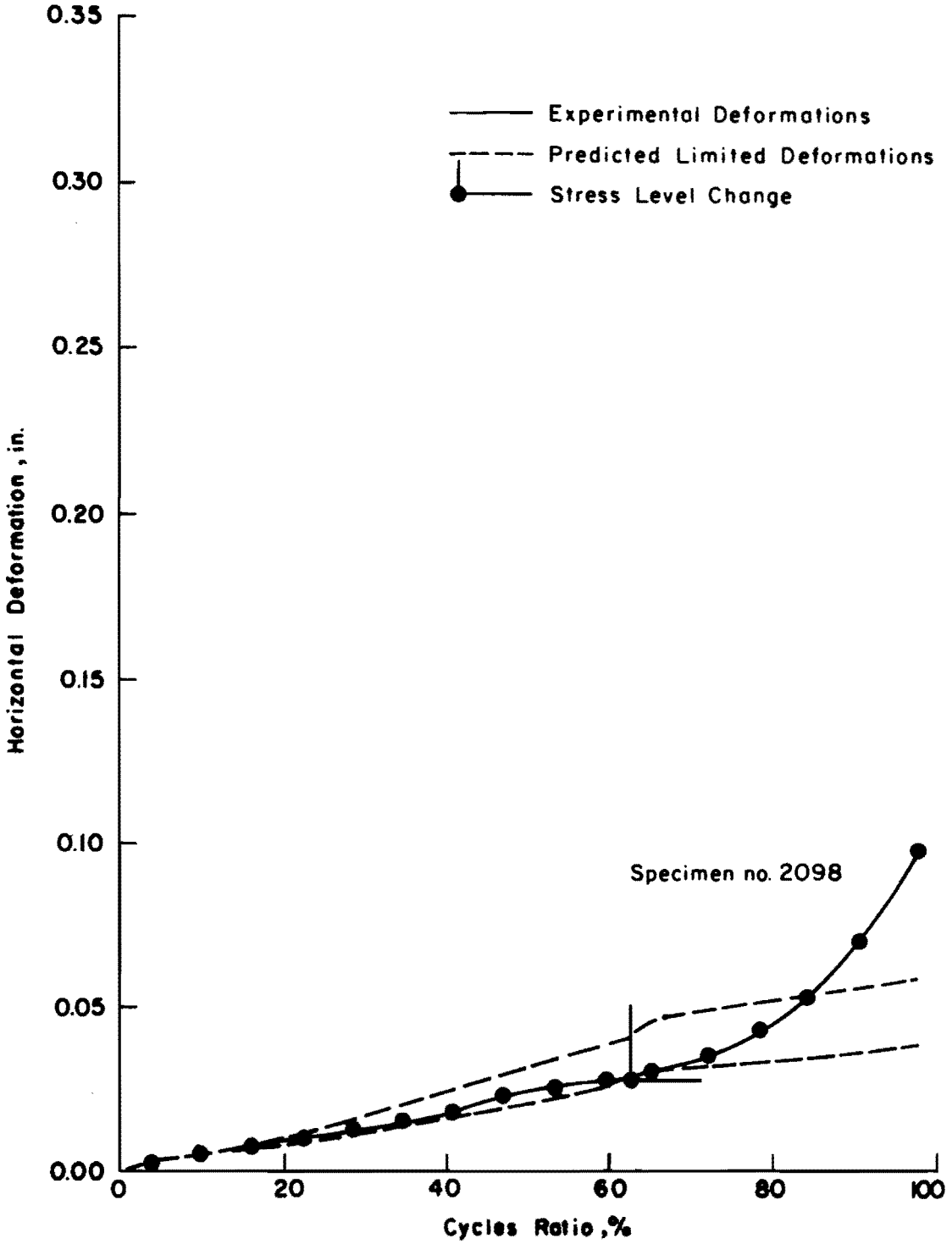

Fig E-6. Comparison of actual and predicted horizontal deformation: 32-40 psi, gravel.

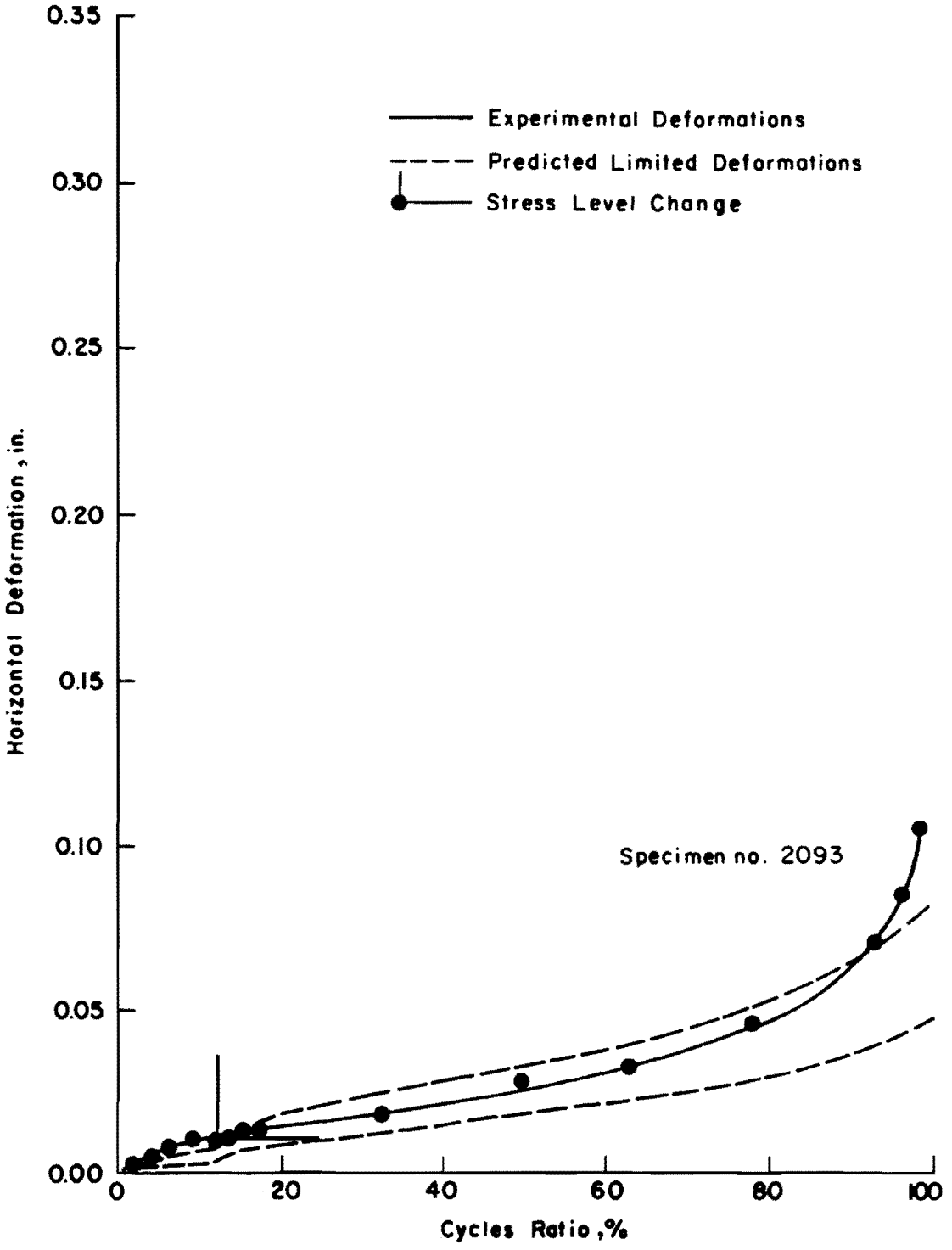

Fig E-7. Comparison of actual and predicted horizontal deformation: 24-16 psi, gravel.

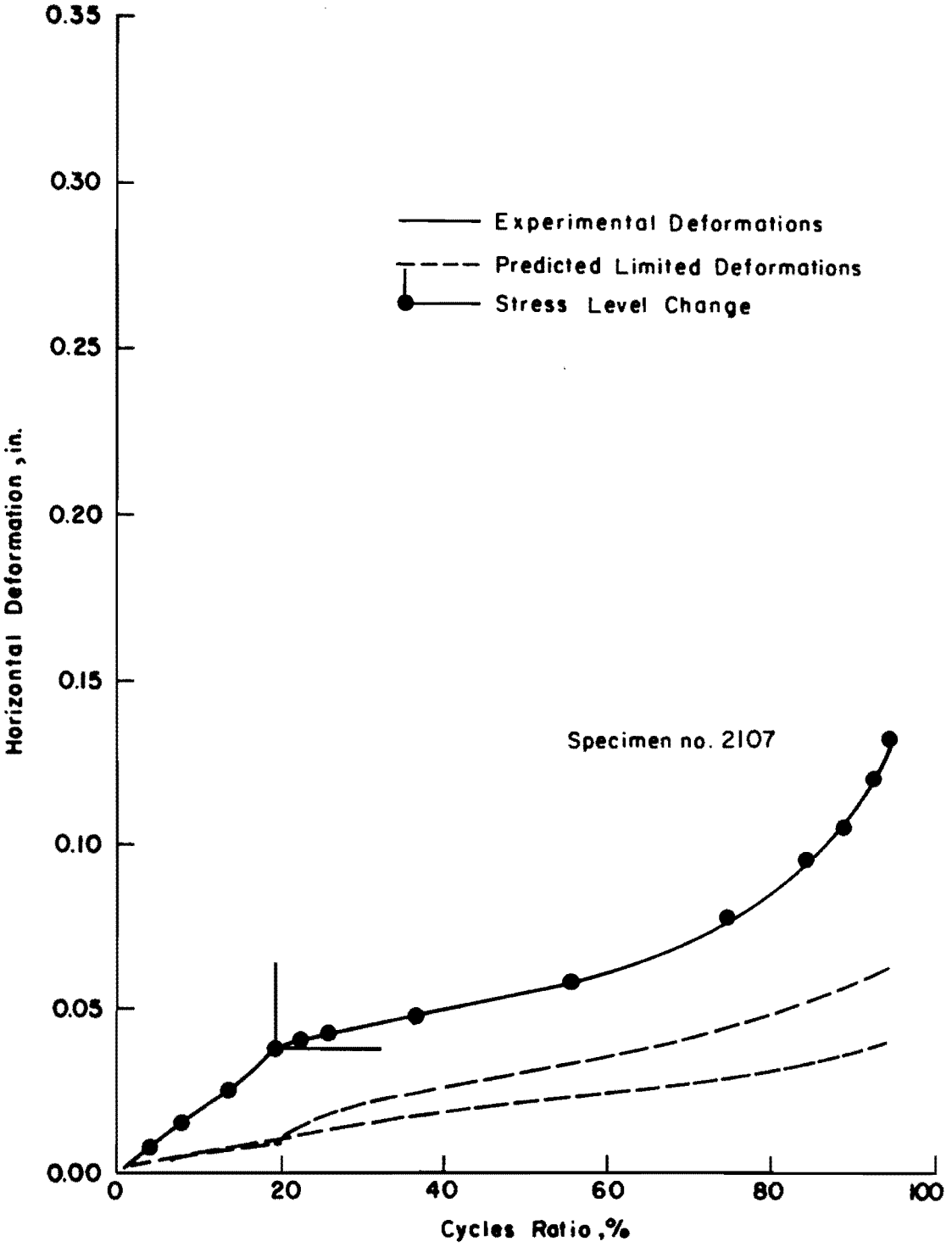

Fig E-8. Comparison of actual and predicted horizontal deformation: 32-16 psi, gravel.

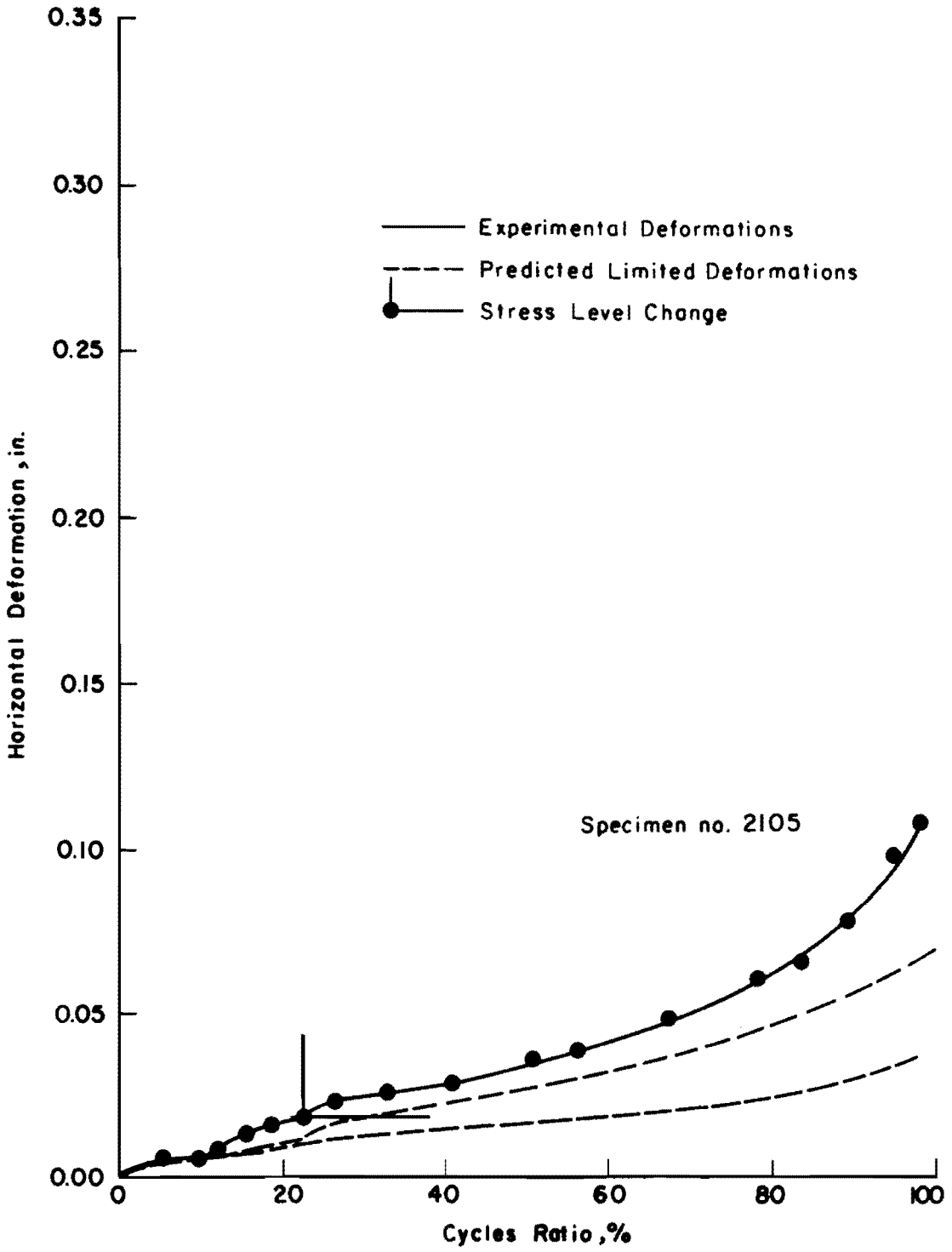

Fig E-9. Comparison of actual and predicted horizontal deformation: 32-24 psi, gravel.

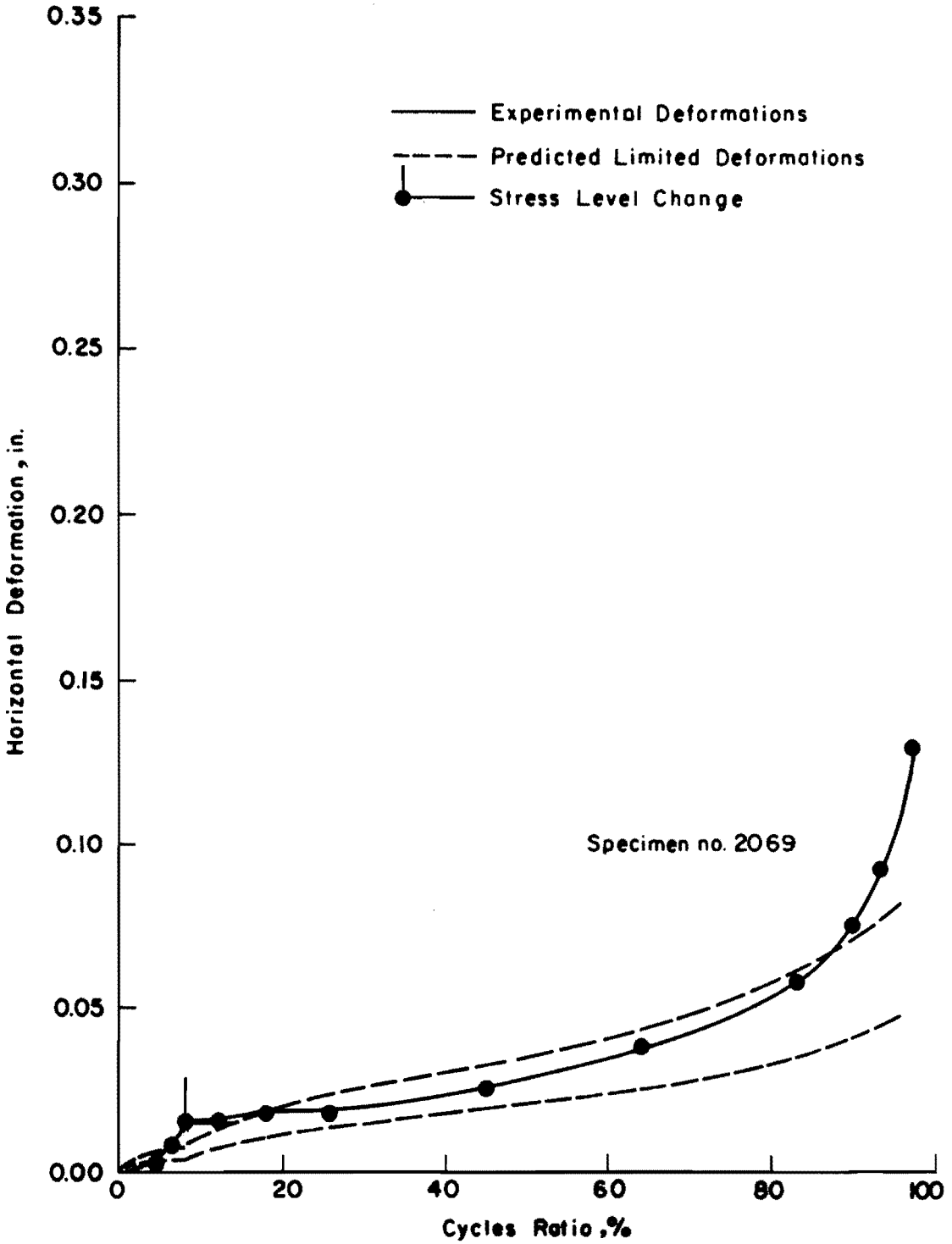

Fig E-10. Comparison of actual and predicted horizontal deformation: 40-16 psi, gravel.

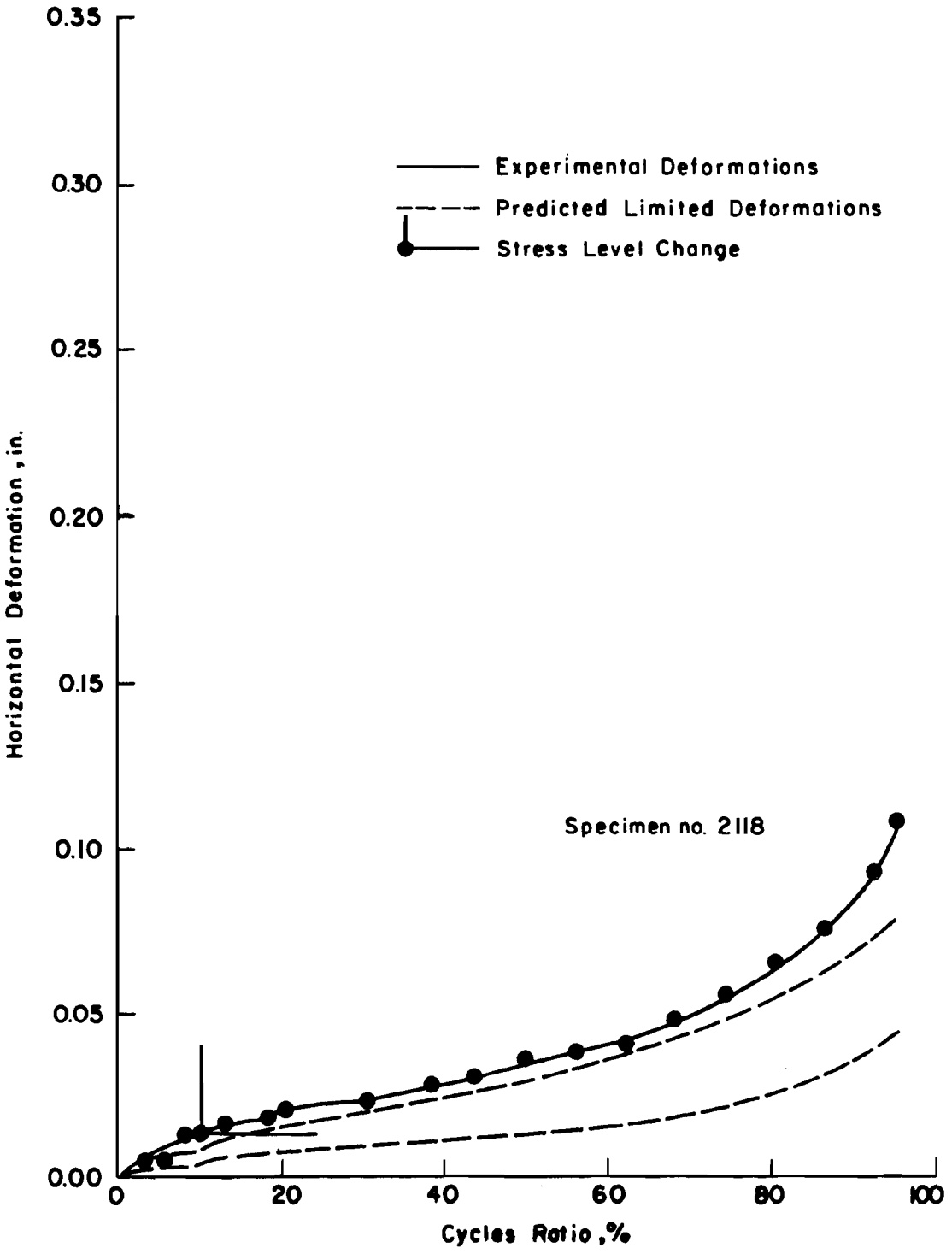

Fig E-11. Comparison of actual and predicted horizontal deformation: 40-24 psi, gravel.

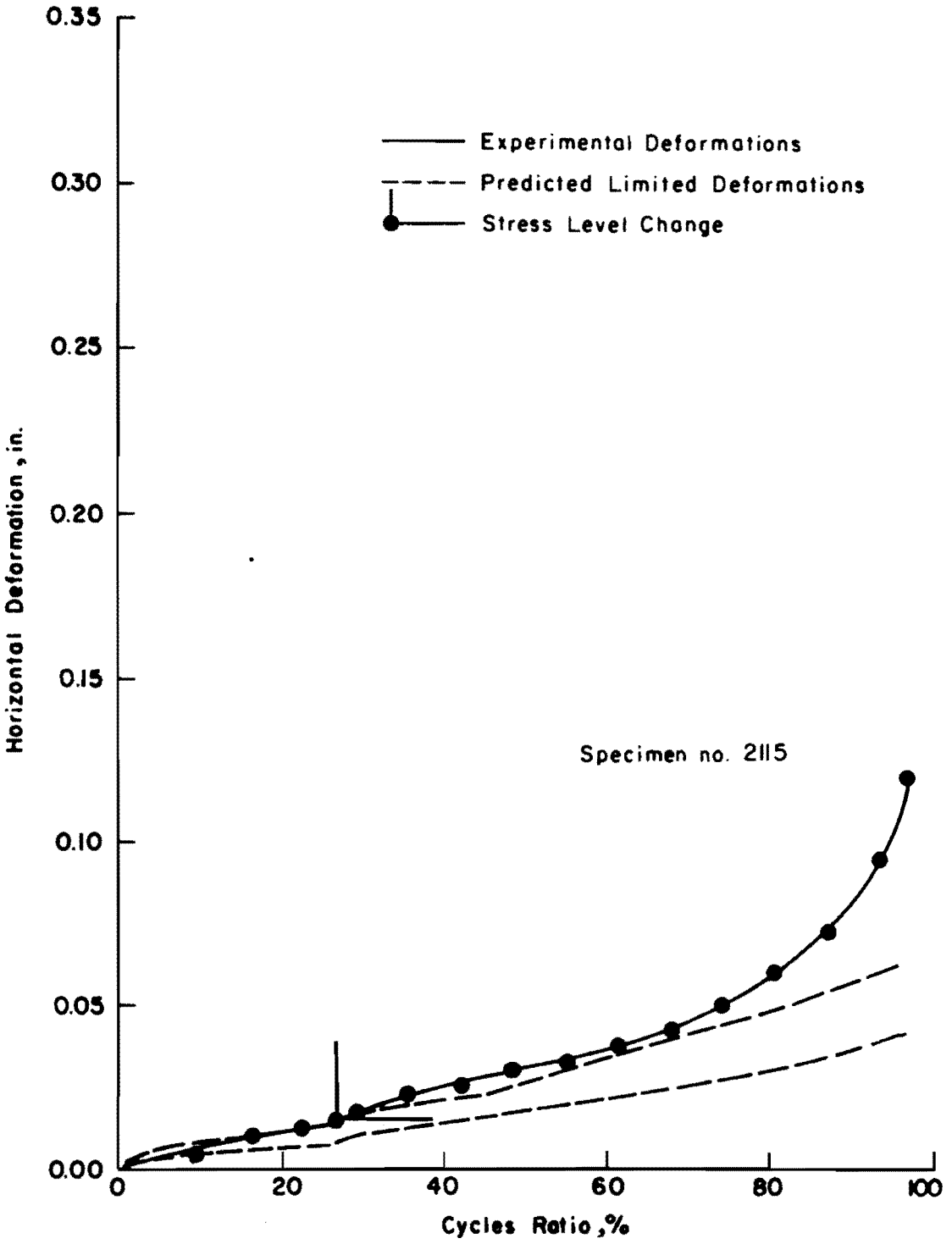

Fig E-12. Comparison of actual and predicted horizontal deformation: 40-32 psi, gravel.

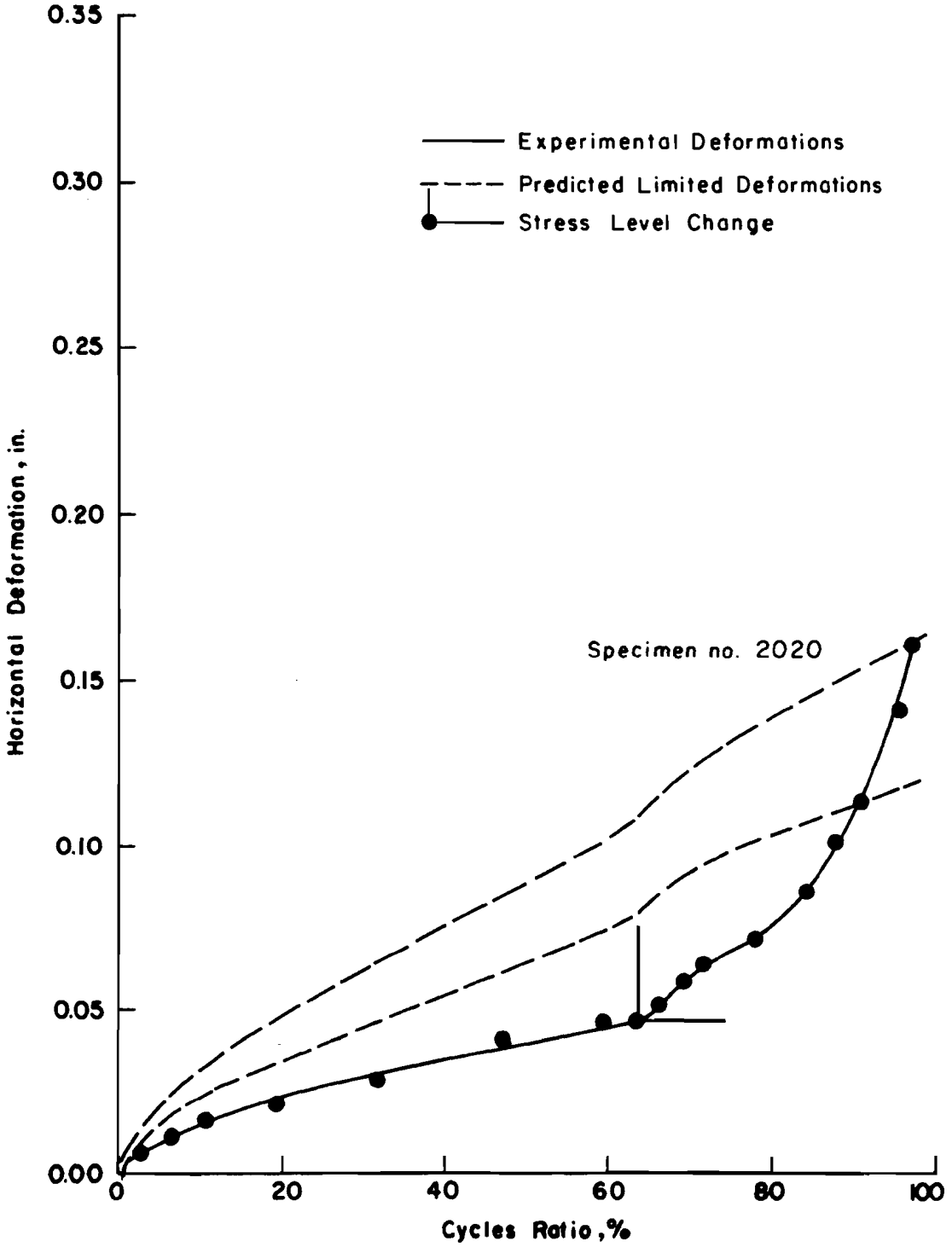

Fig E-13. Comparison of actual and predicted horizontal deformation: 16-24 psi, limestone.

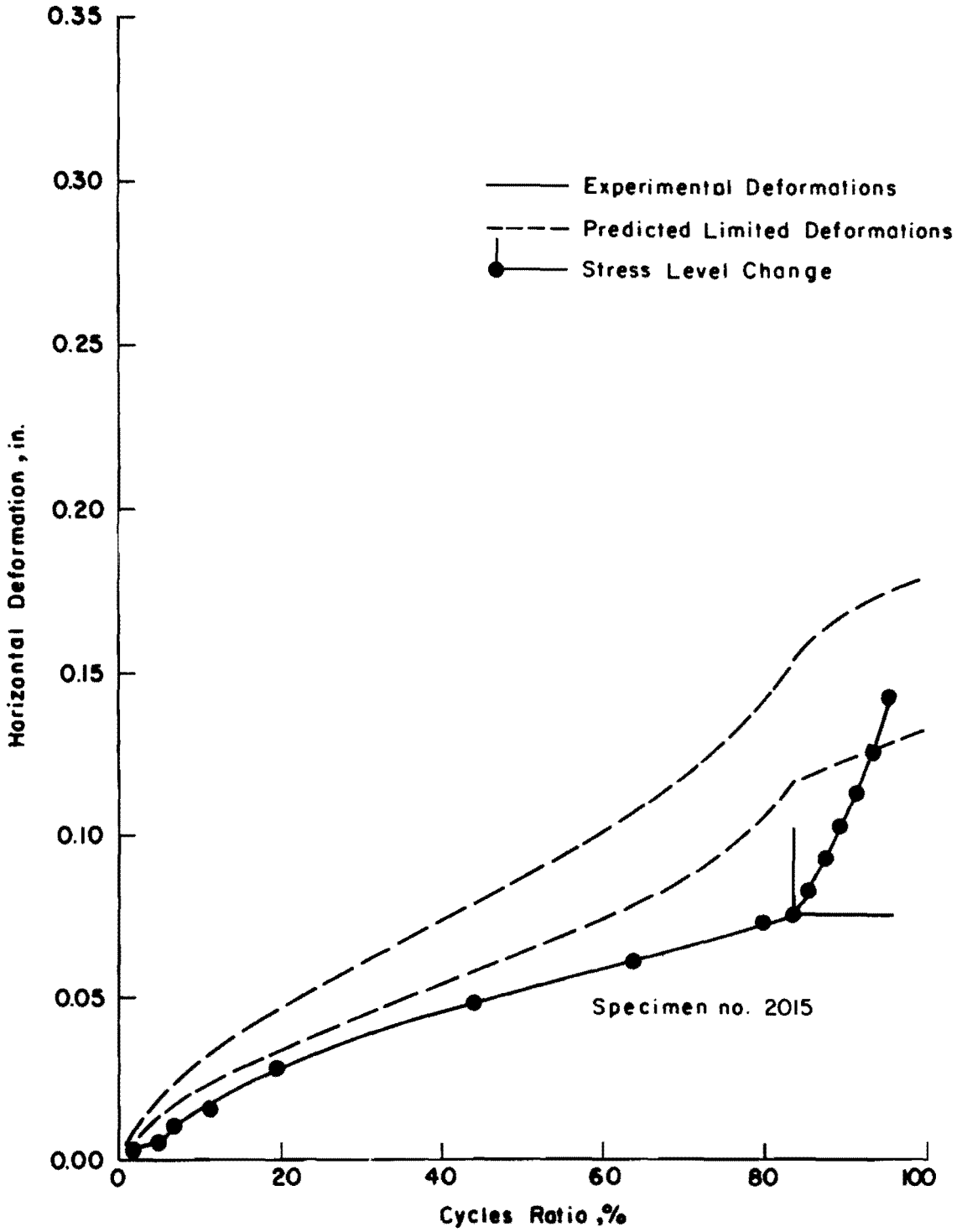

Fig E-14. Comparison of actual and predicted horizontal deformation: 16-32 psi, limestone.

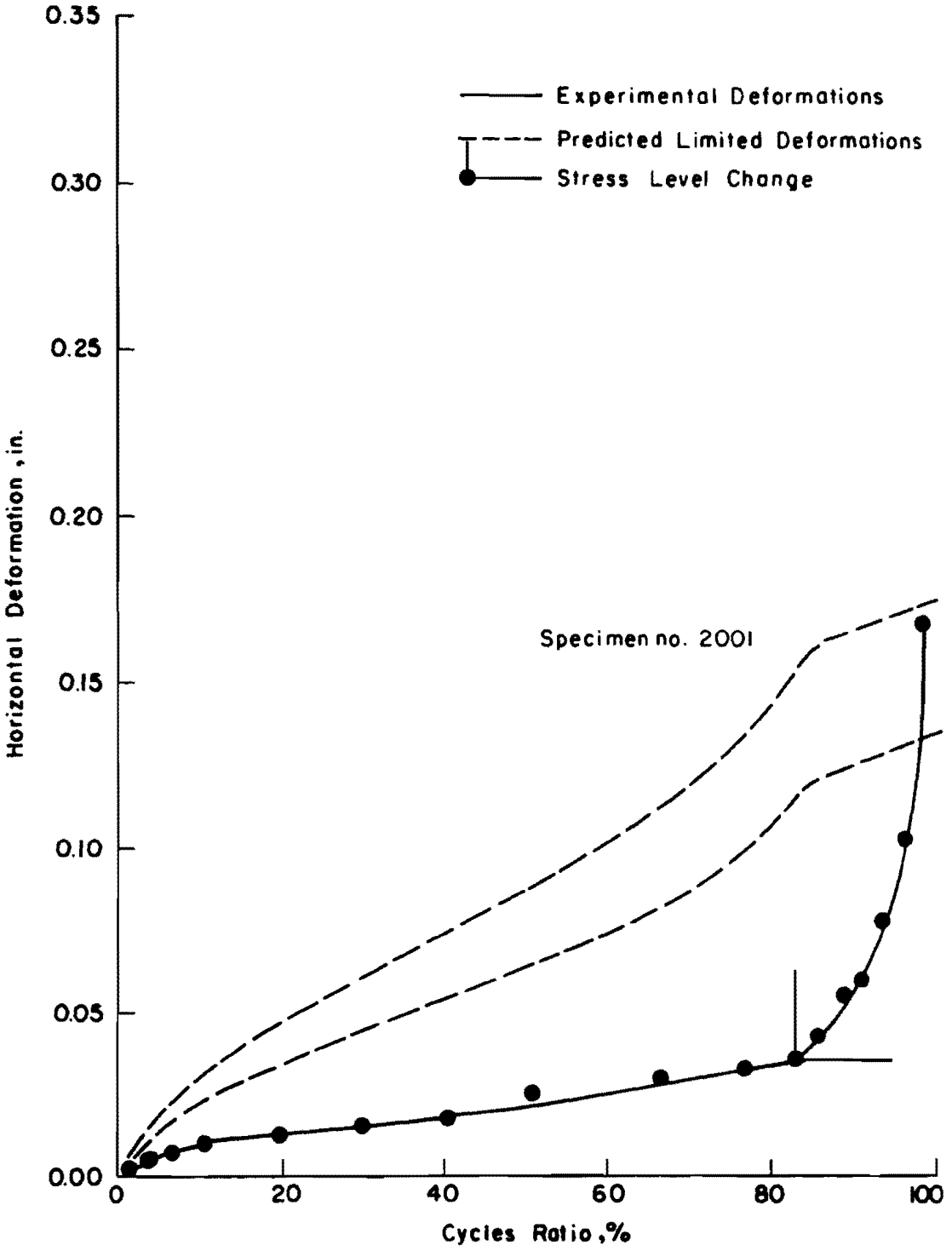

Fig E-15. Comparison of actual and predicted horizontal deformation: 16-40 psi, limestone.

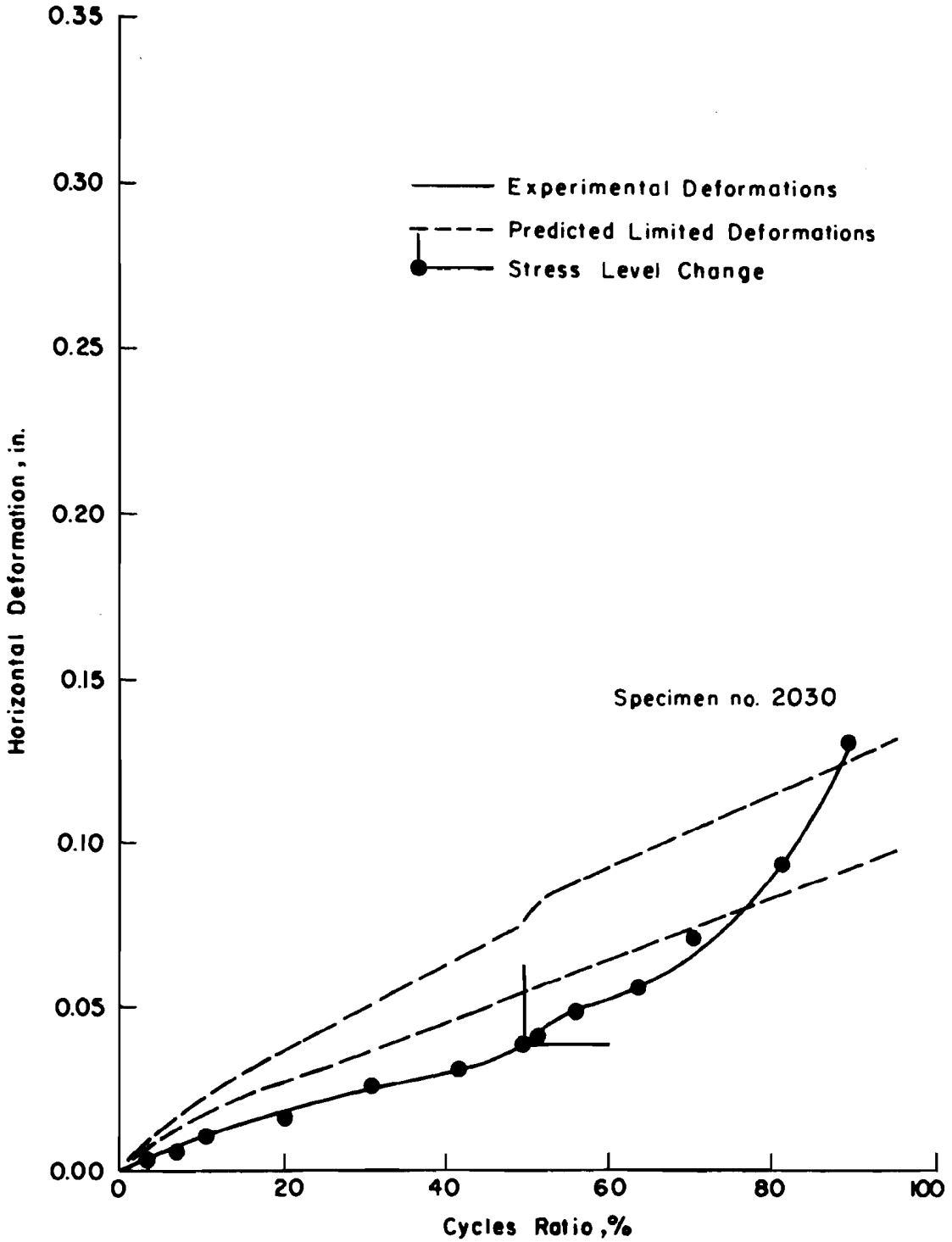

Fig E-16. Comparison of actual and predicted horizontal deformation: 24-32 psi, limestone.

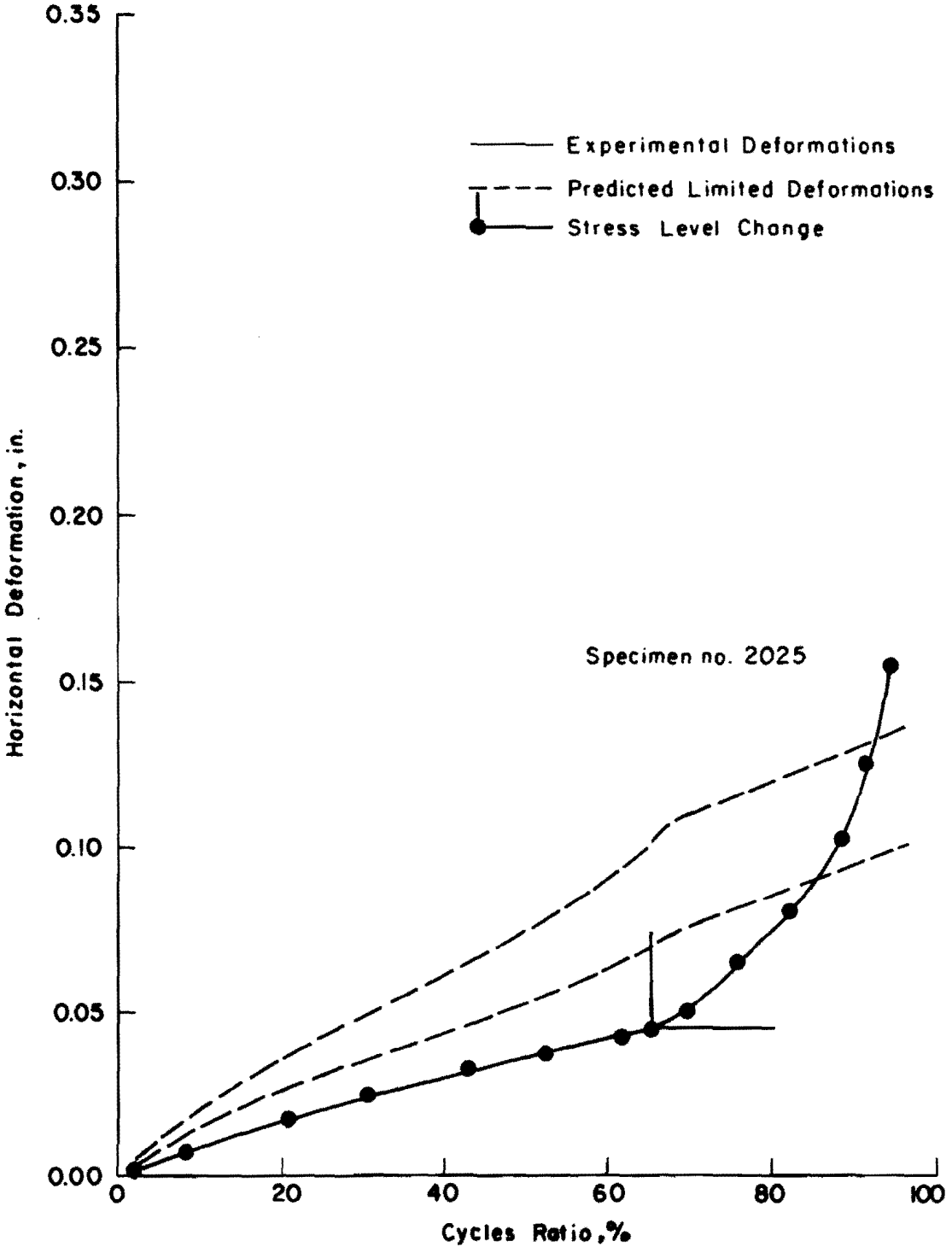

Fig E-17. Comparison of actual and predicted horizontal deformation: 24-40 psi, limestone.

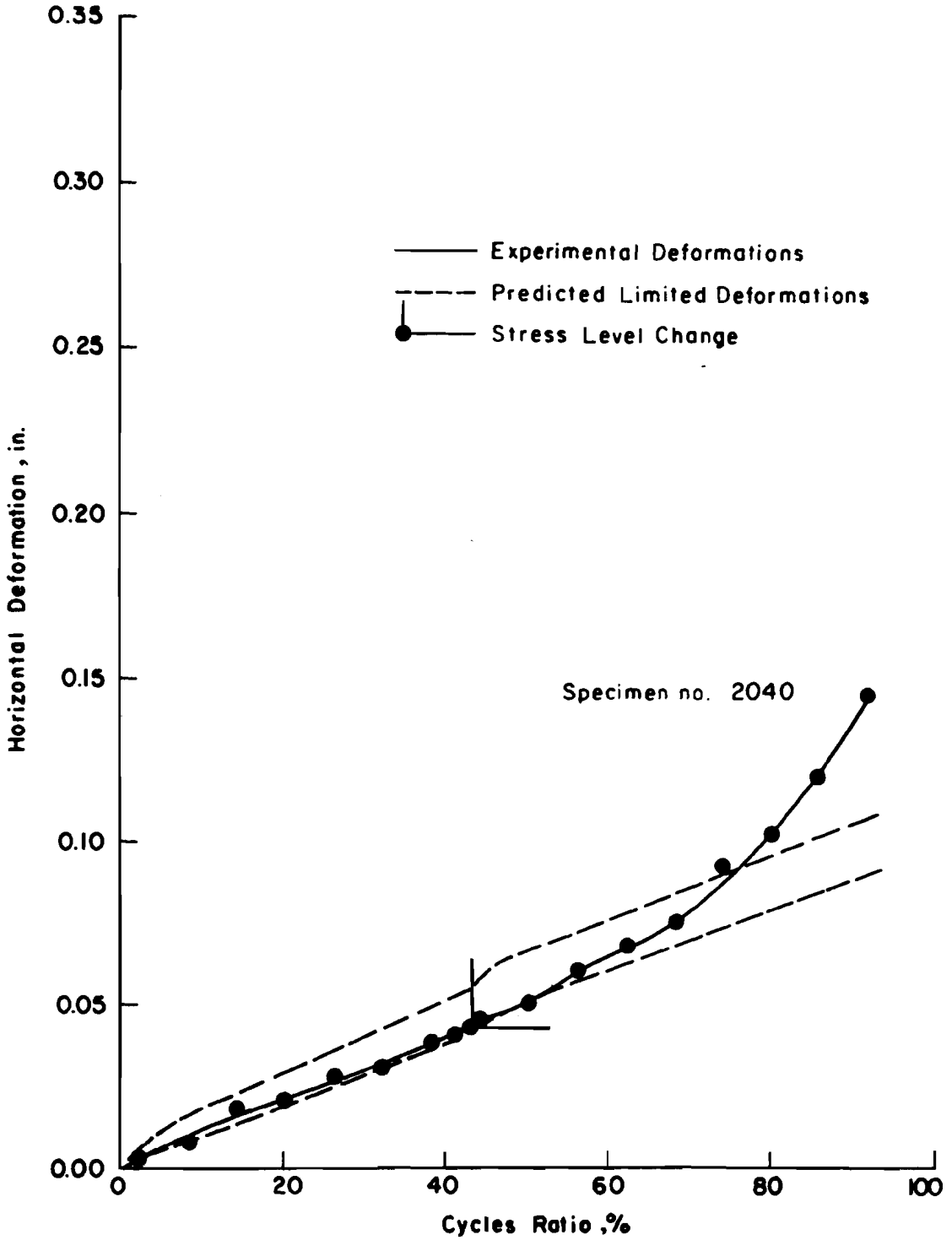

Fig E-18. Comparison of actual and predicted horizontal deformation: 32-40 psi, limestone.

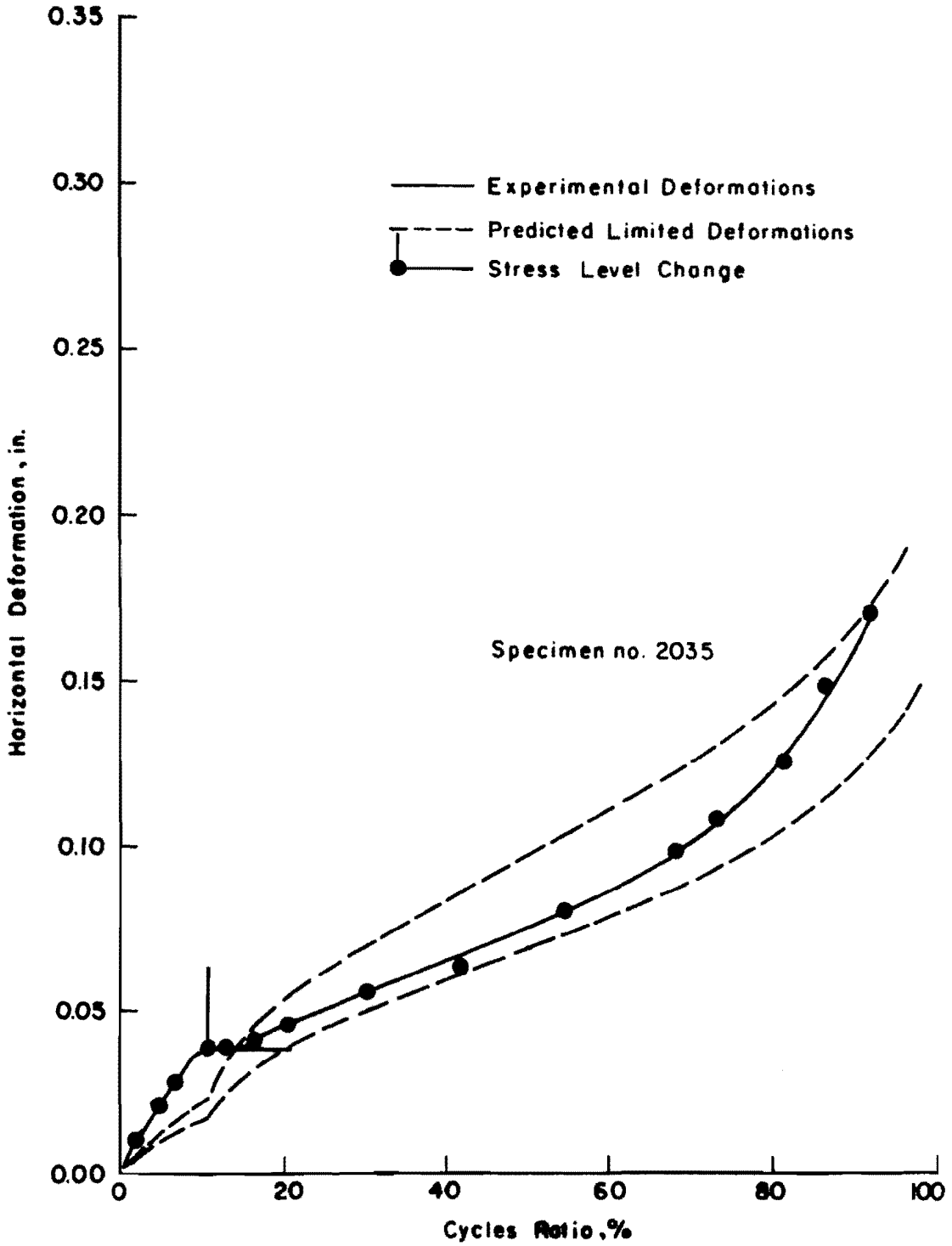

Fig E-19. Comparison of actual and predicted horizontal deformation: 24-16 psi, limestone.

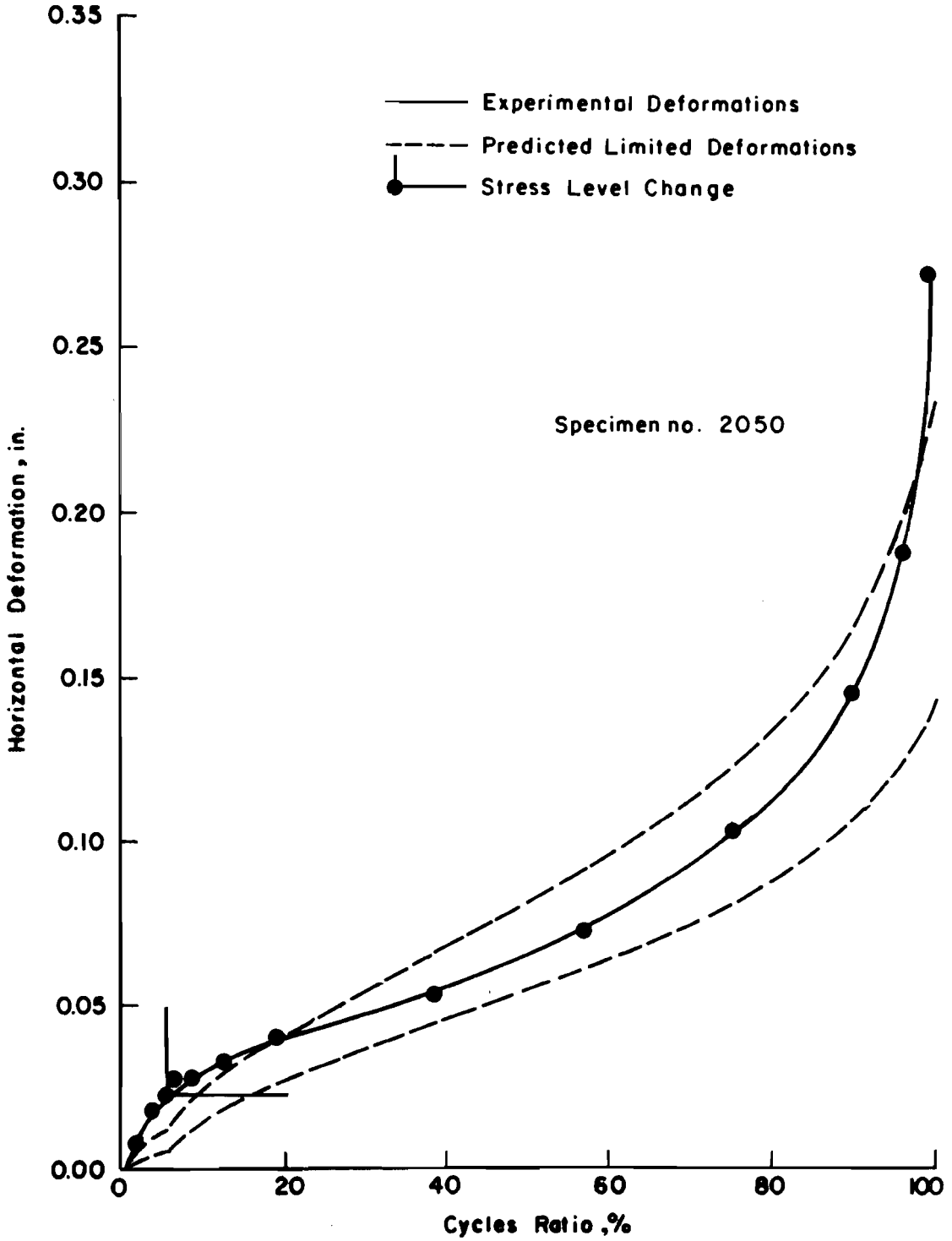

Fig E-20. Comparison of actual and predicted horizontal deformation: 32-16 psi, limestone.

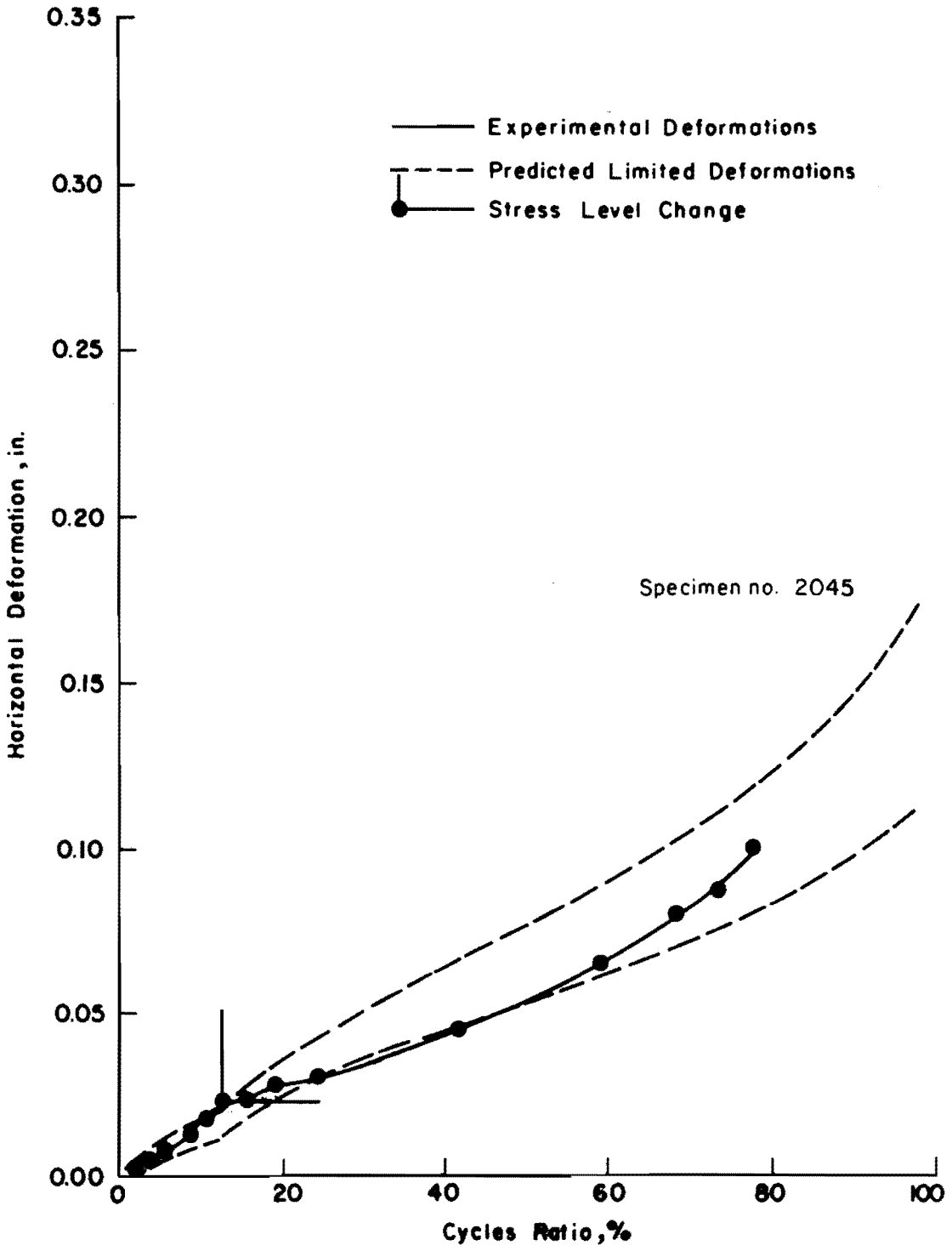

Fig E-21. Comparison of actual and predicted horizontal deformation: 32-24 psi, limestone.

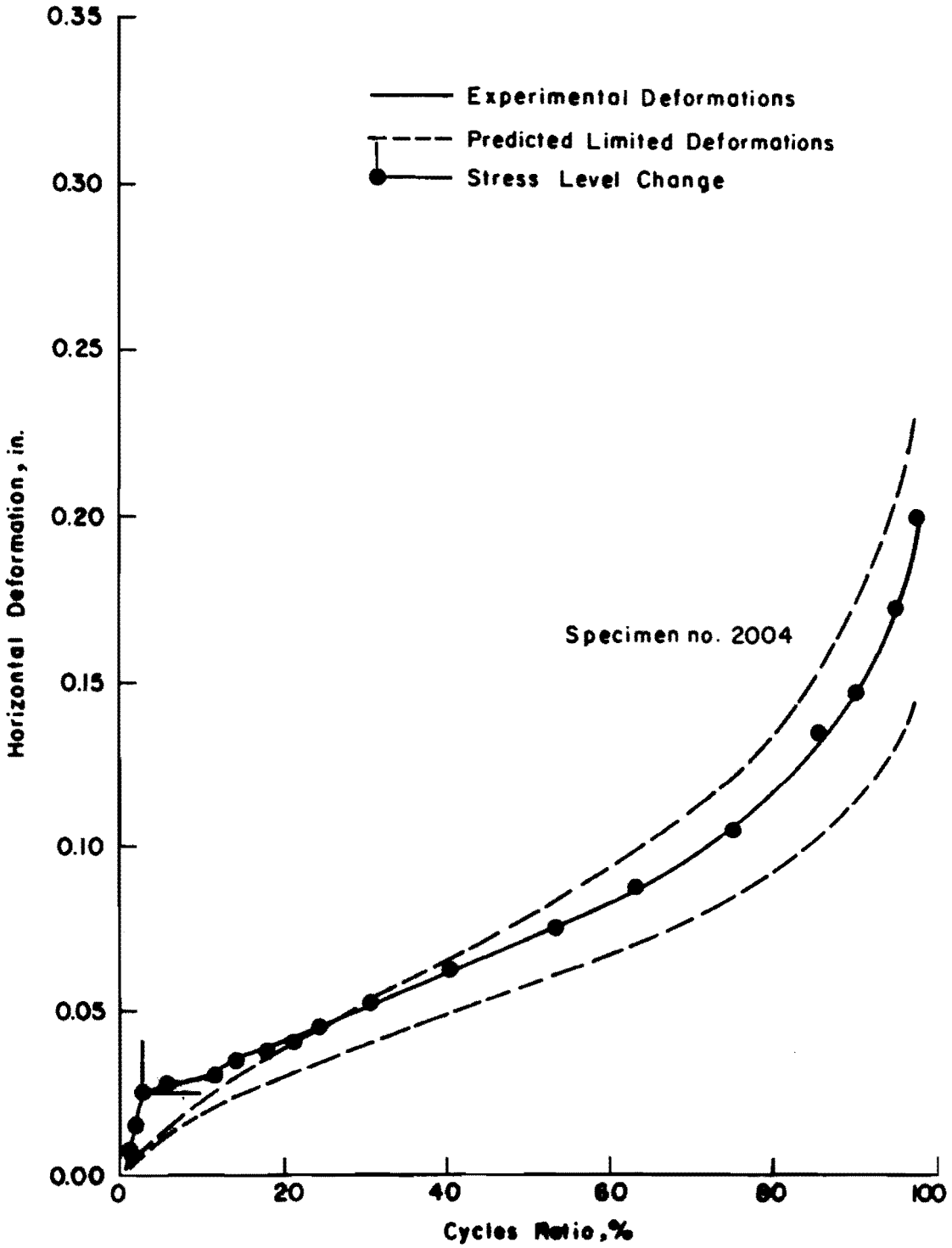

Fig E-22. Comparison of actual and predicted horizontal deformation: 40-16 psi, limestone.

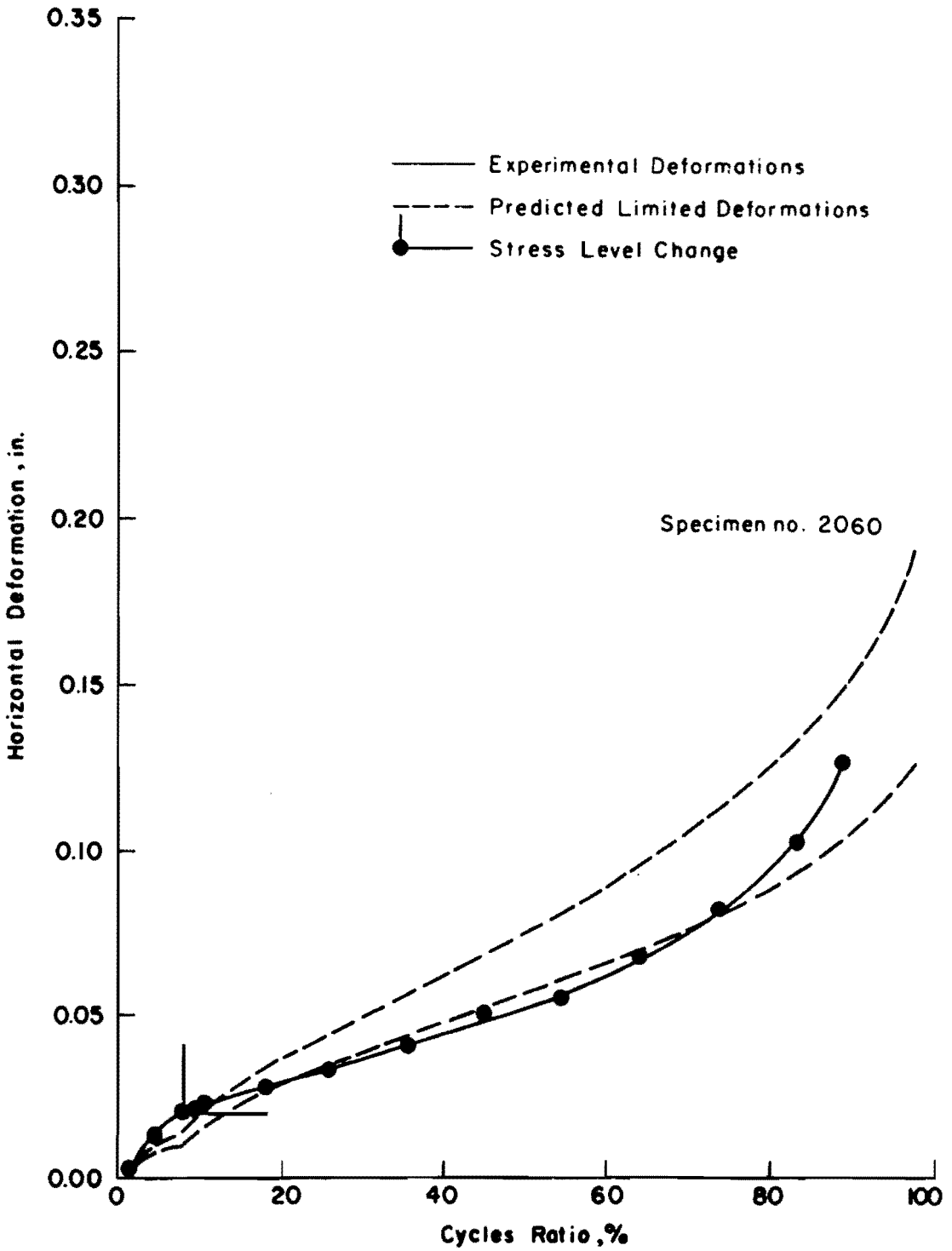

Fig E-23. Comparison of actual and predicted horizontal deformation: 40-24 psi, limestone.

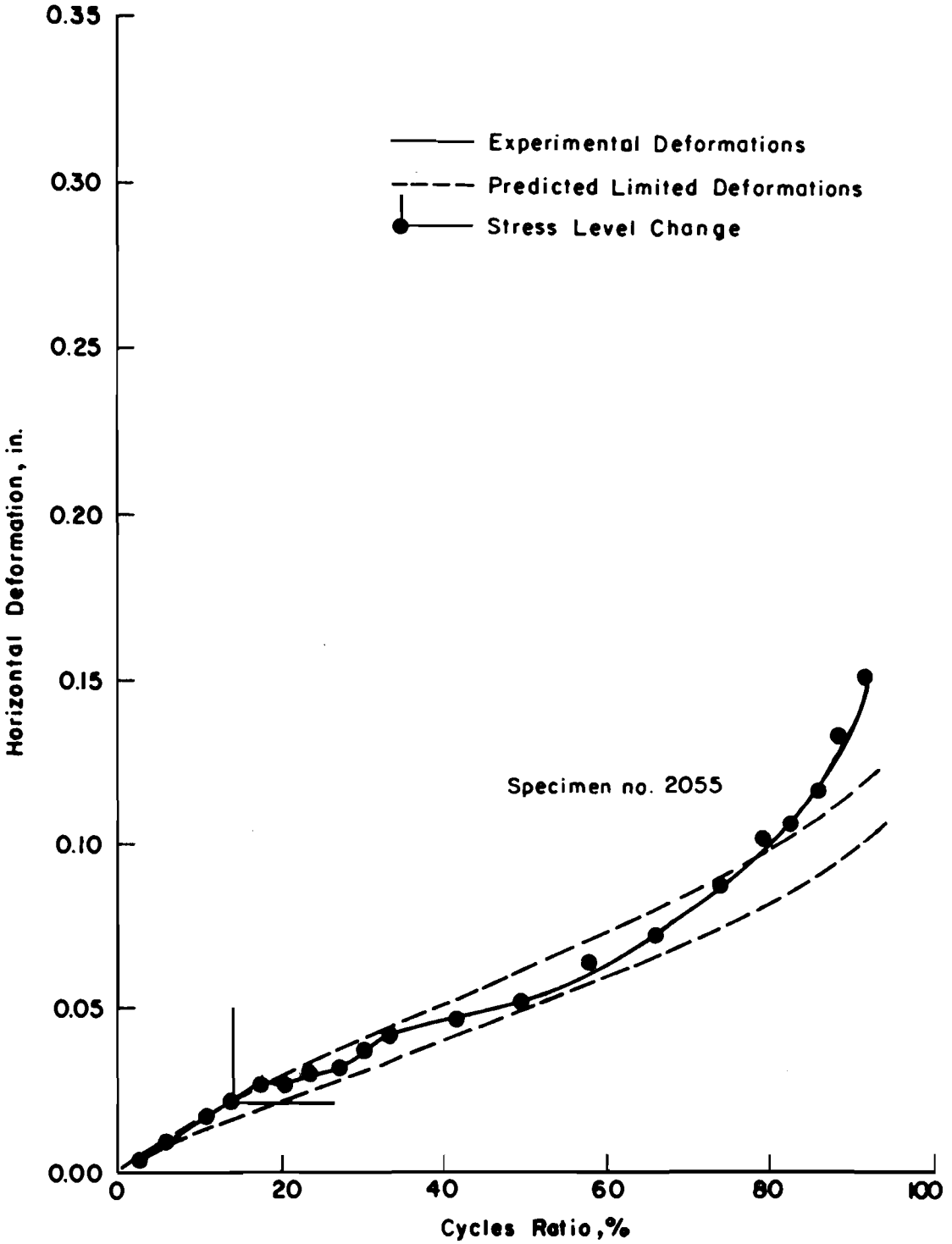

Fig E-24. Comparison of actual and predicted horizontal deformation: 40-32 psi, limestone.